BRAIN ORGANOIDS: MODELING IN NEUROSCIENCE

EDITED BY: Cristina Cereda, Alysson Renato Muotri and Anna Maria Di Giulio

frontiers Research Topics

About Frontiers

Frontiers is more than just an open-access publisher of scholarly articles: it is a pioneering approach to the world of academia, radically improving the way scholarly research is managed. The grand vision of Frontiers is a world where all people have an equal opportunity to seek, share and generate knowledge. Frontiers provides immediate and permanent online open access to all its publications, but this alone is not enough to realize our grand goals.

Frontiers Journal Series

The Frontiers Journal Series is a multi-tier and interdisciplinary set of open-access, online journals, promising a paradigm shift from the current review, selection and dissemination processes in academic publishing. All Frontiers journals are driven by researchers for researchers; therefore, they constitute a service to the scholarly community. At the same time, the Frontiers Journal Series operates on a revolutionary invention, the tiered publishing system, initially addressing specific communities of scholars, and gradually climbing up to broader public understanding, thus serving the interests of the lay society, too.

Dedication to Quality

Each Frontiers article is a landmark of the highest quality, thanks to genuinely collaborative interactions between authors and review editors, who include some of the world's best academicians. Research must be certified by peers before entering a stream of knowledge that may eventually reach the public - and shape society; therefore, Frontiers only applies the most rigorous and unbiased reviews.
Frontiers revolutionizes research publishing by freely delivering the most outstanding research, evaluated with no bias from both the academic and social point of view. By applying the most advanced information technologies, Frontiers is catapulting scholarly publishing into a new generation.

What are Frontiers Research Topics?

Frontiers Research Topics are very popular trademarks of the Frontiers Journals Series: they are collections of at least ten articles, all centered on a particular subject. With their unique mix of varied contributions from Original Research to Review Articles, Frontiers Research Topics unify the most influential researchers, the latest key findings and historical advances in a hot research area! Find out more on how to host your own Frontiers Research Topic or contribute to one as an author by contacting the Frontiers Editorial Office: researchtopics@frontiersin.org

BRAIN ORGANOIDS: MODELING IN NEUROSCIENCE

Topic Editors:
Cristina Cereda, IRCCS Mondino Foundation, Italy
Alysson Renato Muotri, University of California, San Diego, United States
Anna Maria Di Giulio, University of Milan, Italy

Citation: Cereda, C., Muotri, A. R., Di Giulio, A. M., eds. (2020). Brain Organoids: Modeling in Neuroscience. Lausanne: Frontiers Media SA. doi: 10.3389/978-2-88966-264-7

Table of Contents

Editorial: Brain Organoids: Modeling in Neuroscience

Matteo Bordoni[1], Alysson R. Muotri[2,3] and Cristina Cereda[4]*

[1] *Dipartimento di Scienze Farmacologiche e Biomolecolari, Centro di Eccellenza sulle Malattie Neurodegenerative, Università degli Studi di Milano, Milano, Italy,* [2] *Department of Pediatrics, University of California, San Diego, San Diego, CA, United States,* [3] *Department of Cellular and Molecular Medicine, University of California, San Diego, San Diego, CA, United States,* [4] *Genomic and Post-Genomic Center, IRCCS: Istituto di ricovero e cura a carattere scientifico Mondino Foundation, Pavia, Italy*

Editorial on the Research Topic

Brain Organoids: Modeling in Neuroscience

The Research Topic "Brain Organoids: Modeling in Neuroscience" collects both original articles and review that highlight the emergency of novel three dimensional (3D) models, a.k.a. brain organoids, for the study of neurological disorders (NDs). Brain organoids are usually generated from pluripotent stem cells (PSCs) and are defined as multi-cellular, 3D, self-assembled, miniaturized structures that mimic the developing human embryonic and fetal brain (Muotri, 2019). Human brain organoids have recently contributed and represent a promising tool to the understanding of several neurological conditions (Chen et al., 2019).

All the articles reported in the Research Topic are a perfect example to understand the potential of brain organoids for new types of analysis.

The main field in which brain organoids were used is the study of neurodevelopment and the disorders connected to it. For example, brain organoids had a pivotal role in studying congenital and acquired microcephaly that occurs during neurodevelopment (Lancaster et al., 2013; Cugola et al., 2016). All the microcephaly studies conducted on brain organoids were reported in detail in the review article of Gabriel et al..

Original data on neurodevelopmental disorders were published by Benson et al., which exploit iPSC-derived brain organoids to demonstrate the common developmental malformation and transcriptional dysregulations that occur on schizophrenic patients with diverse genetic backgrounds. In particular, thanks to the 3D conformation of brain organoids, they evaluated the organoid region that suffers from a disruption in schizophrenic patients, suggesting the fidelity of organoids to model such disease.

Another neurological disability that occurs in early life is the one caused by the prenatal hypoxic injury. In this case, the disorder is not due to genetic factors. Still, it is produced as effects of hypoxia caused by placental insufficiency, umbilical cord occlusion, premature birth, or obstetric complications (Schump, 2018). However, not all the results of hypoxia are currently known, and this is due to the lack of models to study human corticogenesis. With their works, Daviaud et al. reported the data obtained from their implemented model of brain organoids. They concluded that, in the future, their model could be a starting point for testing new therapeutic approaches to both protect and regenerate the most hit cell population during the neurodevelopmental stage.

Brain organoids are also useful to test the fetal cerebral toxicity of small molecules and other chemicals such as in the article of Zhong et al.. In their work, the authors took advantage of the high reliability of organoids to reproduce the human brain fetal development, in contrast to those conducted in rodents, usually more expensive, time-consuming, and do not always represent the real human pathophysiology.

Brain organoids can also be used in the field of neurodegenerative diseases, such as Alzheimer's disease, Parkinson's disease, Amyotrophic Lateral Sclerosis, and Fronto-Temporal Dementia. For example, Simmnacher et al. widely reviewed in their work the limitations that actual models have for the investigation of the pathogenesis of Parkinson's disease. After the review, the authors presented all the work conducted on different types of organoids, highlighting the importance of cell-cell interactions of a 3D model. The authors also showed the extent to optimize actual protocols to obtain the most realistic 3D model of the pathology.

The research article conducted by Nassor et al. shows another issue connected to organoids generation. Indeed, they developed an episomal method to express a plasmid for the mid and long time because standard methods are not suitable for long-term cultures such as organoids. In particular, they used episomal plasmid to generate an isogenic control for the iPSCs-derived organoid culture of Fronto-Temporal Dementia. Interestingly, the approach presented by this work can be successfully applied not only to other neurodegenerative diseases but also to all models based on iPSCs.

One of the most exciting features of brain organoids is their adaptability. Indeed, brain organoids can reproduce different regions of the brain, such as the neocortex (Heide et al., 2018) and midbrain (Smits and Schwamborn, 2020). Moreover, the protocol of brain organoids can be further optimized to obtain unique features (Qian et al., 2019). Chen et al. reviewed the so-called "assembloid," in which brain organoids are pre-patterned into specific brain regions and

fused to model and recapitulate more complex biological processes of human brain development and related diseases. As explained in the review, such an approach was applied to model many processes, i.e., interneuron migration, neuronal projections, tumor invasion, oligodendrogenesis, forebrain axis establishment, and brain vascularization.

Brain organoids can also be engineered at the genomic level. Fischer et al. reviewed this aspect. In their review, the authors explored both stable and transient genetic modification in all the different stages of brain organoids generation, starting from single-cell techniques to fully develop brain organoids. The authors provided an example of adeno-associated virus delivery and electroporation for the transient transfection, and lentivirus delivery, transposon-like systems, and CRISPR/Cas9 for stable transfection.

In conclusion, the Research "Topic Brain Organoids: Modeling in Neuroscience" provides an intriguing overview of the different approaches that can be applied to human brain organoids, suggesting new techniques for the investigation of NDs. We hope that the reader will find in this Research Topic a useful reference for state of the art in the fast-growing field of brain organoids and their use on the study of brain development and NDs.

AUTHOR CONTRIBUTIONS

MB wrote the editorial. AM revised the editorial. CC wrote, supervised, and revised the editorial. All authors contributed to the article and approved the submitted version.

REFERENCES

Chen, H. I., Song, H., and Ming, G. L. (2019). Applications of human brain organoids to clinical problems. *Dev. Dyn*. 248, 53–64. doi: 10.1002/dvdy.24662

Cugola, F. R., Fernandes, I. R., Russo, F. B., Freitas, B. C., Dias, J. L., Guimaraes, K. P., et al. (2016). The Brazilian Zika virus strain causes birth defects in experimental models. *Nature* 534, 267–271. doi: 10.1038/nature18296

Heide, M., Huttner, W. B., and Mora-Bermúdez, F. (2018). Brain organoids as models to study human neocortex development and evolution. *Curr. Opin. Cell. Biol.* 55, 8–16. doi: 10.1016/j.ceb.2018.06.006

Lancaster, M. A., Renner, M., Martin, C. A., Wenzel, D., Bicknell, L. S., Hurles, M. E., et al. (2013). Cerebral organoids model human brain development and microcephaly. *Nature* 501, 373–379. doi: 10.1038/nature12517

Muotri, A. R. (2019). Brain organoids and insights on human evolution. *F1000Res.* 8:760. doi: 10.12688/f1000research.18495.1

Qian, X., Song, H., and Ming, G. L. (2019). Brain organoids: advances, applications and challenges. *Development* 146:dev166074. doi: 10.1242/dev.166074

Schump, E. A. (2018). Neonatal encephalopathy: current management and future trends. *Crit. Care Nurs. Clin. North Am*. 30, 509–521. doi: 10.1016/j.cnc.2018.07.007

Smits, L. M., and Schwamborn, J. C. (2020). Midbrain organoids: a new tool to investigate Parkinson's disease. *Front. Cell. Dev. Biol.* 19:359. doi: 10.3389/fcell.2020.00359

Check for updates

Distinct Vulnerability and Resilience of Human Neuroprogenitor Subtypes in Cerebral Organoid Model of Prenatal Hypoxic Injury

Nicolas Daviaud[1†], Clément Chevalier[2], Roland H. Friedel[1,3] and Hongyan Zou[1,3*]

[1] Nash Family Department of Neuroscience, Friedman Brain Institute, New York, NY, United States, [2] The Center for Microscopy and Molecular Imaging, Université Libre de Bruxelles, Brussels, Belgium, [3] Department of Neurosurgery, Icahn School of Medicine at Mount Sinai, New York, NY, United States

Prenatal hypoxic injury (HI) is a leading cause of neurological disability. The immediate and long-term effects of hypoxia on progenitor homeostasis and developmental progression during early human brain development remain unclear. This gap is due to difficulty to access human fetal brain tissues and inadequate animal models to study human corticogenesis. Recent optimizations of cerebral organoid models derived from human embryonic stem (ES) cells present new opportunities to investigate pathophysiology of prenatal HI. Here, we implemented a transient HI model using human cerebral organoids with dorsal forebrain specification. We demonstrated that transient hypoxia resulted in immediate and prolonged apoptosis in cerebral organoids, with outer radial glia (oRG), a progenitor population more prominent in primates, and differentiating neuroblasts/immature neurons suffering larger losses. In contrast, neural stem cells in ventricular zone displayed relative resilience to HI and exhibited a shift of cleavage plane angle favoring symmetric division, thereby providing a mechanism to replenish the stem cell pool. Furthermore, we defined the vulnerable window and neurodifferentiation stages that are particularly sensitive to HI. Understanding cell type-specific and stage-dependent effects of prenatal HI on survival and mitotic behavior of human neuroprogenitor subtypes during early human corticogenesis helps elucidate the etiology of neurodevelopmental disorders, and provides a therapeutic starting point to protect the vulnerable populations at critical timeframes.

Keywords: cerebral organoids, prenatal hypoxic injury, human corticogenesis, neural stem cell, neuroprogenitor, outer radial glia

INTRODUCTION

Prenatal hypoxic injury (HI) is a leading cause of neurological disability, with an incidence of 2–4 per 1000 live births (Badr Zahr and Purdy, 2006; Glass and Ferriero, 2007). Deprivation of oxygen due to placental insufficiency, umbilical cord occlusion, premature birth, or obstetric complications can result in immediate cellular damages but also long-term dysfunction of neuroprogenitor cells (NPCs), leading to developmental anomaly and increased risk of neurological disorders later in life

(Schump, 2018). Even a short, transient hypoxic episode, e.g., 30 min, can trigger fetal brain injury at mid-gestation (Mallard et al., 1993; Gunn and Bennet, 2009).

Hypoxic conditions alter brain development as a result of increased apoptosis and a delay in maturation (Salmaso et al., 2014). However, the immediate and long-term effects of hypoxia on NPC homeostasis and differentiation trajectory during early human brain development remain poorly understood, and this is due to relative inaccessibility of human fetal brain tissues and inadequate animal models to study human corticogenesis.

Recent advances in 3D cerebral organoid cultures derived from human embryonic stem cells (hESC) or induced pluripotent stem cells (iPSC) (Kadoshima et al., 2013; Lancaster et al., 2013; Lancaster and Knoblich, 2014; Camp et al., 2015) provide new avenues to implement reproducible models to study cell type- and stage-specific effects of HI on early human cortical development. Cerebral organoid cultures take advantage of the enormous self-organizing potential of neural stem cells (NSCs) and differentiating NPCs to develop into complex structures that mimic early to mid-gestation human brain development (Camp et al., 2015). Cerebral organoids can be differentiated toward dorsal forebrain specification containing ventricle-like structures aligned with ventricular zone (VZ)-like germinal regions populated by NSCs, subventricular zone (SVZ) populated by committed progenitors in various stages of differentiation and migration, and a rudimentary cortical plate (CP) occupied by cortical neurons in a stratified layout (Lancaster et al., 2013). In addition, human cerebral organoids contain a progenitor domain that is more prominent in primates, termed outer SVZ (oSVZ), which is populated by outer radial glia (oRG), which support the evolutionary expansion of human neocortex (Hansen et al., 2010; Dehay et al., 2015; Pollen et al., 2015).

Here, we implemented an organoid-based platform to model prenatal transient HI during early human brain development. As compared to 2D adherent cultures, cerebral organoids contain different neuroprogenitor subtypes that are maintained in a complex 3D cytoarchitecture with stereotypical spatial alignment and proper cell-cell interactions, thus better recapitulating cellular diversity in distinct niches as in developing human brains. The organoid model allows us to address the following fundamental questions not possible with conventional models: (i) relative vulnerability of human neuroprogenitor subtypes to HI, (ii) stability of NSC reserve and potential compensatory mechanisms, and (iii) vulnerable window and differentiation stages that are most affected by HI.

Using the cerebral organoid model, we found that transient HI resulted in immediate and prolonged apoptosis, with FAM107^{+} oRG progenitors and Doublecortin[+] (DCX[+]) neuroblasts/immature neurons suffering larger losses. TBR2^{+} intermediate progenitors (IP) also suffer losses but only at later stages. SOX2^{+} NSCs residing in the VZ-like region remained stable, attributable to intrinsic resilience and a shift of cell division mode for self-expansion. Consistently, timed EdU and BrdU pulse-chase studies of isochronic progenitor cohorts revealed that the differentiating population in SVZ/CP appeared more affected by HI than active cycling NSCs in VZ. Pasca et al. (2019) have recently also reported a transient HI model based on human cortical spheroids (hCS) derived from multiple iPSC lines, which similarly demonstrated particular vulnerability of TBR2^{+} IP to transient HI.

Taken together, human cerebral organoids can be used to implement a reproducible HI paradigm to dissect the etiology of cortical dysgenesis associated with hypoxic insults. Our study and the study of Pasca et al. (2019) demonstrated the broad utility of cerebral organoids for modeling pathophysiology of human neurodevelopmental disorders.

MATERIALS AND METHODS

Cerebral Organoid Generation

Human cerebral organoids were generated from H9 hESCs as described (Lancaster et al., 2013; Lancaster and Knoblich, 2014; Daviaud et al., 2018), with minor modifications. In brief, H9 hESCs were plated in round bottom ultra-low attachment 96-well plates to form embryoid bodies, followed by neural induction. After neuroepithelium emerged, organoids were embedded in Matrigel droplets and cultured in 6 cm Petri dishes for 4 days and were then placed on an orbital shaker at 85 rpm until analyses.

Hypoxia Injury Induction in Cerebral Organoids

Twenty-eight days after differentiation from hESCs, organoids were cultured in a hypoxic chamber (3% O_2, 5% CO_2) (BioSpherix) for 24 h, and then switched back to normoxic condition (21% O_2, 5% CO_2) until analysis.

Labeling of Isochronic NPC Cohorts

Organoids were pulsed with 15 μM of 5-bromo-2′-deoxyuridine (BrdU, Acros Organics) or 10 μM 5-ethynyl-2′-deoxyuridine (EdU, Thermo Fisher) for 30 min. Label-retaining cells (LRCs) were revealed by EdU Click-iT kit (Thermo Fisher) or anti-BrdU antibody (rat, Thermo Scientific MA182718, 1:400).

Quantification and Statistical Analysis

All quantitative analyses were carried out in 100 μm (width) × 300 μm (height) radial columns spanning all cortical layers near organoid surface regions as shown in **Figure 2A**, unless otherwise specified. At least 2–3 different organoids from three independent batches were used for each condition, and 1–3 representative images from each organoid were quantified (Fiji software) (Schindelin et al., 2012). Bar graphs are presented as mean with standard error of the mean (SEM). Box plots represent data extending from 25th to 75th percentiles, with whisker depicting median and min to max (GraphPad Prism 7.0).

For individual comparison between two conditions, normality of data was assessed using a Shapiro–Wilk test followed by a Student t-test. Differences between multiple conditions were determined using a two-way analysis of variance (ANOVA) test, followed by a Tukey post hoc test. To analyze frequencies distribution, a Chi-square test was performed (see **Supplementary Materials** for details).

RESULTS

Establishment and Characterization of HI Model With Human Cerebral Organoids

To develop a reproducible experimental paradigm to model prenatal hypoxia during early human brain development, we adapted the protocol of Lancaster and colleagues with minor modifications to derive consistent cerebral organoids from human ESCs with dorsal forebrain specification (**Supplementary Figure S1A**; Lancaster et al., 2013; Lancaster and Knoblich, 2014). Human ESCs were first differentiated into embryoid bodies, followed by neuroectodermal differentiation. Tissues were then embedded in Matrigel droplets and cultured first in stationary and then rotating condition on an orbital shaker (**Supplementary Figure S1A**). Over the next 4 weeks of culture, we observed rapid maturation of cerebral organoids with appearance of ventricle-like structures aligned with a VZ-like proliferative zone and a rudimental CP, separated by an SVZ-like transitional zone (**Figures 1B,C** and **Supplementary Figure S1B**). Specifically, at D14 after start of differentiation, when culture on orbital shaker started, abundant proliferating cells (Ki67$^+$) expressing radial glia (RG) marker PAX6 were detected in neuroepithelium (**Figure 1B**). From D21 to D42, a majority of Ki67$^+$ cells remained in the VZ, while a small fraction of Ki67$^+$ cells appeared in outer layers representing intermediate progenitors expressing TBR2 (EOMES) and neuroblasts expressing DCX (Hevner et al., 2006; **Figure 1B** and **Supplementary Figure S1B**). During the same period, CP steadily increased in thickness with progressively more cells expressing immature neuronal marker β-III tubulin (TUJ1) and deep layer subcortical projection neuron marker CTIP2 (Molyneaux et al., 2005; **Figure 1B** and **Supplementary Figure S1B**).

Human cerebral organoids also contain a progenitor domain that is much more prominent in primates, populated with oRGs expressing FAM107A (Lancaster et al., 2013; Pollen et al., 2015). It has been shown that the localization of FAM107A$^+$ oRGs during corticogenesis reflects the fetal gestational week (GW) during human embryogenesis (Pollen et al., 2015). Indeed, we found a progressive change of localization of FAM107A$^+$ cells in organoids, from mainly VZ at D14 to mainly outer layers at D42 (**Figure 1C** and **Supplementary Figure S1B**). Based on this correlation, we estimated that our D28–D42 cerebral organoids recapitulated the developmental stage of human fetal cortex at early midgestation (∼GW14.5–18.5).

We next adapted a hypoxia protocol used widely in brain slice cultures for human cerebral organoids (Morales et al., 2007; Wise-Faberowski et al., 2009). We first tested extended exposure of cerebral organoids to 3% oxygen tension for 14 days (D28–D42), which resulted in poorly developed organoids, massive cell death, and cytoarchitectural collapse (**Supplementary Figures S2A,B**). The VZ and cortical layers were highly compromised with markedly diminished NSC pool (SOX2$^+$ or PAX6$^+$) and near obliteration of neuronal populations (β-III tubulin$^+$) (**Supplementary Figure S2C**).

To model milder effects of non-lethal prenatal hypoxia frequently encountered in human newborns, we tested a transient hypoxia paradigm wherein cerebral organoids were subjected to 3% O$_2$ for 24 h from D28–D29, and then returned to normoxia for the remaining culture period (**Figure 1A**). We reasoned that such a transient HI paradigm would preserve overall structural integrity of cerebral organoids without massive cell death and cytoarchitectural collapse, allowing us to study subtle changes from non-lethal HI during early human corticogenesis rather than irreversible cellular damages. Indeed, after transient HI, we found no overt structural alterations in ventricle size or layered organization of VZ and SVZ/CP at D42, i.e., 14-day post initiation of HI (dpi) (**Supplementary Figure S3A**). Immunostaining for radial glia marker SOX2 and immature neuronal marker β-III tubulin also revealed stereotypical organization of germinal zone and cortical layer with no cellular ectopia (**Supplementary Figure S3B**). Similarly, measurement of thickness of cortical columns as a whole, or VZ and SVZ/CP layers separately, indicated no significant differences between HI and control conditions (**Supplementary Figure S3C**).

Hypoxia-inducible factor (HIF) is a protein complex that senses oxygen tension through stabilization of the complex in hypoxic conditions (Maxwell et al., 1999). Immediately after transient hypoxia, we detected an increase of HIF-1α immunostaining in organoids at D29, with cells in outer layers exhibiting higher levels than cells in VZ (**Figure 1D**). Notably, by D42 (14 dpi), HIF-1α levels had returned to baseline with no detectable differences between HI and control conditions (**Figure 1D**). We continued our studies with the transient HI paradigm to model non-lethal prenatal hypoxia corresponding to early human corticogenesis.

Prolonged Apoptosis in Cerebral Organoids After Transient Hypoxia

To assess the effects of transient HI on DNA integrity and cell survival in cerebral organoids, we performed immunofluorescence (IF) staining for γH2AX and cleaved caspase 3 (CC3), markers for DNA double-strand break and apoptosis, respectively. We observed an increase in the prevalence of γH2AX$^+$ cells immediately after HI at D29 (6% in control vs. 15% after HI, $p < 0.001$) (**Figures 2A,B**). The prevalence of γH2AX$^+$ cells only showed a trend of increase by 7 dpi at D35 (14% in control vs. 21% after HI, $p = 0.23$), but had returned to basal levels with even a modest reduction by 14 dpi at D42 (8% in control vs. 6% after HI, $p = 0.005$) (**Figures 2A,B**), perhaps reflecting enhanced DNA repair capability among the surviving population. In parallel, transient HI resulted in a significant increase in apoptotic rates at 1 dpi (14% in control vs. 28% after HI, $p = 0.002$) and 7 dpi (19% in control vs. 27% after HI, $p = 0.002$), but no longer at 14 dpi (20% in control vs. 18% after HI, $p = 0.25$) (**Figures 2A,C**).

To examine if DNA damage or apoptosis occurred predominantly in neural precursors or differentiating populations, we quantified the prevalence of γH2AX$^+$ and CC3$^+$ cells in VZ and outer layers (SVZ/CP) separately. At 1 dpi, we detected a marked increase in the percentage of γH2AX$^+$ cells in VZ (6% in control vs. 15% after HI, $p < 0.01$), but no significant difference in SVZ/CP, consistent with higher
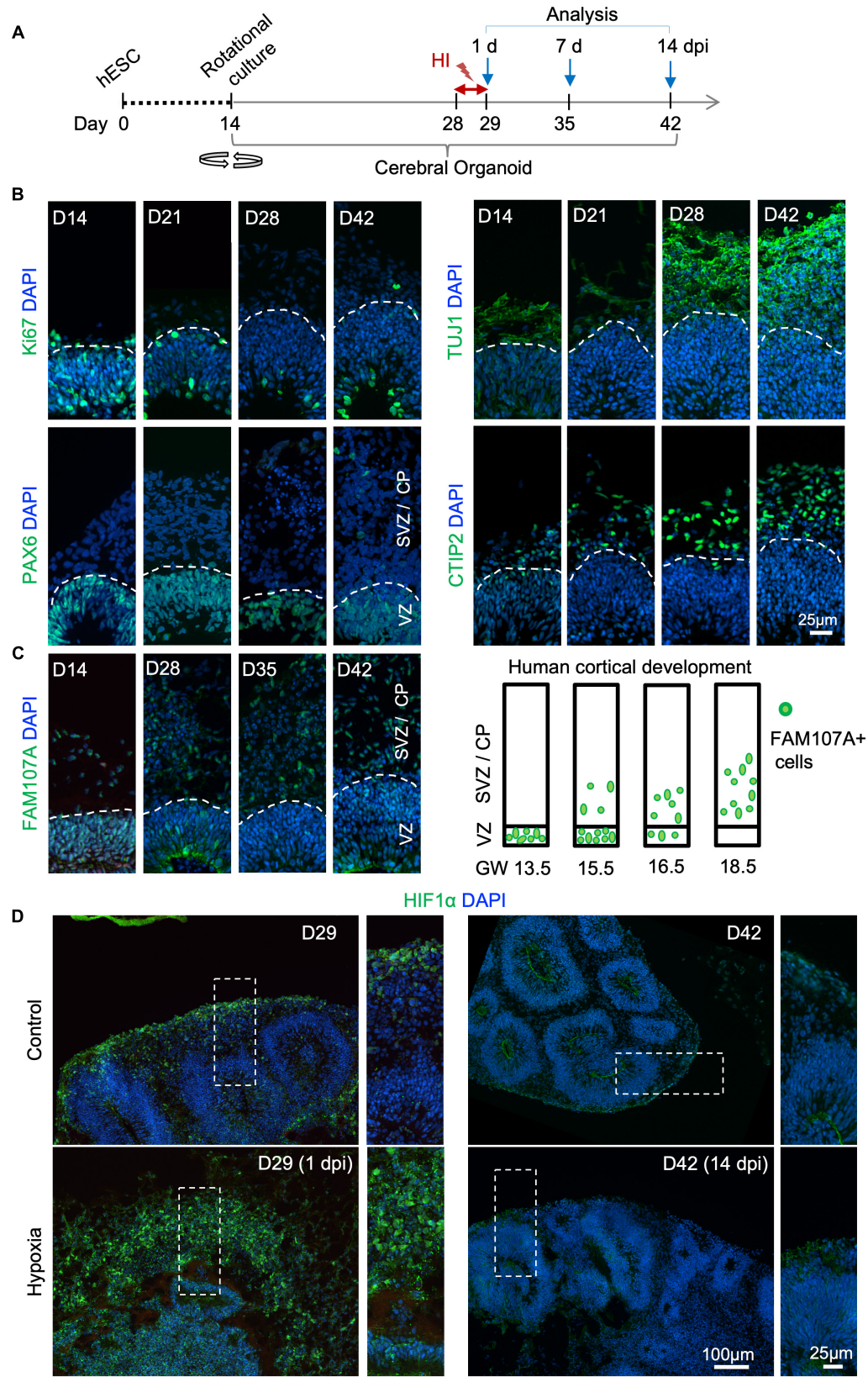
FIGURE 1 | Continued

FIGURE 1 | Transient hypoxia model in human cerebral organoids. **(A)** Schematic diagram of transient hypoxic injury (HI) model with hESC-derived cerebral organoids. D0 represents the starting day of differentiation, D14 denotes the time when organoids were transferred to culture on orbital shaker. At D28, organoids were subjected to 3% O_2 in a hypoxic chamber for 24 h, followed by return to 21% O_2 culture condition for the remaining culture periods until analysis. **(B)** IF images for the indicated markers in cerebral organoids demonstrate progressive development of cortex-like structures and appearance of immature neurons (TUJ1$^+$) and deep-layer cortical neurons (CTIP2$^+$) from D14–D42. Proliferating (Ki67$^+$) NSCs (PAX6$^+$) reside in VZ-like germinal region, and offspring in various stages of differentiation migrate out of VZ to populate outer layers, designated as SVZ/CP-like structures. White dashed lines delineate border between VZ and SVZ/CP. Note higher cellular density in the VZ as visualized by DAPI nuclear counterstaining. **(C)** Left, IF images demonstrate progressive development of oRGs that express FAM107A. Right, schematic depiction of spatial localization of FAM107A$^+$ oRGs during human brain development at the indicated gestational week (GW), adapted from Pollen et al. (2015). **(D)** Representative IF images show stabilization of HIF-1α at D29 (1 dpi) after hypoxia episode as compared to control, while only baseline HIF-1α immunofluorescence was detected at D42 (14 dpi). High magnification images of boxed areas are shown on the right.
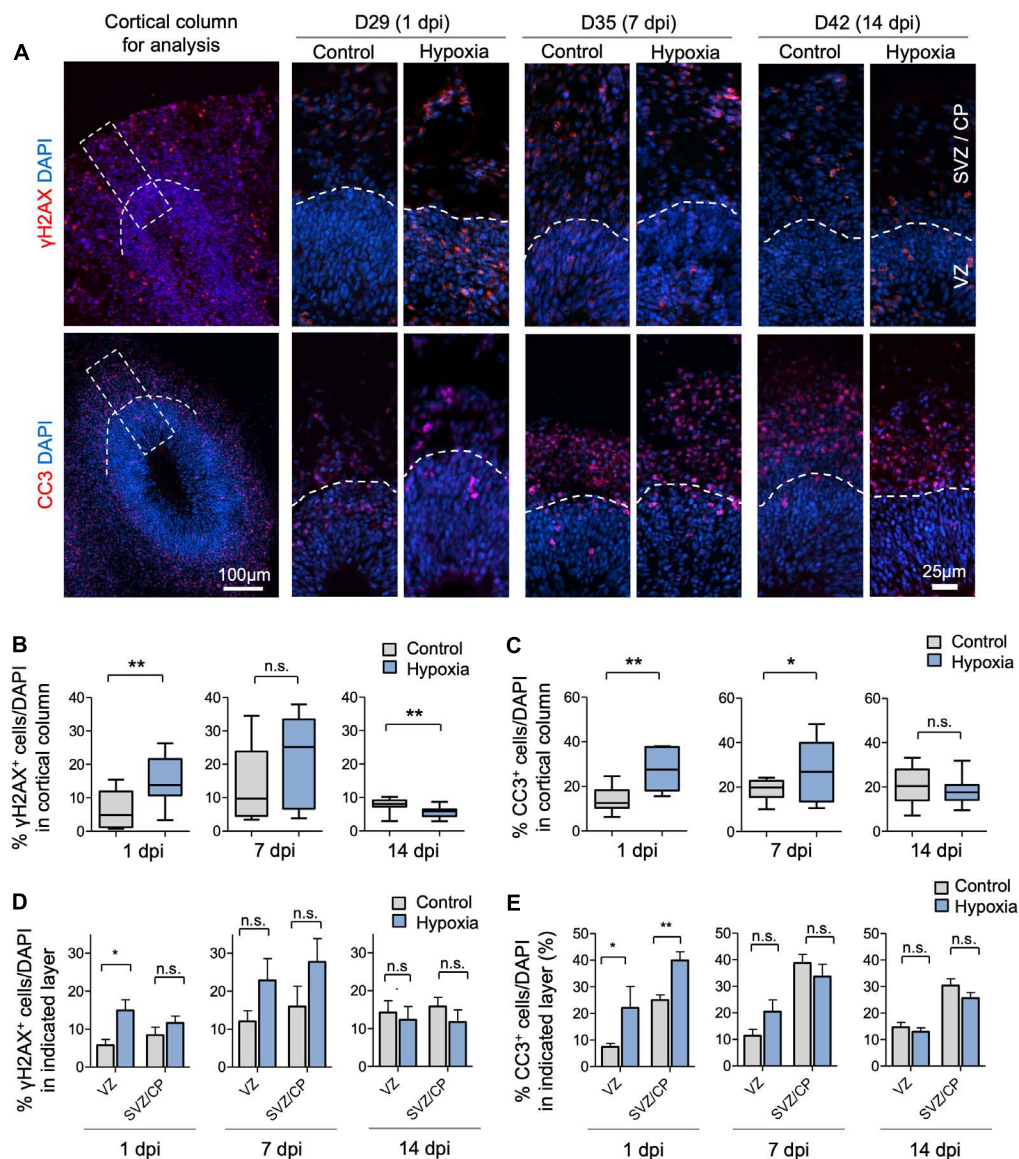
FIGURE 2 | Transient hypoxia induces immediate DNA damage and prolonged apoptosis in cerebral organoids. **(A)** Representative IF images for γH2AX and cleaved caspase 3 (CC3) in cerebral organoids. Boxed area in lower magnification images in left panel denotes the analyzed area, i.e., a 100 μm wide × 300 μm high radial column spanning all cortical layers (VZ, SVZ, and CP). Corresponding cortical areas of the same size were used for all quantifications in our studies to ensure consistency. Higher magnification images are shown in right panels. White dashed lines demarcate VZ and SVZ/CP. **(B,C)** Quantifications show the percentage of DAPI$^+$ cells that are positive for γH2AX **(B)** or CC3 **(C)**. Analyses were carried out in 100 μm × 300 μm cortical column as shown in **(A)**. Student's *t* test, *n* = 9 independent organoids from 3 different batches. **(D,E)** Quantifications of percentage of DAPI$^+$ cells that are positive for γH2AX **(D)** or CC3 **(E)** in VZ or outer layers (SVZ/CP). Two-way ANOVA followed by a Tukey *post hoc* test; *n* = 9. *$p < 0.05$; **$p < 0.01$; n.s., not significant.

replication stress in the proliferative region. However, by 7 and 14 dpi, no significant differences in the prevalence of γH2AX$^+$ cells were detected in either VZ or SVZ/CP between control and hypoxia conditions (**Figure 2D**). Similarly, transient hypoxia induced an increase in apoptotic rates in both VZ and SVZ/CP at 1 dpi, but no significant differences at 7 and 14 dpi (**Figure 2E**). It is worth noting that throughout maturation of cerebral organoids in both control and hypoxia conditions, CC3$^+$ cells were localized predominantly in SVZ/CP relative to VZ ($\sim$25% vs. $\sim$7%, respectively, $p < 0.001$) despite higher replication stress in cells in VZ (**Figures 2D,E**). These results indicated that neural precursors in the VZ might be endowed with better intrinsic capability to cope with DNA damage or hypoxic metabolic stress than their differentiating progenies in SVZ/CP.

Outer Radial Glia and Neuroblasts Display Higher Sensitivity to HI

We next investigated if specific neural cell types might be particularly vulnerable to transient hypoxia. To this end, we compared abundance of different neural populations in control vs. hypoxia conditions at 1, 7, or 14 dpi. Immediately after HI, we found no significant difference in the prevalence of SOX2$^+$ cells, but at 7 dpi, there was a small ($\sim$3%) decrease of the percent of SOX2$^+$ cells after HI relative to control ($p < 0.01$), and by 14 dpi, the number became comparable between conditions (**Figures 3A,B**). Since a majority of SOX2$^+$ cells resided in VZ, but a small proportion were localized in outer layers, representing oRGs (Pollen et al., 2015; Thomsen et al., 2015), we further quantified the number of SOX2$^+$ cells only in VZ, which showed no significant differences between control and HI conditions at all time points. These data revealed stability of the progenitor pool in VZ throughout recovery period after HI, but also suggested that SOX2$^+$ oRG population in oSVZ might be particularly vulnerable to HI.

Indeed, we observed a reduction of the prevalence of FAM107$^+$ cells in cerebral organoids at 7 dpi (45% in control vs. 37% after HI, $p < 0.05$) and at 14 dpi (34% in control vs. 22% after HI, $p < 0.001$), but no immediate drop at 1 dpi (**Figures 3A,C**). Similarly, DCX staining intensity displayed a significant drop at 7 and 14 dpi relative to controls, but not at 1 dpi (**Figures 3A,D**). Likewise, we observed a significant reduction of the percent of TBR2$^+$ IPs in the cortical columns at 14 dpi (25% in control vs. 18% after HI, $p = 0.02$), but no significant differences at 1 and 7 dpi (**Figures 3A,E**).

In comparison, the prevalence of CTIP2$^+$ neurons showed no significant change between conditions at 7 and 14 dpi, but surprisingly an increase at 1 day post HI (**Figures 3A,F**). We suspected that this might stem from a demise of other cell types at 1 dpi when massive cell death occurred in outer layers ($\sim$40% in SVZ/CP, **Figure 2C**). Indeed, when we quantified the absolute number of CTIP2$^+$ cells in radial cortical columns, the difference between HI and control conditions was not statistically significant (**Figure 3F**). Taken together, different neural populations display different sensitivity and resilience to HI, with FAM107A$^+$ oRGs, DCX$^+$ neuroblasts/immature neurons and TBR2$^+$ IPs being more vulnerable even after an

extended recovery period. By comparison, SOX2$^+$ NSCs in VZ and CTIP2$^+$ deep-layer subcortical projection neurons showed relative resilience to HI.

Transient Hypoxia Induces a Shift of Cleavage Plane of Neural Precursors in VZ

To evaluate the effect of HI on cell proliferation, we first assessed the percentage of cells expressing the proliferation marker Ki67, which showed a significant reduction in cortical columns immediately after HI, but also at 7 or 14 dpi as compared to controls (**Figures 4A,B**). We next quantified the percentage of cells expressing the G2/M phase marker phospho-histone H3 (PH3), and found that the vast majority of PH3$^+$ cells resided at apical surface of VZ in both control and HI conditions, indicating that transient hypoxia did not disturb the interkinetic nuclear migration, i.e., cell bodies of radial glia migrate up from the apical VZ surface during G1 phase, and return back after S phase to undergo mitotic division near the VZ surface. HI, however, caused a significant reduction of PH3$^+$ cells at apical surfaces at 1 dpi, but not at 7 or 14 dpi (**Figure 4C**). Put together, the reduced fractions of Ki67$^+$ cells in radial cortical columns, but similar proportions of dividing cells in G2/M phase at apical surfaces of VZ suggest that RG in the VZ niche might have recovered faster from HI-induced proliferation slowdown than other progenitor subtypes in outer layers.

Neural stem cells can expand through symmetric divisions with vertically oriented cleavage planes relative to the apical ventricular surface or undergo neurogenesis through asymmetric divisions with horizontally oriented cleavage planes (Chenn and McConnell, 1995; Mione et al., 1997). To assess whether HI affects cell division mode, we performed IF for the mitotic marker phospho-Vimentin, and measured the cleavage plane angles relative to the apical ventricular surface at different timepoints after HI (**Figures 4D,F**). Quantification showed an increased incidence of vertical cleavage angles at 1, 7, and 14 days after HI (**Figure 4E**). In general, horizontal cleavage angles were more prevalent in control organoids, whereas after HI, vertical cleavage angles became more frequent (**Figures 4E,F**). This change of division mode provides a compensatory mechanism to replenish NSC reserve, but at the expense of neurogenesis, which may further diminish oRG and neuroblast populations.

Isochronic Cohort Analyses Reveal Sensitive Windows and Vulnerability of Differentiating Population in SVZ/CP to HI

To further analyze sensitivity of progenitor populations in different stages of differentiation to HI in the developing cortex, we tracked survival and migration of isochronic progenitor cohorts that were birth-dated at different time points relative to transient HI by timed BrdU or EdU pulse-chase studies. Specifically, cerebral organoids were pulsed with BrdU or EdU for 30 min to label proliferative cells in S phase at D21, 28, 29 or 35. After defined chase periods, the number and spatial location
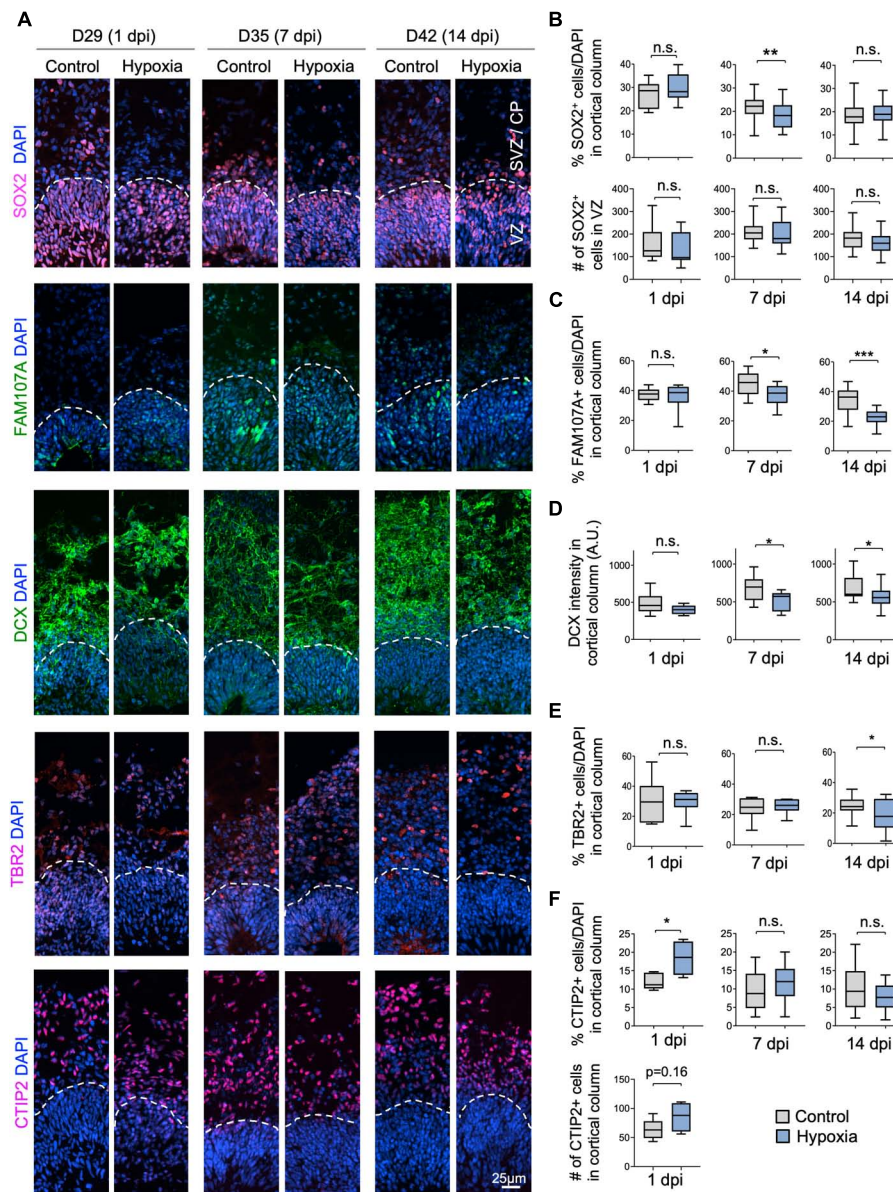
FIGURE 3 | Cellular distinction of different neural populations in response to HI. **(A)** IF images of representative 100 × 300 μm cortical columns labeled for the indicated markers at the indicated time points after hypoxia or control. White dashed lines demarcate VZ and outer layers (SVZ/CP). **(B)** Top graphs: quantifications of the percentage of DAPI$^+$ cells across all cortical layers in radial columns that are positive for SOX2 at the indicated time points after hypoxia or control. Bottom graphs: quantifications of the number of SOX2$^+$ cells in VZ-like layer at the indicated time points. Student's t test, $n = 9$ organoids from three different batches. **(C)** Quantifications of the percentage of DAPI$^+$ cells in cortical columns that are positive for FAM107A. Student's t test, $n = 9$. **(D)** Quantifications of immunostaining intensity for DCX normalized to unit area (expressed as A.U.). Student's t test, $n = 9$. **(E)** Quantifications of the percentage of DAPI$^+$ cells across all cortical layers in radial columns that are positive for TBR2 at the indicated time points after hypoxia or control. **(F)** Top: quantifications of percentage of DAPI$^+$ cells positive for CTIP2 in radial columns. Bottom: quantifications of the number of CTIP2$^+$ cell in radial columns at 1 dpi. Student's t test, $n = 9$. A.U., arbitrary unit. *$p < 0.05$; **$p < 0.01$; ***$p < 0.001$; n.s., not-statistically significant.

of label-retaining cells (LRCs) were analyzed, informing us on the survival, migration and differentiation of a particular isochronic cohort of neural precursors and their offspring (**Figure 5A** and **Supplementary Figure S4A**). It is noteworthy that the abundance of LRCs not only reflects survival but also proliferative history, as fast-dividing cells would dilute EdU or BrdU labels by cell division, leading to reduced number of LRCs.

For cohort 1 cells, birth-dated at D21 by EdU, by the time of HI at D28, a majority of these cells would have already migrated out of VZ and settled in outer layers as committed neuroprogenitors or immature neurons (**Figures 5A,B**). Indeed, as expected, we found few EdU$^+$ cells in VZ by D29 or D42, with no significant differences between control and HI conditions (**Figure 5B**). In contrast, transient HI resulted in a significantly drop in
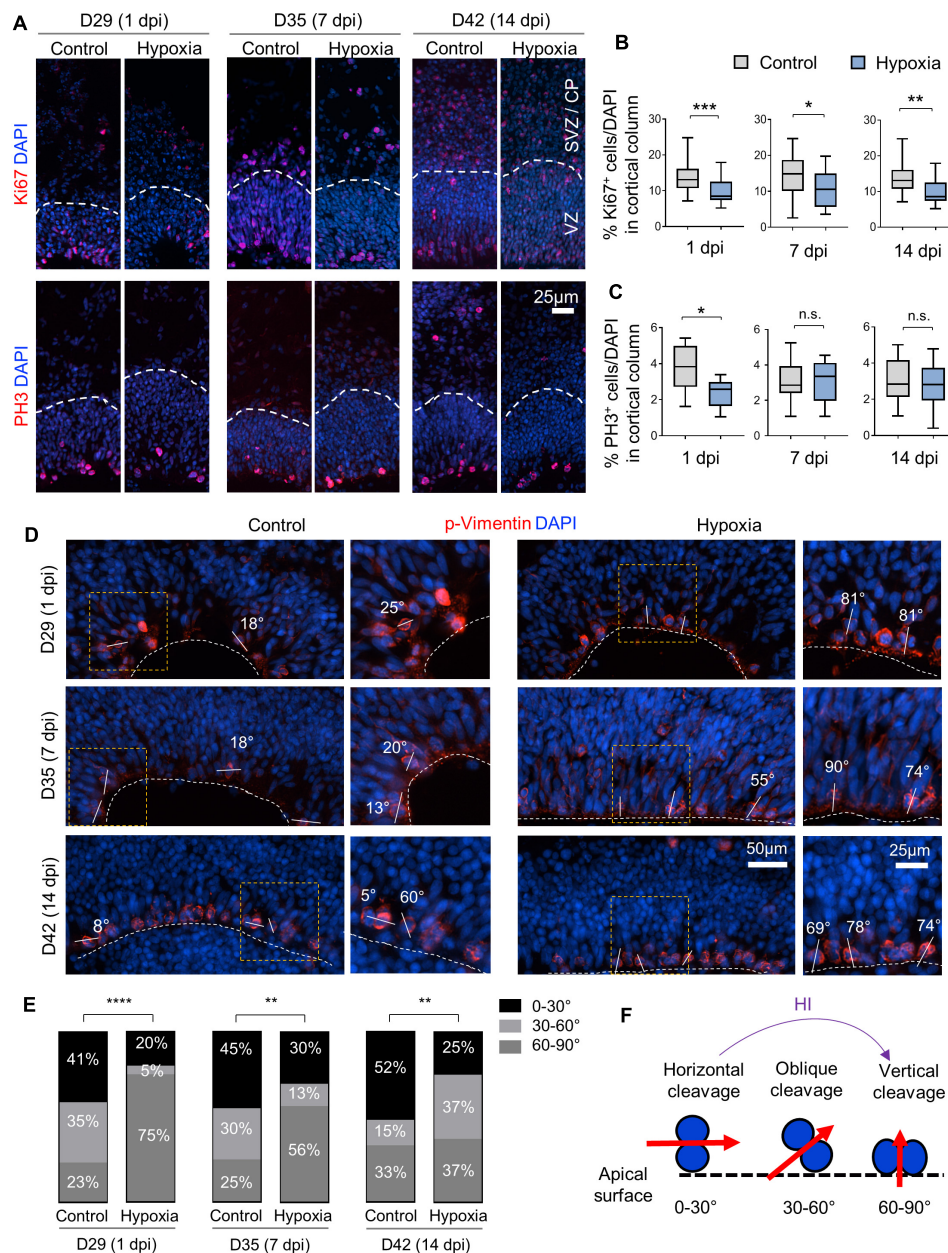
FIGURE 4 | Hypoxic injury reduces proliferation and induces a shift of cell division mode in cerebral organoids. **(A)** IF images for Ki67 and G2/M mitotic marker PH3. White dashed lines delineate VZ and SVZ/CP-like layers in 100 × 300 μm cortical columns. **(B,C)** Quantifications of Ki67+ cells **(B)** and PH3+ cells **(C)** in cortical columns. Student's t test, n = 9 organoids. **(D)** IF images of phospho-Vimentin at apical ventricular surface. Dashed white lines mark the apical surface of ventricle structures. Solid white lines and number labels indicate cleavage plane angle of dividing cells relative to apical surface. High magnification images of boxed area are shown in right panels. **(E)** Quantifications of the prevalence of dividing cells with vertical (defined as 60–90° relative to apical surface), oblique (30–60°), and horizontal (0–30°) cleavage plane at apical ventricular surface of cerebral organoids at indicated time points in control or after HI. Chi-square test, n = 20–25 cells quantified per condition. **(F)** Schematic model of a shift of cleavage plane from horizontal to vertical in proliferating cells at apical ventricular surface induced by transient HI. *$p < 0.05$; **$p < 0.01$; ***$p < 0.001$; ****$p < 0.0001$; n.s., not-statistically significant.

EdU+ LRCs in SVZ/CP at both D29 and D42 as compared to controls (**Figure 5B**). These data indicated a higher vulnerability of the differentiating populations in the SVZ/CP to HI, echoing the finding that FAM107A+ oRGs, TBR2 + IPs, and DCX+ neuroblasts/immature neurons appeared more sensitive to HI than SOX2+ NSCs in VZ.

Cohort 2 cells were labeled by BrdU at D28, thus representing actively cycling cells in S phase at the time of HI (**Supplementary Figure S4A**). Our initial assumption was that HI-induced DNA damage may aggravate the replication stress in actively cycling cells, rendering them more vulnerable to apoptosis or delay in neural maturation. Surprisingly, we found no significant
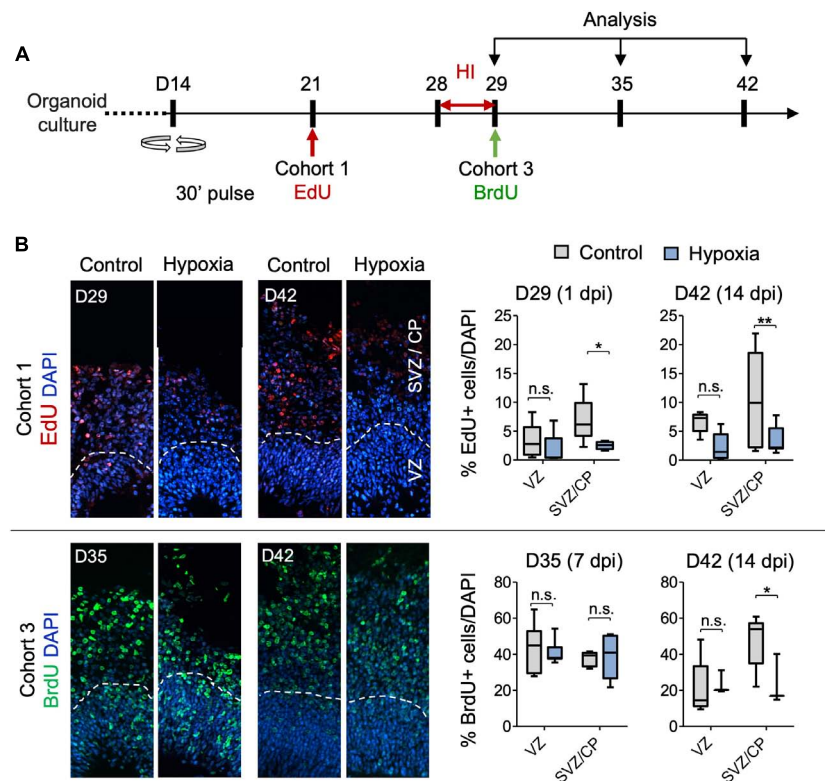
FIGURE 5 | Analysis of isochronic progenitor cohorts reveals vulnerable window and developmental stages affected by HI. **(A)** Timeline of experimental paradigm to analyze different isochronic cohorts (cohort 1 and 3) of neural precursors and their progeny that are birth-dated at different time points relative to transient HI using 30 min EdU or BrdU pulses followed by chase periods until analysis. **(B)** Left: Representative fluorescence images show abundance and spatial distribution of BrdU or EdU LRCs of isochronic cohort 1 or 3 at indicated time points during organoid development in control or after HI. White dashed lines demarcate VZ and SVZ/CP-like layers in $100 \times 300\ \mu m$ radial cortical columns. Right: Quantifications of BrdU$^+$ or EdU$^+$ LRCs in VZ or SVZ/CP layers. Two-way ANOVA followed by a Tukey *post hoc* test; $n = 9$ independent organoids from three different batches. *$p < 0.05$; **$p < 0.01$; n.s., not-statistically significant.

differences in the relative number or spatial location for cohort 2 LRCs between hypoxia and control conditions at either D29 or D42. As expected, at D29, a majority of cohort 2 cells were localized in the VZ, and by D42, they had mostly migrated out of VZ and settled in SVZ/CP. We observed no ectopic locations of LRCs from this cohort (**Supplementary Figure S4B**).

Cohort 3 cells, birth-dated at D29, entered S phase immediately after HI. After 1 week of recovery from HI at D35, we detected no drop in LRCs in either VZ or SVZ/CP layers relative to controls (**Figure 5B**). However by D42, even though most LRCs for this cohort had successfully migrated to outer layers in both conditions with no ectopia, there was a significant drop of LRCs in SVZ/CP in HI group relative to the control cohort during the second week of recovery (**Figure 5B**). Judged from the developmental timeline, this indicated that the differentiating population in SVZ/CP appeared more sensitive to HI, again echoing our finding of higher vulnerability of the differentiating populations (FAM107$^+$, TBR2$^+$, and DCX$^+$) to HI. Of note, the reduced number of LRCs for cohort 3 in SVZ/CP may also stem from a shift of cell division mode from neurogenesis to self-renewal.

Cohort 4 cells were birth-dated at D35, after 1 week of recovery from HI (**Supplementary Figure S4A**). When

analyzed immediately after EdU-pulse, we found that in both conditions, proliferating cells were largely detected in the VZ, but slightly away from the apical ventricular surface, consistent with interkinetic nuclear migration of RG cells, while a smaller fraction was detected in outer layers (**Supplementary Figure S4B**). By D42, LRCs for cohort 4 had mostly migrated out of VZ and settled in outer layers in both conditions, with no significant differences in survival or migration patterns (**Supplementary Figure S4B**).

To further characterize the differentiation stage during which cohort 1 and cohort 3 cells suffered from HI, we co-labeled LRCs for DCX and apoptotic marker CC3 at D42 (**Figure 6A**). In regard to cohort 1, we identified in control organoids many EdU$^+$ cells in SVZ/CP that were positive for DCX, but few were positive for CC3 label; whereas in HI organoids, we found fewer EdU$^+$ LRCs, but they frequently co-labeled for both CC3 and DCX (**Figure 6B**). For cohort 3, we observed that in control organoids at D42, BrdU$^+$ LRCs were largely localized in SVZ/CP, with frequent overlap with DCX, but rarely with CC3. In HI organoids, as expected, fewer BrdU$^+$ cells were detected in SVZ/CP, but we found many examples of apoptotic cells exhibiting fragments of BrdU and DCX labels (**Figure 6C**). Of note, by D42, apoptotic cells induced by HI would have largely been cleared, thus our
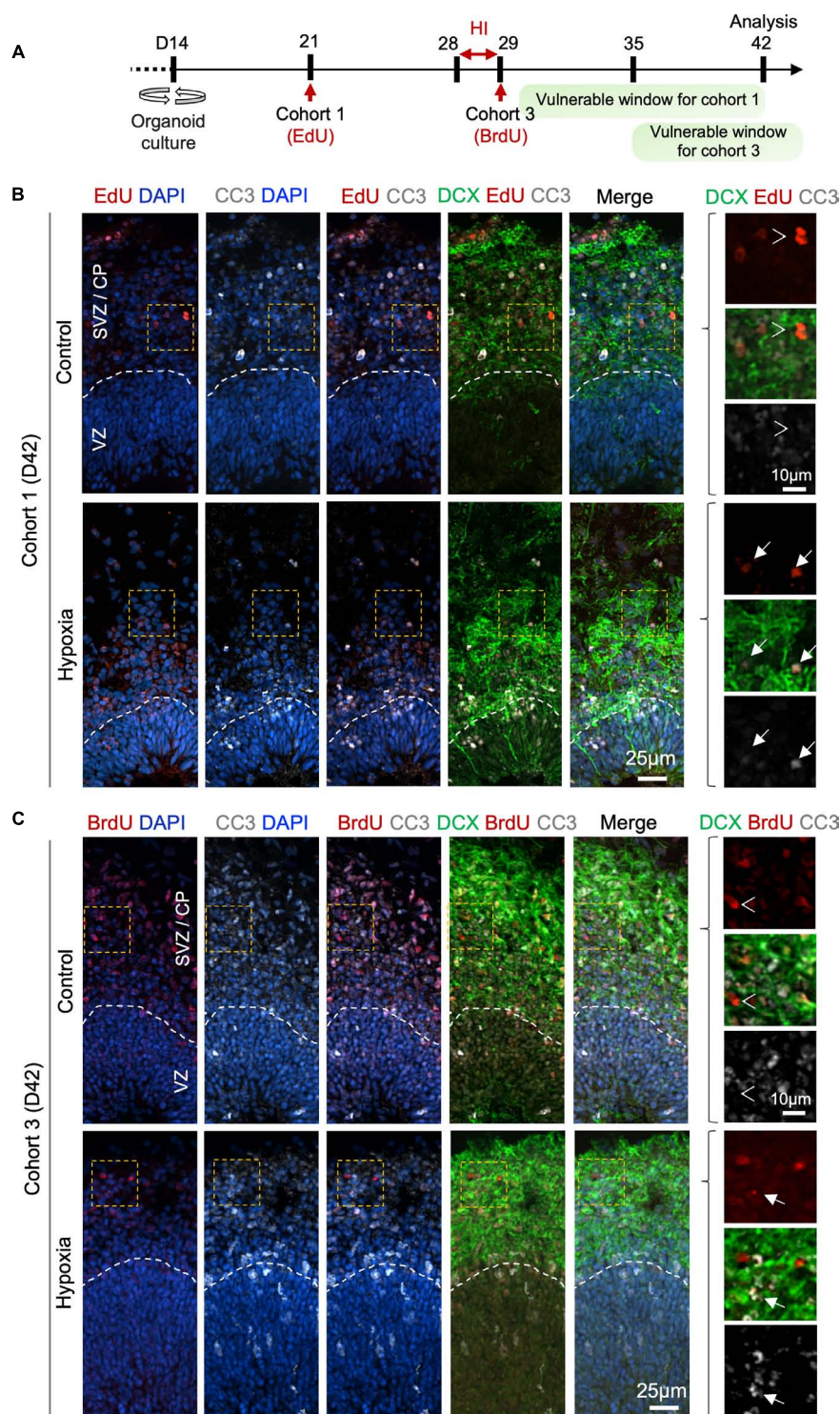
FIGURE 6 | Prolonged effect of transient HI on survival of differentiating population in SVZ. **(A)** Timeline of experimental paradigm to analyze isochronic cohort 1 and 3, birth-dated at D21 or D29 by 30 min EdU or BrdU pulse, respectively, and analyzed at D42 (14 dpi). The vulnerable windows for each cohort are depicted as green bars. **(B,C)** Representative IF images for CC3 and DCX in D42 cerebral organoids. Dashed white lines demarcate VZ and SVZ/CP layers. **(B)** For cohort 1 cells birth-dated at D21 (1 week before HI) and analyzed at D42 (14 dpi), colocalization of EdU, CC3, and DCX staining was observed in HI condition (white arrows), but rarely in control (white arrowheads point to no overlap). **(C)** For cohort 3 cells birth-dated at D29 and analyzed at D42 (14 dpi), no colocalization of BrdU, CC3 and DCX staining was observed in control (white arrowheads), but after HI, apoptotic LRCs with remnant of colocalized DCX and BrdU immunosignals were observed (white arrows). Enlarged images of area outlined by dashed orange box are shown on the right.

analysis might have underestimated the extent of overlap of LRCs with CC3. Also notable is the presence of apoptotic cells even in control organoids, congruent with earlier studies (Qian et al., 2016), but the type of cells undergoing apoptosis awaits further characterization in future.

DISCUSSION

Here, we implemented a transient HI model to study distinct cellular behaviors and coping mechanisms of human neuroprogenitor subtypes in response to hypoxia in human cerebral organoids corresponding to early mid-gestation human brain development. We identified high vulnerability of oRG progenitors but relative resilience of NSCs in VZ niche. We also found a compensatory mechanism to replenish the stem cell reserve after HI through a shift of cell division mode. Furthermore, we defined a critical peri-hypoxia window during which the differentiating neural populations are particularly affected by HI (**Figure 6A**).

Insights into the pathogenesis of prenatal hypoxia have so far been gathered mostly from animal models or limited analyses of postmortem fetal brains. Conventional *in vitro* cultures lack the complexity of 3D cytoarchitecture, thus unsuitable to address cellular distinction of different progenitor subtypes in response to HI. Cerebral organoids provide an alternative platform to study human brain development and model CNS disorders such as microcephaly (Lancaster et al., 2013; Li et al., 2017), autism spectrum disorders (Forsberg et al., 2018) or Zika virus infection (Qian et al., 2016; Watanabe et al., 2017), among others. In our recent study, we demonstrated engraftment and vascularization of human cerebral organoids upon transplantation into mouse host brains, which facilitates the study of human neurodevelopment in the context of vascularization *in vivo* (Daviaud et al., 2018).

Here, we implemented a transient HI model in cerebral organoids with predominantly dorsal forebrain regional specification, which represent a good approximation of early stages of cerebral cortex development *in vivo* (Kadoshima et al., 2013; Lancaster et al., 2013; Lancaster and Knoblich, 2014; Bershteyn et al., 2017). Human cerebral organoids follow a similar developmental progression as human brains from GW10–18 (Camp et al., 2015; Luo et al., 2016). Based on the localization of FAM107A$^+$ oRGs in cortical layers (Pollen et al., 2015), we estimated that our D42 cerebral organoids corresponded to early midgestation human fetal cortex. To ensure reproducibility, we focused our analyses on cortex-like structures close to the surface of organoids.

We found decreased neuroprogenitor proliferation at 1, 7, and 14 dpi, indicating that cell division is an energy demanding process that cannot be met by anaerobic glycolysis alone (De Filippis and Delia, 2011). Different neural cell types at different stages of differentiation fared differently after transient HI. We found a particular vulnerability of oRGs to HI, which highlights the advantage of our species-specific cellular model systems. In comparison, SOX2$^+$ neural stem cell reserve in the germinal zone remained stable in size, perhaps reflecting intrinsic

resilience to HI, better niche protection, and a compensatory mechanism from a shift of the cleavage plane angles favoring self-expansion. However, the change of division mode would further compromise the oRG and neuroblast populations. In the developing human cortex, the oSVZ is greatly expanded (Smart et al., 2002), and oRG progenitors in the oSVZ contribute to upper-layer neurogenesis as a main driver of the evolutionary expansion of human cortical size (Lukaszewicz et al., 2005; Lewitus et al., 2013). A single oRG progenitor can produce hundreds of deep and upper cortical layer neurons (Pollen et al., 2015). Thus, the demise of oRG progenitors and neuroblasts after HI may ultimately result in reduction of cortical neurons, recapitulating clinically relevant scenarios where cortical gray matter is typically reduced in size in individuals who suffered fetal hypoxia. The current study analyzed up to 14 dpi to avoid confounding factors from increased cell death in organoids after prolonged cultures. Long-term effects of diminished FAM107$^+$, TBR2$^+$, and DCX$^+$ cells on neurogenesis and formation of cortical circuitry await future study.

Our data on change of division mode in neural precursor cells after HI are consistent with earlier studies in neurospheres isolated from P6 rat brains after perinatal hypoxia/ischemia injury, which showed that neural precursors exhibited more frequent symmetric division leading to self-expansion (Felling et al., 2006). Similarly, in adult rat, there is a shift from asymmetric to symmetric cell divisions of SVZ cells during recovery from ischemia *in vivo* (Zhang et al., 2004). The distinct vulnerability of progenitor subtypes to HI found in our organoid model is also in congruence with earlier studies in animal models: during early stage of recovery in a perinatal hypoxia model in P6 rat, Nestin$^+$ NSCs in the medial region of dorsolateral SVZ were resilient, whereas the PSA-NCAM$^+$ migrating progenitors in the lateral region of dorsolateral SVZ were vulnerable to HI (Romanko et al., 2004). In a neonatal mouse model, mild-to-moderate HI results in reduced cell numbers of NeuroD1$^+$ neuroblasts and DCX$^+$ neuroblasts/immature neurons, but SOX2$^+$ NSC or TBR2$^+$ IP populations remained stable (Kwak et al., 2015). A recent study of transient HI model in cerebral organoids also reported resilience of PAX6$^+$ radial glia in proliferative zone, but vulnerability of TBR2$^+$ IPs in SVZ (Pasca et al., 2019). However, there are important differences between that study and our current study in regard to differentiation protocol, HI paradigm, developmental stages, duration of analysis, and quantification methods, which warrant careful comparison. For instance, dual SMAD inhibitors, as well as BDNF and NT3 were used in the study of Pasca et al. (2019) but not in our study; Matrigel embedding and rotational culture condition were used in our study to enhance oxygen and nutrient exchange in organoid interior, but not in that study; and 3% O_2 for 24 h was applied in our study vs. 1% O_2 for 48 h in Pasca et al. (2019). Importantly, we analyzed not only immediate, but also long-term impact of HI, which revealed vulnerability of oRGs and DCX$^+$ cells to HI, but only at 7 and 14 dpi, which would have been missed in short term studies. Additional novelty of our study includes: (i) demonstration of massive cell death and cytoarchitectural collapse in developing organoids from continuous hypoxia as compared to transient hypoxia; (ii)

unveiling a shift of division mode for radial glia at apical surface of VZ, thereby providing mechanistic understanding of how the NSC reserve might be maintained after HI; (iii) extensive timed EdU or BrdU pulse-chase studies to track different cohorts of neuroprogenitor populations over extended periods, which provided a dynamic picture and delineated cohort 1 and 3 as particularly affected by HI, as well as gave insights into the vulnerable windows.

The distinct responses to HI in different neural cell types may stem from intrinsic differences in handling hypoxic stress or from diverse extrinsic niche environments. Intrinsically, different progenitor subtypes have diverse metabolic needs and distinct transcriptional states. Single cell transcriptomic studies revealed distinct pathways selectively expressed in oRG but not in ventricular RG (vRG) (Hansen et al., 2010). A recent study of HI in cerebral organoids also revealed distinct changes in unfolded protein response pathway occurring after hypoxia (Pasca et al., 2019). Whether molecular distinction accounts for different stress coping and DNA repair capabilities awaits future studies. Extrinsically, different progenitor subtypes reside in unique niches defined by anatomical location, availability of growth factors, cell morphology, and cell behavior (Fietz et al., 2010).

Our isochronic cohort studies revealed that cells birth-dated a week before HI (cohort 1) and immediately after HI (cohort 3) suffered larger losses, specifically in SVZ/CP, coinciding with the timeframe when they are engaged in an active process of differentiation and migration. Unexpectedly, cells that are cycling during the HI (cohort 2) survived well and progressed through normal development despite high replication stress and energy expenditure of cell division. This may reflect intrinsic resilience but also a protective niche in VZ. Indeed, NSCs greatly rely upon anaerobic respiration; they are equipped with abundant glycogen granules, serving as energy substrate during HI; and they have higher level of anti-apoptotic Bcl-2 and Bcl-X_L, endowing them with resistance to cell death stimuli (Romanko et al., 2004). Future transcriptomic profiling of these cohorts will reveal additional molecular basis for their different coping capability against HI.

Here, we focused our study on HI, which can occur due to inadequate oxygen level in maternal circulation due to cardiopulmonary problems or maternal smoking, but our model also provides a versatile platform to study the effects of other environmental insults, such as cerebral ischemia when disruption of blood flow causes deprivation of both oxygen and glucose. We verified hypoxia in our organoids by the stabilization of HIF-1α when exposed to 3% oxygen, while Pasca et al. (2019) also directly measured the partial pressure of oxygen (pO_2) in cortical spheroids using a fiber-optic oxygen microsensor. As both studies used similar gas-controlled chambers with precise calibration, similar profiles of oxygen tension might be expected.

Our experiments were performed with a single hESC line, leaving reproducibility across different stem cell lines unknown at this point. However, it has been recently reported that cerebral organoids derived from different stem cell lines show consistent reproducibility in neuronal cell types (Velasco et al., 2019). Pasca et al. (2019) described reproducible findings using three iPSC lines. Likewise, in the current study, for each experimental condition, at least 2–3 different organoids from three independent batches were used, and we observed high reproducibility.

Our model also open doors for studies in other region-specific cerebral organoids, e.g., organoids with features of hippocampal or cerebellar cytoarchitecture (Muguruma et al., 2015; Sakaguchi et al., 2015). Cerebral organoids can also be cultured for an extended time period to model later stages of corticogenesis. For instance, 2.5-month old organoids have been shown to transcriptionally map to mid-fetal prenatal brain (19–24 post-conception weeks) (Pasca et al., 2015). Hence, despite notable limitations such as lack of vascularization, absence of immune system, and relative early stage of cortical development, cerebral organoids represent an economic and reproducible experimental paradigm to model prenatal HI during human brain development and to develop therapeutic strategies.

In conclusion, our studies established a novel transient hypoxia model in human cerebral organoids that elucidates HI-associated cerebral dysgenesis and provides a starting point for exploring therapeutic options to protect and replenish the vulnerable progenitor population during the critical window.

DATA AVAILABILITY

All datasets generated for this study are included in the manuscript and/or the **Supplementary Files**.

AUTHOR CONTRIBUTIONS

ND, HZ, and RF conceived and designed the analysis. ND collected the data, performed the analysis and wrote the first draft of the manuscript. CC contributed to data analysis tools. All authors contributed to manuscript revision, read and approved the submitted version.

SUPPLEMENTARY MATERIAL

The Supplementary Material for this article can be found online at: https://www.frontiersin.org/articles/10.3389/fncel.2019.00336/full#supplementary-material

REFERENCES

Badr Zahr, L. K., and Purdy, I. (2006). Brain injury in the infant: the old, the new, and the uncertain. *J. Perinat. Neonatal Nurs.* 20, 163–175. doi: 10.1097/00005237-200604000-00011

Bershteyn, M., Nowakowski, T. J., Pollen, A. A., Di Lullo, E., Nene, A., Wynshaw-Boris, A., et al. (2017). Human iPSC-derived cerebral organoids model cellular features of lissencephaly and reveal prolonged mitosis of outer radial glia. *Cell Stem Cell* 20, 435–449.e4. doi: 10.1016/j.stem.2016.12.007

Camp, J. G., Badsha, F., Florio, M., Kanton, S., Gerber, T., Wilsch-Bräuninger, M., et al. (2015). Human cerebral organoids recapitulate gene expression programs of fetal neocortex development. *Proc. Natl. Acad. Sci. U.S.A.* 112, 15672–15677. doi: 10.1073/pnas.1520760112

Chenn, A., and McConnell, S. K. (1995). Cleavage orientation and the asymmetric inheritance of notch1 immunoreactivity in mammalian neurogenesis. *Cell* 82, 631–641. doi: 10.1016/0092-8674(95)90035-7

Daviaud, N., Friedel, R. H., and Zou, H. (2018). Vascularization and engraftment of transplanted human cerebral organoids in mouse cortex. *eNeuro* 5:ENEURO.0219-18.2018. doi: 10.1523/ENEURO.0219-18.2018

De Filippis, L., and Delia, D. (2011). Hypoxia in the regulation of neural stem cells. *Cell Mol. Life Sci.* 68, 2831–2844. doi: 10.1007/s00018-011-0723

Dehay, C., Kennedy, H., and Kosik, K. S. (2015). The outer subventricular zone and primate-specific cortical complexification. *Neuron* 85, 683–694. doi: 10.1016/j.neuron.2014.12.060

Felling, R. J., Snyder, M. J., Romanko, M. J., Rothstein, R. P., Ziegler, A. N., Yang, Z., et al. (2006). Neural stem/progenitor cells participate in the regenerative response to perinatal hypoxia/ischemia. *J. Neurosci.* 26, 4359–4369. doi: 10.1523/JNEUROSCI.1898-05.2006

Fietz, S. A., Kelava, I., Vogt, J., Wilsch-Brauninger, M., Stenzel, D., Fish, J. L., et al. (2010). OSVZ progenitors of human and ferret neocortex are epithelial-like and expand by integrin signaling. *Nat. Neurosci.* 13, 690–699. doi: 10.1038/nn.2553

Forsberg, S. L., Ilieva, M., and Maria Michel, T. (2018). Epigenetics and cerebral organoids: promising directions in autism spectrum disorders. *Transl. Psychiatry* 8:14. doi: 10.1038/s41398-017-0062-x

Glass, H. C., and Ferriero, D. M. (2007). Treatment of hypoxic-ischemic encephalopathy in newborns. *Curr. Treat Options Neurol.* 9, 414–423. doi: 10.1007/s11940-007-0043-0

Gunn, A. J., and Bennet, L. (2009). Fetal hypoxia insults and patterns of brain injury: insights from animal models. *Clin. Perinatol.* 36, 579–593. doi: 10.1016/j.clp.2009.06.007

Hansen, D. V., Lui, J. H., Parker, P. R., and Kriegstein, A. R. (2010). Neurogenic radial glia in the outer subventricular zone of human neocortex. *Nature* 464, 554–561. doi: 10.1038/nature08845

Hevner, R. F., Hodge, R. D., Daza, R. A., and Englund, C. (2006). Transcription factors in glutamatergic neurogenesis: conserved programs in neocortex, cerebellum, and adult hippocampus. *Neurosci. Res.* 55, 223–233. doi: 10.1016/j.neures.2006.03.004

Kadoshima, T., Sakaguchi, H., Nakano, T., Soen, M., Ando, S., Eiraku, M., et al. (2013). Self-organization of axial polarity, inside-out layer pattern, and species-specific progenitor dynamics in human ES cell-derived neocortex. *Proc. Natl. Acad. Sci. U.S.A.* 110, 20284–20289. doi: 10.1073/pnas.1315710110

Kwak, M., Lim, S., Kang, E., Furmanski, O., Song, H., Ryu, Y. K., et al. (2015). Effects of neonatal hypoxic-ischemic injury and hypothermic neuroprotection on neural progenitor cells in the mouse hippocampus. *Dev. Neurosci.* 37, 428–439. doi: 10.1159/000430862

Lancaster, M. A., and Knoblich, J. A. (2014). Generation of cerebral organoids from human pluripotent stem cells. *Nat. Protoc.* 9, 2329–2340. doi: 10.1038/nprot.2014.158

Lancaster, M. A., Renner, M., Martin, C. A., Wenzel, D., Bicknell, L. S., Hurles, M. E., et al. (2013). Cerebral organoids model human brain development and microcephaly. *Nature* 501, 373–379. doi: 10.1038/nature12517

Lewitus, E., Kelava, I., and Huttner, W. B. (2013). Conical expansion of the outer subventricular zone and the role of neocortical folding in evolution and development. *Front. Hum. Neurosci.* 7:424. doi: 10.3389/fnhum.2013.00424

Li, Y., Muffat, J., Omer, A., Bosch, I., Lancaster, M. A., Sur, M., et al. (2017). Induction of expansion and folding in human cerebral organoids. *Cell Stem Cell* 20, 385–396e3. doi: 10.1016/j.stem.2016.11.017

Lukaszewicz, A., Savatier, P., Cortay, V., Giroud, P., Huissoud, C., Berland, M., et al. (2005). G1 phase regulation, area-specific cell cycle control, and cytoarchitectonics in the primate cortex. *Neuron* 47, 353–364. doi: 10.1016/j.neuron.2005.06.032

Luo, C., Lancaster, M. A., Castanon, R., Nery, J. R., Knoblich, J. A., and Ecker, J. R. (2016). Cerebral organoids recapitulate epigenomic signatures of the human fetal brain. *Cell Rep.* 17, 3369–3384. doi: 10.1016/j.celrep.2016.12.001

Mallard, E. C., Williams, C. E., Gunn, A. J., Gunning, M. I., and Gluckman, P. D. (1993). Frequent episodes of brief ischemia sensitize the fetal sheep brain to neuronal loss and induce striatal injury. *Pediatr. Res.* 33, 61–65. doi: 10.1203/00006450-199301000

Maxwell, P. H., Wiesener, M. S., Chang, G. W., Clifford, S. C., Vaux, E. C., Cockman, M. E., et al. (1999). The tumour suppressor protein VHL targets hypoxia-inducible factors for oxygen-dependent proteolysis. *Nature* 399, 271–275. doi: 10.1038/20459

Mione, M. C., Cavanagh, J. F., Harris, B., and Parnavelas, J. G. (1997). Cell fate specification and symmetrical/asymmetrical divisions in the developing cerebral cortex. *J. Neurosci.* 17, 2018–2029. doi: 10.1523/jneurosci.17-06-02018.1997

Molyneaux, B. J., Arlotta, P., Hirata, T., Hibi, M., and Macklis, J. D. (2005). Fezl is required for the birth and specification of corticospinal motor neurons. *Neuron* 47, 817–831. doi: 10.1016/j.neuron.2005.08.030

Morales, P., Huaiquín, P., Bustamante, D., Fiedler, J., and Herrera-Marschitz, M. (2007). Perinatal asphyxia induces neurogenesis in hippocampus: an organotypic culture study. *Neurotox Res.* 12, 81–84. doi: 10.1007/bf03033903

Muguruma, K., Nishiyama, A., Kawakami, H., Hashimoto, K., and Sasai, Y. (2015). Self-organization of polarized cerebellar tissue in 3D culture of human pluripotent stem cells. *Cell Rep.* 10, 537–550. doi: 10.1016/j.celrep.2014.12.051

Pasca, A. M., Park, J. Y., Shin, H. W., Qi, Q., Revah, O., Krasnoff, R., et al. (2019). Human 3D cellular model of hypoxic brain injury of prematurity. *Nat. Med.* 25, 784–791. doi: 10.1038/s41591-019-0436

Pasca, A. M., Sloan, S. A., Clarke, L. E., Tian, Y., Makinson, C. D., Huber, N., et al. (2015). Functional cortical neurons and astrocytes from human pluripotent stem cells in 3D culture. *Nat. Methods* 12, 671–678. doi: 10.1038/nmeth.3415

Pollen, A. A., Nowakowski, T. J., Chen, J., Retallack, H., Sandoval-Espinosa, C., Nicholas, C. R., et al. (2015). Molecular identity of human outer radial glia during cortical development. *Cell* 163, 55–67. doi: 10.1016/j.cell.2015.09.004

Qian, X., Nguyen, H. N., Song, M. M., Hadiono, C., Ogden, S. C., Hammack, C., et al. (2016). Brain-region-specific organoids using mini-bioreactors for modeling ZIKV exposure. *Cell* 165, 1238–1254. doi: 10.1016/j.cell.2016.04.032

Romanko, M. J., Rothstein, R. P., and Levison, S. W. (2004). Neural stem cells in the subventricular zone are resilient to hypoxia/ischemia whereas progenitors are vulnerable. *J. Cereb. Blood Flow Metab.* 24, 814–825. doi: 10.1097/01.WCB.0000123906.17746.00

Sakaguchi, H., Kadoshima, T., Soen, M., Narii, N., Ishida, Y., Ohgushi, M., et al. (2015). Generation of functional hippocampal neurons from self-organizing human embryonic stem cell-derived dorsomedial telencephalic tissue. *Nat. Commun.* 6:8896. doi: 10.1038/ncomms9896

Salmaso, N., Jablonska, B., Scafidi, J., Vaccarino, F. M., and Gallo, V. (2014). Neurobiology of premature brain injury. *Nat. Neurosci.* 17, 341–346. doi: 10.1038/nn.3604

Schindelin, J., Arganda-Carreras, I., Frise, E., Kaynig, V., Longair, M., Pietzsch, T., et al. (2012). Fiji: an open-source platform for biological-image analysis. *Nat. Methods* 9, 676–682. doi: 10.1038/nmeth.2019

Schump, E. A. (2018). Neonatal encephalopathy: current management and future trends. *Crit. Care Nurs. Clin. North Am.* 30, 509–521. doi: 10.1016/j.cnc.2018.07.007

Smart, I. H., Dehay, C., Giroud, P., Berland, M., and Kennedy, H. (2002). Unique morphological features of the proliferative zones and postmitotic compartments of the neural epithelium giving rise to striate and extrastriate cortex in the monkey. *Cereb. Cortex* 12, 37–53. doi: 10.1093/cercor/12.1.37

Thomsen, E. R., Mich, J. K., Yao, Z., Hodge, R. D., Doyle, A. M., Jang, S., et al. (2015). Fixed single-cell transcriptomic characterization of human radial glial diversity. *Nat. Methods* 13, 87–93. doi: 10.1038/nmeth.3629

Velasco, S., Kedaigle, A. J., Simmons, S. K., Nash, A., Rocha, M., Quadrato, G., et al. (2019). Individual brain organoids reproducibly form cell diversity of

the human cerebral cortex. *Nature* 570, 523–527. doi: 10.1038/s41586-019-1289-x

Watanabe, M., Buth, J. E., Vishlaghi, N., de la Torre-Ubieta, L., Taxidis, J., Khakh, B. S., et al. (2017). Self-Organized cerebral organoids with human-specific features predict effective drugs to combat zika virus infection. *Cell Rep.* 21, 517–532. doi: 10.1016/j.celrep.2017.09.047

Wise-Faberowski, L., Robinson, P. N., Rich, S., and Warner, D. S. (2009). Oxygen and glucose deprivation in an organotypic hippocampal slice model of the developing rat brain: the effects on N-methyl-D-aspartate subunit composition. *Anesth. Analg.* 109, 205–210. doi: 10.1213/ane.0b013e3181a27e37

Zhang, R., Zhang, Z., Zhang, C., Zhang, L., Robin, A., Wang, Y., et al. (2004). Stroke transiently increases subventricular zone cell division from asymmetric to symmetric and increases neuronal differentiation in the adult rat. *J. Neurosci.* 24, 5810–5815. doi: 10.1523/JNEUROSCI.1109-04.2004

Genetic Modification of Brain Organoids

Jan Fischer[†], Michael Heide[*†] and Wieland B. Huttner[*]

Max Planck Institute of Molecular Cell Biology and Genetics, Dresden, Germany

Brain organoids have become increasingly used systems allowing 3D-modeling of human brain development, evolution, and disease. To be able to make full use of these modeling systems, researchers have developed a growing toolkit of genetic modification techniques. These techniques can be applied to mature brain organoids or to the preceding embryoid bodies (EBs) and founding cells. This review will describe techniques used for transient and stable genetic modification of brain organoids and discuss their current use and respective advantages and disadvantages. Transient approaches include adeno-associated virus (AAV) and electroporation-based techniques, whereas stable genetic modification approaches make use of lentivirus (including viral stamping), transposon and CRISPR/Cas9 systems. Finally, an outlook as to likely future developments and applications regarding genetic modifications of brain organoids will be presented.

Keywords: brain organoids, genetic modification, adeno-associated virus, electroporation, lentivirus, transposon, CRISPR/Cas9

INTRODUCTION

The development of brain organoids (Kadoshima et al., 2013; Lancaster et al., 2013) has opened up new ways to study brain development and evolution as well as neurodevelopmental disorders. Brain organoids are multicellular 3D structures that mimic certain aspects of the cytoarchitecture and cell-type composition of certain brain regions over a particular developmental time window (Heide et al., 2018). These structures are generated by differentiation of induced pluripotent stem cells (iPSCs) or embryonic stem cells (ESCs) into embryoid bodies followed by, or combined, with neural induction (Kadoshima et al., 2013; Lancaster et al., 2013). In principle, two different classes of brain organoid protocols can be distinguished, namely: (i) the self-patterning protocols which produce whole-brain organoids; and (ii) the pre-patterning protocols which produce brain region-specific organoids (Heide et al., 2018). However, brain organoids are far from being ideal models of the brain, and notably cortical development (for a review, see Heide et al., 2018). The main issues concern reproducibility and the modeling of later stages of brain development, as mainly early stages of brain development, are modeled correctly. Very recently, approaches have been undertaken to improve the reproducibility through the optimization of protocols (Velasco et al., 2019). Moreover, modeling of later stages has been addressed by introducing organoid slice cultures grown

at the air-liquid interface. This has resulted in increased neuronal survival and improved morphology as well as the generation of axonal tracts (Giandomenico et al., 2019). In future, brain organoid protocols are likely to result in even better 3D models of neural development, evolution and disease. An important step in this direction has been the very recent development of human brain organoids with a vascular-like system (Cakir et al., 2019).

However, even the best 3D model of brain development loses much of its usefulness if one cannot modify it. The ability to genetically modify brain organoids is essential for their utility as models of brain development (Birey et al., 2017), evolution (Mora-Bermúdez et al., 2016) and disease (Bian et al., 2018) as well as their evolving use as drug-screening platforms (Zhou et al., 2017). Genetic modification is a powerful tool that allows for the introduction of alterations ranging from small changes (e.g., point mutations) to the removal or integration of entire genes. This enables researchers to investigate individual genes as well as entire gene cassettes to elicit gene expression patterns, functions, and interactions. Moreover, drugs can be tested in a larger variety of disease states and in different genetic environments.

Rather than focusing on the discussion of the advantages, disadvantages and potential applications of the different brain organoid protocols, which have already been addressed in several excellent reviews (e.g., Kelava and Lancaster, 2016; Quadrato et al., 2016; Di Lullo and Kriegstein, 2017; Heide et al., 2018), the present review will focus on the genetic modification of brain organoids. An overview of the different types and methods of genetic modification in brain organoids will be given, and their advantages and disadvantages, as well as examples of their application, will be discussed.

TYPES OF GENETIC MODIFICATION OF BRAIN ORGANOIDS

Any method of genetic modification needs to address three key issues: (i) the nature of the genetic modification; (ii) the stage, within brain organoid development, at the time of genetic modification; and (iii) the target cells of the genetic modification.

The first issue, namely the nature of the genetic modification, concerns stable vs. transient genetic modification. In a stable modification, the genetic alteration is introduced into the genome of a cell and is thus passed on to future cell generations. In contrast, in transient genetic modifications, genetic cargo (e.g., genes, short interfering RNAs, etc.) is administered to a cell without genomic insertion and the possibility of further replication. The delivered genetic cargo is then progressively degraded and diluted with each cell division. For proliferating cells, in particular, this means that the level of the administered genetic material continuously declines.

The second issue concerns the timepoint of the genetic modification relative to the stage of brain organoid development, which can range from the starting cell line over the embryoid body (EB) stage to mature brain organoids (**Figure 1**). The choice of this timepoint depends mainly on the purpose of the experiment and the proportion of cells to be affected by the genetic modification (**Figure 2**). Stable modifications

are mostly performed at an early stage of brain organoid development, such as in the starting cell line, whereas transient modifications are typically performed at later stages, given the decline of genetic cargo levels due to cell proliferation (**Figure 1**).

Due to the large cellular heterogeneity of brain organoids, the third issue concerns the cell type(s) that is/are targeted within the organoid by the genetic modifications. Approaches can either target cells indiscriminately, regardless of their location and cell type or, contrariwise, target a subset of cells. This can be achieved either through direct visual identification of cells or alternatively by biologically restricting the genetic modification to specific cell types. Visual identification of target cells can be used for single-cell microinjections (Chow et al., 2016; Shull et al., 2019) or approaches such as viral stamping (to be discussed below; Schubert et al., 2018). Biological restriction, on the other hand, makes use of cell type-specific promotors to activate or suppress gene expression (Pasca et al., 2019; Birey et al., 2017). In the following, we will first discuss the various types of transient genetic modifications of brain organoids, and then the various types of stable genetic modifications.

TRANSIENT GENETIC MODIFICATIONS OF BRAIN ORGANOIDS

In transient genetic modifications of brain organoids, gene vectors are used that allow protein expression or the production of short interfering RNAs (siRNAs; Lancaster et al., 2013) for a limited amount of time. Transient expression vectors have therefore been almost exclusively administered into late-stage brain organoids rather than into the cells or EBs that precede them (**Figure 1**). For this type of genetic modification, one of the most important aspects to consider is the mode of plasmid delivery. The two most widely used methods in the case of brain organoids are viral delivery *via* adeno-associated viruses (AAVs) and non-viral delivery *via* electroporation.

Viral Delivery—Adeno-Associated Viruses (AAVs)

AAVs are known to generally produce transient, rather than stable, expression of genetic cargo (e.g., genes or siRNAs). This is in contrast to the frequently used lentiviruses (see below), which typically produce stable transfections. However, it is important to note that AAVs can integrate genes into the genome of targeted cells at very low rates, particularly in dividing cells and at the AAV-safe loci (AAVS1; Deyle and Russell, 2009). AAVs have been successfully used in brain organoids to achieve fluorescence specifically in neurons (Deverman et al., 2016; Bershteyn et al., 2017; Birey et al., 2017). These experiments avoided targeting proliferative cell populations and primarily focused on neuronal migration within brain organoids. However, in organoid slice cultures, proliferative cell populations have been targeted using adenoviruses, which allowed for detectable fluorescence in these cells for 2–5 days (Bershteyn et al., 2017).

In most cases, AAVs are simply added to the cell culture medium, which results in scattered mosaic expression
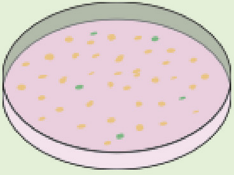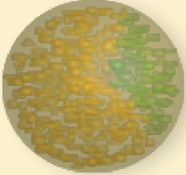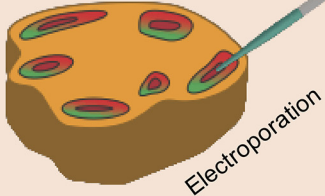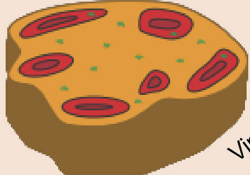
Stage	Approach	References	Stable / Transient	Degree of mosaicism following transfection
Single Cells	Cas9 nickase KO	Karzbrun et al., 2018	Stable	
	Cas9 oligonucleotide knock-in	Seo et al., 2017	Stable	
	TALEN inducible gene knock-in	Cederquist et al., 2019	Stable	
	PiggyBac fluorescence (+FACS)	Karzbrun et al., 2018	Stable	
	Lentivirus fluorescence (+selection)	Mansour et al., 2018 Daviaud et al., 2018	Stable	
Embryoid Bodies	Sleeping Beauty nucleofection	Bian et al., 2018	Stable	
	CRISPR/Cas9 KO nucleofection	Bian et al., 2018	Stable	
Organoids	AAV fluorescence	Birey et al., 2017, Bershteyn et al., 2017, Deverman et al., 2016	Transient	
	Plasmid (gene rescue)	Lancaster et al., 2013	Transient	
	Plasmid (fluorescence)	Lancaster et al., 2013, Lancaster et al., 2017	Transient	
	shRNA	Lancaster et al., 2013	Transient	
	Lentivirus fluorescence	Pasca et al., 2015, Birey et al., 2017	Stable	
	Viral stamping	Schubert et al., 2017	Stable	
	Cas9 oncogene knock-in & suppressor KO	Ogawa et al., 2018	Stable	
	Sleeping Beauty (GFP)	Giandomenico et al., 2019, Renner et al., 2017	Stable	

FIGURE 1 | Overview of the transient and stable approaches for genetic modification in brain organoids. Techniques are listed by the stage of organoid development in which they have been used. Schematic representation of mosaicism and spatial distribution of genetically modified cells (green) following respective modification approaches.

throughout the entire organoid or slice (**Figure 2F**). However, this mode of administration precludes a more focused targeting of individual regions within the brain organoid. Further drawbacks of AAVs include: (i) the need of special facility-requiring safety precautions; (ii) a greater amount of work in comparison to non-viral delivery due to the production and titration of virus particles; and (iii) a limit of 5 kilobases of cargo DNA (Grieger and Samulski, 2005).

Non-viral Delivery—Electroporation

An important alternative to genetic cargo delivery *via* AAVs is electroporation. Analogous to *in utero* electroporations of embryonic mouse (Saito and Nakatsuji, 2001; LoTurco et al., 2009) and ferret (Kawasaki et al., 2012) neocortex, in which plasmid DNA is injected into the brain ventricles prior to the electroporation, ventricle-like structures in brain organoids can be identified and injected with plasmid DNA and subsequently
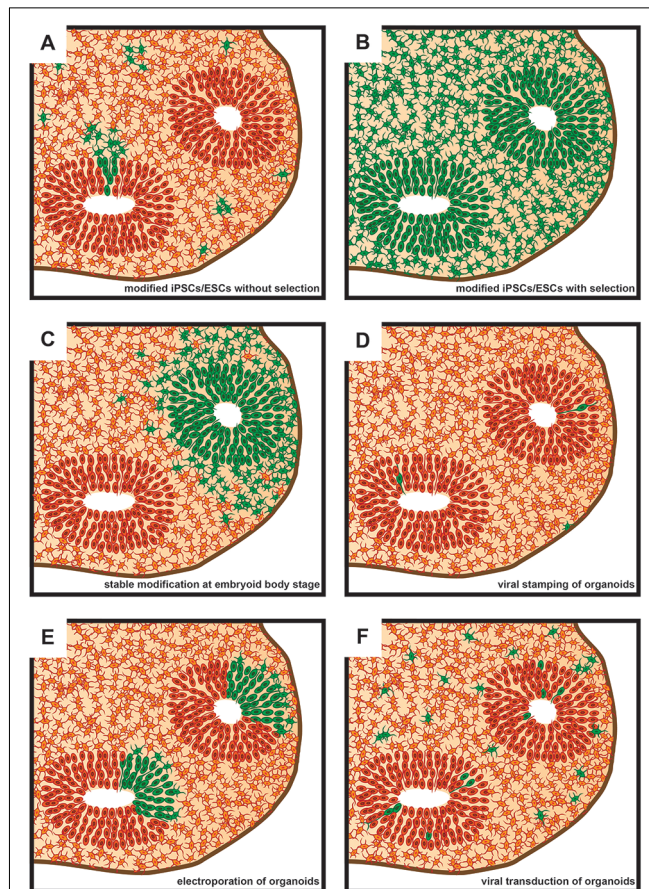
FIGURE 2 | Schematic representation of sections of brain organoids as seen subsequent to various approaches of genetic modification. Green denotes genetically modified cells. **(A)** Brain organoid derived from genetically modified induced pluripotent stem cells (iPSCs)/embryonic stem cells (ESCs) that did not undergo subsequent positive selection. **(B)** Brain organoid derived from genetically modified iPSCs/ESCs that underwent subsequent positive selection using FACS or antibiotic resistance. The vast majority of cells within the brain organoid will contain the genetic modification. **(C)** Brain organoids derived from an embryoid body (EB) that underwent regional genetic modification through the use of an electroporation-based approach. Note that a ventricle-like structure will only show genetic modification if transfection efficiency and cell survival is sufficiently high in the targeted region of the EB. **(D)** Brain organoid following genetic modifications being targeted to single cells using viral stamping. Cells both at and away from, the brain organoid surface can be targeted. **(E)** Brain organoid following the electroporation of genetic cargo into ventricle-like structures. **(F)** Brain organoid following virus-based (e.g., lentivirus or adeno-associated virus, AAV) genetic modification approaches. The proportion of genetically modified cells can vary greatly depending on incubation times of brain organoids in medium containing viral vectors.

electroporated (Lancaster et al., 2013; Li et al., 2017). Here, electrical pulses lead to pore formation in the cell's plasma membrane to allow for plasmid uptake (Kar et al., 2018). However, particularly in older brain organoids (>2 months old), targeting of ventricles by injection becomes increasingly difficult due to a reduction in tissue translucency. This can partly be overcome by confining the manipulation to the outer regions of a brain organoid where ventricles are located, which can be blindly targeted by injection. However, this approach frequently

results in increased mechanical damage of the brain organoid and decreased transfection efficiency (our own observations).

When the ventricles of brain organoids can be specifically targeted, electroporation has a much higher transfection efficiency than genetic cargo delivery *via* AAVs. Analogous to *in utero* electroporation, efficiencies of up to almost half of the cells lining the ventricular surface of the targeted region can be achieved (dal Maschio et al., 2012). Such high efficiencies allow for regionally confining the area of cell transfection within a given ventricular structure of the brain organoid (**Figure 2E**), depending on electrode placement. Thereby a comparison between transfected and untransfected areas within the same ventricular structure in the brain organoid can be made. A further benefit of electroporation over viral delivery is that cells are transfected at the same timepoint, whereas upon viral delivery transfection occurs over a temporal range. Yet, these benefits come at the risk of cellular toxicity due to the electrical pulses that are applied. However, if the voltages for electroporation are kept low (≤80 V), cell viability usually remains high (Lancaster et al., 2013). Importantly, reflecting the decline of genetic cargo levels over time prior to EB embedding, transient genetic modification using electroporation has been found to be limited to mature brain organoids (Lancaster et al., 2013; Li et al., 2017; **Figure 1**).

STABLE GENETIC MODIFICATIONS OF BRAIN ORGANOIDS

Whilst transient genetic modification of brain organoids is suitable for many experimental approaches, it is insufficient for setups in which proliferative cells require modifications for longer periods of time. Not only can stable genetic modification approaches resolve this issue, but if applied to the brain organoid founder cells they can also greatly reduce mosaic expression patterns (**Figures 2A,B**). Stable genetic modification methods also heavily rely on viral delivery or electroporation (although the use of lipofection is also conceivable) in order to introduce genetic cargo into the cells. As above, genetic cargo is any nucleic acid from an exogenous source that is delivered into the cells to bring about a change in gene expression. However, unlike transient genetic modification, stable genetic modification is typically achieved by delivering a piece of machinery into the cells that subsequently will mediate the introduction of genetic modifications (from point mutations to integration of transgenes) into the host cell's genome. A variety of tools that involve such a machinery have been developed to achieve genomic integration into the cells forming brain organoids, namely viruses with reverse transcriptase activity (lentiviruses), transposon systems, and CRISPR/Cas9.

Viral Delivery—Lentiviruses

Retrovirus-based, in particular, lentivirus-based, transduction is an efficient, fast and easy-to-use method to achieve stable genetic modification of cells. Replication-deficient lentiviral vectors are one of the most widely used tools for this purpose (Janssens et al., 2019). These commonly are human immunodeficiency viruses pseudotyped with a vesicular stomatitis virus envelope, which allows infection of most cell types (Vigna and Naldini, 2000;

Merten et al., 2016). In this system, the genetic cargo (referred to as transfer plasmid) and the viral components (structural proteins and the enzymes needed for the integration of the genetic cargo, collectively referred to as packaging plasmids) are contained on different plasmids. To generate functional viral particles, these plasmids are introduced into a packaging cell line, typical HEK293, and the thus generated viral particles are then collected from the cell culture supernatant. These viral particles contain only the genetic cargo but no genes for the packaging machinery, which implies that after infection of the target cells, the genetic cargo can be integrated into the host genome, but new viral particles cannot be produced by the infected cell (Vigna and Naldini, 2000).

Lentiviral vectors have been administered to brain organoids to induce fluorescence in target cells through the use of cell-type-specific promotors (Pasca et al., 2019; Birey et al., 2017). Due to relatively low transfection efficiencies, significant mosaicism results from the use of these vectors when they are simply added to the cell culture medium of brain organoids (**Figure 2A**). To overcome this, brain organoid founder cells can be virally targeted, with subsequent antibiotic selection or fluorescence-activated cell sorting in order to obtain a more homogeneous cell pool for brain organoid generation (Daviaud et al., 2018; Mansour et al., 2018; Janssens et al., 2019; **Figure 2B**).

Moreover, researchers will in the future not only be limited to the aforementioned approaches using lentiviral vectors, which infect without cell-type specificity, on bulk cell populations or tissue. Rather, selected single cells can be targeted using such viral vectors (Schubert et al., 2018; **Figure 2D**). This procedure makes use of a technique termed viral stamping, in which viral vectors are brought into direct physical contact with single target cells (Schubert et al., 2018). This approach is not limited to targeting cells at the surface of brain organoids, but can also target those that lie within them. In the latter case, using a so-called shielded approach, the viral particles, which are linked to magnetic nanoparticles, are only exposed to cell surfaces upon an electromagnetic pulse. Using viral stamping, individual cells within brain organoids have been successfully targeted at a depth of up to 150 μm from the organoid's surface, with an efficiency of 10%–25% of the targeted cells (Schubert et al., 2018).

Regardless of approach, however, lentiviral vectors have several notable drawbacks. Although lentiviral vectors have a greater size capacity for genetic cargo than AAVs, only 10–12 kb of genetic cargo have been efficiently transduced, thereby placing limits on more complex gene constructs (Kumar et al., 2001; Counsell et al., 2017). A further disadvantage is that random genomic insertion of genes can lead to unwanted and unpredictable effects, ranging from cell apoptosis to uncontrolled proliferation through activation of proto-oncogenes.

Non-viral Delivery

In contrast to viral delivery through lentiviruses, which introduces into the host cell both the genetic cargo and the machinery for its integration into the genome, non-viral delivery mediated by electroporation or lipofection may introduce only genetic cargo into the host cell. If so, non-viral delivery needs to include, or be combined with, introducing machinery into the host cell that mediates the integration of the genetic cargo into the genome. The two most often used such machinery are transposon-like systems and nuclease-based tools (nowadays mainly CRISPR/Cas9).

Transposon-Like Systems

Transposon-like systems used to obtain stable genetic modification are based on mobile DNA elements. These elements can move ("transpose") their position within the genome using a "cut and paste" mechanism (McClintock, 1950; Grabundzija et al., 2010). This is made possible by the presence of a transposase that is able to recognize inverted terminal repeats (ITRs) flanking the transposon, which is then excised and inserted at a different site. In current transposon-like systems, the DNA cargo of interest is tagged with flanking ITRs, and the appropriate transposase is provided in trans, leading to the integration of the DNA cargo into the target genome (Ni et al., 2008). Two of the most notable transposon-like systems that have been developed are Sleeping Beauty (Ivics et al., 1997) and PiggyBac (Ding et al., 2005; Wilson et al., 2007).

With regard to brain organoids, these transposon-like systems have been used not only to achieve GFP reporter expression (Lancaster et al., 2017; Renner et al., 2017; Karzbrun et al., 2018; Giandomenico et al., 2019), but also to introduce oncogenes (Bian et al., 2018). With generally higher genomic insertion efficiencies than retroviral vectors (Ding et al., 2005; Chen et al., 2015), transposon-like systems can be delivered, typically *via* electroporation, not only into brain organoid founder cells, often followed by selection of expressing cells, but also into EBs (Bian et al., 2018) and even mature organoids. The aim of this approach is to achieve expression in targeted cell populations and their progeny within the brain organoid (**Figure 2C**).

Despite several advantages, including the potentially large size of the transposable elements of up to 14 kb, some notable drawbacks of transposon-like systems exist (Ding et al., 2005). Thus, uncertainty as to the level of gene expression when using these systems can be a major disadvantage. Specifically, transgenes may have integrated a variable number of times into the genome of a given cell type, leading to significant differences in expression from cell to cell. Furthermore, the genomic integration of the cargo DNA can interfere with the expression of endogenous genes, leading to unwanted side effects.

CRISPR/Cas9

An alternative to achieve stable genetic modification is to make use of nuclease-based tools. A variety of nuclease-based tools have been developed to induce targeted mutations and gene insertions, ranging from Transcription Activator-Like Effector Nucleases (TALENs; Boch et al., 2009) and Zinc Finger Nucleases (ZFNs; Kim et al., 1996) to the now very popular Clustered Regularly Interspaced Short Palindromic Repeats/Cas9 (CRISPR/Cas9; Jinek et al., 2012; Cong et al., 2013; Mali et al., 2013) system. Although there is still some use of TALENs (Cederquist et al., 2019) and ZFNs in the context of stable genetic modifications of brain organoids, these nuclease-based tools have now largely been replaced by the CRISPR/Cas9 system due to its relative ease of use and high efficiency. This system uses a guide

RNA to target the nuclease Cas9 to a specific genomic locus to then cause a double-strand break, thereby activating endogenous DNA repair processes. These can be non-homologous end joining (NHEJ) or homologous-directed repair (HDR). NHEJ has a high propensity for generating small deletions or insertions during repair, thus enabling the generation of knockouts or knockdowns of targeted genes. HDR, on the other hand, is useful for introducing changes (ranging from point mutations to transgene insertions) in the presence of a DNA template to instruct the repair DNA synthesis (Doudna and Charpentier, 2014; Harrison et al., 2014; Hsu et al., 2014). It is, however, important to note that NHEJ has also been shown to play an important role in the insertion of transgenes particularly in postmitotic cells which show significantly reduced HDR (Suzuki et al., 2016; Suzuki and Belmonte, 2018). CRISPR/Cas9-mediated genetic modifications are usually conducted on brain organoid founder cells, that is, ESCs and iPSCs (Bershteyn et al., 2017; Iefremova et al., 2017; Li et al., 2017; Matsui et al., 2017; Fiddes et al., 2018; Karzbrun et al., 2018). Cells containing the desired genomic change are then selected and can be used to grow brain organoids. This approach has the advantage that all cells in the organoid will contain the previously introduced genetic modification (**Figure 2B**).

However, the use of CRISPR/Cas9-mediated genetic modifications is not limited to brain organoid founder cells. Plasmid vectors containing Cas9 along with one or more guide RNAs, or *in vitro* formed complexes of recombinant Cas9 protein and guide RNAs (Kalebic et al., 2016), can be electroporated directly into EBs or early organoids to result in loss of function mutations (Bian et al., 2018). This has been explored in organoid models of central nervous system (CNS) tumors in which tumor suppressor genes were targeted to provoke neoplasia (Bian et al., 2018). A further example is the combined use of a CRISPR/Cas9-directed tumor suppressor (TP53) knock-out combined with a CRISPR/Cas9-directed oncogene (KRAS) knock-in in 4 months-old human brain organoids (Ogawa et al., 2018). By generating cells with a glioblastoma-like proliferative potential, only a few cells needed to successfully undergo stable genetic modification.

In certain cases, especially for knock-outs of genes that exert essential functions at certain stages of brain organoid development, it would be beneficial to have temporal control of CRISPR/Cas9 activity. To this end, one may consider using CRISPR/Cas9 as an inducible system. For example, Tet- or Lac-based systems could be combined with Cas9 and guide RNA (Sun et al., 2019). Once this system is introduced into the ESC or iPSC genome, it would allow for a time-specific knockout of the gene of interest. Transcription of Cas9 would be induced by the addition of doxycycline (Tet) or isopropyl ß-D-1-thiogalactopyranoside (Lac) to the culture medium.

Of note, Cas9 activity in cells over long periods of time increases the risk of off-target effects, thereby having unforeseen effects on cell survival and phenotype. To reduce such effects, paired Cas9 nickases can be used (Ran et al., 2013). Cas9 nickases can only produce single-strand cuts rather than the double-strand cuts of wild-type Cas9. This means that two nickases need to target sequences in very close proximity to one another to result in a successful genetic modification event. This significantly increases target specificity, albeit at the cost of genetic modification efficiency.

One prime application of the CRISPR/Cas9 system in brain organoids is its use in modeling neurodevelopmental and neurodegenerative diseases. Here, either patient mutations can be introduced into control iPS cell lines, or patient iPS cells can be "repaired" to generate isogenic controls (Iefremova et al., 2017; Matsui et al., 2017; Fiddes et al., 2018). This was for example successfully applied in the modeling of retinoblastoma (Matsui et al., 2017) and Miller-Dieker Syndrome (Bershteyn et al., 2017; Iefremova et al., 2017).

OUTLOOK AND FUTURE APPLICATIONS

In summary, different modes and methods of genetic modifications have been successfully applied at various time points of brain organoid development. The spectrum of potential applications has so far ranged from the simple expression of fluorescent marker proteins (Pasca et al., 2019; Renner et al., 2017) to the study of gene function (Lancaster et al., 2013) to the modeling of disease conditions (Bershteyn et al., 2017; Iefremova et al., 2017; Matsui et al., 2017). Yet, significant untapped potential still remains.

In the case of transient genetic modification, the electroporation of mature organoids—although already successfully applied in the first report of cerebral organoids (Lancaster et al., 2013)—is not frequently employed. Many labs successfully utilize *in utero* electroporation of mice (Saito and Nakatsuji, 2001; LoTurco et al., 2009) and less frequently rat (Szczurkowska et al., 2016) and ferret (Kawasaki et al., 2013) developing neocortex to study gene function. Brain organoids could provide a potential replacement here, especially if their capacity to model 3D neural tissue is further improved. Moreover, the use of human or chimpanzee brain organoids (Mora-Bermúdez et al., 2016; Otani et al., 2016; Heide et al., 2018; Kanton et al., 2019; Pollen et al., 2019) for electroporations represents a huge opportunity as these organoids provide an environment that is comparable to the early stages of fetal human neocortex development in terms of gene expression and cell-type composition (Camp et al., 2015; Velasco et al., 2019). This could prove to be particularly beneficial for the study of human-specific genes that are expressed during cortical development either in progenitors or newborn neurons (Florio et al., 2018; Suzuki et al., 2018). Electroporation of chimpanzee brain organoids would be a relatively quick and powerful test to examine the function of these genes and would be one of the very few possible ways to study them in our closest living relative of the Hominidae family.

In the case of stable genetic modification, CRISPR/Cas9 is, and most likely will be, the method of choice to introduce such modifications in brain organoids. It is easy to use, does not require special safety precautions and is very efficient in comparison to other targeted genetic modification techniques. At present, a major application of CRISPR/Cas9 in brain organoids is the generation of disease models and is primarily focused on monogenic neurodevelopmental diseases as well as oncogenic

mutations. A major future challenge will be to study more complex disease states that are oligo- or polygenic in nature.

Nonetheless, viral and transposon systems will still play a significant role in future brain organoid studies. This is due to the versatility of these tools and their greater genetic modification efficiencies in comparison to CRISPR/Cas9, particularly in EBs and mature brain organoids. Notably, the use of viruses in combination with viral stamping may prove useful in tracing axonal connections within single brain organoids as well as organoid assembloids (Pasca, 2019; Schwarz and Remy, 2019). Furthermore, advanced techniques to control the behavior of individual neurons, such as optogenetics, should also open up new avenues for brain organoid studies (Frank et al., 2019). In this context, the demonstration of oscillating electrical waves within cortical organoids (Trujillo et al., 2019) is of major relevance.

A major focus of future applications of stable genetic modifications of brain organoids will likely be cell lineage tracing. A multitude of methods have been devised in various systems that employ CRISPR/Cas9, viral vectors or transposons in order to track the developmental origin and fate of individual cells (Figueres-Oñate et al., 2016; Kebschull and Zador, 2018; McKenna and Gagnon, 2019). These methods make use of a differential expression of fluorophore combinations or other cell barcoding techniques. As to brain organoids, these approaches of cell lineage tracing could constitute a vital experimental avenue to confirm and complement *in silico* lineage analyses derived from single-cell sequencing (Camp and Treutlein, 2017; Camp et al., 2018). A significant advance in this context would be the transcriptomic analysis of defined cell subpopulations with an identified location within brain organoids, labeled *via* lineage-specific expression of fluorescent proteins.

Finally, combinations of stable and transient genetic modifications will likely hold great promise for studying various aspects of brain organoid development and performance in the future. For example, such combination may prove advantageous for rescue experiments of a given phenotype. On a general note, combinations of stable and transient genetic modifications will allow for the modeling and dissection of increasingly complex disease states as well as developmental and evolutionary processes in brain organoids.

AUTHOR CONTRIBUTIONS

FUNDING

ACKNOWLEDGMENTS

REFERENCES

Bershteyn, M., Nowakowski, T. J., Pollen, A. A., Di Lullo, E., Nene, A., Wynshaw-Boris, A., et al. (2017). Human iPSC-derived cerebral organoids model cellular features of lissencephaly and reveal prolonged mitosis of outer radial glia. *Cell Stem Cell* 20, 435.e4–449.e4. doi: 10.1016/j.stem.2016.12.007

Bian, S., Repic, M., Guo, Z., Kavirayani, A., Burkard, T., Bagley, J. A., et al. (2018). Genetically engineered cerebral organoids model brain tumor formation. *Nat. Methods* 15, 631–639. doi: 10.1038/s41592-018-0070-7

Birey, F., Andersen, J., Makinson, C. D., Islam, S., Wei, W., Huber, N., et al. (2017). Assembly of functionally integrated human forebrain spheroids. *Nature* 545, 54–59. doi: 10.1038/nature22330

Boch, J., Scholze, H., Schornack, S., Landgraf, A., Hahn, S., Kay, S., et al. (2009). Breaking the code of DNA binding specificity of TAL-type III effectors. *Science* 326, 1509–1512. doi: 10.1126/science.1178811

Cakir, B., Xiang, Y., Tanaka, Y., Kural, M. H., Parent, M., Kang, Y. J., et al. (2019). Engineering of human brain organoids with a functional vascular-like system. *Nat. Methods* 16, 1169–1175. doi: 10.1038/s41592-019-0586-5

Camp, J. G., and Treutlein, B. (2017). Human organomics: a fresh approach to understanding human development using single-cell transcriptomics. *Development* 144, 1584–1587. doi: 10.1242/dev.150458

Camp, J. G., Badsha, F., Florio, M., Kanton, S., Gerber, T., Wilsch-Bräuninger, M., et al. (2015). Human cerebral organoids recapitulate gene expression programs of fetal neocortex development. *Proc. Natl. Acad. Sci. U S A* 112, 15672–15677. doi: 10.1073/pnas.1520760112

Camp, J. G., Wollny, D., and Treutlein, B. (2018). Single-cell genomics to guide human stem cell and tissue engineering. *Nat. Methods* 15, 661–667. doi: 10.1038/s41592-018-0113-0

Cederquist, G. Y., Asciolla, J. J., Tchieu, J., Walsh, R. M., Cornacchia, D., Resh, M. D., et al. (2019). Specification of positional identity in forebrain organoids. *Nat. Biotechnol.* 37, 436–444. doi: 10.1038/s41587-019-0085-3

Chen, X., Cui, J., Yan, Z., Zhang, H., Chen, X., Wang, N., et al. (2015). Sustained high level transgene expression in mammalian cells mediated by the optimized piggyBac transposon system. *Genes Dis.* 2, 96–105. doi: 10.1016/j.gendis.2014.12.001

Chow, Y. T., Chen, S., Wang, R., Liu, C., Kong, C. W., Li, R. A., et al. (2016). Single cell transfection through precise microinjection with quantitatively controlled injection volumes. *Sci. Rep.* 6:24127. doi: 10.1038/srep24127

Cong, L., Ran, F. A., Cox, D., Lin, S. L., Barretto, R., Habib, N., et al. (2013). Multiplex genome engineering using CRISPR/cas systems. *Science* 339, 819–823. doi: 10.1126/science.1231143

Counsell, J. R., Asgarian, Z., Meng, J., Ferrer, V., Vink, C. A., Howe, S. J., et al. (2017). Lentiviral vectors can be used for full-length dystrophin gene therapy. *Sci. Rep.* 7:79. doi: 10.1038/s41598-017-00152-5

dal Maschio, M., Ghezzi, D., Bony, G., Alabastri, A., Deidda, G., Brondi, M., et al. (2012). High-performance and site-directed *in utero* electroporation by a triple-electrode probe. *Nat. Commun.* 3:960. doi: 10.1038/ncomms1961

Daviaud, N., Friedel, R. H., and Zou, H. (2018). Vascularization and engraftment of transplanted human cerebral organoids in mouse cortex. *eNeuro* 5:ENEURO.0219-18.2018. doi: 10.1523/ENEURO.0219-18.2018

Deverman, B. E., Pravdo, P. L., Simpson, B. P., Kumar, S. R., Chan, K. Y., Banerjee, A., et al. (2016). Cre-dependent selection yields AAV variants for widespread gene transfer to the adult brain. *Nat. Biotechnol.* 34, 204–209. doi: 10.1038/nbt.3440

Deyle, D. R., and Russell, D. W. (2009). Adeno-associated virus vector integration. *Curr. Opin. Mol. Ther.* 11, 442–447.

Di Lullo, E., and Kriegstein, A. R. (2017). The use of brain organoids to investigate neural development and disease. *Nat. Rev. Neurosci.* 18, 573–584. doi: 10.1038/nrn.2017.107

Ding, S., Wu, X., Li, G., Han, M., Zhuang, Y., and Xu, T. (2005). Efficient transposition of the piggyBac (PB) transposon in mammalian cells and mice. *Cell* 122, 473–483. doi: 10.1016/j.cell.2005.07.013

Doudna, J. A., and Charpentier, E. (2014). Genome editing. The new frontier of genome engineering with CRISPR-Cas9. *Science* 346:1258096. doi: 10.1126/science.1258096

Fiddes, I. T., Lodewijk, G. A., Mooring, M., Bosworth, C. M., Ewing, A. D., Mantalas, G. L., et al. (2018). Human-specific NOTCH2NL genes affect notch signaling and cortical neurogenesis. *Cell* 173, 1356.e22–1369.e22. doi: 10.1016/j.cell.2018.03.051

Figueres-Oñate, M., García-Marqués, J., and López-Mascaraque, L. (2016). UbC-StarTrack, a clonal method to target the entire progeny of individual progenitors. *Sci. Rep.* 6:33896. doi: 10.1038/srep33896

Florio, M., Heide, M., Pinson, A., Brandl, H., Albert, M., Winkler, S., et al. (2018). Evolution and cell-type specificity of human-specific genes preferentially expressed in progenitors of fetal neocortex. *Elife* 7:e32332. doi: 10.7554/eLife.32332

Frank, J. A., Antonini, M. J., and Anikeeva, P. (2019). Next-generation interfaces for studying neural function. *Nat. Biotechnol.* 37, 1013–1023. doi: 10.1038/s41587-019-0198-8

Giandomenico, S. L., Mierau, S. B., Gibbons, G. M., Wenger, L. M. D., Masullo, L., Sit, T., et al. (2019). Cerebral organoids at the air-liquid interface generate diverse nerve tracts with functional output. *Nat. Neurosci.* 22, 669–679. doi: 10.1038/s41593-019-0350-2

Grabundzija, I., Irgang, M., Mates, L., Belay, E., Matrai, J., Gogol-Doring, A., et al. (2010). Comparative analysis of transposable element vector systems in human cells. *Mol. Ther.* 18, 1200–1209. doi: 10.1038/mt.2010.47

Grieger, J. C., and Samulski, R. J. (2005). Packaging capacity of adeno-associated virus serotypes: impact of larger genomes on infectivity and postentry steps. *J. Virol.* 79, 9933–9944. doi: 10.1128/JVI.79.15.9933-9944.2005

Harrison, M. M., Jenkins, B. V., O'Connor-Giles, K. M., and Wildonger, J. (2014). A CRISPR view of development. *Genes Dev.* 28, 1859–1872. doi: 10.1101/gad.248252.114

Heide, M., Huttner, W. B., and Mora-Bermudez, F. (2018). Brain organoids as models to study human neocortex development and evolution. *Curr. Opin. Cell Biol.* 55, 8–16. doi: 10.1016/j.ceb.2018.06.006

Hsu, P. D., Lander, E. S., and Zhang, F. (2014). Development and applications of CRISPR-Cas9 for genome engineering. *Cell* 157, 1262–1278. doi: 10.1016/j.cell.2014.05.010

Iefremova, V., Manikakis, G., Krefft, O., Jabali, A., Weynans, K., Wilkens, R., et al. (2017). An organoid-based model of cortical development identifies non-cell-autonomous defects in wnt signaling contributing to miller-dieker syndrome. *Cell Rep.* 19, 50–59. doi: 10.1016/j.celrep.2017.03.047

Ivics, Z., Hackett, P. B., Plasterk, R. H., and Izsvak, Z. (1997). Molecular reconstruction of sleeping beauty, a Tc1-like transposon from fish and its transposition in human cells. *Cell* 91, 501–510. doi: 10.1016/s0092-8674(00)80436-5

Janssens, S., Schotsaert, M., Manganaro, L., Dejosez, M., Simon, V., Garcia-Sastre, A., et al. (2019). FACS-mediated isolation of neuronal cell populations from virus-infected human embryonic stem cell-derived cerebral organoid cultures. *Curr. Protoc. Stem Cell Biol.* 48:e65. doi: 10.1002/cpsc.65

Jinek, M., Chylinski, K., Fonfara, I., Hauer, M., Doudna, J. A., and Charpentier, E. (2012). A programmable dual-RNA-guided DNA endonuclease in adaptive bacterial immunity. *Science* 337, 816–821. doi: 10.1126/science.1225829

Kadoshima, T., Sakaguchi, H., Nakano, T., Soen, M., Ando, S., Eiraku, M., et al. (2013). Self-organization of axial polarity, inside-out layer pattern and species-specific progenitor dynamics in human ES cell-derived neocortex. *Proc. Natl. Acad. Sci. U S A* 110, 20284–20289. doi: 10.1073/pnas.1315710110

Kalebic, N., Taverna, E., Tavano, S., Wong, F. K., Suchold, D., Winkler, S., et al. (2016). CRISPR/Cas9-induced disruption of gene expression in mouse embryonic brain and single neural stem cells in vivo. *EMBO Rep.* 17, 338–348. doi: 10.15252/embr.201541715

Kanton, S., Boyle, M. J., He, Z. S., Santel, M., Weigert, A., Sanchis-Calleja, F., et al. (2019). Organoid single-cell genomic atlas uncovers human-specific features of brain development. *Nature* 574, 418–422. doi: 10.1038/s41586-019-1654-9

Kar, S., Loganathan, M., Dey, K., Shinde, P., Chang, H.-Y., Nagai, M., et al. (2018). Single-cell electroporation: current trends, applications and future prospects. *J. Micromech. Microeng.* 28:123002. doi: 10.1088/1361-6439/aae5ae

Karzbrun, E., Kshirsagar, A., Cohen, S. R., Hanna, J. H., and Reiner, O. (2018). Human brain organoids on a chip reveal the physics of folding. *Nat. Phys.* 14, 515–522. doi: 10.1038/s41567-018-0046-7

Kawasaki, H., Iwai, L., and Tanno, K. (2012). Rapid and efficient genetic manipulation of gyrencephalic carnivores using in utero electroporation. *Mol. Brain* 5:24. doi: 10.1186/1756-6606-5-24

Kawasaki, H., Toda, T., and Tanno, K. (2013). *In vivo* genetic manipulation of cortical progenitors in gyrencephalic carnivores using in utero electroporation. *Biol. Open* 2, 95–100. doi: 10.1242/bio.20123160

Kebschull, J. M., and Zador, A. M. (2018). Cellular barcoding: lineage tracing, screening and beyond. *Nat. Methods* 15, 871–879. doi: 10.1038/s41592-018-0185-x

Kelava, I., and Lancaster, M. A. (2016). Stem cell models of human brain development. *Cell Stem Cell* 18, 736–748. doi: 10.1016/j.stem.2016.05.022

Kim, Y. G., Cha, J., and Chandrasegaran, S. (1996). Hybrid restriction enzymes: zinc finger fusions to Fok I cleavage domain. *Proc. Natl. Acad. Sci. U S A* 93, 1156–1160. doi: 10.1073/pnas.93.3.1156

Kumar, M., Keller, B., Makalou, N., and Sutton, R. E. (2001). Systematic determination of the packaging limit of lentiviral vectors. *Hum. Gene Ther.* 12, 1893–1905. doi: 10.1089/104303401753153947

Lancaster, M. A., Corsini, N. S., Wolfinger, S., Gustafson, E. H., Phillips, A. W., Burkard, T. R., et al. (2017). Guided self-organization and cortical plate formation in human brain organoids. *Nat. Biotechnol.* 35, 659–666. doi: 10.1038/nbt.3906

Lancaster, M. A., Renner, M., Martin, C. A., Wenzel, D., Bicknell, L. S., Hurles, M. E., et al. (2013). Cerebral organoids model human brain development and microcephaly. *Nature* 501, 373–379. doi: 10.1038/nature12517

Li, Y., Muffat, J., Omer, A., Bosch, I., Lancaster, M. A., Sur, M., et al. (2017). Induction of expansion and folding in human cerebral organoids. *Cell Stem Cell* 20, 385.e3–396.e3. doi: 10.1016/j.stem.2016.11.017

LoTurco, J., Manent, J. B., and Sidiqi, F. (2009). New and improved tools for in utero electroporation studies of developing cerebral cortex. *Cereb. Cortex* 19, i120–i125. doi: 10.1093/cercor/bhp033

Mali, P., Yang, L. H., Esvelt, K. M., Aach, J., Guell, M., DiCarlo, J. E., et al. (2013). RNA-guided human genome engineering via Cas9. *Science* 339, 823–826. doi: 10.1126/science.1232033

Mansour, A. A., Gonçalves, J. T., Bloyd, C. W., Li, H., Fernandes, S., Quang, D., et al. (2018). An in vivo model of functional and vascularized human brain organoids. *Nat. Biotechnol.* 36, 432–441. doi: 10.1038/nbt.4127

Matsui, T., Nieto-Estevez, V., Kyrychenko, S., Schneider, J. W., and Hsieh, J. (2017). Retinoblastoma protein controls growth, survival and neuronal migration in human cerebral organoids. *Development* 144, 1025–1034. doi: 10.1242/dev.143636

McClintock, B. (1950). The origin and behavior of mutable loci in maize. *Proc. Natl. Acad. Sci. U S A* 36, 344–355. doi: 10.1073/pnas.36.6.344

McKenna, A., and Gagnon, J. A. (2019). Recording development with single cell dynamic lineage tracing. *Development* 146:dev169730. doi: 10.1242/dev.169730

Merten, O. W., Hebben, M., and Bovolenta, C. (2016). Production of lentiviral vectors. *Mol. Ther. Methods Clin. Dev.* 3:16017. doi: 10.1038/mtm.2016.17

Mora-Bermúdez, F., Badsha, F., Kanton, S., Camp, J. G., Vernot, B., Kohler, K., et al. (2016). Differences and similarities between human and chimpanzee neural progenitors during cerebral cortex development. *eLife* 5:e18683. doi: 10.7554/eLife.18683

Ni, J., Clark, K. J., Fahrenkrug, S. C., and Ekker, S. C. (2008). Transposon tools hopping in vertebrates. *Brief. Funct. Genomic. Proteomic.* 7, 444–453. doi: 10.1093/bfgp/eln049

Ogawa, J., Pao, G. M., Shokhirev, M. N., and Verma, I. M. (2018). Glioblastoma model using human cerebral organoids. *Cell Rep.* 23, 1220–1229. doi: 10.1016/j.celrep.2018.03.105

Otani, T., Marchetto, M. C., Gage, F. H., Simons, B. D., and Livesey, F. J. (2016). 2D and 3D stem cell models of primate cortical development identify species-specific differences in progenitor behavior contributing to brain size. *Cell Stem Cell* 18, 467–480. doi: 10.1016/j.stem.2016.03.003

Pasca, A. M., Sloan, S. A., Clarke, L. E., Tian, Y., Makinson, C. D., Huber, N., et al. (2019). Functional cortical neurons and astrocytes from human pluripotent stem cells in 3D culture. *Nat. Methods* 12, 671–678. doi: 10.1038/nmeth.3415

Pasca, S. P. (2019). Assembling human brain organoids. *Science* 363, 126–127. doi: 10.1126/science.aau5729

Pollen, A. A., Bhaduri, A., Andrews, M. G., Nowakowski, T. J., Meyerson, O. S., Mostajo-Radji, M. A., et al. (2019). Establishing cerebral organoids as models of human-specific brain evolution. *Cell* 176, 743.e717–756.e717. doi: 10.1016/j.cell.2019.01.017

Quadrato, G., Brown, J., and Arlotta, P. (2016). The promises and challenges of human brain organoids as models of neuropsychiatric disease. *Nat. Med.* 22, 1220–1228. doi: 10.1038/nm.4214

Ran, F. A., Hsu, P. D., Lin, C. Y., Gootenberg, J. S., Konermann, S., Trevino, A. E., et al. (2013). Double nicking by RNA-guided CRISPR Cas9 for enhanced genome editing specificity. *Cell* 154, 1380–1389. doi: 10.1016/j.cell.2013.08.021

Renner, M., Lancaster, M. A., Bian, S., Choi, H., Ku, T., Peer, A., et al. (2017). Self-organized developmental patterning and differentiation in cerebral organoids. *EMBO J.* 36, 1316–1329. doi: 10.15252/embj.201694700

Saito, T., and Nakatsuji, N. (2001). Efficient gene transfer into the embryonic mouse brain using *in vivo* electroporation. *Dev. Biol.* 240, 237–246. doi: 10.1006/dbio.2001.0439

Schubert, R., Trenholm, S., Balint, K., Kosche, G., Cowan, C. S., Mohr, M. A., et al. (2018). Virus stamping for targeted single-cell infection *in vitro* and *in vivo*. *Nat. Biotechnol.* 36, 81–88. doi: 10.1038/nbt.4034

Schwarz, M. K., and Remy, S. (2019). Rabies virus-mediated connectivity tracing from single neurons. *J. Neurosci. Methods* 325:108365. doi: 10.1016/j.jneumeth.2019.108365

Shull, G., Haffner, C., Huttner, W. B., Kodandaramaiah, S. B., and Taverna, E. (2019). Robotic platform for microinjection into single cells in brain tissue. *EMBO Rep.* 20:e47880. doi: 10.15252/embr.201947880

Sun, N., Petiwala, S., Wang, R., Lu, C., Hu, M., Ghosh, S., et al. (2019). Development of drug-inducible CRISPR-Cas9 systems for large-scale functional screening. *BMC Genomics* 20:225. doi: 10.1186/s12864-019-5601-9

Suzuki, I. K., Gacquer, D., Van Heurck, R., Kumar, D., Wojno, M., Bilheu, A., et al. (2018). Human-specific NOTCH2NL genes expand cortical neurogenesis through Delta/Notch regulation. *Cell* 173, 1370.e1316–1384.e1316. doi: 10.1016/j.cell.2018.03.067

Suzuki, K., and Belmonte, J. C. I. (2018). *In vivo* genome editing *via* the HITI method as a tool for gene therapy. *J. Hum. Genet.* 63, 157–164. doi: 10.1038/s10038-017-0352-4

Suzuki, K., Tsunekawa, Y., Hernandez-Benitez, R., Wu, J., Zhu, J., Kim, E. J., et al. (2016). *In vivo* genome editing *via* CRISPR/Cas9 mediated homology-independent targeted integration. *Nature* 540, 144–149. doi: 10.1038/nature20565

Szczurkowska, J., Cwetsch, A. W., dal Maschio, M., Ghezzi, D., Ratto, G. M., and Cancedda, L. (2016). Targeted *in vivo* genetic manipulation of the mouse or rat brain by *in utero* electroporation with a triple-electrode probe. *Nat. Protoc.* 11, 399–412. doi: 10.1038/nprot.2016.014

Trujillo, C. A., Gao, R., Negraes, P. D., Gu, J., Buchanan, J., Preissl, S., et al. (2019). Complex oscillatory waves emerging from cortical organoids model early human brain network development. *Cell Stem Cell* 25, 558.e557–569.e557. doi: 10.1016/j.stem.2019.08.002

Velasco, S., Kedaigle, A. J., Simmons, S. K., Nash, A., Rocha, M., Quadrato, G., et al. (2019). Individual brain organoids reproducibly form cell diversity of the human cerebral cortex. *Nature* 570, 523–527. doi: 10.1038/s41586-019-1289-x

Vigna, E., and Naldini, L. (2000). Lentiviral vectors: excellent tools for experimental gene transfer and promising candidates for gene therapy. *J. Gene Med.* 2, 308–316. doi: 10.1002/1521-2254(200009/10)2:5<308::AID-JGM131>;3.0.CO;2-3

Wilson, M. H., Coates, C. J., and George, A. L. Jr. (2007). PiggyBac transposon-mediated gene transfer in human cells. *Mol. Ther.* 15, 139–145. doi: 10.1038/sj.mt.6300028

Zhou, T., Tan, L., Cederquist, G. Y., Fan, Y., Hartley, B. J., Mukherjee, S., et al. (2017). High-content screening in hPSC-neural progenitors identifies drug candidates that inhibit zika virus infection in fetal-like organoids and adult brain. *Cell Stem Cell* 21, 274.e275–283.e275. doi: 10.1016/j.stem.2017.06.017

Check for updates

Modeling Cell-Cell Interactions in Parkinson's Disease Using Human Stem Cell-Based Models

Katrin Simmnacher[†], Jonas Lanfer[†], Tania Rizo[†], Johanna Kaindl[†] and Beate Winner *

Department of Stem Cell Biology, Friedrich-Alexander-Universität Erlangen-Nürnberg, Erlangen, Germany

Parkinson's disease (PD) is the most frequently occurring movement disorder, with an increasing incidence due to an aging population. For many years, the post-mortem brain was regarded as the gold standard for the analysis of the human pathology of this disease. However, modern stem cell technologies, including the analysis of patient-specific neurons and glial cells, have opened up new avenues for dissecting the pathologic mechanisms of PD. Most data on morphological changes, such as cell death or changes in neurite complexity, or functional deficits were acquired in 2D and few in 3D models. This review will examine the prerequisites for human disease modeling in PD, covering the generation of midbrain neurons, 3D organoid midbrain models, the selection of controls including genetically engineered lines, and the study of cell-cell interactions. We will present major disease phenotypes in human *in vitro* models of PD, focusing on those phenotypes that have been detected in genetic and sporadic PD models. An additional point covered in this review will be the use of induced pluripotent stem cell (iPSC)-derived technologies to model cell-cell interactions in PD.

Keywords: Parkinson's disease, iPSC, neurodegeneration, organoid, dopaminergic neuron, disease modeling, inflammation, glia

INTRODUCTION PARKINSON'S DISEASE

Parkinson's disease (PD) is the second most frequently occurring neurodegenerative disorder. Clinically, PD patients suffer from motor symptoms, such as bradykinesia, rigor, and tremor, with varying degrees of severity (Postuma et al., 2015). Neuropathological hallmarks of PD include the selective loss of midbrain dopaminergic (mDA) neurons in the pars compacta of the substantia nigra (SNpc), and the presence of α-synuclein-protein (α-Syn) in intracytoplasmic and intraneuritic eosinophilic inclusions, termed Lewy bodies and Lewy neurites, respectively (Pakkenberg et al., 1991; Braak and Braak, 2000). Around 90% of PD patients are diagnosed with sporadic PD, which has a largely unknown etiology. In attempting to decipher this complex etiology, environmental toxins such as heavy metals and pesticides, as well as psychostimulants, have gained increasing attention, alongside multifactorial genetic processes (Ball et al., 2019). To date, the majority of research has focused on familial PD, despite the fact that this constitutes less than 10% of all PD cases. Pathogenic variants in genes including *SNCA*, *LRRK2*, *PINK1*, and *PRKN2*, as well as rare mutations in e.g., *DJ-1*, *ATP13A2*, *PLA2G6*, and *GBA*, have been identified as critical for this disease (Singleton et al., 2013).

The gold-standard treatment for motor symptoms in PD is the pharmacological replacement of dopamine in the brain, either by increasing dopamine concentrations or by stimulating dopamine receptors (Connolly and Lang, 2014). In most PD cases, dopaminergic (DA) therapy results in a significant amelioration of motor symptoms, though this is merely symptomatic and may lose efficiency over time (Kalia and Lang, 2015). Surgical procedures, such as deep-brain stimulation, offer additional symptomatic benefits and in particular have been reported to improve on-off periods of motor symptoms observed at later stages of the disease (Limousin et al., 1998; Castrioto et al., 2014). However, no existing therapies target the neurodegenerative process itself. Furthermore, it is becoming increasingly evident that neuronal loss in PD does not arise solely from a neuron-intrinsic degenerative mechanism, but is rather the result of a complex process involving neurons and other CNS-resident and non-resident cell types (Hirsch et al., 2013).

Due to difficulties in accessing patient brain tissue, the majority of knowledge regarding PD pathology was originally obtained from the study of postmortem brains (Baba et al., 1998; Walker et al., 1998; Hunot et al., 1999). However, the development of human stem cell-based technologies has provided new possibilities for furthering our understanding of PD pathophysiology and developing new therapeutic strategies. Replacement strategies involving the transplantation of dopamine-producing human stem cells into PD patients' striatum have been implemented and are currently evaluated by a worldwide consortium. Clinical studies are evaluating the potential of this method to improve motor symptoms while reducing or eliminating the need for DA medication (Barker et al., 2015; Studer et al., 2019). Moreover, human stem cell-based disease modeling provides a means of studying both genetic and sporadic PD and also of testing for suitable compounds that may target the neurodegenerative process in PD (Marchetto et al., 2010; Durnaoglu et al., 2011). The ongoing optimization of stem cell differentiation protocols for the generation of various cell types and multicellular structures paves the way for PD disease modeling in more complex intercellular settings (Lancaster et al., 2013; Smits et al., 2019). In this review article, we will first address the pre-requisites of stem cell-based PD research: the efficient generation of relevant models of functional mDA neurons in 2D and 3D settings. We will then provide an overview of recent stem cell-based findings in genetic and sporadic PD and describe both two- and three-dimensional approaches to the disease modeling of various cell-cell interactions.

HUMAN STEM CELL-DERIVED MODELS FOR PD MODELING

Recent advances in stem cell biology have established technologies to reprogram somatic cells to a state of pluripotency comparable to human embryonic stem cells (hESCs). The first reprogrammed cells termed induced pluripotent stem cells (iPSCs), were generated by retroviral expression of four transcription factors *Oct3/4, Sox2, Klf4,* and *c-myc (or alternatively Nanog)* from adult fibroblasts jump-starting their

continuous expression (Takahashi et al., 2007). The resulting possibility to differentiate these iPSCs further into neurons of various neurotransmitter phenotypes opens new horizons for the study of CNS diseases, where human brain tissue is otherwise difficult to approach (Tao and Zhang, 2016). Alternative resources for human disease models include ESCs derived from the blastocyst, which are also able to generate a source for brain cells.

Initial midbrain differentiation protocols mimicked embryonic development by the formation of embryoid bodies or the use of undefined co-culture systems (Kawasaki et al., 2000; Perrier et al., 2004). The Studer lab later pioneered the conversion of human pluripotent cells into a primitive neuroectoderm by inhibiting the TGFβ/activin/nodal and BMP pathways, both of which signal *via* SMAD2/3 and SMAD1/5 (Heldin et al., 1997; Bond et al., 2012). This dual SMAD inhibition method was further refined by adding sonic hedgehog (Shh) pathway agonists for anterior floor plate identity and appropriately activating the WNT signaling pathway [e.g., using the GSK3β inhibitor Chiron (CHIR99021)] resulting in a majority of TH-positive floor plate derived neurons (Chambers et al., 2009; Kriks et al., 2011).

In addition to the advances made in differentiating DA neurons, the differentiation of other CNS resident cell types from iPSCs and ESCs have made considerable progress in recent years. Protocols for the differentiation of iPSC derived astrocytes and microglia-like cells now enable disease modeling using heterotopic 2D cell-cell interaction models (Abud et al., 2017; di Domenico et al., 2019).

Given the complex etiology of PD, investigating the role of spatial tissue organization, cell-cell- and cell-matrix connections is likely to be crucial in determining new mechanisms in PD pathogenesis. The possibility to differentiate stem cells into 3D organ-like structures termed *organoids* now offers a variety of opportunities to study neurodegenerative diseases (Kadoshima et al., 2013; Lancaster et al., 2013). Specifically, the patterning of organoid differentiation toward distinct brain-region specific fates, including midbrain-like organoids containing DA neurons, is of particular relevance in terms of PD (Qian et al., 2016; Smits et al., 2019).

However, despite this astonishing progress, disease modeling using human stem cells is still accompanied by a number of caveats. Line-to-line variability is a prominent challenge in identifying even subtle disease phenotypes in stem cell-derived PD models. Consequently, genome editing techniques have become highly important for the control of genetic variation as they enable the introduction of a pathogenic mutation into a control line (Soldner et al., 2016) or the correction of a mutation in a patient line (Reinhardt et al., 2013b). The development of CRISPR technology by Doudna and Charpentier (Jinek et al., 2012) has thus greatly facilitated the generation of isogenic iPSC lines, i.e., lines that have the same genetic background, differing only in the mutation of interest.

An additional pitfall of iPSC and ESC derived model system arises from the reprogramming process itself, which has been shown to reset the epigenetic landscape of the derived cells into a more embryonic-like state (Maherali et al., 2007; Guenther et al., 2010). As aging constitutes one of the major risk factors for

neurodegenerative diseases, it is not surprising that age-specific epigenetic signatures emerge as potential additional drivers in their pathogenesis (Hwang et al., 2017). Transdifferentiation protocols, which allow the direct reprogramming of human fibroblasts into neurons without an intermediate stem cell state, has thus been pushed forward in order to preserve possible patient-associated epigenetic changes (Ladewig et al., 2012; Liu et al., 2013).

In summary, extremely productive efforts by the stem cell field in recent years have greatly expanded the toolbox available for PD disease modeling (see **Figure 1**). This toolbox has been essential in identifying pathological phenotypes in human stem cell models of familial and sporadic PD. In the next section, we will provide an overview of the major phenotypes that were recently identified.

MAJOR PHENOTYPES IN HUMAN iPSC MODELS OF PD

Neurite Defects

Human iPSC technology offers a unique opportunity to analyze specific neuronal structures, such as neurites, during maturation and development of pathological features. Studies employing these techniques have revealed abnormalities in iPSC-derived neurons to be one of the most consistent features across different neurodegenerative diseases. In PD pathology, changes in neurite morphology have been associated with mutations in *PARK2*, *LRRK2*, and *SNCA* (Ren et al., 2015; Lin et al., 2016; Kouroupi et al., 2017; Korecka et al., 2019; see **Figure 2**).

In *PARK2* iPSC derived neurons, decreased microtubule stability affects neurite complexity. It was possible to rescue neurite complexity by overexpressing parkin or by stabilizing the microtubule network using microtubule-stabilizing compounds. Long term culture of $LRRK2^{G2019S}$ mDA neurons displayed decreased neurite length, as well as a number of neurites per neuron, which is further exacerbated by the treatment with 6-OHDA and Mg132 (Sánchez-Danés et al., 2012; Lin et al., 2016). $LRRK2^{G2019S}$ mDA neurites are also especially susceptible to decreases in Ca^{2+} influx, as chronic treatment with thapsigargin resulted in neurite collapse (Korecka et al., 2019). A decreased neurite outgrowth rate in $LRRK2^{G2019S}$ patient-derived neurons was also reported by Reinhardt et al. (2013b), who were able to restore outgrowth velocities to the level of wild-type controls using targeted gene correction. This phenotype was recapitulated by introducing the G2019S mutation into the *LRRK2* loci of a control line. The impairment in neurite outgrowth was also detectable after 5 days of differentiation. At this differentiation stage $LRRK2^{G2019S}$, immature neurons display a shorter, but considerably more complex, neurite branching (Borgs et al., 2016).

Mutations in *LRRK2* also affect sensory neurons: while neurite length and complexity of sensory neurons were not affected by *LRRK2* mutations, increased neurite swellings containing cytoskeletal proteins, including tau and p-Tau, were present (Schwab and Ebert, 2015).

In addition to neurite morphology, functional parameters such as synaptic connectivity and axonal transport are impaired in PD (Kouroupi et al., 2017; Prots et al., 2018). The proportion of mobile mitochondria was reportedly increased in iPSC-derived neurons from symptomatic and presymptomatic PD patients carrying $LRRK2^{G2019S}$ and $LRRK2^{R1441C}$ mutations, respectively (Cooper et al., 2012). Although the mechanism behind these impairments remains elusive, the conformation, degree of aggregation and phosphorylation of α-Syn evidently has a role in the maintenance or formation of neurites (Qing et al., 2017; Prots et al., 2018).

It is important to note that mutations in *GBA* and *LRRK2* alter the levels of *SNCA* (Woodard et al., 2014; Oliveira et al., 2015; Lin et al., 2016). An interesting study carried out in monozygotic twins harboring a heterozygous GBA mutation showed displaced α-syn in the affected twin only, further suggesting that the quantity of α-Syn and its distribution along the neurons play a key role in neurite support (Woodard et al., 2014). The same study also indicated that not only the genetic predisposition but also additional factors contribute to the penetrance of PD. In this regard, studies on sporadic PD cases are especially valuable to shed light on which additional factors may alter disease onset and progression. Different cohorts of iPSC derived DA neurons from sporadic PD patients reported impairments in neurite complexity; an autologous PD Lymphocyte/iPSC-DA Neuron co-culture model for neuroinflammation, and prolonged differentiation of 2D DA neuronal cultures (Sánchez-Danés et al., 2012; Marrone et al., 2018; Sommer et al., 2018). These studies showed stress-related decreased neurite complexity in PD patients, suggesting that impairments in morphology and neurite outgrowth might be a general feature in PD pathology.

Aggregation

The pathological hallmarks of PD are Lewy bodies and Lewy neurites, which are principally composed of aggregated α-Syn. The importance of α-Syn is further emphasized by *SNCA* mutations that have been shown to cause familial forms of parkinsonism with early-onset and fast disease progression. *SNCA* duplications or triplications and point mutations (A53T, A30P, E46K) cause PD by increasing the gene dosage or altering the biochemical properties of α-Syn (Kang et al., 2011). iPSC-derived neurons generated from PD patients or mutations introduced by CRISPR technology were able to model α-Syn aggregation as the major pathological hallmark of the disease (see **Figure 2**). Furthermore, iPSC derived models could replicate important mechanisms of α-Syn aggregation, such as oligomerization, phosphorylation, or secretion.

α-Syn accumulation has been demonstrated in iPSC derived PD neurons of *SNCA* duplication (Prots et al., 2018), *SNCA* triplication (Byers et al., 2011; Devine et al., 2011; Flierl et al., 2014; Oliveira et al., 2015; Reyes et al., 2015; Heman-Ackah et al., 2017; Vasquez et al., 2017) and point mutations in $SNCA^{A53T}$ (Ryan et al., 2014; Kouroupi et al., 2017), $LRRK2^{G2019S}$ (Nguyen et al., 2011; Reinhardt et al., 2013b), $PARK2^{V324A}$ (Imaizumi et al., 2012; Chung et al., 2016), $PINK1^{Q456X}$ (Chung et al., 2016) and GBA^{N370S} (Woodard et al., 2014; Kim et al., 2018). A study

FIGURE 1 | The growing induced pluripotent stem cell (iPSC) toolbox for Parkinson's disease (PD) disease modeling.

FIGURE 2 | Major phenotypes observed in iPSC-derived dopaminergic (DA) neurons. The accumulation and aggregation of α-synuclein in PD models of iPSC derived neurons was shown in the following publications: Byers et al. (2011), Devine et al. (2011), Nguyen et al. (2011), Imaizumi et al. (2012), Reinhardt et al. (2013a), Ryan et al. (2013), Flierl et al. (2014), Woodard et al. (2014), Oliveira et al. (2015), Reyes et al. (2015), Chung et al. (2016), Mazzulli et al. (2016), Heman-Ackah et al. (2017), Kouroupi et al. (2017), Vasquez et al. (2017), Kim et al. (2018), Ludtmann et al. (2018), Prots et al. (2018), Hu et al. (2019), Tagliafierro et al. (2019) and Zambon et al. (2019). The phenotype of aberrant neurite morphology was described in Sánchez-Danés et al. (2012), Reinhardt et al. (2013b), Woodard et al. (2014), Schwab and Ebert (2015), Borgs et al. (2016), Lin et al. (2016), Kouroupi et al. (2017), Sommer et al. (2018) and Korecka et al. (2019). Increased cell death without additional stressors could be detected in Sánchez-Danés et al. (2012) and Bogetofte et al. (2019). Several publications detected increased cell death rate in PD models of iPSC derived neurons adding additional stressors: Byers et al. (2011), Nguyen et al. (2011), Miller et al. (2013), Reinhardt et al. (2013b), Flierl et al. (2014), Ryan et al. (2014), Shaltouki et al. (2015), Chung et al. (2016), Lin et al. (2016), Sommer et al. (2018).

introducing a PD-associated risk variant in an isogenic iPSC line using CRISPR technology was able to determine an enhancer element that regulates α-Syn expression (Soldner et al., 2016).

The accumulation of insoluble α-Syn, expected to be part of the aggregation cascade of α-Syn, was detected in a diverse set of genetic PD models such as *SNCA* duplication (Prots et al., 2018), *SNCA* triplication (Mazzulli et al., 2016; Ludtmann et al., 2018; Tagliafierro et al., 2019) and the point mutations *SNCA*[A53T] (Ryan et al., 2013; Kouroupi et al., 2017) *PARK2*[V324A] (Chung et al., 2016), *PINK1*[Q456X] (Chung et al., 2016) and *GBA*[N370S] (Kim et al., 2018). This reproduces aggregation as the shared disease process of PD and underlines iPSC-derived models as an adequate tool to investigate synucleinopathies on a cellular level. The higher aggregation propensity of α-Syn was detected by detergent-insoluble α-Syn (Chung et al., 2016; Mazzulli et al., 2016; Kim et al., 2018; Prots et al., 2018), as well as Thioflavin staining (Ryan et al., 2013; Kouroupi et al., 2017).

Together with the higher aggregation rate, changes such as phosphorylation and oligomerization were recapitulated in iPSC PD models. Increased Ser129-phosphorylation of α-Syn could be detected in iPSC models of *SNCA* triplication (Lin et al., 2016) *SNCA*[A53T] point mutation (Ryan et al., 2013; Kouroupi et al., 2017; Hu et al., 2019) and the *PARK2* mutation (Ryan et al., 2013; Lin et al., 2016; Kouroupi et al., 2017). Oligomers were previously shown to be a neurotoxic α-Syn species (Winner et al., 2011). Multiple iPSC-derived *SNCA* triplication models could show an increase in α-Syn oligomers that were connected to axonal transport impairments (Prots et al., 2018) and activation of the mitochondrial transition pore (Ludtmann et al., 2018).

The main physiological α-Syn species remains controversial. Studies detected a physiological tetrameric α-Syn species, resistant to aggregation (Bartels et al., 2011; Wang et al., 2011; Dettmer et al., 2015b). A *SNCA*[A53T] point mutation (Dettmer et al., 2015a) and *GBA*[N370S] mutations (Kim et al., 2018) were shown to disrupt this tetrameric form and increase the monomeric α-Syn level in iPSC derived neurons.

Braak stated the hypothesis of spreading α-Syn pathology with the course of the disease (Braak and Braak, 2000). One route of α-Syn spreading is thought to be the secretion of α-Syn into the extracellular space. IPSC-derived models could show increased extracellular levels of α-Syn in *GBA*[N370S] mutations (Fernandes et al., 2016) and *SNCA* triplication cases (Zambon et al., 2019). A recent study identified *LRRK2*[G2019S] astrocytes as another source of α-Syn spreading to neurons (di Domenico et al., 2019). This study stresses the flexibility of the iPSC models to answer cell-type-specific questions, as co-cultures of control astrocytes and *LRRK2*[G2019S] mutated neurons and vice versa could give indications about the effect of certain cell types on one another.

Recently, premature aging was introduced to iPSC models of *SNCA* triplication by extended passaging at the NPC state. These aged neurons showed a higher α-Syn aggregation rate compared to the young *SNCA* triplication neurons (Tagliafierro et al., 2019). The incorporation of aging adds an additional layer of complexity that can be modeled by iPSC-derived PD neurons. Thus, iPSC-derived models enable us to test hypotheses about how PD-causing mutations affect α-Syn species and the aggregation process.

Cell Death

Loss of DA neurons in the SNpc is another hallmark of PD. The current hypothesis is that both genetic and environmental factors contribute to PD-linked neuronal cell death (Ball et al., 2019). This combination makes it challenging to study the disease *in vitro* since the exposure to specific environmental factors is usually difficult to trace back. *PARK2* KO derived neurons showed a decreased survival after 14 days of differentiation compared to isogenic WT lines (Shaltouki et al., 2015) and displayed higher levels of necrosis after 25 days (Bogetofte et al., 2019). However, besides these studies, neuronal cell death is rarely reported in iPSC-derived neuronal cultures without a prior stressor challenge (see **Figure 2**). One of the best-studied mutations in PD is the *LRRK2*[G2019S]. However, in the majority of studies, no changes in cell viability were reported under basal conditions. Sánchez-Danés et al. (2012) were able to find increased cell death occurring in sporadic and familial cases of *LRRK2*- related PD *in vitro* after prolonged differentiation. This can be attributed to the increased maturity of the neuronal culture. Longer neuronal cultures can also be achieved by generating brain organoids. However, to date only two studies have modeled PD using PD-patient derived midbrain organoids (Kim et al., 2019; Smits et al., 2019) and cell death was reported in only one of these (Kim et al., 2019).

One possible explanation for the lack of cell death in iPSC-derived cultures under basal conditions may be the use of well-adjusted cell culture media and supplements, which were specially developed to support neuronal survival and counteract oxidative stress. In addition, for neuronal differentiation, this media is usually supplemented with additional neurotrophic factors, including BDNF and GDNF (Björklund et al., 1997; Zuccato and Cattaneo, 2009). Thus, this media combination may mask some of the neurodegenerative phenotypes we wish to model.

A second explanation for the lack of cell death may be the loss of age-related markers, which inevitably occurs during the process of reprogramming (Marion et al., 2009). These age-related traits that are lost are not regained even in longer *in vitro* maturation and consequently, these neurons still do not faithfully mimic the age-related traits of an e.g., 50-year-old PD patient neuron. Transdifferentiation might be an option to retain age-related epigenetic traits for future experiments (Mertens et al., 2015).

Despite these drawbacks, such neuronal cultures are especially valuable when investigating early transcriptomic and proteomic pathological changes, which may ultimately lead to activation of apoptotic pathways. Transcriptomic analysis of *SNCA* triplication in cortical neurons suggest that endoplasmatic reticulum stress followed by activation of the IRE1a/XBP arm of the unfolded protein response might be responsible for cell death in PD (Heman-Ackah et al., 2017). Microarray analysis of DA neurons derived from two patients with A53T mutation in *SNCA* was associated with S-nitrosylation of the anti-apoptotic transcription factor MEF2C contributing

to mitochondrial dysfunction (Ryan et al., 2013). Moreover, increase in oxidative stress and inflammation was associated with induction of the necroptotic pathway in OPA-1 derived NPCs (Iannielli et al., 2018). An autologous mDA-lymphocyte co-culture suggested activation of the NFkB pathway, bringing neuroinflammation into the spotlight (Sommer et al., 2018). Finally, proteomic analysis of *PARK2* KO iPSC-derived neurons and isogenic lines used as controls identified dysregulation of proteins involved in oxidative stress defense, mitochondria respiration, cell cycle control and cell viability (Bogetofte et al., 2019). Further, "omic" studies may shed some light on early-associated PD-specific dysregulated pathways.

Stressor Response

A set of publications has been able to link cell death pathways to dysregulated upstream cellular functions in PD patients' cells. These studies indicate a decrease in viability upon exposure to stressors that challenge these dysregulated functions. An example of these studies identifying and then challenging the dysregulated pathway is published by Nguyen et al. (2011). They first showed increased expression of genes involved in oxidative stress response in iPSC-derived $LRRK2^{G2019S}$ patient neurons. When adding the oxidative stressor H_2O_2, the patients' derived DA neurons revealed a higher cell death rate (Wang et al., 2011). Thus, this study demonstrated that iPSC models are a powerful tool to study the environmental component *in vitro*. As previously mentioned, both environmental and genetic factors contribute to the current hypothesis of PD pathogenesis. Oxidative stress, mitochondrial dysfunction, proteasome inhibition, and aging factors have all been identified as playing a role in PD. The following four paragraphs describe publications that have combined these factors with genetic iPSC PD models.

Mitochondrial dysfunction is a core pathomechanism of PD (Franco-Iborra et al., 2018). This is underlined by the environmental risk factor rotenone, which inhibits the complex I of the mitochondrial electron transport chain and is epidemiologically linked to PD (Tanner et al., 2011). Another mitochondrial stressor inhibiting mitochondrial complex I, MPTP, also causes PD symptoms within days of exposure (Langston, 2017). An increased susceptibility towards rotenone (Cooper et al., 2012; Ryan et al., 2013; Flierl et al., 2014; Mittal et al., 2017; Tabata et al., 2018) and MPTP (Kim et al., 2019) was also determined in neurons and organoids from iPSC-derived PD patients'. Carbonyl cyanide m-chlorophenyl hydrazine (CCCP) decreases the mitochondrial membrane potential and *PINK1* and *PARK2* iPSC-derived DA neurons were more prone to cell death after treatment with CCCP (Chung et al., 2016).

Oxidative stress is one of the major biochemical processes thought to impair the vulnerability of DA neurons in PD. Pesticides and heavy metals (Tanner et al., 2011; Farina et al., 2013), as well as PD-causing mutations (e.g., *PARK2*, *PINK1*, *SNCA*, *LRRK2*; Blesa et al., 2015), have been shown to induce oxidative stress. Several factors known to induce oxidative stress are used in iPSC PD studies, such as the pesticide paraquat, the synthetic dopamine analog 6-hydroxydopamine (6-OHDA) and

the reactive oxygen species H_2O_2. Paraquat is epidemiologically linked to PD (Tanner et al., 2011) and increased susceptibility to this pesticide could be determined in iPSC PD neurons (Ryan et al., 2013; Lin et al., 2016). 6-OHDA is a synthetic neurotoxin, taken up *via* the dopamine transporter and selectively damaging DA neurons due to ROS generation (Hernandez-Baltazar et al., 2017). An increased vulnerability of PD patients' derived neurons towards 6-OHDA has been determined (Nguyen et al., 2011; Lin et al., 2016). Adding the reactive oxygen species H_2O_2 to $LRRK2^{G2019S}$ (Nguyen et al., 2011), $LRRK2^{I2020T}$ (Ohta et al., 2015) or *SNCA* triplication neurons (Byers et al., 2011), revealed a higher vulnerability of cells carrying PD-causing mutations towards oxidative stress. There is evidence linking heavy metal exposure to the development of PD, thought to be at least partly due to the generation of oxidative stress (Ball et al., 2019). An increased susceptibility towards the heavy metals copper (Aboud et al., 2015), cadmium (Aboud et al., 2015), and manganese (Aboud et al., 2012) were determined in iPSC-derived PD patients' neurons.

The proteasome system, which plays a central role in degrading dysfunctional proteins, has been shown to be impaired in the postmortem substantia nigra (SN) of PD patients (Bentea et al., 2017). Exposure to the proteasomal inhibitor carbobenzoxyl-L-leucyl-L-leucyl-L-leucine (MG-132) determined a higher susceptibility in PD patients' cells (Nguyen et al., 2011; Lin et al., 2016).

Aging is a major risk factor for PD. Reprogramming has been shown to rejuvenate the cells by resetting aging markers, e.g., mitochondrial ROS, nuclear morphology markers and DNA damage markers (Miller et al., 2013). Aging is known to drive major pathomechanisms of PD, e.g., mitochondrial and oxidative stress (Rodriguez et al., 2015). The addition of aging factors can provide a way of determining higher susceptibility within iPSC models of genetic PD that is compensated for during the rejuvenation in the iPSC model. Studies have so far added a variety of aging factors together with different PD-causing mutations, all of which resulted in a higher susceptibility. Several strategies have been applied to induce premature aging, e.g., telomerase inhibition (Vera et al., 2016), progerin expression (Miller et al., 2013) and higher NPC passaging (Tagliafierro et al., 2019). The susceptibility towards the aging factors was not specific to a certain mutation, as shown for $PARK2^{V324A}$ (Miller et al., 2013) $PINK1^{Q456X}$ (Miller et al., 2013; Vera et al., 2016) and SNCA triplication cases (Miller et al., 2013; Vera et al., 2016; Oh, 2019).

IPSC technology and epidemiology can both provide valuable insights into Parkinson disease. The addition of environmental risk factors to iPSC-derived models generates PD models that can investigate the combinatorial effects of genes and the environment. This allows a deeper insight into the interactions and dependencies between the affected cellular processes critical to the cell to maintain homeostasis. This can help to determine the key cellular pathways challenged by multiple exposures occurring over a lifetime, recently summarized by the concept of the "neuroexposome." These combinatorial effects may be of particular significance when investigating genetic risk factors e.g., SNPs identified in genome-wide association (GWAS) studies.

While genetic risk factors increase the risk for developing PD, they are not causative and depend on the presence of other risk factors, including environmental factors. This interplay of genetic risk factors that render DA neurons more susceptible to environmental factors takes place in sporadic PD. Indeed, our lab was able to identify an increased vulnerability of iPSC-derived, sporadic PD patients' neurons towards interleukin 17. The cell death rate of sporadic PD patients' cells was equal to cells from healthy individuals in unstressed conditions, but significantly higher when exposed to IL-17 secreting T helper 17 cells (Sommer et al., 2018).

Neurodegenerative phenotypes in PD patients' neurons become more evident with the addition of cellular stressors. Yet the comparability of different studies remains problematic, as differentiation protocols, maturation time as well as stressor dosage and duration tend to vary between different studies.

MODELING CELL-CELL INTERACTIONS IN PD USING HUMAN iPSC-DERIVED MODELS

As mentioned above, mounting evidence indicates that neurodegeneration in PD is not a neuron-autonomous process, but rather the result of a complex detrimental interplay between a variety of different cell types (Hirsch et al., 2013). Recent advances in the differentiation of human iPSCs and ESCs have now expanded the toolbox available for studying PD *via* 2D co-culture models as well as 3D organoid models. In the following section, we discuss recent findings of studies using these models, highlighting specific cell-cell interactions as well as organoid models. Moreover, we also address new possibilities for future investigations of cell-cell interactions in PD.

Neuron—Astrocyte

Although the majority of existing studies on PD aimed to investigate neuronal function, there is now increasing evidence that astrocytes play an important role in PD pathogenesis. Recent transcriptomic analyses using human and rodent CNS-resident cells have shown that a variety of PD associated genes are expressed in human astrocytes to a similar, and sometimes even larger extent, compared to neurons (Zhang et al., 2016). Astrocyte-specific functions have been identified for a variety of genes known to be causative for PD, including *DJ-1, SNCA, PARK1, PARK2, PARK7, PLA2G6,* and *ATP13A2*. These functions include regulation of astrocyte neurotrophic properties and their response to inflammatory stimuli, as well as astrocytic glutamate transport and mitochondrial function (reviewed extensively in Booth et al., 2017). Most of these studies were conducted in both rodent models and in post-mortem human brain tissue. While stem-cell-derived technologies now open up many possibilities to study astrocyte function in a human system (Krencik and Zhang, 2011; Roybon et al., 2013; Santos et al., 2017; Tcw et al., 2017; Perriot et al., 2018), studies on astrocyte function in PD using iPSC- or ES-derived cellular systems remain scarce.

Using a co-culture system of iPSC-derived neural progenitor cells and astrocytes, astrocytes exerted a protective effect. Interestingly, while treatment with mitochondrial stressors

rotenone and potassium cyanide led to a significant decrease in NPC maturation into DA neurons, co-culture with iPSC-derived astrocytes rescued differentiation deficits and mitochondrial dysfunction in iPSC-derived DA neurons (Du et al., 2018). These results clearly highlight the important role of astrocytes in regulating mitochondrial homeostasis of DA neurons under stress conditions. However, it has yet to be determined how this protective effect during differentiation may be translated into a PD disease context, given the fact that neurodegeneration in PD sets in after maturation of DA neurons. Moreover, it is not clear whether PD-causing pathogenic variants may lead to a disturbance of these protective astrocyte functions during differentiation.

A recent study by di Domenico et al. (2019) made use of a neuron-astrocyte co-culture approach to study the effect of a PD-causing *LRRK2* mutation on neuron-astrocyte crosstalk (G2019S). Remarkably, the co-culture of control iPSC-derived mDA neurons with patient-derived astrocytes harboring the LRRK2 G2019S mutation exerted a neurodegenerative phenotype, while co-culture with control astrocytes did not result in this effect. The neurodegenerative phenotype was characterized by decreased cell survival and morphological alterations in mDA neurons, as well as an accumulation of α-Syn in mDA neurons and mutant astrocytes. Activation of chaperone-mediated autophagy was, at least in part, able to rescue these effects (di Domenico et al., 2019).

These results emphasize the dual role astrocytes may play during PD pathogenesis. On the one hand, the loss of astrocytic neurotrophic and neuroprotective properties might be an important driver of PD pathogenesis. On the other hand, astrocytes could gain neurotoxic abilities upon progression of the disease and may themselves release neurotoxic factors. As an inadequate response and higher vulnerability to environmental stressors are possible causes for sporadic PD, modeling sporadic PD *via* neuron-astrocyte interactions upon different stressor conditions may be of particular interest. Interestingly, recent studies showed that PD patient brain samples harbor an increased number of senescent astrocytes (Chinta et al., 2018). Whether these senescent astrocytes contribute to neurodegeneration *via* the loss of their neuroprotective function or the release of neurotoxic factors remains to be elucidated. Stem-cell derived co-culture systems may provide a valuable platform in deciphering the role of these astrocytes in PD pathogenesis. However, it may be difficult to model the late-stage effects of an aberrant astrocyte-neuron interaction in PD using iPS derived 2D co-culture approaches due to the fetal identity of iPS derived neurons and astrocytes. The addition of stressors inducing aging effects may thus be needed in the co-culture set up in order to gain insights into the contribution of astrocytes to later time points of PD pathogenesis.

Neuron—Immune Cells

Microglia represent the resident macrophage population in the central nervous system (CNS). In response to a variety of disease-associated stimuli, including microbes or even unfolded and aggregated proteins like α-Syn oligomers

and fibrils, microglia can become activated and initiate an inflammatory response in CNS (Wolf et al., 2017). Several studies have provided direct evidence for a microglia-mediated inflammatory response in neurodegenerative diseases including PD (reviewed in Song and Colonna, 2018). In post-mortem studies of PD patient brains, as well as in living patients, microglia activation has been demonstrated (Hirsch et al., 2003; McGeer and McGeer, 2008). Interestingly, epidemiological studies were able to show that the risk of PD is reduced in patients receiving long-term treatment with certain nonsteroidal anti-inflammatory medications, supporting the idea that inflammatory pathways contribute to PD progression (Bartels et al., 2010; Rees et al., 2011). Until now, the vast majority of studies on microglial function in health and disease have relied on rodent models. As recent studies indicated major transcriptomic differences between human and rodent microglia (Butovsky et al., 2014; Gosselin et al., 2017), the investigation of microglial function in a human system is urgently required to delineate the mechanisms and functional consequences of microglia activation in human neurodegenerative diseases. Protocols generating microglia-like cells (iMGLs) from iPSCs may provide a valuable resource in characterizing human microglial function. As microglia originate from hematopoietic stem cells of the yolk sac (Ginhoux et al., 2010), microglia differentiation differs extensively from differentiation procedures of neuroectoderm-derived cells such as neurons, oligodendrocytes, and astrocytes. Muffat et al. (2016) were the first to report a protocol for microglia differentiation based on the induction of cystic embryoid bodies resembling yolk-sac-like cells and subsequent maturation with colony-stimulating factor 1 and IL-34. A feeder and serum-free differentiation method, which exhibited good scalability and high purity were first described by Abud et al. (2017). They made use a two-step differentiation in which iPSCs were first differentiated into hematopoietic stem/progenitor cells (HSPCs) and afterward matured into iMGLs.

Thus far, existing literature delineating the role of microglia in neurodegenerative diseases using iMGLs remains sparse. Nevertheless, a number of studies in other neurodegenerative diseases point toward the possible impact of iMGLs. A study by Lin et al. (2016) showed morphological alterations and a reduced capacity of extracellular amyloid-beta clearance in iPSC-derived microglia-like cells carrying the ApoE4 risk variant for Alzheimer's disease compared to controls. Using iPSC cells from patients carrying a disease-causing variant of the TREM2 protein, another study was able to show that TREM2 deficient microglia show specific deficits in phagocytosis of apoptotic cells (Garcia-Reitboeck et al., 2018). Like astrocytes, microglia may play a dual role in PD pathophysiology by exerting both a protective and detrimental effect dependent on the disease-state.
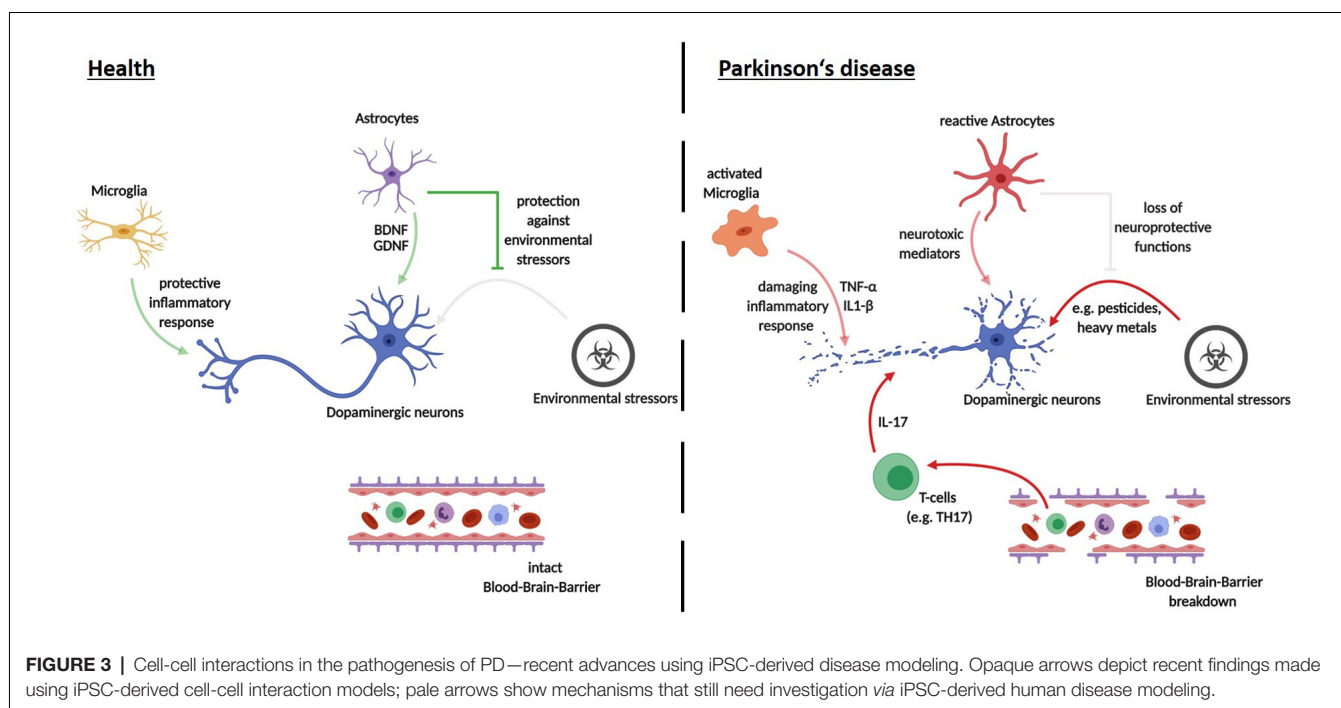
A number of different concepts and hypotheses for the role of microglia in neurodegeneration have been developed in an effort to summarize the existing data. The concept of "microglia-priming" assumes that microglia exhibit an inherently aberrant response to disease-associated proinflammatory stimuli in neurodegeneration—potentially

initiating and exacerbating the course of the disease (Perry and Holmes, 2014). Another possibility is that microglia respond adequately to neuroinflammatory stimuli before disease onset, but then undergo a phenotypic switch towards detrimental "degeneration-associated-microglia" as a result of accumulating inflammatory stimuli and aging effects (Song and Colonna, 2018). An investigation of the human microglia response to different PD associated stimuli may shed light on these different concepts in Parkinson disease. However, it has to be taken into account that microglial identity and function strongly relies on the presence of paracrine and juxtacrine cues provided by surrounding cells of the CNS including neurons (Abud et al., 2017; Gosselin et al., 2017; Hasselmann et al., 2019). Thus, a co-culture of iMGLs with iPSC-derived mDA neurons, in particular, may represent a valuable system in deciphering the effect of microglia on DA neurons under steady-state and stress conditions in a more physiological environment. As iMGLs and iPSC-derived mDA neurons have been shown to more closely resemble their fetal cellular counterparts, an iMGL-mDA neuron co-culture may be of specific value for the investigation of a possible "primed microglia" phenotype. Nevertheless, more sophisticated 2D co-culture systems also including other glial cells as transducers or even more complex 3D culture systems may be needed to more closely model *in vivo* human microglial function in a PD disease context (see "Organoids" section).

The concept of neuroinflammation in PD has long been principally attributed to innate immune cells of the CNS, like microglia (Muffat et al., 2016). However, studies that demonstrated the activation of T lymphocytes by α-Syn, as well as T-cell subset alterations in blood samples of PD patients, raised the possibility of a peripheral immunity involvement in PD pathogenesis (Baba et al., 2005; Stevens et al., 2012; Sulzer et al., 2017). Animal models have provided some functional evidence for a T-lymphocyte involvement in PD pathology (Brochard et al., 2009; Reynolds et al., 2010; Sommer et al., 2016). In addition, a recent study by Sommer et al. (2018) made use of a co-culture system between T-lymphocytes and iPSC-derived midbrain neurons to enumerate the role of T-cells in sporadic PD. Strikingly, the autologous co-culture of patient midbrain neurons with patient IL-17 producing T-cells leads to increased cell death in neurons compared to a non-autologous co-culture. This effect was dependent on IL-17 receptor signaling, as blockage of IL-17 or IL-17 receptor rescued neuronal death (Sommer et al., 2018). These results emphasize the possible role of adaptive immune cells in PD pathogenesis. Adding microglia to a co-culture system of T-cells and neurons may thus provide a means of determining how the interplay between adaptive and innate immunity shapes PD pathogenesis.

Organoids

Generation of human iPSC-derived DA neurons from PD patients could recapitulate certain disease phenotypes such as neurite pathology or neuronal cell death. Although the co-culture of DA neurons and different cell types such as astrocytes or microglia may bring the *in vitro* model closer to the *in vivo* situation, the complex organization of the

FIGURE 3 | Cell-cell interactions in the pathogenesis of PD—recent advances using iPSC-derived disease modeling. Opaque arrows depict recent findings made using iPSC-derived cell-cell interaction models; pale arrows show mechanisms that still need investigation *via* iPSC-derived human disease modeling.

human brain remains a major challenge. One of the difficulties in modeling late-onset neurodegenerative diseases like PD is the immaturity of human iPSC-derived DA neurons *in vitro*. Moreover, current 2D culture systems lack cell-cell interactions of neurons and non-neuronal cells such as glia cells in a spatially organized environment.

Recent advances in the generation of 3D cell culture systems, so-called organoids, open up new possibilities for iPSC-based disease modeling of PD. Differentiation protocols for human brain organoids make use of the intrinsic self-organization capability of pluripotent stem cells. Aggregation of single-cell iPSCs into embryoid bodies mimics the organization of the three germ layers during embryonic development. Culturing in minimal medium enables the differentiation of the outer layer to ectodermal fate. Embedding of these structures in extracellular matrices leads to a further outgrowth of neuroepithelium by serving as a supporting scaffold and induction of the apical-basal polarity as it is seen for the neural tube during embryonic neurodevelopment. Consequently, brain-region specific organoids offer enormous possibilities for long-term disease modeling of human neurodegeneration in specialized brain regions, such as the SN in PD.

Similar to the 2D differentiation of human iPSC-derived DA neurons, human midbrain organoids (hMOs) containing DA neurons are generated by patterning of iPSCs to midbrain fate. Either human iPSCs (Jo et al., 2016; Qian et al., 2016; Kim et al., 2019) or already patterned neural stem cells (Monzel et al., 2017; Smits et al., 2019) are aggregated as single cells to form hMOs.

Midbrain specific differentiation approaches led to radially organized midbrain organoids consisting of a proliferative ventral zone, an intermediate zone, and an outer neuronal layer.

After around 2 months, the hMOs express the respective midbrain markers (e.g., FOXA2, dopamine transporter DAT) and contain 54%–65% TH-positive DA neurons. Electrophysiological analysis by whole-cell patch clamping and multielectrode arrays (MEA) revealed functional neurons and synchronized neuronal networks. Moreover, the accumulation of neuromelanin, a byproduct of dopamine metabolism in 2 months old hMOs, represents an intriguing line of inquiry for disease modeling.

To date, only two studies describe disease modeling of PD using hMOs (Kim et al., 2019; Smits et al., 2019). In both cases, the focus was on a specific *LRRK2* mutation (G2019S). *LRRK2*^G2019S hMOs have deficits as indicated by a decreased number of TH-positive neurons and a reduction of neuronal complexity. In addition, increased MPTP-induced cell death of DA neurons in mutant organoids and abnormal localization of phosphorylated α-Syn was present. Inhibition of LRRK2 kinase activity resulted in a reduction of DA cell death and a reduction of phosphorylated α-Syn.

These results indicate that hMOs can indeed recapitulate aspects of PD pathology that have been already shown in 2D models. However, human brain organoids lack some glial cell types like oligodendrocytes or microglia (Quadrato et al., 2017; Sloan et al., 2017). As a result, co-culture models of midbrain organoids and non-neuronal cell types are required. Recent transcriptomic studies on human microglia were able to determine that their transcriptional identity is heavily dependent on intercellular, three-dimensional cues (Gosselin et al., 2017). It will be challenging to establish applicable 3D co-culture models due to the appropriate timing of differentiation and media compositions to introduce one or more additional cell types into the organoids. Moreover, activation of apoptosis

within larger organoids due to lack of oxygen and nutrients (Mansour et al., 2018) might interfere with PD models focusing on oxidative stress.

It is suspected that the leakiness of the blood-brain-barrier (BBB) may lead to the observed infiltration of peripheral immune cells (Sommer et al., 2018). Consequently, 3D culture conditions need to be further optimized for the co-culture of hMOs and, for example, patient-derived blood lymphocytes. Nonetheless, one needs to consider that stem cell-based models still resemble fetal stages of neurodevelopment and that even premature aging using substances like progerin creates an artificial model of age-related phenotypes as seen in PD.

OUTLOOK

Since the first report describing successful reprogramming of human fibroblasts into iPSCs over a decade ago, recent progress has underscored the importance of iPSCs as a powerful tool to model neurodegenerative diseases, including PD, in a human system. As a pre-requisite, various iPSC-differentiation protocols now enable the generation of DA neurons, astrocytes, and microglia as well as complex three-dimensional neuronal structures, termed organoids. Future innovation and optimization of differentiation protocols should be able to accelerate research progress in this field even further.

It should be noted that while studies on iPSC-derived midbrain dopaminergic (mDA) neurons in isolated culture systems were able to recapitulate major pathological hallmarks of PD, including neurite defects and aggregation of α-Syn, they found very little cell death. The addition of further stressors appears to be an essential step in observing cell death in iPSC-derived model systems of PD (see **Figure 2**). These stressors have been shown to include toxins, aging effects and the addition of other cell types to the culture system. Major reasons for limited

pathology in PD models are that cultivation media are optimized to prevent neurodegeneration, the iPSC derived neural models mimic a fetal developmental stage and that major epigenetic traits are lost during reprogramming. Given the complex etiology of the neurodegenerative process in PD, co-culture approaches of different neural cell types provide unique opportunities for future disease modeling (depicted in **Figure 3**).

AUTHOR CONTRIBUTIONS

BW, KS, JL, TR and JK wrote and critically discussed this manuscript. BW, JK, TR, JL and KS generated the figures, revised the manuscript and approved the final manuscript.

FUNDING

ACKNOWLEDGMENTS

REFERENCES

Aboud, A. A., Tidball, A. M., Kumar, K. K., Neely, M. D., Ess, K. C., Erikson, K. M., et al. (2012). Genetic risk for Parkinson's disease correlates with alterations in neuronal manganese sensitivity between two human subjects. *Neurotoxicology* 33, 1443–1449. doi: 10.1016/j.neuro.2012.10.009

Aboud, A. A., Tidball, A. M., Kumar, K. K., Neely, M. D., Han, B., Ess, K. C., et al. (2015). PARK2 patient neuroprogenitors show increased mitochondrial sensitivity to copper. *Neurobiol. Dis.* 73, 204–212. doi: 10.1016/j.nbd.2014.10.002

Aboud, E. M., Ramirez, R. N., Martinez, E. S., Healy, L. M., Nguyen, C. H. H., Newman, S. A., et al. (2017). iPSC-derived human microglia-like cells to study neurological diseases. *Neuron* 94, 278.e9–293.e9. doi: 10.1016/j.neuron.2017.03.042

Baba, Y., Kuroiwa, A., Uitti, R. J., Wszolek, Z. K., and Yamada, T. (2005). Alterations of T-lymphocyte populations in Parkinson disease. *Parkinsonism Relat. Disord.* 11, 493–498. doi: 10.1016/j.parkreldis.2005.07.005

Baba, M., Nakajo, S., Tu, P. H., Tomita, T., Nakaya, K., Lee, V. M., et al. (1998). Aggregation of α-synuclein in Lewy bodies of sporadic Parkinson's disease and dementia with Lewy bodies. *Am. J. Pathol.* 152, 879–884.

Ball, N., Teo, W. P., Chandra, S., and Chapman, J. (2019). Parkinson's disease and the environment. *Front. Neurol.* 10:218. doi: 10.3389/fneur.2019.00218

Barker, R. A., Drouin-Ouellet, J., and Parmar, M. (2015). Cell-based therapies for Parkinson disease-past insights and future potential. *Nat. Rev. Neurol.* 11, 492–503. doi: 10.1038/nrneurol.2015.123

Bartels, T., Choi, J. G., and Selkoe, D. J. (2011). α-synuclein occurs physiologically as a helically folded tetramer that resists aggregation. *Nature* 477, 107–110. doi: 10.1038/nature10324

Bartels, A. L., Willemsen, A. T., Doorduin, J., de Vries, E. F., Dierckx, R. A., and Leenders, K. L. (2010). [11C]-PK11195 PET: quantification of neuroinflammation and a monitor of anti-inflammatory treatment in Parkinson's disease? *Parkinsonism Relat. Disord.* 16, 57–59. doi: 10.1016/j.parkreldis.2009.05.005

Bentea, E., Verbruggen, L., and Massie, A. (2017). The proteasome inhibition model of Parkinson's disease. *J. Parkinsons Dis.* 7, 31–63. doi: 10.3233/JPD-160921

Björklund, A., Rosenblad, C., Winkler, C., and Kirik, D. (1997). Studies on neuroprotective and regenerative effects of GDNF in a partial lesion model of Parkinson's disease. *Neurobiol. Dis.* 4, 186–200. doi: 10.1006/nbdi.1997.0151

Blesa, J., Trigo-Damas, I., Quiroga-Varela, A., and Jackson-Lewis, V. R. (2015). Oxidative stress and Parkinson's disease. *Front. Neuroanat.* 9:91. doi: 10.3389/fnana.2015.00091

Bogetofte, H., Jensen, P., Ryding, M., Schmidt, S. I., Okarmus, J., Ritter, L., et al. (2019). PARK2 mutation causes metabolic disturbances and impaired

survival of human iPSC-derived neurons. *Front. Cell. Neurosci.* 13:297. doi: 10.3389/fncel.2019.00297

Bond, A. M., Bhalala, O. G., and Kessler, J. A. (2012). The dynamic role of bone morphogenetic proteins in neural stem cell fate and maturation. *Dev. Neurobiol.* 72, 1068–1084. doi: 10.1002/dneu.22022

Booth, H. D. E., Hirst, W. D., and Wade-Martins, R. (2017). The role of astrocyte dysfunction in Parkinson's disease pathogenesis. *Trends Neurosci.* 40, 358–370. doi: 10.1016/j.tins.2017.04.001

Borgs, L., Peyre, E., Alix, P., Hanon, K., Grobarczyk, B., Godin, J. D., et al. (2016). Dopaminergic neurons differentiating from LRRK2 G2019S induced pluripotent stem cells show early neuritic branching defects. *Sci. Rep.* 6:33377. doi: 10.1038/srep33377

Braak, H., and Braak, E. (2000). Pathoanatomy of Parkinson's disease. *J. Neurol.* 247, II3–II10. doi: 10.1007/PL00007758

Brochard, V., Combadiere, B., Prigent, A., Laouar, Y., Perrin, A., Beray-Berthat, V., et al. (2009). Infiltration of CD4+ lymphocytes into the brain contributes to neurodegeneration in a mouse model of Parkinson disease. *J. Clin. Invest.* 119, 182–192. doi: 10.1172/JCI36470

Brownjohn, P. W., Smith, J., Solanki, R., Lohmann, E., Houlden, H., Hardy, J., et al. (2018). Functional studies of missense TREM2 mutations in human stem cell-derived microglia. *Stem Cell Rep.* 10, 1294–1307. doi: 10.1016/j.stemcr.2018.03.003

Butovsky, O., Jedrychowski, M. P., Moore, C. S., Cialic, R., Lanser, A. J., Gabriely, G., et al. (2014). Identification of a unique TGF-β-dependent molecular and functional signature in microglia. *Nat. Neurosci.* 17:131. doi: 10.1038/nn.3599

Byers, B., Cord, B., Nguyen, H. N., Schule, B., Fenno, L., Lee, P. C., et al. (2011). SNCA triplication Parkinson's patient's iPSC-derived DA neurons accumulate α-synuclein and are susceptible to oxidative stress. *PLoS One* 6:e26159. doi: 10.1371/journal.pone.0026159

Castrioto, A., Lhommée, E., Moro, E., and Krack, P. (2014). Mood and behavioural effects of subthalamic stimulation in Parkinson's disease. *Lancet Neurol.* 13, 287–305. doi: 10.1016/s1474-4422(13)70294-1

Chambers, S. M., Fasano, C. A., Papapetrou, E. P., Tomishima, M., Sadelain, M., and Studer, L. (2009). Highly efficient neural conversion of human ES and iPS cells by dual inhibition of SMAD signaling. *Nat. Biotechnol.* 27, 275–280. doi: 10.1038/nbt.1529

Chinta, S. J., Woods, G., Demaria, M., Rane, A., Zou, Y., McQuade, A., et al. (2018). Cellular senescence is induced by the environmental neurotoxin paraquat and contributes to neuropathology linked to Parkinson's disease. *Cell Rep.* 22, 930–940. doi: 10.1016/j.celrep.2017.12.092

Chung, S. Y., Kishinevsky, S., Mazzulli, J. R., Graziotto, J., Mrejeru, A., Mosharov, E. V., et al. (2016). Parkin and PINK1 patient iPSC-derived midbrain dopamine neurons exhibit mitochondrial dysfunction and α-synuclein accumulation. *Stem Cell Reports* 7, 664–677. doi: 10.1016/j.stemcr.2016.08.012

Connolly, B. S., and Lang, A. E. (2014). Pharmacological treatment of Parkinson disease: a review. *JAMA* 311, 1670–1683. doi: 10.1001/jama.2014.3654

Cooper, O., Seo, H., Andrabi, S., Guardia-Laguarta, C., Graziotto, J., Sundberg, M., et al. (2012). Pharmacological rescue of mitochondrial deficits in iPSC-derived neural cells from patients with familial Parkinson's disease. *Sci. Transl. Med.* 4:141ra190. doi: 10.1126/scitranslmed.3003985

Dettmer, U., Newman, A. J., Soldner, F., Luth, E. S., Kim, N. C., von Saucken, V. E., et al. (2015a). Parkinson-causing α-synuclein missense mutations shift native tetramers to monomers as a mechanism for disease initiation. *Nat. Commun.* 6:8008. doi: 10.1038/ncomms9008

Dettmer, U., Newman, A. J., von Saucken, V. E., Bartels, T., and Selkoe, D. (2015b). KTKEGV repeat motifs are key mediators of normal α-synuclein tetramerization: their mutation causes excess monomers and neurotoxicity. *Proc. Natl. Acad. Sci. U S A* 112, 9596–9601. doi: 10.1073/pnas.1505953112

Devine, M. J., Ryten, M., Vodicka, P., Thomson, A. J., Burdon, T., Houlden, H., et al. (2011). Parkinson's disease induced pluripotent stem cells with triplication of the α-synuclein locus. *Nat. Commun.* 2:440. doi: 10.1038/ncomms1453

di Domenico, A., Carola, G., Calatayud, C., Pons-Espinal, M., Muñoz, J. P., Richaud-Patin, Y., et al. (2019). Patient-specific iPSC-derived astrocytes contribute to non-cell-autonomous neurodegeneration in Parkinson's disease. *Stem Cell Reports* 12, 213–229. doi: 10.1016/j.stemcr.2018.12.011

Du, F., Yu, Q., Chen, A., Chen, D., and Yan, S. S. (2018). Astrocytes attenuate mitochondrial dysfunctions in human dopaminergic neurons derived from iPSC. *Stem Cell Reports* 10, 366–374. doi: 10.1016/j.stemcr.2017.12.021

Durnaoglu, S., Genc, S., and Genc, K. (2011). Patient-specific pluripotent stem cells in neurological diseases. *Stem Cells Int.* 2011:212487. doi: 10.4061/2011/212487

Farina, M., Avila, D. S., da Rocha, J. B. T., and Aschner, M. (2013). Metals, oxidative stress and neurodegeneration: a focus on iron, manganese and mercury. *Neurochem. Int.* 62, 575–594. doi: 10.1016/j.neuint.2012.12.006

Fernandes, H. J., Hartfield, E. M., Christian, H. C., Emmanoulidou, E., Zheng, Y., Booth, H., et al. (2016). ER stress and autophagic perturbations lead to elevated extracellular α-synuclein in GBA-N370S Parkinson's iPSC-derived dopamine neurons. *Stem Cell Reports* 6, 342–356. doi: 10.1016/j.stemcr.2016.01.013

Flierl, A., Oliveira, L. M., Falomir-Lockhart, L. J., Mak, S. K., Hesley, J., Soldner, F., et al. (2014). Higher vulnerability and stress sensitivity of neuronal precursor cells carrying an α-synuclein gene triplication. *PLoS One* 9:e112413. doi: 10.1371/journal.pone.0112413

Franco-Iborra, S., Cuadros, T., Parent, A., Romero-Gimenez, J., Vila, M., and Perier, C. (2018). Defective mitochondrial protein import contributes to complex I-induced mitochondrial dysfunction and neurodegeneration in Parkinson's disease. *Cell Death Dis.* 9:1122. doi: 10.1038/s41419-018-1154-0

Garcia-Reitboeck, P., Phillips, A., Piers, T. M., Villegas-Llerena, C., Butler, M., Mallach, A., et al. (2018). Human induced pluripotent stem cell-derived microglia-like cells harboring TREM2 missense mutations show specific deficits in phagocytosis. *Cell Rep.* 24, 2300–2311. doi: 10.1016/j.celrep.2018.07.094

Ginhoux, F., Greter, M., Leboeuf, M., Nandi, S., See, P., Gokhan, S., et al. (2010). Fate mapping analysis reveals that adult microglia derive from primitive macrophages. *Science* 330, 841–845. doi: 10.1126/science.1194637

Gosselin, D., Skola, D., Coufal, N. G., Holtman, I. R., Schlachetzki, J. C. M., Sajti, E., et al. (2017). An environment-dependent transcriptional network specifies human microglia identity. *Science* 356:eaal3222. doi: 10.1126/science.aal3222

Guenther, M. G., Frampton, G. M., Soldner, F., Hockemeyer, D., Mitalipova, M., Jaenisch, R., et al. (2010). Chromatin structure and gene expression programs of human embryonic and induced pluripotent stem cells. *Cell Stem Cell* 7, 249–257. doi: 10.1016/j.stem.2010.06.015

Hasselmann, J., Coburn, M. A., England, W., Figueroa Velez, D. X., Kiani Shabestari, S., Tu, C. H., et al. (2019). Development of a chimeric model to study and manipulate human microglia *in vivo*. *Neuron* 103, 1016.e10–1033.e10. doi: 10.1016/j.neuron.2019.07.002

Heldin, C. H., Miyazono, K., and ten Dijke, P. (1997). TGF-β signalling from cell membrane to nucleus through SMAD proteins. *Nature* 390, 465–471. doi: 10.1038/37284

Heman-Ackah, S. M., Manzano, R., Hoozemans, J. J. M., Scheper, W., Flynn, R., Haerty, W., et al. (2017). α-synuclein induces the unfolded protein response in Parkinson's disease SNCA triplication iPSC-derived neurons. *Hum. Mol. Genet.* 26, 4441–4450. doi: 10.1093/hmg/ddx331

Hernandez-Baltazar, D., Zavala-Flores, L. M., and Villanueva-Olivo, A. (2017). The 6-hydroxydopamine model and parkinsonian pathophysiology: novel findings in an older model. *Neurologia* 32, 533–539. doi: 10.1016/j.nrl.2015.06.011

Hirsch, E. C., Breidert, T., Rousselet, E., Hunot, S., Hartmann, A., and Michel, P. P. (2003). The role of glial reaction and inflammation in Parkinson's disease. *Ann. N Y Acad. Sci.* 991, 214–228. doi: 10.1111/j.1749-6632.2003.tb07478.x

Hirsch, E. C., Jenner, P., and Przedborski, S. (2013). Pathogenesis of Parkinson's disease. *Mov. Disord.* 28, 24–30. doi: 10.1002/mds.25032

Hu, D., Sun, X., Liao, X., Zhang, X., Zarabi, S., Schimmer, A., et al. (2019). α-synuclein suppresses mitochondrial protease ClpP to trigger mitochondrial oxidative damage and neurotoxicity. *Acta Neuropathol.* 137, 939–960. doi: 10.1007/s00401-019-01993-2

Hunot, S., Dugas, N., Faucheux, B., Hartmann, A., Tardieu, M., Debre, P., et al. (1999). FcepsilonRII/CD23 is expressed in Parkinson's disease and induces, *in vitro*, production of nitric oxide and tumor necrosis factor-α in glial cells. *J. Neurosci.* 19, 3440–3447. doi: 10.1523/jneurosci.19-09-03440.1999

Hwang, J. Y., Aromolaran, K. A., and Zukin, R. S. (2017). The emerging field of epigenetics in neurodegeneration and neuroprotection. *Nat. Rev. Neurosci.* 18, 347–361. doi: 10.1038/nrn.2017.46

Iannielli, A., Bido, S., Folladori, L., Segnali, A., Cancellieri, C., Maresca, A., et al. (2018). Pharmacological inhibition of necroptosis protects from dopaminergic neuronal cell death in Parkinson's disease models. *Cell Rep.* 22, 2066–2079. doi: 10.1016/j.celrep.2018.01.089

Imaizumi, Y., Okada, Y., Akamatsu, W., Koike, M., Kuzumaki, N., Hayakawa, H., et al. (2012). Mitochondrial dysfunction associated with increased oxidative stress and α-synuclein accumulation in PARK2 iPSC-derived neurons and postmortem brain tissue. *Mol. Brain* 5:35. doi: 10.1186/1756-6606-5-35

Jinek, M., Chylinski, K., Fonfara, I., Hauer, M., Doudna, J. A., and Charpentier, E. (2012). A programmable dual-RNA-guided DNA endonuclease in adaptive bacterial immunity. *Science* 337, 816–821. doi: 10.1126/science.1225829

Jo, J., Xiao, Y., Sun, A. X., Cukuroglu, E., Tran, H. D., Goke, J., et al. (2016). Midbrain-like organoids from human pluripotent stem cells contain functional dopaminergic and neuromelanin-producing neurons. *Cell Stem Cell* 19, 248–257. doi: 10.1016/j.stem.2016.07.005

Kadoshima, T., Sakaguchi, H., Nakano, T., Soen, M., Ando, S., Eiraku, M., et al. (2013). Self-organization of axial polarity, inside-out layer pattern and species-specific progenitor dynamics in human ES cell-derived neocortex. *Proc. Natl. Acad. Sci. U S A* 110, 20284–20289. doi: 10.1073/pnas.1315710110

Kalia, L. V., and Lang, A. E. (2015). Parkinson's disease. *Lancet* 386, 896–912. doi: 10.1016/S0140-6736(14)61393-3

Kang, L., Wu, K. P., Vendruscolo, M., and Baum, J. (2011). The A53T mutation is key in defining the differences in the aggregation kinetics of human and mouse α-synuclein. *J. Am. Chem. Soc.* 133, 13465–13470. doi: 10.1021/ja203979j

Kawasaki, H., Mizuseki, K., Nishikawa, S., Kaneko, S., Kuwana, Y., Nakanishi, S., et al. (2000). Induction of midbrain dopaminergic neurons from ES cells by stromal cell-derived inducing activity. *Neuron* 28, 31–40. doi: 10.1016/s0896-6273(00)00083-0

Kim, H., Park, H. J., Choi, H., Chang, Y., Park, H., Shin, J., et al. (2019). Modeling G2019S-LRRK2 sporadic Parkinson's disease in 3D midbrain organoids. *Stem Cell Reports* 12, 518–531. doi: 10.1016/j.stemcr.2019.01.020

Kim, S., Yun, S. P., Lee, S., Umanah, G. E., Bandaru, V. V. R., Yin, X., et al. (2018). GBA1 deficiency negatively affects physiological α-synuclein tetramers and related multimers. *Proc. Natl. Acad. Sci. U S A* 115, 798–803. doi: 10.1073/pnas.1700465115

Korecka, J. A., Talbot, S., Osborn, T. M., de Leeuw, S. M., Levy, S. A., Ferrari, E. J., et al. (2019). Neurite collapse and altered ER Ca^{2+} control in human parkinson disease patient iPSC-derived neurons with LRRK2 G2019S mutation. *Stem Cell Reports* 12, 29–41. doi: 10.1016/j.stemcr.2018.11.021

Kouroupi, G., Taoufik, E., Vlachos, I. S., Tsioras, K., Antoniou, N., Papastefanaki, F., et al. (2017). Defective synaptic connectivity and axonal neuropathology in a human iPSC-based model of familial Parkinson's disease. *Proc. Natl. Acad. Sci. U S A* 114, E3679–E3688. doi: 10.1073/pnas.1617259114

Krencik, R., and Zhang, S. C. (2011). Directed differentiation of functional astroglial subtypes from human pluripotent stem cells. *Nat. Protoc.* 6, 1710–1717. doi: 10.1038/nprot.2011.405

Kriks, S., Shim, J. W., Piao, J., Ganat, Y. M., Wakeman, D. R., Xie, Z., et al. (2011). Dopamine neurons derived from human ES cells efficiently engraft in animal models of Parkinson's disease. *Nature* 480, 547–551. doi: 10.1038/nature10648

Ladewig, J., Mertens, J., Kesavan, J., Doerr, J., Poppe, D., Glaue, F., et al. (2012). Small molecules enable highly efficient neuronal conversion of human fibroblasts. *Nat. Methods* 9, 575–578. doi: 10.1038/nmeth.1972

Lancaster, M. A., Renner, M., Martin, C.-A., Wenzel, D., Bicknell, L. S., Hurles, M. E., et al. (2013). Cerebral organoids model human brain development and microcephaly. *Nature* 501, 373–379. doi: 10.1038/nature12517

Langston, J. W. (2017). The MPTP story. *J. Parkinsons Dis.* 7, S11–S19. doi: 10.3233/jpd-179006

Limousin, P., Krack, P., Pollak, P., Benazzouz, A., Ardouin, C., Hoffmann, D., et al. (1998). Electrical stimulation of the subthalamic nucleus in advanced Parkinson's disease. *N. Engl. J. Med.* 339, 1105–1111. doi: 10.1056/NEJM199810153391603

Lin, L., Göke, J., Cukuroglu, E., Dranias, M. R., VanDongen, A. M., and Stanton, L. W. (2016). Molecular features underlying neurodegeneration identified through *in vitro* modeling of genetically diverse Parkinson's disease patients. *Cell Rep.* 15, 2411–2426. doi: 10.1016/j.celrep.2016.05.022

Liu, M. L., Zang, T., Zou, Y., Chang, J. C., Gibson, J. R., Huber, K. M., et al. (2013). Small molecules enable neurogenin 2 to efficiently convert human fibroblasts into cholinergic neurons. *Nat. Commun.* 4:2183. doi: 10.1038/ncomms3183

Ludtmann, M. H. R., Angelova, P. R., Horrocks, M. H., Choi, M. L., Rodrigues, M., Baev, A. Y., et al. (2018). α-synuclein oligomers interact with ATP synthase and open the permeability transition pore in Parkinson's disease. *Nat. Commun.* 9:2293. doi: 10.1038/s41467-018-04422-2

Maherali, N., Sridharan, R., Xie, W., Utikal, J., Eminli, S., Arnold, K., et al. (2007). Directly reprogrammed fibroblasts show global epigenetic remodeling and widespread tissue contribution. *Cell Stem Cell* 1, 55–70. doi: 10.1016/j.stem.2007.05.014

Mansour, A. A., Goncalves, J. T., Bloyd, C. W., Li, H., Fernandes, S., Quang, D., et al. (2018). An *in vivo* model of functional and vascularized human brain organoids. *Nat. Biotechnol.* 36, 432–441. doi: 10.1038/nbt.4127

Marchetto, M. C., Winner, B., and Gage, F. H. (2010). Pluripotent stem cells in neurodegenerative and neurodevelopmental diseases. *Hum. Mol. Genet.* 19, R71–R76. doi: 10.1093/hmg/ddq159

Marion, R. M., Strati, K., Li, H., Tejera, A., Schoeftner, S., Ortega, S., et al. (2009). Telomeres acquire embryonic stem cell characteristics in induced pluripotent stem cells. *Cell Stem Cell* 4, 141–154. doi: 10.1016/j.stem.2008.12.010

Marrone, L., Bus, C., Schondorf, D., Fitzgerald, J. C., Kubler, M., Schmid, B., et al. (2018). Generation of iPSCs carrying a common LRRK2 risk allele for *in vitro* modeling of idiopathic Parkinson's disease. *PLoS One* 13:e0192497. doi: 10.1371/journal.pone.0192497

Mazzulli, J. R., Zunke, F., Isacson, O., Studer, L., and Krainc, D. (2016). α-synuclein-induced lysosomal dysfunction occurs through disruptions in protein trafficking in human midbrain synucleinopathy models. *Proc. Natl. Acad. Sci. U S A* 113, 1931–1936. doi: 10.1073/pnas.1520335113

McGeer, P. L., and McGeer, E. G. (2008). Glial reactions in Parkinson's disease. *Mov. Disord.* 23, 474–483. doi: 10.1002/mds.21751

Mertens, J., Paquola, A. C. M., Ku, M., Hatch, E., Bohnke, L., Ladjevardi, S., et al. (2015). Directly reprogrammed human neurons retain aging-associated transcriptomic signatures and reveal age-related nucleocytoplasmic defects. *Cell Stem Cell* 17, 705–718. doi: 10.1016/j.stem.2015.09.001

Miller, J. D., Ganat, Y. M., Kishinevsky, S., Bowman, R. L., Liu, B., Tu, E. Y., et al. (2013). Human iPSC-based modeling of late-onset disease *via* progerin-induced aging. *Cell Stem Cell* 13, 691–705. doi: 10.1016/j.stem.2013.11.006

Mittal, S., Bjørnevik, K., Im, D. S., Flierl, A., Dong, X., Locascio, J. J., et al. (2017). β2-adrenoreceptor is a regulator of the α-synuclein gene driving risk of Parkinson's disease. *Science* 357, 891–898. doi: 10.1126/science.aaf3934

Monzel, A. S., Smits, L. M., Hemmer, K., Hachi, S., Moreno, E. L., van Wuellen, T., et al. (2017). Derivation of human midbrain-specific organoids from neuroepithelial stem cells. *Stem Cell Reports* 8, 1144–1154. doi: 10.1016/j.stemcr.2017.03.010

Muffat, J., Li, Y., Yuan, B., Mitalipova, M., Omer, A., Corcoran, S., et al. (2016). Efficient derivation of microglia-like cells from human pluripotent stem cells. *Nat. Med.* 22, 1358–1367. doi: 10.1038/nm.4189

Nguyen, H. N., Byers, B., Cord, B., Shcheglovitov, A., Byrne, J., Gujar, P., et al. (2011). LRRK2 mutant iPSC-derived DA neurons demonstrate increased susceptibility to oxidative stress. *Cell Stem Cell* 8, 267–280. doi: 10.1016/j.stem.2011.01.013

Oh, Y. (2019). Patient-specific pluripotent stem cell-based Parkinson's disease models showing endogenous α-synuclein aggregation. *BMB Rep.* 52, 349–359. doi: 10.5483/bmbrep.2019.52.6.142

Ohta, E., Nihira, T., Uchino, A., Imaizumi, Y., Okada, Y., Akamatsu, W., et al. (2015). I2020T mutant LRRK2 iPSC-derived neurons in the Sagamihara family exhibit increased Tau phosphorylation through the AKT/GSK-3β signaling pathway. *Hum. Mol. Genet.* 24, 4879–4900. doi: 10.1093/hmg/ddv212

Oliveira, L. M. A., Falomir-Lockhart, L. J., Botelho, M. G., Lin, K.-H., Wales, P., Koch, J. C., et al. (2015). Elevated α-synuclein caused by SNCA gene triplication impairs neuronal differentiation and maturation in Parkinson's patient-derived induced pluripotent stem cells. *Cell Death Dis.* 6:e1994. doi: 10.1038/cddis.2015.318

Pakkenberg, B., Moller, A., Gundersen, H. J., Mouritzen Dam, A., and Pakkenberg, H. (1991). The absolute number of nerve cells in substantia nigra in normal subjects and in patients with Parkinson's disease estimated with

an unbiased stereological method. *J. Neurol. Neurosurg. Psychiatry* 54, 30–33. doi: 10.1136/jnnp.54.1.30

Perrier, A. L., Tabar, V., Barberi, T., Rubio, M. E., Bruses, J., Topf, N., et al. (2004). Derivation of midbrain dopamine neurons from human embryonic stem cells. *Proc. Natl. Acad. Sci. U S A* 101, 12543–12548. doi: 10.1073/pnas.0404700101

Perriot, S., Mathias, A., Perriard, G., Canales, M., Jonkmans, N., Merienne, N., et al. (2018). Human induced pluripotent stem cell-derived astrocytes are differentially activated by multiple sclerosis-associated cytokines. *Stem Cell Reports* 11, 1199–1210. doi: 10.1016/j.stemcr.2018.09.015

Perry, V. H., and Holmes, C. (2014). Microglial priming in neurodegenerative disease. *Nat. Rev. Neurol.* 10, 217–224. doi: 10.1038/nrneurol.2014.38

Postuma, R. B., Berg, D., Stern, M., Poewe, W., Olanow, C. W., Oertel, W., et al. (2015). MDS clinical diagnostic criteria for Parkinson's disease. *Mov. Disord.* 30, 1591–1601. doi: 10.1002/mds.26424

Prots, I., Grosch, J., Brazdis, R.-M., Simmnacher, K., Veber, V., Havlicek, S., et al. (2018). α-synuclein oligomers induce early axonal dysfunction in human iPSC-based models of synucleinopathies. *Proc. Natl. Acad. Sci. U S A* 115, 7813–7818. doi: 10.1073/pnas.1713129115

Qian, X., Nguyen, H. N., Song, M. M., Hadiono, C., Ogden, S. C., Hammack, C., et al. (2016). Brain-region-specific organoids using mini-bioreactors for modeling ZIKV exposure. *Cell* 165, 1238–1254. doi: 10.1016/j.cell.2016.04.032

Qian, X., Jacob, F., Song, M. M., Nguyen, H. N., Song, H., and Ming, G.-L., et al. (2018). Generation of human brain region–specific organoids using a miniaturized spinning bioreactor. *Nat. Protoc.* 13, 565–580. doi: 10.1038/nprot.2017.152

Qing, X., Walter, J., Jarazo, J., Arias-Fuenzalida, J., Hillje, A. L., and Schwamborn, J. C. (2017). CRISPR/Cas9 and piggyBac-mediated footprint-free LRRK2–G2019S knock-in reveals neuronal complexity phenotypes and α-synuclein modulation in dopaminergic neurons. *Stem Cell Res.* 24, 44–50. doi: 10.1016/j.scr.2017.08.013

Quadrato, G., Nguyen, T., Macosko, E. Z., Sherwood, J. L., Min Yang, S., Berger, D. R., et al. (2017). Cell diversity and network dynamics in photosensitive human brain organoids. *Nature* 545, 48–53. doi: 10.1038/nature22047

Rees, K., Stowe, R., Patel, S., Ives, N., Breen, K., Clarke, C. E., et al. (2011). Non-steroidal anti-inflammatory drugs as disease-modifying agents for Parkinson's disease: evidence from observational studies. *Cochrane Database Syst. Rev.* 11:Cd008454. doi: 10.1002/14651858.cd008454.pub2

Reinhardt, P., Glatza, M., Hemmer, K., Tsytsyura, Y., Thiel, C. S., Höing, S., et al. (2013a). Derivation and expansion using only small molecules of human neural progenitors for neurodegenerative disease modeling. *PLoS One* 8:e59252. doi: 10.1371/journal.pone.0059252

Reinhardt, P., Schmid, B., Burbulla, L. F., Schöndorf, D. C., Wagner, L., Glatza, M., et al. (2013b). Genetic correction of a LRRK2 mutation in human iPSCs links parkinsonian neurodegeneration to ERK-dependent changes in gene expression. *Cell Stem Cell* 12, 354–367. doi: 10.1016/j.stem.2013.01.008

Ren, Y., Jiang, H., Hu, Z., Fan, K., Wang, J., Janoschka, S., et al. (2015). Parkin mutations reduce the complexity of neuronal processes in iPSC-derived human neurons. *Stem Cells* 33, 68–78. doi: 10.1002/stem.1854

Reyes, J. F., Olsson, T. T., Lamberts, J. T., Devine, M. J., Kunath, T., and Brundin, P. (2015). A cell culture model for monitoring α-synuclein cell-to-cell transfer. *Neurobiol. Dis.* 77, 266–275. doi: 10.1016/j.nbd.2014.07.003

Reynolds, A. D., Stone, D. K., Hutter, J. A., Benner, E. J., Mosley, R. L., and Gendelman, H. E. (2010). Regulatory T cells attenuate Th17 cell-mediated nigrostriatal dopaminergic neurodegeneration in a model of Parkinson's disease. *J. Immunol.* 184, 2261–2271. doi: 10.4049/jimmunol.0901852

Rodriguez, M., Rodriguez-Sabate, C., Morales, I., Sanchez, A., and Sabate, M. (2015). Parkinson's disease as a result of aging. *Aging Cell* 14, 293–308. doi: 10.1111/acel.12312

Roybon, L., Lamas, N. J., Garcia, A. D., Yang, E. J., Sattler, R., Lewis, V. J., et al. (2013). Human stem cell-derived spinal cord astrocytes with defined mature or reactive phenotypes. *Front. Immunol.* 4, 1035–1048. doi: 10.1016/j.celrep.2013.06.021

Ryan, S. D., Dolatabadi, N., Chan, S. F., Zhang, X., Akhtar, M. W., Parker, J., et al. (2013). Isogenic human iPSC Parkinson's model shows nitrosative stress-induced dysfunction in MEF2-PGC1α transcription. *Cell* 155, 1351–1364. doi: 10.1016/j.cell.2013.11.009

Ryan, B. J., Lourenco-Venda, L. L., Crabtree, M. J., Hale, A. B., Channon, K. M., and Wade-Martins, R. (2014). α-Synuclein and mitochondrial bioenergetics regulate tetrahydrobiopterin levels in a human dopaminergic model of Parkinson disease. *Free Radic. Biol. Med.* 67, 58–68. doi: 10.1016/j.freeradbiomed.2013.10.008

Sánchez-Danés, A., Richaud-Patin, Y., Carballo-Carbajal, I., Jiménez-Delgado, S., Caig, C., Mora, S., et al. (2012). Disease-specific phenotypes in dopamine neurons from human iPS-based models of genetic and sporadic Parkinson's disease. *EMBO Mol. Med.* 4, 380–395. doi: 10.1002/emmm.201200215

Santos, R., Vadodaria, K. C., Jaeger, B. N., Mei, A., Lefcochilos-Fogelquist, S., Mendes, A. P. D., et al. (2017). Differentiation of inflammation-responsive astrocytes from glial progenitors generated from human induced pluripotent stem cells. *Stem Cell Reports* 8, 1757–1769. doi: 10.1016/j.stemcr.2017.05.011

Schwab, A. J., and Ebert, A. D. (2015). Neurite aggregation and calcium dysfunction in iPSC-derived sensory neurons with Parkinson's disease-related lrrk2 g2019s mutation. *Stem Cell Reports* 5, 1039–1052. doi: 10.1016/j.stemcr.2015.11.004

Shaltouki, A., Sivapatham, R., Pei, Y., Gerencser, A. A., Momcilovic, O., Rao, M. S., et al. (2015). Mitochondrial alterations by PARKIN in dopaminergic neurons using PARK2 patient-specific and PARK2 knockout isogenic iPSC lines. *Stem Cell Reports* 4, 847–859. doi: 10.1016/j.stemcr.2015.02.019

Singleton, A. B., Farrer, M. J., and Bonifati, V. (2013). The genetics of Parkinson's disease: progress and therapeutic implications. *Mov. Disord.* 28, 14–23. doi: 10.1002/mds.25249

Sloan, S. A., Darmanis, S., Huber, N., Khan, T. A., Birey, F., Caneda, C., et al. (2017). Human astrocyte maturation captured in 3D cerebral cortical spheroids derived from pluripotent stem cells. *Neuron* 95, 779.e6–790.e6. doi: 10.1016/j.neuron.2017.07.035

Smits, L. M., Reinhardt, L., Reinhardt, P., Glatza, M., Monzel, A. S., Stanslowsky, N., et al. (2019). Modeling Parkinson's disease in midbrain-like organoids. *NPJ Parkinsons Dis.* 5:5. doi: 10.1038/s41531-019-0078-4

Soldner, F., Stelzer, Y., Shivalila, C. S., Abraham, B. J., Latourelle, J. C., Barrasa, M. I., et al. (2016). Parkinson-associated risk variant in distal enhancer of α-synuclein modulates target gene expression. *Nature* 533, 95–99. doi: 10.1038/nature17939

Sommer, A., Fadler, T., Dorfmeister, E., Hoffmann, A. C., Xiang, W., Winner, B., et al. (2016). Infiltrating T lymphocytes reduce myeloid phagocytosis activity in synucleinopathy model. *J. Neuroinflammation* 13:174. doi: 10.1186/s12974-016-0632-5

Sommer, A., Marxreiter, F., Krach, F., Fadler, T., Grosch, J., Maroni, M., et al. (2018). Th17 lymphocytes induce neuronal cell death in a human iPSC-based model of Parkinson's disease. *Cell Stem Cell* 23, 123.e6–131.e6. doi: 10.1016/j.stem.2018.06.015

Song, W. M., and Colonna, M. (2018). The identity and function of microglia in neurodegeneration. *Nat. Immunol.* 19, 1048–1058. doi: 10.1038/s41590-018-0212-1

Stevens, C. H., Rowe, D., Morel-Kopp, M. C., Orr, C., Russell, T., Ranola, M., et al. (2012). Reduced T helper and B lymphocytes in Parkinson's disease. *J. Neuroimmunol.* 252, 95–99. doi: 10.1016/j.jneuroim.2012.07.015

Studer, L. T. J., Parmar, M., and Barker, R. (2019). *G-Force PD Webpage.* Available online at: http://www.gforce-pd.com. Accessed 2019.

Sulzer, D., Alcalay, R. N., Garretti, F., Cote, L., Kanter, E., Agin-Liebes, J., et al. (2017). T cells from patients with Parkinson's disease recognize α-synuclein peptides. *Nature* 546, 656–661. doi: 10.1038/nature22815

Tabata, Y., Imaizumi, Y., Sugawara, M., Andoh-Noda, T., Banno, S., Chai, M., et al. (2018). T-type calcium channels determine the vulnerability of dopaminergic neurons to mitochondrial stress in familial Parkinson disease. *Stem Cell Reports* 11, 1171–1184. doi: 10.1016/j.stemcr.2018.09.006

Tagliafierro, L., Zamora, M. E., and Chiba-Falek, O. (2019). Multiplication of the SNCA locus exacerbates neuronal nuclear aging. *Hum. Mol. Genet.* 28, 407–421. doi: 10.1093/hmg/ddy355

Takahashi, K., Tanabe, K., Ohnuki, M., Narita, M., Ichisaka, T., Tomoda, K., et al. (2007). Induction of pluripotent stem cells from adult human fibroblasts by defined factors. *Cell* 131, 861–872. doi: 10.1016/j.cell.2007.11.019

Tanner, C. M., Kamel, F., Ross, G. W., Hoppin, J. A., Goldman, S. M., Korell, M., et al. (2011). Rotenone, paraquat, and Parkinson's disease. *Environ. Health Perspect.* 119, 866–872. doi: 10.1289/ehp.1002839

Tao, Y., and Zhang, S. C. (2016). Neural subtype specification from human pluripotent stem cells. *Cell Stem Cell* 19, 573–586. doi: 10.1016/j.stem.2016.10.015

Tcw, J., Wang, M., Pimenova, A. A., Bowles, K. R., Hartley, B. J., Lacin, E., et al. (2017). An efficient platform for astrocyte differentiation from human induced pluripotent stem cells. *Stem Cell Reports* 9, 600–614. doi: 10.1016/j.stemcr.2017.06.018

Vasquez, V., Mitra, J., Hegde, P. M., Pandey, A., Sengupta, S., Mitra, S., et al. (2017). Chromatin-bound oxidized α-synuclein causes strand breaks in neuronal genomes in *in vitro* models of Parkinson's disease. *J. Alzheimers Dis.* 60, S133–S150. doi: 10.3233/JAD-170342

Vera, E., Bosco, N., and Studer, L. (2016). Generating late-onset human iPSC-based disease models by inducing neuronal age-related phenotypes through telomerase manipulation. *Cell Rep.* 17, 1184–1192. doi: 10.1016/j.celrep.2016.09.062

Walker, D. G., Terai, K., Matsuo, A., Beach, T. G., McGeer, E. G., and McGeer, P. L. (1998). Immunohistochemical analyses of fibroblast growth factor receptor-1 in the human substantia nigra. Comparison between normal and Parkinson's disease cases. *Brain Res.* 794, 181–187. doi: 10.1016/s0006-8993(98)00132-2

Wang, W., Perovic, I., Chittuluru, J., Kaganovich, A., Nguyen, L. T., Liao, J., et al. (2011). A soluble α-synuclein construct forms a dynamic tetramer. *Proc. Natl. Acad. Sci. U S A* 108, 17797–17802. doi: 10.1073/pnas.1113260108

Winner, B., Jappelli, R., Maji, S. K., Desplats, P. A., Boyer, L., Aigner, S., et al. (2011). *In vivo* demonstration that α-synuclein oligomers are toxic. *Proc. Natl. Acad. Sci. U S A* 108, 4194–4199. doi: 10.1073/pnas.1100976108

Wolf, S. A., Boddeke, H. W. G. M., and Kettenmann, H. (2017). Microglia in physiology and disease. *Annu. Rev. Physiol.* 79, 619–643. doi: 10.1146/annurev-physiol-022516-034406

Woodard, C. M., Campos, B. A., Kuo, S. H., Nirenberg, M. J., Nestor, M. W., Zimmer, M., et al. (2014). iPSC-derived dopamine neurons reveal differences between monozygotic twins discordant for Parkinson's disease. *Cell Rep.* 9, 1173–1182. doi: 10.1016/j.celrep.2014.10.023

Zambon, F., Cherubini, M., Fernandes, H. J. R., Lang, C., Ryan, B. J., Volpato, V., et al. (2019). Cellular α-synuclein pathology is associated with bioenergetic dysfunction in Parkinson's iPSC-derived dopamine neurons. *Hum. Mol. Genet.* 28, 2001–2013. doi: 10.1093/hmg/ddz038

Zhang, Y., Sloan, S. A., Clarke, L. E., Caneda, C., Plaza, C. A., Blumenthal, P. D., et al. (2016). Purification and characterization of progenitor and mature human astrocytes reveals transcriptional and functional differences with mouse. *Neuron* 89, 37–53. doi: 10.1016/j.neuron.2015.11.013

Zuccato, C., and Cattaneo, E. (2009). Brain-derived neurotrophic factor in neurodegenerative diseases. *Nat. Rev. Neurol.* 5, 311–322. doi: 10.1038/nrneurol.2009.54

Check for updates

Long Term Gene Expression in Human Induced Pluripotent Stem Cells and Cerebral Organoids to Model a Neurodegenerative Disease

Ferid Nassor[1,2], Rafika Jarray[1,2], Denis S. F. Biard[1], Auriane Maïza[3], Dulce Papy-Garcia[3], Serena Pavoni[1], Jean-Philippe Deslys[1] and Frank Yates[1,2]*

[1]Service d'Etude des Prions et des Infections Atypiques (SEPIA), Institut François Jacob, Commissariat à l'Energie Atomique et aux Energies Alternatives (CEA), Université Paris Saclay, Fontenay-aux-Roses, France, [2]CellTechs Laboratory, Sup'Biotech, Villejuif, France, [3]Glycobiology, Cell Growth, Tissue Repair and Regeneration (Gly-CRRET), UPEC 4397, Université Paris Est Créteil, Créteil, France

Human brain organoids (mini-brains) consist of self-organized three-dimensional (3D) neural tissue which can be derived from reprogrammed adult cells and maintained for months in culture. These 3D structures manifest substantial potential for the modeling of neurodegenerative diseases and pave the way for personalized medicine. However, as these 3D brain models can express the whole human genetic complexity, it is critical to have access to isogenic mini-brains that only differ in specific and controlled genetic variables. Genetic engineering based on retroviral vectors is incompatible with the long-term modeling needed here and implies a risk of random integration while methods using CRISPR-Cas9 are still too complex to adapt to stem cells. We demonstrate in this study that our strategy which relies on an episomal plasmid vector derived from the Epstein-Barr virus (EBV) offers a simple and robust approach, avoiding the remaining caveats of mini-brain models. For this proof-of-concept, we used a normal tau protein with a fluorescent tag and a mutant genetic form (P301S) leading to Fronto-Temporal Dementia. Isogenic cell lines were obtained which were stable for more than 30 passages expressing either form. We show that the presence of the plasmid in the cells does not interfere with the mini-brain differentiation protocol and obtain the development of a pathologically relevant phenotype in cerebral organoids, with pathological hyperphosphorylation of the tau protein. Such a simple and versatile genetic strategy opens up the full potential of human organoids to contribute to disease modeling, personalized medicine and testing of therapeutics.

Keywords: stem cells, cerebral organoid, neurodegenerative disease, fronto-temporal dementia, Alzheimer, IPS, disease modeling

INTRODUCTION

The prevalence of neurodegenerative diseases has amplified continuously over the years, notably due to an increasingly elderly population, and has become a major concern for many facets of society. The development of accurate modeling tools for human neurodegenerative diseases is therefore of vital interest for public health entities. With the development of human brain organoids, three-dimensional (3D) structures highly reminiscent of certain human brain regions, we are now a step closer to the accurate modeling of the human brain

in vitro (Lancaster et al., 2013). Moreover, with the possibility of reprogramming patient cells to obtain induced pluripotent stem cells (iPSCs) while maintaining the original genetic characteristics of patients, we can now better decipher the events leading to the pathology. One of the initial hurdles identified regarding this model was its incompatibility with the modeling of events occurring late in the evolution of neurodegenerative diseases because of its embryonic/fetal nature (Camp et al., 2015). However, recent publications have shown that the cerebral organoid model is relevant for neurodegenerative diseases: specific markers, such as an imbalance of Aβ secretion, tau hyperphosphorylation and protein aggregation leading to the formation of amyloid fibrils have been described in organoids (Raja et al., 2016; Gonzalez et al., 2018; Pavoni et al., 2018). Nonetheless, one of the major issues for accurate modeling using patient-derived cerebral organoids is the control used for comparison. Indeed, because of the multiplicity of genetic and epigenetic factors when comparing cells from two individuals, there is a risk of missing crucial information (Vitale et al., 2012). To circumvent the issues surrounding this comparison, researchers have used additive (additional??) gene transfer strategies to express proteins of interest in a stable manner using retroviral approaches. Nonetheless, issues such as random integration, viral copy numbers, silencing, etc. hinder the potential of these applications in stem cells, especially in long term modeling approaches, where numerous cell passages and divisions are to be expected (Liew et al., 2007; Xia et al., 2007). Gene editing techniques based on CRISPR-Cas9 in human stem cells (embryonic or induced pluripotent), have been applied to create isogenic cell lines by adding or correcting a mutation (Grobarczyk et al., 2015; Li et al., 2015; Paquet et al., 2016). This novel approach circumvents the difficulty of finding isogenic controls, but the method requires both time and major resources, preventing a wide application of this technology. A different approach applicable to stem cells has been described by several authors with the use of episomal plasmid vectors derived from the Epstein-Barr virus (EBV; Ren et al., 2006; Thyagarajan et al., 2009). This plasmid allows the expression of a transgene able to replicate in the normal cell cycle due to the presence of OriP on the episome, without integration in the genome. The maintenance of the plasmid as an extrachromosomal element in a low-copy state has been attributed to the EBNA-1 region and its maintenance in the cell can be achieved through antibiotic selection (Lupton and Levine, 1985). In this report, the plasmid used was initially designed for gene silencing studies in tumor cell lines and has been extensively studied since (Biard et al., 2005). Existing approaches using EBV-based plasmids have been limited so far to the establishment of proofs of concept in stem cell lines, expressing fluorescent proteins, and do not show long term modeling approaches or validation for disease modeling.

This study describes the use of an EBV-based plasmid for pathological modeling using iPSCs and demonstrates the possibilities of its application in cerebral organoids to obtain isogenic cell lines that differ only in the expression of a single gene of interest. To do so, we developed a model based on a 4R tauopathy, the fronto-temporal dementia, which can be triggered with a mutation in the exon 10 of the MAPT gene, resulting in the conversion of a proline in a serine at the amino acid 301 in the tau protein (P301S; Hutton et al., 1998; Bugiani et al., 1999). This pathology constitutes a proof of concept, as tau protein can be tagged without affecting symptoms of its pathological progression, such as its aggregation capacity, as described by others (Frost et al., 2009). Notably, this pathology has been extensively described as a good modeling approach to understand the tauopathy underlying Alzheimer's disease (Goedert et al., 2012). As described in patients, and elucidated in animal models, this 4R tauopathy manifests the following indications in the brain throughout the pathological progress: a synaptic loss, followed by hyperphosphorylation of the tau protein, leading to neurofibrillary degeneration, ultimately resulting in neuronal loss (Spillantini et al., 1998; Yoshiyama et al., 2007). Our goal in this work is to establish the capacity to model a neurodegenerative disease with episomal vectors on isogenic iPSCs differentiated in cerebral organoids in order to evaluate the development of a pathological state.

MATERIALS AND METHODS

iPSCs Cell Culture

iPSCs were obtained by reprogramming BJ Fibroblasts obtained from ATCC (CRL-2522) in a previous study (Pavoni et al., 2018). Briefly, fibroblasts were reprogrammed using the Sendai virus reprogramming method as recommended by the manufacturer (Life Technologies). iPSCs were grown under feeder-free conditions on Matrigel-coated plates in E8 Flex Medium (Invitrogen). Seventy to eighty percent confluent iPSCs were passaged (ReleSR, Stem Cell Technologies) 1:5 and transferred to new wells in feeder-free conditions and incubated at 37°C, 5% CO_2. Media were changed every 2 days and the cells split every 7 days. When cells possessed an EBV-based plasmid, the passaging medium used contained 0.5 µg/mL of puromycin in order to maintain the vector.

EBV-Based Plasmid Generation

TauWT-YFP or TauP301S-YFP mutant open reading frames were introduced into puromycin-resistant EBV-based plasmid (pEBV) downstream of a CAG promoter to obtain the constructions of interest (Biard et al., 2005).

iPSCs Electroporation

From a 35 mm dish, when iPSCs reached 70–80% confluence, cells were dissociated in a single-cell suspension using accutase. Electroporation was performed using an electro-square-porator (BTX 830, Harvard Apparatus) set on Low Voltage, using a 2 mm wide cuvette in PBS + 125 mM HEPES buffer with 1 pulse at 250 V of 1 ms, followed by three pulses at 50 V of 50 ms at 1 s interval. Ten microgram of plasmid DNA was used per electroporation. After electroporation, cells were plated on a Matrigel-coated plate with ROCK inhibitor (10 µM) present in the media for 24 h.

Characterization of iPSCs

PCR Analysis of Gene Expression

Total RNA was isolated from iPSCs with the NucleoSpin RNA II kit (Macherey Nagel), in accordance with the manufacturer's protocol. One microgram of each RNA sample was used to generate cDNA, with an iScript cDNA Synthesis Kit (Bio-Rad). RT-PCR was performed with the GoTaq DNA Polymerase kit (Promega). PCR products were separated by electrophoresis in a 1% agarose gel and analyzed with Gel Doc-it (UVP). RT-PCR for the 5′ coding region was performed with primers specific for OCT4 (sense primer 5′-AGCGAACCAGTATCGAGAAC-3′ and reverse primer 5′-TTACAGAACCACACTCGGAC-3′), SOX2 (sense primer 5′-AGCTACAGCATGATGCAGGA-3′ and reverse primer 5′-GGTCATGGAGTTGTACTGCA-3′), NANOG (sense primer 5′-TGAACCTCAGCTACAAACAG -3′ and reverse primer 5′-TGGTGGTAGGAAGAGTAAAG-3′), RPLP0 (sense primer 5′-CATTGCCCCATGTGAAGTC-3′ and reverse primer 5′-GCTCCCACTTTGTCTCCAGT-3′), REX1 (sense primer 5′-CAGTCCAGCAGGTGTTTGC-3′ and reverse primer 5′-GCATTCTATGTAACAGTCTGAGA-3′). The analysis was conducted at the population level at two different passages to confirm the presence and maintenance of the expression of pluripotency genes.

Teratoma Formation

iPSCs, whether expressing an EBV-based plasmid or not, were harvested at 70–80% confluence using ReleSR, collected into tubes, and centrifuged. The pellets were suspended in 50% Matrigel (Corning). Approximately 10^6 cells were injected subcutaneously into NSG mice (NOD.Cg-Prkdc[scid] Il2rg[tm1Wjl]/SzJ). Teratomas formed within 8–12 weeks. They were excised and fixed. Histological analysis was performed on sections stained with hematoxylin-eosin. One teratoma assay per cell line was performed. All animals were treated according to protocols approved by the local animal ethics advisory committee, registered with the French Ministry of Research and in accordance with French national regulations (national transposition of European directive 2010/63/CE). All animal experiments were approved by the Commissariat à l'énergie atomique et aux énergies alternatives (CEA), 92265 Fontenay-aux-Roses, France.

Cerebral Organoid Formation

To generate cerebral organoids, we followed our previously described method (Pavoni et al., 2018) with minor modifications. Briefly, embryoid bodies (EBs) were formed by the hanging drop method with 10,000 cells per drop on the inside of a 10 cm dish lid. The lid was then placed on a dish filled with PBS to avoid evaporation. The dishes were transferred to an incubator at 37 C° with 95% relative humidity and 5% CO_2. Media used in EB culture consisted of DMEM/F12 supplemented with KSR (20% v/v), MEM-NEAA (1×), 2-mercaptoethanol (0.1 mM), ROCK inhibitor (50 μM), dual SMAD inhibitors (SB431532 10 μM and LDN193189 100 nM) and bFGF (4 ng/mL). After 2 days, EBs were transferred to a 24-well plate and kept in this media up to day-6. On day 6, the culture medium was replaced with neural induction medium containing DMEM/F12-Glutamax

medium supplemented with N2 supplement (1×), MEM-NEAA (1×) and antibiotic-antimycotic solution (1×). On days 11 and 12 of the protocol, cerebral organoids were embedded in growth factor-reduced Matrigel drops (BD Biosciences) and cultured in ultra-low attachment six-well plates (four cerebral organoids per well) in a differentiation medium containing DMEM/F12-Glutamax and Neurobasal medium (1:1 ratio) supplemented with N2 supplement (0.5×), B27 supplement without vitamin A (1×), 2-mercaptoethanol (0.2 μM), human insulin solution (2.5 μg/ml), MEM-NEAA (0.5×) and antibiotic-antimycotic solution (1×). On days 15 and 16, cerebral organoids were transferred to the same differentiation medium (the same as that described above with B27 supplemented with vitamin A) and the plates were placed in an orbital shaker (Infors) set at 70 rpm. The culture medium was replaced every 7 days.

Western Blot

Cerebral Organoids were collected at 30 days. They were washed twice with PBS, snap-frozen in liquid nitrogen and stored at −80°C. To prepare the tissue homogenates, the samples were thawed partially on ice, resuspended (20% v/v) in ice-cold PBS containing protease (complete cocktail, Roche) and phosphatase inhibitors (50 mM NaF, 0.2 mM $Na_3 3VO_4$) and lysed using a close-fitting rotating plunger. The protein concentration was estimated by the bicinchoninic acid method (BCA, Pierce). The supernatant was resuspended in SDS sample buffer (containing 33 mM dithiothreitol), boiled for 10 min, and electrophoresed through 4–12% Bis-Tris precast gels (Invitrogen). Proteins were transferred onto a PVDF (0.2 μm, Bio-Rad) membrane. Membranes were incubated with 5% non-fat milk for blocking. Phosphorylated tau (p-tau) was identified using the AT8 antibody and total tau (t-tau) using the TAU5 antibody. The blot was subsequently incubated with the appropriate horseradish peroxidase-conjugated secondary antibody. The blots were developed with ECL Plus reagents (Amersham GE Healthcare), and the immunoreactive bands were visualized by scanning with a Bio-Rad image analysis system. Each group of samples analyzed by western blot was collected from three independent cultures.

Statistical Analysis

The data were plotted using GraphPad Prism software. Groups were compared via Student's two-tailed t-test (two groups) or one-way analysis of variance (ANOVA; multiple groups).

RESULTS

Generation of Transgene-Expressing iPSCs

iPSCs obtained from reprogrammed fibroblasts in the laboratory were electroporated with EBV-based plasmids. As shown in **Figure 1A** the EBV-based plasmid expresses resistance to puromycin under an SV40 promoter allowing for an antibiotic selection of the cells. Forty-eight hours post-electroporation, puromycin was added for 24 h and cells then allowed to recover for up to 2 weeks, as shown in **Figure 1B**. After this point, the

FIGURE 1 | Generation of modified induced pluripotent stem cells (iPSCs) using an epstein-barr virus (EBV)-based plasmid. **(A)** Map of the EBV-based plasmid used in iPSCs, transgene expression under CAG promoter regulation, puromycin resistance under SV40 promoter regulation. **(B)** Workflow for EBV-based plasmid expressing iPSCs generation. **(C)** iPSCs colony after 30 passages post-electroporation expressing either wild type Tau 2N4R or mutated (P301S) form fused to YFP.

culture was maintained until colonies are ready for passaging with the expected morphological characteristics as shown in **Supplementary Figure S1**. At each passage, the media was supplemented with puromycin (0.5 µg/ml) for 24 h allowing for the maintenance of the episomal vector in the cells. We did not observe the repression of the reporter YFP gene up to 30 passages in the presence of puromycin (**Figure 1C**).

Characterization of Transgene-Expressing iPSCs

The newly established iPSCs lines maintaining an EBV-based plasmid were characterized to verify whether the presence of the plasmid or the expression of the transgenes interferes with the phenotypical and functional characteristics of pluripotent stem cells. The pluripotency of iPSCs electroporated with the EBV-based plasmid expressing either TauWT-YFP or TauP301S-YFP fusion protein was investigated. This analysis was performed by assessing the expression of the endogenous pluripotency marker genes SOX2, OCT4, NANOG and REX-1 by RT-PCR. RPLP0 gene expression was used as an internal control for this assay. The pluripotency markers were strongly expressed in all iPSC clones but not in the initial fibroblasts as expected and shown in **Figure 2A**. We assayed the teratoma-forming potential of episome-transfected iPSC and carried out a histological analysis of tumors derived from these cells. These teratoma assays provided a clear evaluation of the impact on differentiation and proliferation of these iPSCs *in vivo* over a period of several weeks. Histological analysis of the tumors showed that these cells had differentiated into endodermal, ectodermal and mesodermal tissues (bone precursor, intestinal cavities and melanocytes) as shown in **Figure 2B**. The tissues were well-differentiated, without malignancy, in all the structures observed.

Pathological Modeling Using Cerebral Organoids

Next, for pathological modeling, the cerebral organoid model was used as a method to obtain a heterogeneous composition of neural cells, representative of the complexity of the human brain. Cerebral organoids have already been used for their potential to model neurodegenerative phenotypes (Raja et al., 2016; Gonzalez et al., 2018). Furthermore, we have previously shown that chemical compounds added to the culture medium can induce an imbalance of the Aβ42/Aβ40 ratio comparable to that seen in human Alzheimer's disease patients (Pavoni et al., 2018).

It was first ensured that the modifications introduced to the original Lancaster et al.'s (2013) protocol and the expression of transgenes on the EBV-based plasmid did not interfere with the differentiation steps of our model. *in vitro* differentiation was performed while avoiding antibiotic selection to avoid any toxicity. This choice was also guided by preliminary results showing that the number of divisions occurring to obtain an organoid was compatible with growth in absence of antibiotic selection, without losing the vector. As shown in **Figure 3A**, the differentiation pattern is not hampered by the presence of the episomal vector. Both expression markers and immunohistochemical characterization point towards an internal organization coherent with what has previously been described for the cerebral organoid by others (Lancaster et al., 2013). Real-time PCR analysis shows the presence of different neural cells (Neurons, Astrocytes and Oligodendrocytes) whose proportions increase during culture (**Figure 3B**). On the immunohistochemical sections, the development of a neural stem cell niche can be discerned developing outwards in neuronal cells supported in a radial organization as shown with laminin staining (**Figure 3C**).
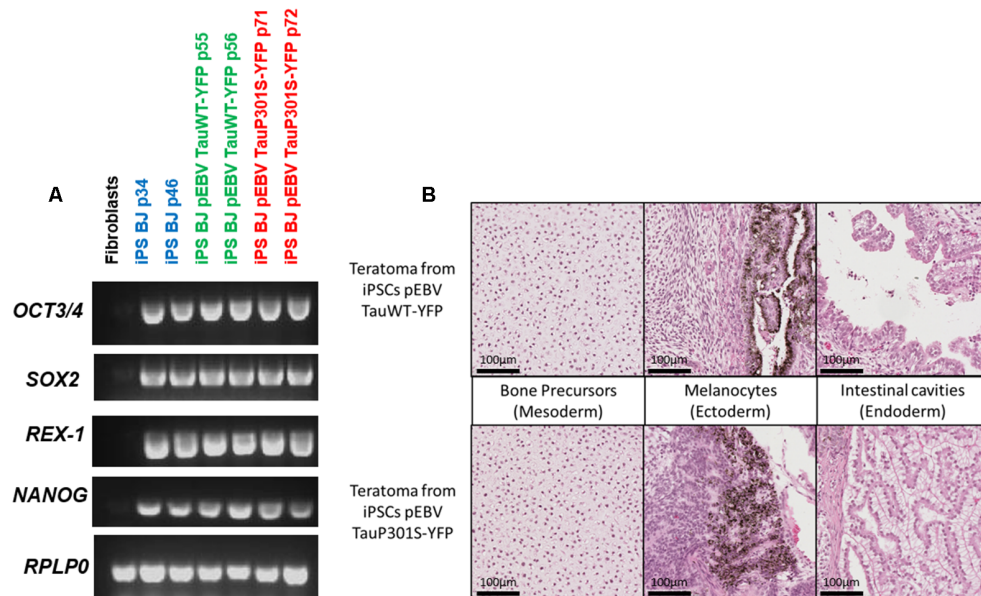
FIGURE 2 | Pluripotency characterization of transgenic iPSCs. **(A)** Assessment of pluripotency by semi-quantitative PCR to confirm the expression of pluripotency markers in the control iPS line BJ and in EBV-based plasmid expressing lines. PCR analysis shows the expression of pluripotency markers OCT4, SOX2, NANOG and REX-1. BJ fibroblasts were used as a control and RPLP0 as a housekeeping gene. **(B)** H&E staining of a section of teratomas obtained from iPSCs expressing either Tau WT or P301S using an EBV-based plasmid showing the development of structures specific to the three germ layers.
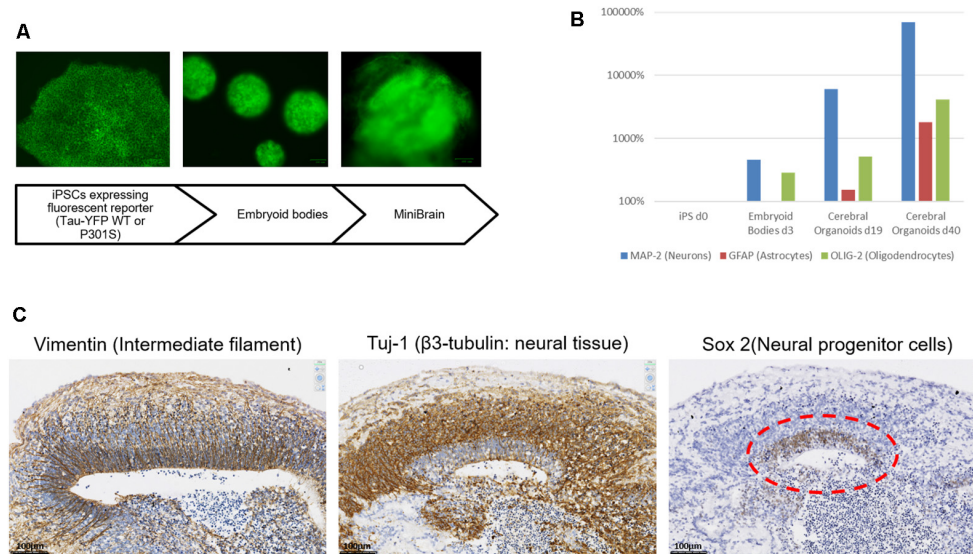
FIGURE 3 | MiniBrain generation with modified iPSCs for pathological modeling. **(A)** Diagram showing the major steps of the MiniBrain protocol from iPSCs to cerebral organoids. **(B)** Real-time PCR analysis shows the expression of different neural markers at different time points in the cerebral organoid formation protocol, MAP-2 for neuron evaluation, GFAP for astrocyte evaluation and Olig-2 for oligodendrocyte evaluation. **(C)** Tissue sections of a 30-day cerebral organoid showing the development of neural rosettes with a radial organization, as shown with vimentin staining. Sox-2 staining reveals a neural stem cell niche, from which a neuronal network is developing as can be seen with the Tuj1 staining.

To verify the continuous presence of the episomally expressed forms of tau a western blot of organoids was performed after 30 days of culture. The DNA construct used, with a protein fused to a fluorescent reporter, enables the endogenous tau to be distinguished from the exogenous tau (i.e., the tau protein translated from the transgene carried by the episomal vector) by the differences in their sizes (addition of 27 kDa due to the YFP). As has been described by others (Yoshiyama et al., 2007), one of the first pathological symptoms of the frontotemporal disease is a hyperphosphorylation of
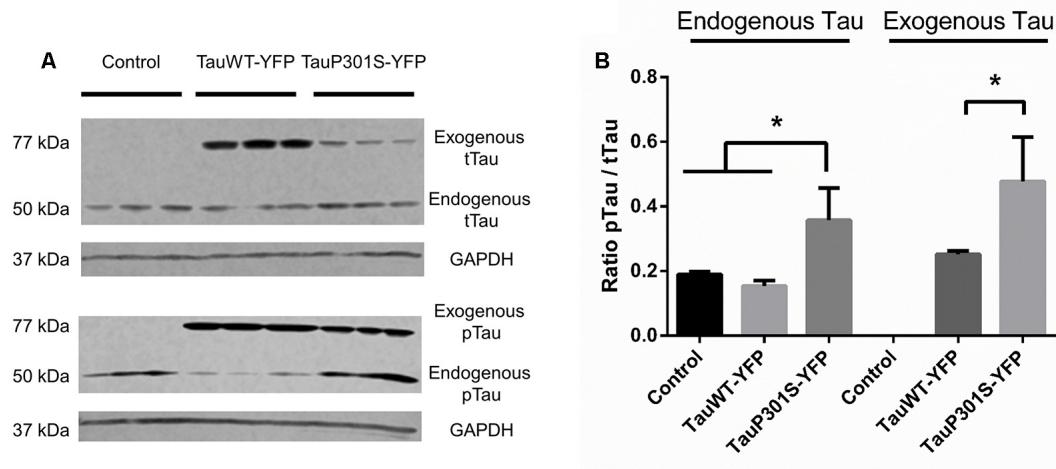
FIGURE 4 | FTD pathological modeling using modified iPSCs expressing an EBV-based plasmid. **(A)** Western Blot analysis of total tau protein (tTau, TAU5 antibody) and phosphorylated tau protein (pTau, AT8 antibody). The expression of a fusion protein enables the endogenously expressed tau protein to be distinguished from the exogeneous form expressed using the EBV-based plasmid. **(B)** Ratio of phosphorylated tau protein over total tau against GAPDH for endogenous and exogenous tau. Statistical analysis: one-way analysis of variance (ANOVA; multiple groups). On charts *$p < 0.05$.

the tau protein. Immunoblotting was therefore performed using the AT8 antibody, recognizing the first site to be phosphorylated of the tau protein in tauopathies, to assess the phosphorylation of the protein and one using TAU5 antibody, recognizing all tau isoforms, to have an estimation of total tau. As shown in **Figure 4**, there are no significant differences between control cells and the overexpression of Tau2N4RWT for the phosphorylation ratio of tau. However, from the P301S overexpression, hyperphosphorylation of the exogenous P301S mutant form compared to controls can be seen, as can hyperphosphorylation of the endogenous form of tau, which is not mutated. These results are also confirmed through IHC, which shows a significant change in the surface ratio of p-tau as shown in **Supplementary Figure S2**.

DISCUSSION

The novel approach described here shows the possibilities offered by an episomal vector for disease modeling using iPSCs in a long-term approach with matching isogenic controls. We have been able to express different proteins using this system and the versatility of the plasmid allows a promoter of interest to be chosen. Here a CAG promoter was used. However, because of the dissociation between the expression of antibiotic resistance and that of the protein of interest, the construct can easily be modified. The establishment of a modified cell line based on electroporation of an EBV-based plasmid has proven to be simple, fast and reliable.

As the episomal vector is extrachromosomal, it allows the expression of transgene without the usual risk of random insertion encountered with lentiviral approaches. In addition, the benefits of the episomal vector approach for other applications is demonstrable, notably in gene therapy (Ehrhardt et al., 2008).

This modeling approach in a cerebral organoid shows that the vector is maintained during differentiation, without measurable silencing and allows the development of a relevant phenotype associated with the disease. In the present case, the absence of measurable protein aggregation can be attributed to a longer development of the disease which provides a rare opportunity to observe the pathology at its source and at a cellular level. For further investigation, artificial aging of our model *in vitro* could be used, as many systems have been described by studying progeroid syndromes. For instance, an inducible progerin expression or a chemically induced telomerase manipulation might provide the necessary cues for modeling aging *in vitro* (Miller et al., 2013; Carrero et al., 2016; Vera et al., 2016).

The methodology used here allows for the development of a pipeline for the large-scale production of isogenic lines for studying genetic diseases with the differentiation in complex models, such as cerebral organoids. However, this same technique could be used in all models based on pluripotent stem cells, becoming the basis for full-body modeling. This, in turn, can allow the advantage to be taken off the full potential of human organoids to contribute to disease modeling, personalized medicine and testing of therapeutics.

DATA AVAILABILITY STATEMENT

The datasets generated for this study are available on request to the corresponding author.

ETHICS STATEMENT

The animal study was reviewed and approved by Commissariat à l'Energie Atomique.

AUTHOR CONTRIBUTIONS

FN, RJ, DB, AM, and SP performed the experiments. FN, RJ, DP-G, J-PD, and FY analyzed the data. FN, RJ, J-PD, and FY conceived the study, wrote and revised the manuscript.

SUPPLEMENTARY MATERIAL

The Supplementary Material for this article can be found online at: https://www.frontiersin.org/articles/10.3389/fncel.2020.000 14/full#supplementary-material.

REFERENCES

Biard, D. S. F., Despras, E., Sarasin, A., and Angulo, J. F. (2005). Development of new EBV-based vectors for stable expression of small interfering RNA to mimick human syndromes: application to NER gene silencing. *Mol. Cancer Res.* 3, 519–529. doi: 10.1158/1541-7786.mcr-05-0044

Bugiani, O., Murrell, J. R., Giaccone, G., Hasegawa, M., Ghigo, G., Tabaton, M., et al. (1999). Frontotemporal dementia and corticobasal degeneration in a family with a P301S mutation in tau. *J. Neuropathol. Exp. Neurol.* 58, 667–677. doi: 10.1097/00005072-199906000-00011

Camp, J. G., Badsha, F., Florio, M., Kanton, S., Gerber, T., Wilsch-Bräuninger, M., et al. (2015). Human cerebral organoids recapitulate gene expression programs of fetal neocortex development. *Proc. Natl. Acad. Sci. U S A* 112, 15672–15677. doi: 10.1073/pnas.1520760112

Carrero, D., Soria-Valles, C., and López-Otín, C. (2016). Hallmarks of progeroid syndromes: lessons from mice and reprogrammed cells. *Dis. Models Mech.* 9, 719–735. doi: 10.1242/dmm.024711

Ehrhardt, A., Haase, R., Schepers, A., Deutsch, M. J., Lipps, H. J., and Baiker, A. (2008). Episomal vectors for gene therapy. *Curr. Gene Ther.* 8, 147–161. doi: 10.2174/156652308784746440

Frost, B., Jacks, R. L., and Diamond, M. I. (2009). Propagation of tau misfolding from the outside to the inside of a cell. *J. Biol. Chem.* 284, 12845–12852. doi: 10.1074/jbc.m808759200

Goedert, M., Ghetti, B., and Spillantini, M. G. (2012). Frontotemporal dementia: implications for understanding Alzheimer disease. *Cold Spring Harb. Perspect. Med.* 2, a006254–a006254. doi: 10.1101/cshperspect. a006254

Gonzalez, C., Armijo, E., Bravo-Alegria, J., Becerra-Calixto, A., Mays, C. E., and Soto, C. (2018). Modeling amyloid-β and tau pathology in human cerebral organoids. *Mol. Psychiatry* 23, 2363–2374. doi: 10.1038/s41380-018-0229-8

Grobarczyk, B., Franco, B., Hanon, K., and Malgrange, B. (2015). Generation of isogenic human IPS cell line precisely corrected by genome editing using the CRISPR/Cas9 system. *Stem Cell Rev. Rep.* 11, 774–787. doi: 10.1007/s12015-015-9600-1

Hutton, M., Lendon, C. L., Rizzu, P., Baker, M., Froelich, S., Houlden, H., et al. (1998). Association of missense and 5'-splice-site mutations in tau with the inherited dementia FTDP-17. *Nature* 393, 702–705. doi: 10.1038/31508

Lancaster, M. A., Renner, M., Martin, C.-A., Wenzel, D., Bicknell, L. S., Hurles, M. E., et al. (2013). Cerebral organoids model human brain development and microcephaly. *Nature* 501, 373–379. doi: 10.1038/nature12517

Li, H. L., Gee, P., Ishida, K., and Hotta, A. (2015). Efficient genomic correction methods in human IPS cells using CRISPR-Cas9 system. *Methods* 101, 27–35. doi: 10.1016/j.ymeth.2015.10.015

Liew, C.-G., Draper, J. S., Walsh, J., Moore, H., and Andrews, P. W. (2007). Transient and stable transgene expression in human embryonic stem cells. *Stem Cells* 25, 1521–1528. doi: 10.1634/stemcells.2006-0634

Lupton, S., and Levine, A. J. (1985). Mapping genetic elements of epstein-barr virus that facilitate extrachromosomal persistence of epstein-barr virus-derived plasmids in human cells. *Mol. Cell. Biol.* 5, 2533–2542. doi: 10.1128/mcb.5.10.2533

Miller, J. D., Ganat, Y. M., Kishinevsky, S., Bowman, R. L., Liu, B., Tu, E. Y., et al. (2013). Human IPSC-based modeling of late-onset disease *via* progerin-induced aging. *Cell Stem Cell* 13, 691–705. doi: 10.1016/j.stem.2013.11.006

Paquet, D., Kwart, D., Chen, A., Sproul, A., Jacob, S., Teo, S., et al. (2016). Efficient introduction of specific homozygous and heterozygous mutations using CRISPR/Cas9. *Nature* 533, 125–129. doi: 10.1038/nature17664

Pavoni, S., Jarray, R., Nassor, F., Guyot, A.-C., Cottin, S., Rontard, J., et al. (2018). Small-molecule induction of Aβ-42 peptide production in human cerebral organoids to model Alzheimer's disease associated phenotypes. *PLoS One* 13:e0209150. doi: 10.1371/journal.pone.0209150

Raja, W. K., Mungenast, A. E., Lin, Y.-T., Ko, T., Abdurrob, F., Seo, J., et al. (2016). Self-organizing 3D human neural tissue derived from induced pluripotent stem cells recapitulate Alzheimer's disease phenotypes. *PLoS One* 11:e0161969. doi: 10.1371/journal.pone.0161969

Ren, C., Zhao, M., Yang, X., Li, D., Jiang, X., Wang, L., et al. (2006). Establishment and applications of epstein-barr virus-based episomal vectors in human embryonic stem cells. *Stem Cells* 24, 1338–1347. doi: 10.1634/stemcells.2005-0338

Spillantini, M. G., Bird, T. D., and Ghetti, B. (1998). Frontotemporal dementia and parkinsonism linked to chromosome 17: a new group of tauopathies. *Brain Pathol.* 8, 387–402. doi: 10.1111/j.1750-3639.1998.tb00162.x

Thyagarajan, B., Scheyhing, K., Xue, H., Fontes, A., Chesnut, J., Rao, M., et al. (2009). A single EBV-based vector for stable episomal maintenance and expression of GFP in human embryonic stem cells. *Regen. Med.* 4, 239–250. doi: 10.2217/17460751.4.2.239

Vera, E., Bosco, N., and Studer, L. (2016). Generating late-onset human IPSC-based disease models by inducing neuronal age-related phenotypes through telomerase manipulation. *Cell Rep.* 17, 1184–1192. doi: 10.1016/j.celrep.2016.09.062

Vitale, A. M., Matigian, N. A., Ravishankar, S., Bellette, B., Wood, S. A., Wolvetang, E. J., et al. (2012). Variability in the generation of induced pluripotent stem cells: importance for disease modeling. *Stem Cells Transl. Med.* 1, 641–650. doi: 10.5966/sctm.2012-0043

Xia, X., Zhang, Y., Zieth, C. R., and Zhang, S.-C. (2007). Transgenes delivered by lentiviral vector are suppressed in human embryonic stem cells in a promoter-dependent manner. *Stem Cells Dev.* 16, 167–176. doi: 10.1089/scd.2006.0057

Yoshiyama, Y., Higuchi, M., Zhang, B., Huang, S. M., Iwata, N., Saido, T. C., et al. (2007). Synapse loss and microglial activation precede tangles in a P301S tauopathy mouse model. *Neuron* 53, 337–351. doi: 10.1016/j.neuron.2007.01.010

Antidepressant Paroxetine Exerts Developmental Neurotoxicity in an iPSC-Derived 3D Human Brain Model

Xiali Zhong[1,2], Georgina Harris[1], Lena Smirnova[1], Valentin Zufferey[3],
Rita de Cássia da Silveira e Sá[4], Fabiele Baldino Russo[5], Patricia Cristina Baleeiro Beltrao
Braga[5,6], Megan Chesnut[1], Marie-Gabrielle Zurich[3], Helena T. Hogberg[1],
Thomas Hartung[1,7] and David Pamies[1,3]*

[1]Center for Alternatives to Animal Testing (CAAT), Johns Hopkins Bloomberg School of Public Health, Baltimore, MD, United States, [2]Guangdong Provincial Key Laboratory of Food, Nutrition and Health, Department of Toxicology, School of Public Health, Sun Yat-sen University, Guangzhou, China, [3]Department of Physiology, Lausanne and Swiss Centre for Applied Human Toxicology (SCAHT), University of Lausanne, Lausanne, Switzerland, [4]Department of Physiology and Pathology, Federal University of Paraíba, João Pessoa, Brazil, [5]Department of Microbiology, Institute of Biomedical Sciences, University of São Paulo, São Paulo, Brazil, [6]Department of Obstetrics, School of Arts Sciences and Humanities, São Paulo, Brazil, [7]CAAT-Europe, University of Konstanz, Konstanz, Germany

Selective serotonin reuptake inhibitors (SSRIs) are frequently used to treat depression during pregnancy. Various concerns have been raised about the possible effects of these drugs on fetal development. Current developmental neurotoxicity (DNT) testing conducted in rodents is expensive, time-consuming, and does not necessarily represent human pathophysiology. A human, *in vitro* testing battery to cover key events of brain development, could potentially overcome these challenges. In this study, we assess the DNT of paroxetine—a widely used SSRI which has shown contradictory evidence regarding effects on human brain development using a versatile, organotypic human induced pluripotent stem cell (iPSC)-derived brain model (BrainSpheres). At therapeutic blood concentrations, which lie between 20 and 60 ng/ml, Paroxetine led to an 80% decrease in the expression of synaptic markers, a 60% decrease in neurite outgrowth and a 40–75% decrease in the overall oligodendrocyte cell population, compared to controls. These results were consistently shown in two different iPSC lines and indicate that relevant therapeutic concentrations of Paroxetine induce brain cell development abnormalities which could lead to adverse effects.

Keywords: paroxetine, SSRI, organoid, neurotoxicity, developmental neurotoxicity, 3D, iPSC

INTRODUCTION

Between 7 and 12% of pregnant women suffer from depression (Bennett et al., 2004). Selective serotonin reuptake inhibitors (SSRIs) are one of the most commonly used treatments (Andrade et al., 2008; Alwan et al., 2011). Several concerns about the possible developmental neurotoxicity (DNT) effects of different SSRIs have been raised over the years (i.e., antidepressants such as fluoxetine, paroxetine, citalopram, and sertraline). Indeed, neurobehavioral studies involving SSRIs have shown adverse effects on neonates (Zeskind and Stephens, 2004; Alwan and Friedman, 2009; Gentile and Galbally, 2011), infants and young children.

Paroxetine was shown to cross the placental barrier (Hendrick et al., 2003) and was often the center of attention for possible adverse effects (Nevels et al., 2016), including autism

(Posey et al., 1999; Harrington et al., 2013; Boukhris et al., 2016). Croen et al. (2011) followed 145,456 full-term infants for a total of 904,035 person-years; they reported increased risk from 1% to 1.87%, with a 95% CI of 1.15–3.04, but several shortcomings of the study were noted (Croen et al., 2011; Nevels et al., 2016). A systematic review in 2016 (Boukhris et al., 2016) reported an odds ratio of 2.13 (95% CI: 1.66–2.73) for developing autism in children prenatally exposed to SSRIs compared to an odds ratio of 1.81 (95% CI: 1.47–2.24) in those unexposed.

The use of paroxetine in pregnancy has declined substantially (Meunier et al., 2013) due to the US FDA warning in 2005 regarding the potential risk for cardiac defects in the fetus (Cole et al., 2007) and some evidence of major congenital malformations, especially in children (Berard et al., 2016; Gao et al., 2018). However, the effects are not clear and there are contradictory results (Ellfolk and Malm, 2010; Alwan et al., 2016). Even though the use during the first trimester is contraindicated, paroxetine is still used later in pregnancy and during breastfeeding. To the best of our knowledge, there are no studies that explore the consequences of long-term exposure of the developing brain to SSRIs. In this project, we aim to study the possible deleterious effects of the SSRI paroxetine may exert on different key processes during brain development.

DNT is of high concern, however, no routine testing for DNT is carried out in any regulatory program worldwide. Indeed, DNT testing is not required unless triggered by the observation of neurotoxic or endocrine effects in adult rodents. Furthermore, as described in the OECD guidelines, DNT experiments are also extremely expensive (1.4 million per substance), as well as time- and animal-consuming (1,400 pups per compound). Moreover, human brain complexity may not be completely reflected in animal models. The same shortcomings apply for toxicity testing of drugs developed in the pharmaceutical industry. Thus, thousands of drugs and chemicals reach the market without proper classification regarding DNT.

There is consensus in the field that more reliable and efficient screening and assessment tools are required for better identification and evaluation of DNT chemicals and drugs. Over the last 15 years, there has been a process to develop an *in vitro* testing battery to cover key events of neurodevelopment, such as neural stem cell proliferation and differentiation, migration, neurite outgrowth, synaptogenesis, neuronal network formation, myelination, and apoptosis (Bal-Price et al., 2012; Smirnova et al., 2014). Furthermore, the use of more human-relevant models, based on 3D organotypic induced pluripotent stem cell (iPSC)-derived systems, has been recommended as an alternative to classical *in vitro* models (Bal-Price et al., 2012; Fritsche et al., 2018a,b; Smirnova et al., 2018).

The previously described 3D human iPSC-derived brain model (BrainSpheres) recapitulates some of the key events of neurodevelopment (Pamies et al., 2017). BrainSpheres are very reproducible in terms of size and cellular composition and do not display necrotic centers. They not only contain neurons and astrocytes but also functional oligodendrocytes with 40–50% axonal myelination, which is rarely observed *in vitro* (Pamies et al., 2017). In this study, we used the BrainSphere model to study the effects of paroxetine on different processes of brain development. Exposure to human-relevant therapeutic blood concentrations of paroxetine (Tomita et al., 2014) led to alterations in synaptic markers expression, myelination, neurite outgrowth and oligodendrocyte numbers in BrainSpheres differentiated from two independent iPSCs lines, strongly suggesting paroxetine as a DNT toxicant.

MATERIALS AND METHODS

Chemicals and Exposure

Paroxetine was supplied by Sigma. A stock of 10 µg/ml was prepared in DMSO Hybri-Max (Sigma) and stored at −20°C. DMSO (0.072%) was used as vehicle control to match the amount of DMSO in the highest paroxetine concentration of 60 ng/ml.

BrainSphere Differentiation

The CRL-2097 line was derived from CCD-1079Sk ATCC® CRL-2097™ fibroblasts purchased from ATCC and was kindly provided by Dr. Hongjun Song within our joint NIH NCATS funded project (Pamies et al., 2017; #1U18TR000547-01). The iPS2C1 line was kindly provided by Dr. Herbert Lachman. All studies followed Institutional Review Board protocols approved by the Johns Hopkins University School of Medicine. Differentiation from iPSCs to NPCs has been previously described (Wen et al., 2014). The BrainSpheres were generated as described in Pamies et al. (2017). Briefly, at 90% confluency, NPCs were detached mechanically and counted. The 2×10^6 cells per well were plated in uncoated six well-plates. After 2 days, NPC medium was changed to differentiation medium (Neurobasal® electro Medium (Gibco) supplemented with 2% B-27® Electrophysiology (Gibco), 1% Glutamax (Gibco), 0.01 µg/ml human recombinant GDNF (Gemini), 0.01 µg/ml human recombinant BDNF (Gemini). Cultures were kept at 37°C in an atmosphere of 5% CO_2 under constant gyratory shaking (88 rpm, 19 mm orbit) for up to 8 weeks. The medium was partly exchanged three times a week.

Cell Viability

Cytotoxicity to BrainSpheres was assessed after exposure to 0, 20 and 60 ng/ml of paroxetine continuously for 8 weeks. After drug exposure, resazurin reduction assay was performed. One-hunderd microliter of 2 mg/ml Resazurin were added directly to 6-well plates (2 ml/well). The plates were incubated for 3 h at 37°C, 5% CO_2. Subsequently, 50 µl of medium from each well were transferred to 96-well plates and the fluorescence of resorufin was measured at 530 nm/590 nm (excitation/emission) using a multi-well fluorometric reader CytoFluor series 4000 (PerSeptive Biosystems, Inc., Framingham, MA, USA). To determine statistical significance, an one-way ANOVA test was performed with *post hoc* Bonferroni test. All data given are the means ± SD of three independent experiments performed with three technical replicates in both cell lines.

Mitochondrial Membrane Potential Assay

Mitochondrial dysfunction was measured by MitoTracker Red CMXRos (Life Technologies, Carlsbad, CA, USA) following the protocol described in Pamies et al. (2018). Briefly, after 8 weeks of

exposure to 0, 20 or 60 ng/ml of paroxetine, 10 BrainSpheres per condition were plated in 24-well-plates (500 μl). One microliter of MitoTracker Red CMXRos was added to the medium and incubated for 30 min at 37°C, 5% CO_2. The BrainSpheres were then washed twice and fixed with 4% paraformaldehyde (PFA) for 1 h and washed again twice with PBS. The Shandon Immuno-Mount (Thermo Fisher Scientific, Waltham, MA, USA) was used to mount the spheroids onto microscope cover slides (Thermo Fisher Scientific, Waltham, MA, USA). Images were taken using a Olympus BX60. The fluorescence was quantified using ImageJ software[1] and normalized to the size of the aggregates. To determine statistical significance, one-way ANOVA was performed with *post hoc* Bonferroni test. All data given are the means ± SD of three independent experiments performed with 10 technical replicates.

Immunohistochemistry

BrainSpheres were collected at 8 weeks of differentiation, washed three times for 5 min with PBS and fixed with 4% PFA for 1 h at room temperature followed by two washing steps with PBS. BrainSpheres were incubated for 1 h in blocking solution consisting of 5% normal goat serum (NGS) in PBS with 0.4% Triton-X100 (Sigma). BrainSpheres were then incubated for 48 h at 4 °C with a combination of primary antibodies (**Table 1**) diluted in PBS containing 3% NGS and 0.1% Triton-X100. After this incubation, BrainSpheres were washed three times for 15 min in 1× PBS and incubated 1 h with secondary antibodies (**Table 1**) diluted in PBS with 3% NGS at room temperature. Subsequently, BrainSpheres were washed three times for 5 min each with PBS, the nuclei were stained with Hoechst 33342 (1:10,000, Thermo Fisher Scientific, Waltham, MA, USA) for 60 min. BrainSpheres were mounted on glass slides by using Shandon Immu-mount. The images were taken using a Zeiss UV-LSM 510 confocal microscope and a Zeiss LSM 780 GaAsP.

Neuronal Synaptic Pixel Quantification

After 8 weeks of differentiation, BrainSpheres were fixed and stained for synaptophysin (SYP, pre-synaptic protein; **Table 1**), along with Neurofilament Protein (NF200; **Table 1**), for cell identification. In addition, the same final cell density was confirmed by Hoechst staining for each condition. Immunofluorescent images were taken randomly for each condition at 63× and SYP pixels were quantified after three-dimensional reconstruction of z-stack confocal images considering the number of pixels for neurite length, using ImageJ. Quantification was performed blindly.

Western Blot Analysis

BrainSpheres were collected after paroxetine exposure for 8 weeks. One-hundred and fifty micro liter RIPA lysis buffer (Sigma–Adrich, St. Louis, MO, USA) containing 1× protease inhibitor cocktails (Sigma–Adrich, St. Louis, MO, USA) was added to each sample and incubated on ice for 30 min to lyse the cells. Then the samples were centrifuged at 12,000 rpm, 4°C for 15 min, the supernatant was transferred to a new tube and incubated with pierce[TM] lance marker reducing

sample buffer (Thermo Fisher Scientific, Waltham, MA, USA) at 95°C for 5 min. The protein concentration was measured with the pierce[TM] BCA protein assay kit (Thermo Fisher Scientific, Waltham, MA, USA). A total of 30 μg protein was separated on a 4–15% gradient SDS-polyacrylamide gel with 80 V for 120 min and transferred to a polyvinylidene difluoride membrane by electroblotting with 200 mA on ice for 2 h. The non-specific membrane binding was blocked with a blocking solution (PBS, 0.5% Tween-20, 5% non-fat dry milk, pH 7.4) for 1 h at room temperature. Subsequently, the membrane was incubated with primary antibodies Synaptophysin, 1:800, Sigma–Adrich, St. Louis, MO, USA; PSD95, 1:1,000, Thermo Fisher Scientific, Waltham, MA, USA; GAPDH, 1:1,000, Cell Signaling Technology, Danvers, MA, USA) in blocking solution overnight at 4°C. The membrane was washed thoroughly with PBS-T and incubated with HRP-conjugated goat anti-mouse or goat-anti-rabbit secondary antibodies anti-mouse, 1:3,000, BIO-RAD; anti-rabbit, 1:2,000, Cell Signaling Technology, Danvers, MA, USA)in blocking solution at room temperature for 1 h. The blotting bands were detected by chemiluminescence reagent plus (BIO-RAD, Hercules, CA, USA), and exposed to the X-ray film.

Neurite Outgrowth and Astrocytes Staining

BrainSpheres were cultivated as described above. After 8 weeks of exposure to 0, 20 or 60 ng/ml of paroxetine, BrainSpheres were seeded on Matrigel[TM] (BD Biosciences) pre-coated, flat-bottom, black 24-well plates (Thermo Fisher Scientific, Waltham, MA, USA). After 24 h, the BrainSpheres were fixed in 4% PFA, stained with anti-β-III-Tubulin (neuronal marker) and GFAP (astrocytes marker) as described above and imaged using a confocal microscope Zeiss UV-LSM 510 and analyzed using the Sholl ImageJ Software[2]. For data analysis, the number of intersections/distance from spheroid center was calculated and the mean plotted. Significance was calculated by using the Area Under the Curve. ANOVA with Dunnett's post-test was performed comparing each treatment with the control. $**P < 0.01$. Intersections were counted after 300 μm diameter (average size of the spheroids).

Oligodendrocyte Quantification

BrainSpheres were exposed for 8 weeks to 0, 20 or 60 ng/ml of Paroxetine, fixed with 4% PFA and stained with anti-O4 antibody. Immunohistochemistry was performed as described above. O4-positive cells were counted in four different experiments by four different individuals, median and standard deviation (SD) were calculated from the count of each individual.

RESULTS

Therapeutic Concentrations of Paroxetine Do Not Alter Cell Viability, Mitochondrial Function and Neuronal/Astrocyte Phenotype

To determine, if therapeutic concentrations could produce general cytotoxicity, resazurin assay, and mitotracker analysis

---

[1]https://imagej.nih.gov/ij/

[2]https://imagej.net/Sholl_Analysis

TABLE 1 | Primary antibodies for immunohistochemistry.

Antibody	Host	Type	Source	Dilution
NF200	Rabbit	Polyclonal	Sigma	1:200
GFAP	Rabbit	Polyclonal	Dako	1:500
βTUBIII	Rabbit	Polyclonal	R&D	1:200
S100β	Rabbit	Polyclonal	Santa Cruz	1:200
O4	Mouse	Monoclonal	R&D	1:200
O1	Mouse	Monoclonal	Millipore	1:500
MBP	Mouse	Monoclonal	Biolegend	1:200
Synaptophysin	Mouse	Monoclonal	Sigma	1:200
PSD95	Rabbit	Monoclonal	Life technologies	1:200
Secondary antibodies for immunohistochemistry				
Alexa Fluor 488 goat anti-mouse			Life Technologies	1:500
Alexa Fluor 658 goat anti-rabbit			Life Technologies	1:500

were performed after 8 weeks of exposure to paroxetine (0, 20 and 60 ng/ml) in two cell lines (**Figures 1A,B** and data not shown). No significant difference in cell viability and mitochondrial membrane potential (**Figure 1C**) was observed at the concentrations studied. Immunohistochemistry for astrocyte markers (S100β and GFAP) and neuronal markers (NF200 and βTUBIII) also showed no changes upon exposure to paroxetine (**Figure 1D**).

Paroxetine Exposure Alters the Expression of Synaptic Markers in BrainSpheres

BrainSpheres were exposed to therapeutic-relevant paroxetine concentrations (Tomita et al., 2014) for the 8 weeks of differentiation. After 8 weeks of treatment, BrainSpheres were collected, fixed and stained with different antibodies as described in materials and methods. SYP quantification showed a statistically significant decrease in this marker in BrainSpheres generated from both iPSC lines (**Figure 2A**). In the iPS2C1 line, a 60 and 70% decrease in SYP staining was observed, at both concentrations. The CLR-2097 line showed a dose-dependent reduction of approximately 40 and 80%, at 20 and 60 ng/ml, respectively (**Figure 2A**). Western blot results confirmed the decrease in SYP and PSD95 markers in both iPSC lines (**Figures 2B,C**). By western blot, a stronger effect on SYP levels was observed in the iPS2C1 line. The CLR-2097 line showed a dose-dependent decrease in SYP, similar to the immunohistochemistry quantification results (**Figures 2A,B**). Paroxetine exposure also decreased a post-synaptic marker (PSD95) in both cell lines but to a lesser extent than SYP, as shown by immunohistochemistry (**Figure 2D**). These results show a consistent decrease in SYP and PSD95 markers after paroxetine exposure which may result in adverse effects on synaptogenesis during neural differentiation.

BrainSpheres Neurite Outgrowth Capability Is Reduced After Paroxetine Exposure

BrainSpheres were cultivated for 8 weeks with and without the presence of paroxetine (20 or 60 ng/ml). In order to quantify neurite outgrowth, BrainSpheres were attached to Matrigel-coated 24-well plates after 8 weeks of exposure to paroxetine and cultured for further 24 h. Neurite outgrowth analysis

showed a consistent statistically significant decrease in neurite density in both cell lines treated with 60 ng/ml of paroxetine in different experiments (**Figures 3A,C**). The iPS2C1 line showed a higher number of neurites and in consequence a higher number of intersections (**Figure 3A**). iPS2C1-derived BrainSpheres presented reproducibility across experiments with around 187 ± 35 intersections 400 μm from the BrainSphere center in experiment 1 and 178 ± 39 intersections 410 μm from the BrainSphere center in experiment 2. Cells treated with 60 ng/ml presented a 60% decrease in the number of intersections (neurites). However, some variability was found at 20 ng/ml exposure (light green, **Figure 3C**); leading to a statistically significant dose-dependent decrease in number of neurites in experiment 1 and no effects compared to control in experiment 2 (**Figure 3C**). In the CRL-2097 line, BrainSpheres presented a maximum of intersections 114 ± 26 at 290 μm from the center, with a 25% decrease in the number of neurites at both 20 and 60 ng/ml. The area under the curve was used to compare treatments with controls, showing a consistent decrease in number of neurites at 60 ng/ml and significant change in two of three experiments at 20 ng/ml paroxetine treatment (**Figure 3C**). Since we observed that 20 ng/ml paroxetine reduced neurite outgrowth in two out of three experiments performed in two lines, and 60 ng/ml paroxetine reduced neurite outgrowth consistently in all experiments, we concluded that paroxetine at therapeutic concentrations has the potential to affect neurite outgrowth during brain development. Additionally, no changes were observed in astrocyte morphology by immunostaining after treatments with paroxetine (**Figures 1C, 3B**).

Paroxetine Affects Oligodendrocyte Population

BrainSpheres were cultivated for 8 weeks in the presence and absence of paroxetine (0, 20 or 60 ng/ml). After 8 weeks of treatment, BrainSpheres were collected, fixed and stained with different antibodies as described in materials and methods (**Figures 4A,C**). Although O1 is considered a marker for mature oligodendrocytes and O4 a marker for immature oligodendrocytes, both antibodies presented a similar pattern within BrainSpheres (**Figures 4A,D**). This co-expression of O4 and O1 has been described by several authors (Silbereis et al., 2010; Fröhlich et al., 2011; Traiffort et al., 2016). The
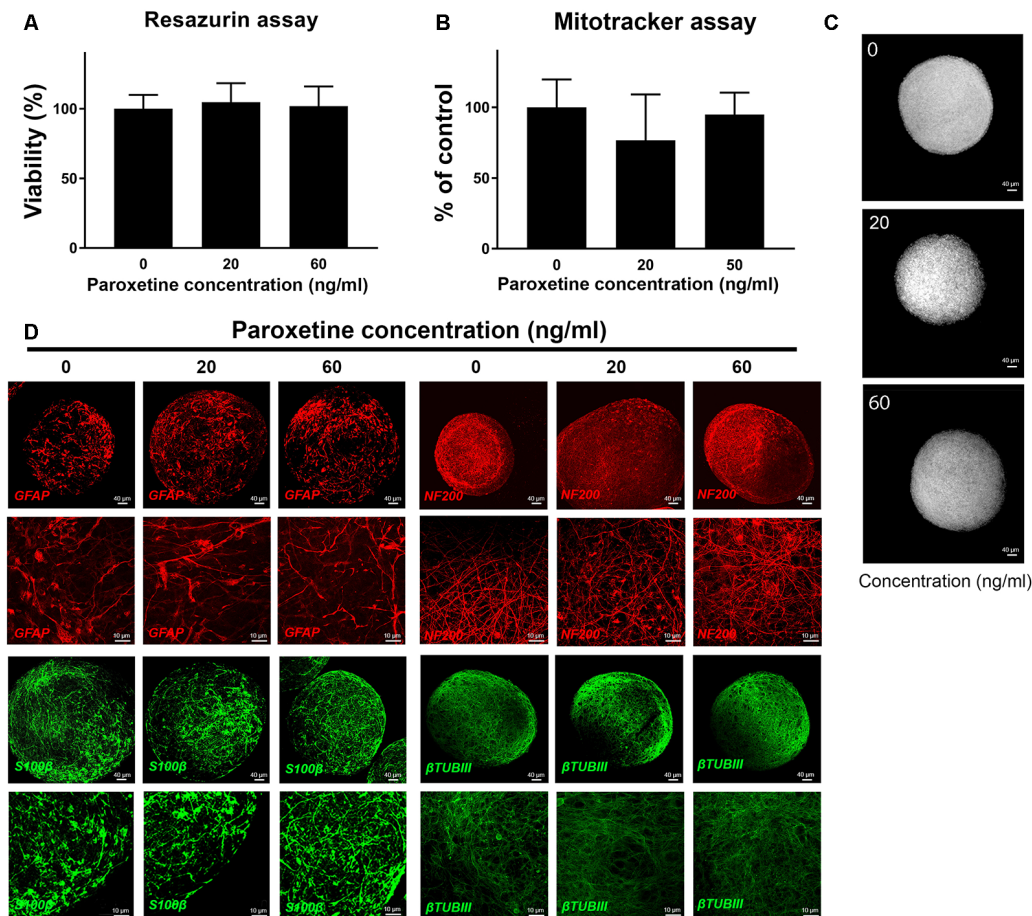
FIGURE 1 | Cell viability, mitochondria function and immunohistochemistry of BS after exposure to paroxetine. BrainSpheres were treated during the differentiation process (8 weeks) with 20 or 60 ng/ml paroxetine. This is a representative figure of the experiment performed, both cell lines have shown similar results. **(A)** Percentage of viable cells in paroxetine-treated BrainSpheres, normalized to the vehicle control as measured by resazurin assay. Data are presented as mean ± SD from three independent experiments. **(B)** Mitochondrial membrane potential measured (MMP) by mitotracker assay. Vehicle-treated control was used to set 100% MMP. **(C)** Representative images of mitotracker assay. **(D)** Immunohistochemistry with astrocyte markers (GFAP, S100β) and neuronal markers (NF200, βTUBIII).

fact that cells in this model still express O4 indicates that in the BrainSpheres, oligodendrocytes do not reach full maturation within 8 weeks. Since, O4 presented better cell body definition and less background immunostaining, it was selected for oligodendrocyte quantification in four independent experiments that were performed, two per cell line. Confocal images for O4 (**Supplementary Figure S1**) were blindly quantified by four different experimenters and represented graphically (**Figure 4B**). The results showed a statistically significant decrease of O4-positive cells in all BrainSpheres treated with paroxetine except in the second experiment using the iPS2C1 line treated with 60 ng/ml paroxetine where the observed decrease was not significant. Myelination of axons was quantified in one independent experiment (10 replicates) as described in material and methods and was decreased in paroxetine-treated BrainSpheres (**Supplementary Figure S2**). A decrease in myelination was observed in further three experiments with both cell lines, however, were not quantified due to noisy staining with the MBP antibody.

DISCUSSION

Paroxetine, a SSRI is contraindicated during the first trimester of pregnancy mainly because of the increased risk of cardiac and other congenital malformations (Cole et al., 2007). However, this drug is still used after this period (second and third trimester) as well as during breastfeeding (Orsolini and Bellantuono, 2015). Very few studies can be found addressing neurobehavioral effects after chronic prenatal exposure to paroxetine, however, negative effects have been reported in neonates (Zeskind and Stephens, 2004; Alwan et al., 2007; Gentile and Galbally, 2011; Klinger et al., 2011), infants and young children (Casper et al., 2003, 2011; Oberlander et al., 2005, 2010; Klinger et al., 2011; Harrington et al., 2013; Rai et al., 2013). Rat studies have shown that pharmacological or genetic modifications of serotonin levels in the developing brain produce adverse effects on adult emotional behavior (Lisboa et al., 2007; Olivier et al., 2011; Glover et al., 2015; Glover and Clinton, 2016; Zohar et al., 2016). In addition, studies in infants whose mothers were treated
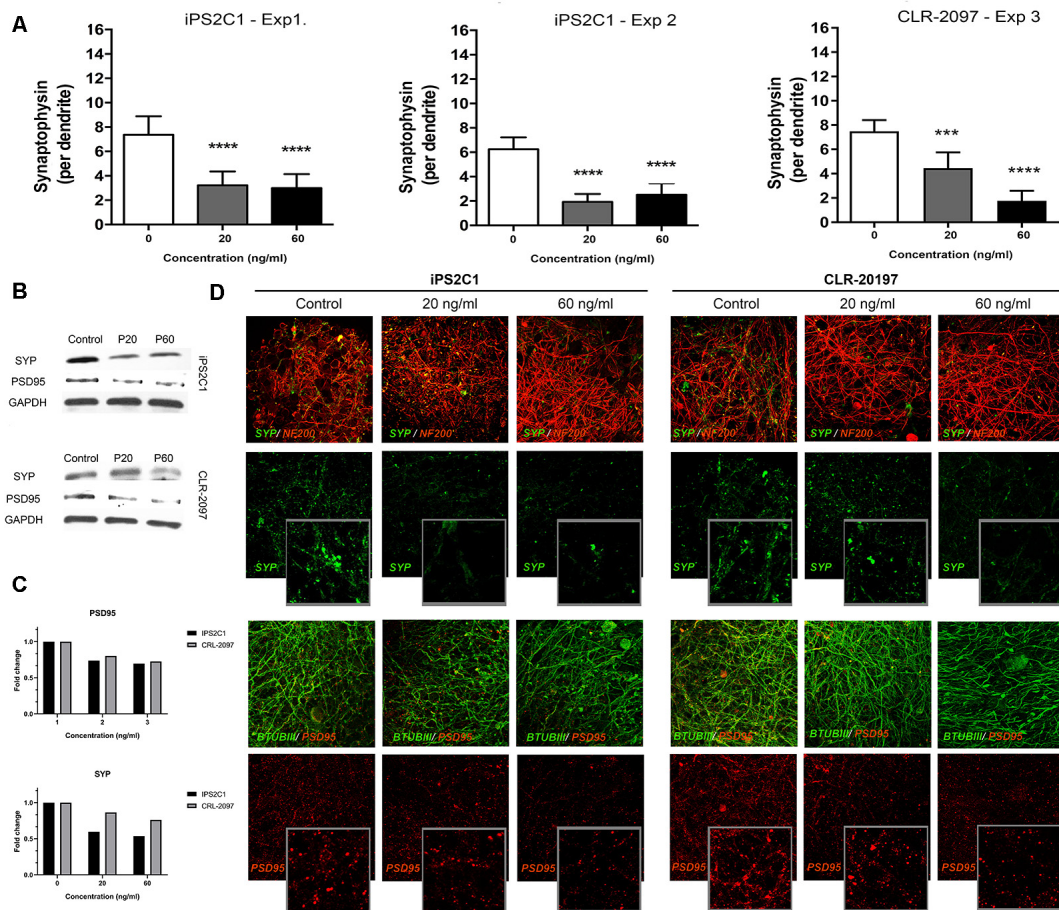
FIGURE 2 | Synaptic markers analysis after paroxetine exposure. BrainSpheres were exposed to paroxetine (0, 20 or 60 ng/ml) for 8 weeks of differentiation. After 8 weeks BrainSpheres were collected to perform immunohistochemistry and Western blot. **(A)** Blinded quantification of synaptophysin (SYP) pixels after three-dimensional reconstruction of z-stack confocal images from three different experiments (two for iPS2C1 and one for CLR-2097). At least 10 spheroids were imaged for each experiment. **(B)** Western blot analyses of SYP, PSD95, and GAPDH. **(C)** Densitometry of western blot analysis. **(D)** Representative images for synaptic markers. Upper panel: SYP (green) co-stained with neuronal marker NF200 (red); lower panel: postsynaptic marker PSD95 (red) co-stained with neuronal marker βTUBIII (green). ***$P < 0.01$; ****$P < 0.001$.

with paroxetine during breastfeeding have shown deficits in alertness, sleepiness, irritability, as well as low body temperature, uncontrollable crying, eating and sleeping disorders (Costei et al., 2002; Hale et al., 2010; Uguz and Arpaci, 2016; Uguz, 2018). However, it has remained a challenge to correlate these symptoms with exposure to paroxetine during development (National Library of Medicine, 2006).

First and early second trimesters of pregnancy are vital for the development of the heart (Mäkikallio et al., 2005; Valenti et al., 2011). Serotonin plays an important role in heart formation and has been reported to be involved in the regulation of proliferation in the embryonic heart (Frishman and Grewall, 2000; Nebigil et al., 2000, 2003; Nebigil and Maroteaux, 2001). Deregulation of this developmental process by the excess of serotonin due to paroxetine treatment during the first trimester of pregnancy may explain cardiac malfunction. The much longer duration needed for proper brain development, which extends until adolescence (Epstein,

1986), increases the period of vulnerability of the brain to developmental toxins.

Serotonin plays an important role in cognitive processes, such as memory and learning (Berridge et al., 2009) and is crucial during brain development (Buznikov et al., 2001). Therefore, subtle modulation of serotonin levels by paroxetine during brain development may have important deleterious consequences later in life. Manipulations of serotonin levels in rodent brains during early development were shown to alter the formation of the whisker (barrel) representation in the primary somatosensory cortex and promote aggressive and/or anxiety-related behaviors (Cases et al., 1995; Persico et al., 2000, 2001; Holmes et al., 2003). Behavioral changes were also observed when serotonin levels are modified in rodents' early-life (Welker et al., 1996; Yang et al., 2001; Esaki et al., 2005).

Effects of paroxetine on key processes of brain development have to be established in order to evaluate its potential DNT. However, current DNT testing is facing numerous challenges.
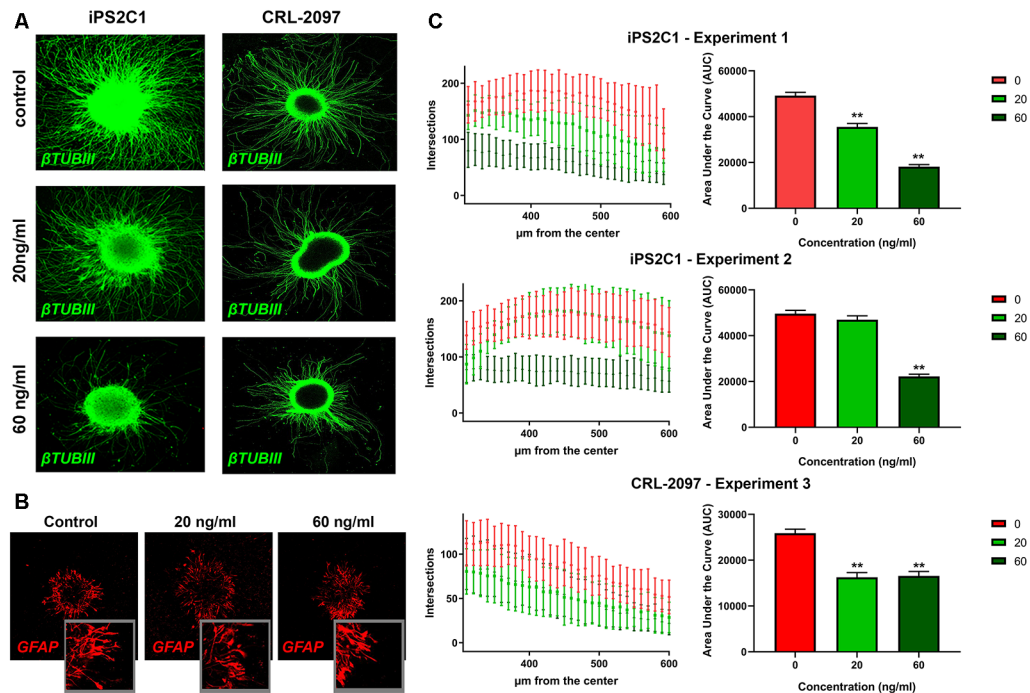
FIGURE 3 | Neurite outgrowth analysis after paroxetine exposure. BrainSpheres were cultivated for 8 weeks with and without paroxetine (20 or 60 ng/ml). After treatment, cells were seeded on Matrigel® for 24 h and fixed for immunohistochemistry. **(A)** βTUBIII staining of attached BrainSpheres after 24 h for both cell lines. **(C)** Sholl ImageJ neurite outgrowth quantification for a total of three experiments in two different cell lines. In the left panel the X-axis represents radius from the center while the Y-axis represents the number of intersections with the concentric circles produced by the software. In the right panel, the area under the curve is shown for the three experiments. The red line represents vehicle control; light green represents 20 ng/ml of paroxetine; dark green represents 60 ng/ml paroxetine treatment. **(B)** Immunohistochemistry with anti-GFAP antibody on attached spheres (24 h) for iPS2C1 line after 8 weeks of treatment with the different concentrations. Statistical analysis was performed by using ANOVA with Dunnett's post-test comparing treated with control (untreated). **$P < 0.01$.
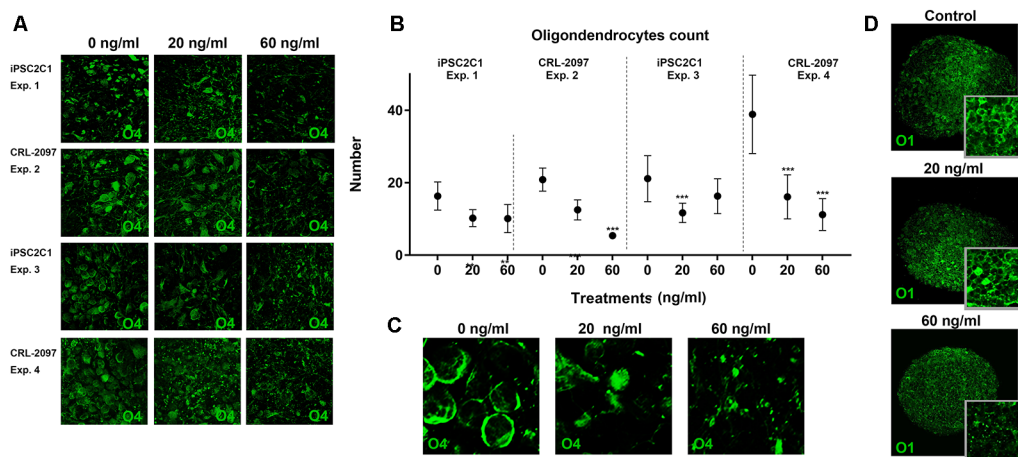
FIGURE 4 | Quantification of oligodendrocytes population. BrainSpheres were cultivated for 8 weeks with and without the presence of paroxetine (0, 20 or 60 ng/ml). After treatment, spheres were fixed for immunohistochemistry. **(A)** O4 staining of BrainSpheres from both cell lines (two independent experiments per line). **(B)** O4-positive cells quantification from four experiments. **(C)** Blow-up of a representative 04 staining. **(D)** O1 staining of BrainSpheres from CLR-2097 line. Statistical analysis was performed by using ANOVA with Dunnett's post-test comparing treated with control (untreated). ***$P < 0.01$.

DNT experts have raised concerns about the relevance of animal data for human risk assessment and have recommended substituting the expensive and time-consuming rodent guidelines for an *in vitro* testing battery comprising human-relevant models such as 3D organo-typic iPSC-derived systems (Bal-Price et al., 2012), covering key events of neurodevelopment.

The goal of this study was to establish a battery to help the identification of DNT compounds. Here, we took advantage of our 3D iPSC-derived human *in vitro* model, the BrainSpheres, enabling the study of various key events, such as a neuron, astrocyte and oligodendrocyte differentiation and maturation, neurite outgrowth, synaptogenesis, and myelination, to study the potentially deleterious effects of paroxetine. Our model allows performing multiple assays covering different key events in a single model system facilitating its applicability. For this study, relevant, therapeutic-blood concentrations of 20 and 60 ng/ml paroxetine (Tomita et al., 2014) were chosen. BrainSpheres were exposed during the entire differentiation process. In order to show robust results, we decided to use two different iPSC lines to generate the BrainSpheres and used at least three independent experiments per assay. Between 5 and 10 technical replicates (spheroids) were analyzed for each experiment.

BrainSpheres exposed to 20 or 60 ng/ml paroxetine for 8 weeks did not present any cytotoxic effects or mitochondrial dysfunction (**Figures 1A,B**) in either of the lines studied. Moreover, immunohistochemistry for astrocytic markers (GFAP and S100β) and neuronal markers (NEF200 and BTUBIII) did not show any changes after paroxetine treatment (**Figure 1D**). However, our functional assays showed some DNT effects produced by paroxetine exposure, in line with different animal studies indicating that serotonin or 5-hydroxytryptamine (5-HT), together with other neurotransmitters, is implicated in developmental processes such as proliferation, migration, differentiation, and morphogenesis (Buznikov et al., 2001).

Gene expression analysis for the serotonin transporter (SLC6A4; **Supplementary Figure S3**) showed a decrease after paroxetine exposure, however, this change was not statistically significant. The synaptic marker (SYP) was quantified in BrainSpheres derived from both iPSCs line (iPS2C1 and CLR-2097), showing a consistent statistical significant reduction over the experiments and lines (**Figure 2A**). We also observed that BrainSpheres derived from the line CLR-2097 were slightly less sensitive to 20 ng/ml paroxetine than BrainSpheres derived from iPS2C1, indicating that studies involving different cell lines might provide insight towards different individual sensitivity to paroxetine effects. These results were also confirmed by Western blot analysis, showing a stronger reduction of SYP in the iPS2C1 line than CLR-2097 (**Figures 2A,B**). Furthermore, staining for a postsynaptic marker, PSD95, showed a decrease in expression of this protein. These results show a consistent reduction of pre- and postsynaptic markers (SYP and PSD95, respectively) after paroxetine exposure, indicating this antidepressant may affect synaptogenesis during neural differentiation. Animal studies have shown that serotonin depletion during brain development disrupts normal synaptogenesis, producing decreased synaptic density (Mazer et al., 1997). On the other side, the SSRI fluoxetine has been reported to reduce monoamine oxidase gene expression, the primary metabolizing enzyme for serotonin (Bond et al., 2020). Furthermore, some SSRIs have been shown to modulate sodium channels (Thériault et al., 2015; Nakatani and Amano, 2018), which are thought to play a pivotal role during CNS

development, since action potential propagation and excitatory transmission are vital for neuronal maturation (Shatz, 1990). Although changes in serotonin levels in the brain of the fetus after maternal exposure to SSRI are not clear, changes in levels of this important neurotransmitter in the brain could have severe consequences on synaptogenesis.

We also observed a statistically significant decrease in neurite outgrowth at 60 ng/ml in all the experiments with both lines, however, 20 ng/ml presented differing results (**Figures 3A,C**) potentially. CLR-2097 showed practically the same results at 20 and 60 ng/ml, while in iPS2C1 we observed statistically significant changes only in one of two experiments, albeit a decreasing trend (**Figure 3C**). The differences between the two lines could be due to the higher neurite outgrowth in iPS2C1 than CLR-2097, or because of different sensitivity to paroxetine. It is possible, that 20 ng/ml is close to the threshold that affects this specific endpoint leading to the observed experimental variability (**Figures 3A,C**). The decrease in neurite outgrowth observed in BrainSpheres after paroxetine exposure is in line with the role of serotonin in this developmental process (Rojas et al., 2014). It is known, that neurotransmitters such serotonin and dopamine are involved in neurite outgrowth and synapse formation (Haydon et al., 1984; Lipton and Kater, 1989; van Kesteren and Spencer, 2003; Daubert and Condron, 2010), therefore, alterations in the level of these neurotransmitters could lead to adverse effects on these key processes. Our data shows disruption on neurite outgrowth and decrease expression of synaptic markers, indicating that changes in serotonin levels may be directly or indirectly responsible for these disruptions (**Figures 2, 3**).

Oligodendrocyte differentiation and myelin formation are two key events of neural development that have remained difficult to cover in DNT test batteries due to the difficulty to differentiate oligodendrocytes *in vitro*. Myelination is one of the strongest features of the BrainSphere model since this process is rarely observed *in vitro*. Few *in vitro* protocols have been developed recently to obtain oligodendrocytes from human embryonic stem cells or iPSCs (Czepiel et al., 2011; Stacpoole et al., 2013; Wang et al., 2013; Douvaras et al., 2014; Piao et al., 2015; Ehrlich et al., 2017) and other stem cell sources (Najm et al., 2013; Yang et al., 2013). However, to our knowledge, BrainSpheres is one of the few human *in vitro* systems able to produce oligodendrocytes in a 3D model enabling the winding of oligodendrocytes processes around the axons. By using image analysis we were able to show a decreased number of oligodendrocytes accompanied by a decreased expression of MBP (**Figure 4** and **Supplementary Figure S2**) after Paroxetine exposure. In line with our data, previous *in vitro* studies have suggested that an increase of serotonin levels may disrupt oligodendrocytes maturation and myelin formation (Fan et al., 2015). Moreover, exposure to other SSRIs, such as fluoxetine have shown to produce long-term changes in the expression of genes involved in myelination in adult rats (Kroeze et al., 2016). This also correlated with our data on oligodendrocyte quantification (**Figure 4**) and may indicate that changes in serotonin levels in BrainSphereshave an adverse effect on oligodendrocyte maturation and myelin formation.

In conclusion, some indications from clinical studies suggested that paroxetine may affect brain development, but these results were inconsistent. By using a battery of assays that cover several key events of neural development in BrainSpheres we were able to detect alterations in neurite outgrowth, reduction of synaptic marker expression and a decrease in the number of oligodendrocytes after exposure to paroxetine at relevant therapeutic concentrations. These results identify paroxetine as a potential human developmental neurotoxicant, and suggest that the contraindication for its use should be evaluated and possibly extended far beyond the first trimester of pregnancy. In addition, we show that BrainSpheres allow to cover different aspects of brain development in one single system and constitute a novel tool to study and identify potential developmental neurotoxicants among chemicals and drugs, before their entry to the market.

DATA AVAILABILITY STATEMENT

The datasets generated for this study are available on request to the corresponding author.

AUTHOR CONTRIBUTIONS

XZ: western blots, stainings, and some cultures. GH: neurite outgrowth. LS: neurite outgrowth, immunohistochemistry, and supervision XZ, VZ, and MC: myelin and oligodendrocytes quantification. M-GZ: oligodendrocytes quantification, writing and revision of the manuscript. RS: BS cultures, viability assays, and mitochondrial function. FB and PB: synapsis quantification. PB: Synapsis quantification. HH: revision of the manuscript. TH: project idea, PI funding, head of laboratory, and revision of the manuscript. DP: cultures, immunohistochemistry, neurite outgrowth analysis, statistical analysis, coordinator of the experiments, and writer of the manuscript.

FUNDING

SUPPLEMENTARY MATERIAL

The Supplementary Material for this article can be found online at: https://www.frontiersin.org/articles/10.3389/fncel.2020.000 25/full#supplementary-material.

FIGURE S1 | BrainSpheres oligodendrocytes quantification panel. Confocal imagines of O4 positive marker for the four different experiments used for quantification.

FIGURE S2 | Myelin quantification assay. BrainSphere myelination was quantified using a protocol adapted from Kerman et al. (2015) for computer-assisted evaluation of myelin formation on ImageJ. Myelination, is defined by the pixels overlapping between binary single-channel images of MBP staining and axons NF200 staining. **(A)** CEM quantification of one independent experiment (10 individual spheroids per condition) with the CLR–2097 line. The X-axis represents the concentration of paroxetine while the Y-axis represents the % of myelinated axons quantified by CEM plug-in. **(B)** Representative pictures of binary overlap between NF200 and MBP used for quantification. **(C)** Representative picture of BrainSpheres for neuronal marker (NF200) and myelin marker (MBP). Statistical analysis was performed by using ANOVA with Dunnett's post-test comparing treated with control (untreated). $*P < 0.01$.

FIGURE S3 | Gene expression of SLC6A4. BrainSphere gene expression of SLC6A4 was quantified using qPCR. Housekeeping was Actin. No statistically significant changes were found.

REFERENCES

Alwan, S., and Friedman, J. M. (2009). Safety of selective serotonin reuptake inhibitors in pregnancy. *CNS Drugs* 23, 493–509. doi: 10.2165/00023210-200923060-00004

Alwan, S., Friedman, J. M., and Chambers, C. (2016). Safety of selective serotonin reuptake inhibitors in pregnancy: a review of current evidence. *CNS Drugs* 30, 499–515. doi: 10.1007/s40263-016-0338-3

Alwan, S., Reefhuis, J., Rasmussen, S. A., Friedman, J. M., and National Birth Defects Prevention Study. (2011). Patterns of antidepressant medication use among pregnant women in a United States population. *J. Clin. Pharmacol.* 51, 264–270. doi: 10.1177/0091270010373928

Alwan, S., Reefhuis, J., Rasmussen, S. A., Olney, R. S., Friedman, J. M., and National Birth Defects Prevention Study. (2007). Use of selective serotonin-reuptake inhibitors in pregnancy and the risk of birth defects. *N. Engl. J. Med.* 356, 2684–2692. doi: 10.1056/NEJMoa066584

Andrade, S. E., Raebel, M. A., Brown, J., Lane, K., Livingston, J., Boudreau, D., et al. (2008). Use of antidepressant medications during pregnancy: a multisite study. *Am. J. Obstet. Gynecol.* 198, 194.e1–194.e5. doi: 10.1016/j.ajog.2007.07.036

Bal-Price, A. K., Coecke, S., Costa, L., Crofton, K. M., Fritsche, E., Goldberg, A., et al. (2012). Advancing the science of developmental neurotoxicity (DNT): testing for better safety evaluation. *ALTEX* 29, 202–215. doi: 10.14573/altex.2012.2.202

Bennett, H. A., Einarson, A., Taddio, A., Koren, G., and Einarson, T. R. (2004). Prevalence of depression during pregnancy: systematic review. *Obstet. Gynecol.* 103, 698–709. doi: 10.1097/01.aog.0000116689.75396.5f

Berard, A., Iessa, N., Chaabane, S., Muanda, F. T., Boukhris, T. and Zhao, J.-P. (2016). The risk of major cardiac malformations associated with paroxetine use during the first trimester of pregnancy: a systematic review and meta-analysis. *Br. J. Clin. Pharmacol.* 81, 589–604. doi: 10.1111/bcp.12849

Berridge, K. C., Robinson, T. E., and Aldridge, J. W. (2009). Dissecting components of reward: 'liking', 'wanting', and learning. *Curr. Opin. Pharmacol.* 9, 65–73. doi: 10.1016/j.coph.2008.12.014

Bond, C. M., Johnson, J. C., Chaudhary, V., McCarthy, E. M., McWhorter, M. L., and Woehrle, N. S. (2020). Perinatal fluoxetine exposure results in social deficits and reduced monoamine oxidase gene expression in mice. *Brain Res.* 1727:S0006-8993(19)30328-2. doi: 10.1016/j.brainres.2019.06.001

Boukhris, T., Sheehy, O., Mottron, L., and Bérard, A. (2016). Antidepressant use during pregnancy and the risk of autism spectrum disorder in children. *JAMA Pediatr.* 170, 117–124. doi: 10.1001/jamapediatrics.2015.3356

Buznikov, G. A., Lambert, H. W., and Lauder, J. J. (2001). Serotonin and serotonin-like substances as regulators of early embryogenesis and morphogenesis. *Cell Tissue Res.* 305, 177–186. doi: 10.1007/s004410100408

Cases, O., Seif, I., Grimsby, J., Gaspar, P., Chen, K., Pournin, S., et al. (1995). Aggressive behavior and altered amounts of brain serotonin and norepinephrine in mice lacking MAOA. *Science* 268, 1763–1766. doi: 10.1126/science.7792602

Casper, R. C., Fleisher, B. E., Lee-Ancajas, J. C., Gilles, A., Gaylor, E., DeBattista, A., et al. (2003). Follow-up of children of depressed mothers exposed or not exposed to antidepressant drugs during pregnancy. *J. Pediatr.* 142, 402–408. doi: 10.1067/mpd.2003.139

Casper, R. C., Gilles, A. A., Fleisher, B. E., Baran, J., Enns, G., and Lazzeroni, L. C. (2011). Length of prenatal exposure to selective serotonin reuptake inhibitor (SSRI) antidepressants: effects on neonatal adaptation and psychomotor development. *Psychopharmacology* 217, 211–219. doi: 10.1007/s00213-011-2270-z

Cole, J. A., Ephross, S. A., Cosmatos, I. S., and Walker, A. M. (2007). Paroxetine in the first trimester and the prevalence of congenital malformations. *Pharmacoepidemiol. Drug Saf.* 16, 1075–1085. doi: 10.1002/pds.1463

Costei, A. M., Kozer, E., Ho, T., Ito, S., and Koren, G. (2002). Perinatal outcome following third trimester exposure to paroxetine. *Arch. Pediatr. Adolesc. Med.* 156, 1129–1132. doi: 10.1001/archpedi.156.11.1129

Croen, L. A., Grether, J. K., Yoshida, C. K., Odouli, R., and Hendrick, V. (2011). Antidepressant use during pregnancy and childhood autism spectrum disorders. *Arch. Gen. Psychiatry* 68, 1104–1112. doi: 10.1001/archgenpsychiatry.2011.73

Czepiel, M., Balasubramaniyan, V., Schaafsma, W., Stancic, M., Mikkers, H., Huisman, C., et al. (2011). Differentiation of induced pluripotent stem cells into functional oligodendrocytes. *Glia* 59, 882–892. doi: 10.1002/glia.21159

Daubert, E. A., and Condron, B. G. (2010). Serotonin: a regulator of neuronal morphology and circuitry. *Trends Neurosci.* 33, 424–434. doi: 10.1016/j.tins.2010.05.005

Douvaras, P., Wang, J., Zimmer, M., Hanchuk, S., O'Bara, M. A., Sadiq, S., et al. (2014). Efficient generation of myelinating oligodendrocytes from primary progressive multiple sclerosis patients by induced pluripotent stem cells. *Stem Cell Reports* 3, 250–259. doi: 10.1016/j.stemcr.2014.06.012

Ehrlich, M., Mozafari, S., Glatza, M., Starost, L., Velychko, S., Hallmann, A. L., et al. (2017). Rapid and efficient generation of oligodendrocytes from human induced pluripotent stem cells using transcription factors. *Proc. Natl. Acad. Sci. U S A* 114, E2243–E2252. doi: 10.1073/pnas.1614412114

Ellfolk, M., and Malm, H. (2010). Risks associated with *in utero* and lactation exposure to selective serotonin reuptake inhibitors (SSRIs). *Reprod. Toxicol.* 30, 249–260. doi: 10.1016/j.reprotox.2010.04.015

Epstein, H. T. (1986). Stages in human brain development. *Brain Res.* 395, 114–119. doi: 10.1016/s0006-8993(86)80017-8

Esaki, T., Cook, M., Shimoji, K., Murphy, D. L., Sokoloff, L., and Holmes, A. (2005). Developmental disruption of serotonin transporter function impairs cerebral responses to whisker stimulation in mice. *Proc. Natl. Acad. Sci. U S A* 102, 5582–5587. doi: 10.1073/pnas.0501509102

Fan, L. W., Bhatt, A., Tien, L. T., Zheng, B., Simpson, K. L., Lin, R. C., et al. (2015). Exposure to serotonin adversely affects oligodendrocyte development and myelination *in vitro*. *J. Neurochem.* 133, 532–543. doi: 10.1111/jnc.12988

Frishman, W. H., and Grewall, P. (2000). Serotonin and the heart. *Ann. Med.* 32, 195–209. doi: 10.3109/07853890008998827

Fritsche, E., Barenys, M., Klose, J., Masjosthusmann, S., Nimtz, L., Schmuck, M., et al. (2018a). Corrigendum to "current availability of stem cell-based *in vitro* methods for developmental neurotoxicity (DNT) testing". *Toxicol. Sci.* 165:531. doi: 10.1093/toxsci/kfy195

Fritsche, E., Barenys, M., Klose, J., Masjosthusmann, S., Nimtz, L., Schmuck, M., et al. (2018b). Current availability of stem cell-based *in vitro* methods for developmental neurotoxicity (DNT) testing. *Toxicol. Sci.* 165, 21–30. doi: 10.1093/toxsci/kfy178

Fröhlich, N., Nagy, B., Hovhannisyan, A., and Kukley, M. (2011). Fate of neuron-glia synapses during proliferation and differentiation of NG2 cells. *J. Anat.* 219, 18–32. doi: 10.1111/j.1469-7580.2011.01392.x

Gao, S.-Y., Wu, Q.-J., Sun, C., Zhang, T.-N., Shen, Z.-Q., Liu, C.-X., et al. (2018). Selective serotonin reuptake inhibitor use during early pregnancy and congenital malformations: a systematic review and meta-analysis of cohort studies of more than 9 million births. *BMC Med.* 16:205. doi: 10.1186/s12916-018-1193-5

Gentile, S., and Galbally, M. (2011). Prenatal exposure to antidepressant medications and neurodevelopmental outcomes: a systematic review. *J. Affect. Disord.* 128, 1–9. doi: 10.1016/j.jad.2010.02.125

Glover, M. E., and Clinton, S. M. (2016). Of rodents and humans: a comparative review of the neurobehavioral effects of early life SSRI exposure in preclinical and clinical research. *Int. J. Dev. Neurosci.* 51, 50–72. doi: 10.1016/j.ijdevneu.2016.04.008

Glover, M. E., Pugh, P. C., Jackson, N. L., Cohen, J. L., Fant, A. D., Akil, H., et al. (2015). Early-life exposure to the SSRI paroxetine exacerbates depression-like behavior in anxiety/depression-prone rats. *Neuroscience* 284, 775–797. doi: 10.1016/j.neuroscience.2014.10.044

Hale, T. W., Kendall-Tackett, K., Cong, Z., Votta, R., and McCurdy, F. (2010). Discontinuation syndrome in newborns whose mothers took antidepressants while pregnant or breastfeeding. *Breastfeed. Med.* 5, 283–288. doi: 10.1089/bfm.2010.0011

Harrington, R. A., Lee, L. C., Crum, R. M., Zimmerman, A. W., and Hertz-Picciotto, I. (2013). Serotonin hypothesis of autism: implications for selective serotonin reuptake inhibitor use during pregnancy. *Autism Res.* 6, 149–168. doi: 10.1002/aur.1288

Haydon, P. G., McCobb, D. P., and Kater, S. B. (1984). Serotonin selectively inhibits growth cone motility and synaptogenesis of specific identified neurons. *Science* 226, 561–564. doi: 10.1126/science.6093252

Hendrick, V., Stowe, Z. N., Altshuler, L. L., Hwang, S., Lee, E., and Haynes, D. (2003). Placental passage of antidepressant medications. *Am. J. Psychiatry* 160, 993–996. doi: 10.1176/appi.ajp.160.5.993

Holmes, A., Yang, R. J., Lesch, K. P., Crawley, J. N., and Murphy, D. L. (2003). Mice lacking the serotonin transporter exhibit 5-HT(1A) receptor-mediated abnormalities in tests for anxiety-like behavior. *Neuropsychopharmacology* 28, 2077–2088. doi: 10.1038/sj.npp.1300266

Kerman, B. E., Kim, H. J., Padmanabhan, K., Mei, A., Georges, S., Joens, M. S., et al. (2015). *In vitro* myelin formation using embryonic stem cells. *Development* 142, 2213–2225. doi: 10.1242/dev.116517

Klinger, G., Frankenthal, D., Merlob, P., Diamond, G., Sirota, L., Levinson-Castiel, R., et al. (2011). Long-term outcome following selective serotonin reuptake inhibitor induced neonatal abstinence syndrome. *J. Perinatol.* 31, 615–620. doi: 10.1038/jp.2010.211

Kroeze, Y., Peeters, D., Boulle, F., van den Hove, D. L., van Bokhoven, H., Zhou, H., et al. (2016). Long-term consequences of chronic fluoxetine exposure on the expression of myelination-related genes in the rat hippocampus. *Transl. Psychiatry* 6:e779. doi: 10.1038/tp.2016.60

Lipton, S. A., and Kater, S. B. (1989). Neurotransmitter regulation of neuronal outgrowth, plasticity and survival. *Trends Neurosci.* 12, 265–270. doi: 10.1016/0166-2236(89)90026-x

Lisboa, S. F., Oliveira, P. E., Costa, L. C., Venâncio, E. J., and Moreira, E. G. (2007). Behavioral evaluation of male and female mice pups exposed to fluoxetine during pregnancy and lactation. *Pharmacology* 80, 49–56. doi: 10.1159/000103097

Mäkikallio, K., Jouppila, P., and Rasanen, J. (2005). Human fetal cardiac function during the first trimester of pregnancy. *Heart* 91, 334–338. doi: 10.1136/hrt.2003.029736

Mazer, C., Muneyyirci, J., Taheny, K., Raio, N., Borella, A., and Whitaker-Azmitia, P. (1997). Serotonin depletion during synaptogenesis leads to decreased synaptic density and learning deficits in the adult rat: a possible model of neurodevelopmental disorders with cognitive deficits. *Brain Res.* 760, 68–73. doi: 10.1016/s0006-8993(97)00297-7

Meunier, M. R., Bennett, I. M., and Coco, A. S. (2013). Use of antidepressant medication in the united states during pregnancy, 2002–2010. *Psychiatr. Serv.* 64, 1157–1160. doi: 10.1176/appi.ps.201200455

Najm, F. J., Lager, A. M., Zaremba, A., Wyatt, K., Caprariello, A. V., Factor, D. C., et al. (2013). Transcription factor-mediated reprogramming of fibroblasts to expandable, myelinogenic oligodendrocyte progenitor cells. *Nat. Biotechnol.* 31, 426–433. doi: 10.1038/nbt.2561

Nakatani, Y., and Amano, T. (2018). Functional modulation of $Na_v1.2$ voltage-gated sodium channels induced by escitalopram. *Biol. Pharm. Bull.* 41, 1471–1474. doi: 10.1248/bpb.b18-00214

National Library of Medicine. (2006). *Paroxetine in Drugs and Lactation Database (LactMed)*. Bethesda, MD: National Library of Medicine.

Nebigil, C. G., Choi, D. S., Dierich, A., Hickel, P., Le Meur, M., Messaddeq, N., et al. (2000). Serotonin 2B receptor is required for heart development. *Proc. Natl. Acad. Sci. U S A* 97, 9508–9513. doi: 10.1073/pnas.97.17.9508

Nebigil, C. G., Etienne, N., Messaddeq, N., and Maroteaux, L. (2003). Serotonin is a novel survival factor of cardiomyocytes: mitochondria as a target of 5-HT2B receptor signaling. *FASEB J.* 17, 1373–1375. doi: 10.1096/fj.02-1122fje

Nebigil, C. G., and Maroteaux, L. (2001). A novel role for serotonin in heart. *Trends Cardiovasc. Med.* 11, 329–335. doi: 10.1016/s1050-1738(01)00135-9

Nevels, R. M., Gontkovsky, S. T., and Williams, B. E. (2016). Paroxetine-the antidepressant from hell? Probably not, but caution required. *Psychopharmacol. Bull.* 46, 77–104.

Oberlander, T. F., Grunau, R. E., Fitzgerald, C., Papsdorf, M., Rurak, D., and Riggs, W. (2005). Pain reactivity in 2-month-old infants after prenatal and postnatal serotonin reuptake inhibitor medication exposure. *Pediatrics* 115, 411–425. doi: 10.1542/peds.2004-0420

Oberlander, T. F., Papsdorf, M., Brain, U. M., Misri, S., Ross, C., and Grunau, R. E. (2010). Prenatal effects of selective serotonin reuptake inhibitor antidepressants, serotonin transporter promoter genotype (SLC6A4) and maternal mood on child behavior at 3 years of age. *Arch. Pediatr. Adolesc. Med.* 164, 444–451. doi: 10.1001/archpediatrics.2010.51

Olivier, J. D. A., Vallès, A., van Heesch, F., Afrasiab-Middelman, A., Roelofs, J. J., Jonkers, M., et al. (2011). Fluoxetine administration to pregnant rats increases anxiety-related behavior in the offspring. *Psychopharmacology* 217, 419–432. doi: 10.1007/s00213-011-2299-z

Orsolini, L., and Bellantuono, C. (2015). Serotonin reuptake inhibitors and breastfeeding: a systematic review. *Hum. Psychopharmacol.* 30, 4–20. doi: 10.1002/hup.2451

Pamies, D., Barreras, P., Block, K., Makri, G., Kumar, A., Wiersma, D., et al. (2017). A human brain microphysiological system derived from induced pluripotent stem cells to study neurological diseases and toxicity. *ALTEX* 34, 362–376. doi: 10.14573/altex.1609122

Pamies, D., Block, K., Lau, P., Gribaldo, L., Pardo, C. A., Barreras, P., et al. (2018). Rotenone exerts developmental neurotoxicity in a human brain spheroid model. *Toxicol. Appl. Pharmacol.* 354, 101–114. doi: 10.1016/j.taap.2018.02.003

Persico, A. M., Altamura, C., Calia, E., Puglisi-Allegra, S., Ventura, R., Lucchese, F., et al. (2000). Serotonin depletion and barrel cortex development: impact of growth impairment vs. serotonin effects on thalamocortical endings. *Cereb. Cortex* 10, 181–191. doi: 10.1093/cercor/10.2.181

Persico, A. M., Mengual, E., Moessner, R., Hall, F. S., Revay, R. S., Sora, I., et al. (2001). Barrel pattern formation requires serotonin uptake by thalamocortical afferents and not vesicular monoamine release. *J. Neurosci.* 21, 6862–6873. doi: 10.1523/jneurosci.21-17-06862.2001

Piao, J. H., Major, T., Auyeung, G., Policarpio, E., Menon, J., Droms, L., et al. (2015). Human embryonic stem cell-derived oligodendrocyte progenitors remyelinate the brain and rescue behavioral deficits following radiation. *Cell Stem Cell* 16, 198–210. doi: 10.1016/j.stem.2015.01.004

Posey, D. I., Litwiller, M., Koburn, A., and McDougle, C. J. (1999). Paroxetine in autism. *J. Am. Acad. Child Adolesc. Psychiatry* 38, 111–112. doi: 10.1097/00004583-199902000-00004

Rai, D., Lee, B. K., Dalman, C., Golding, J., Lewis, G., and Magnusson, C. (2013). Parental depression, maternal antidepressant use during pregnancy, and risk of autism spectrum disorders: population based case-control study. *BMJ* 346:f2059. doi: 10.1136/bmj.f2059

Rojas, P. S., Neira, D., Muñoz, M., Lavandero, S., and Fiedler, J. L. (2014). Serotonin (5-HT) regulates neurite outgrowth through 5-HT1A and 5-HT7 receptors in cultured hippocampal neurons. *J. Neurosci. Res.* 92, 1000–1009. doi: 10.1002/jnr.23390

Shatz, C. J. (1990). Impulse activity and the patterning of connections during CNS development. *Neuron* 5, 745–756. doi: 10.1016/0896-6273(90)90333-b

Silbereis, J. C., Huang, E. J., Back, S. A., and Rowitch, D. H. (2010). Towards improved animal models of neonatal white matter injury associated with cerebral palsy. *Dis. Model. Mech.* 3, 678–688. doi: 10.1242/dmm.002915

Smirnova, L., Hogberg, H. T., Leist, M., and Hartung, T. (2014). Developmental neurotoxicity—challenges in the 21st century and in vitro opportunities. *ALTEX* 31, 129–156. doi: 10.14573/altex.1403271

Smirnova, L., Kleinstreuer, N., Corvi, R., Levchenko, A., Fitzpatrick, S. C., and Hartung, T. (2018). 3S - Systematic, systemic, and systems biology and toxicology. *ALTEX* 35, 139–162. doi: 10.14573/altex.1804051

Stacpoole, S. R. L., Spitzer, S., Bilican, B., Compston, A., Karadottir, R., Chandran, S., et al. (2013). High yields of oligodendrocyte lineage cells from human embryonic stem cells at physiological oxygen tensions for evaluation of translational biology. *Stem Cell Reports* 1, 437–450. doi: 10.1016/j.stemcr.2013.09.006

Thériault, O., Poulin, H., Beaulieu, J. M., and Chahine, M. (2015). Differential modulation of Nav1.7 and Nav1.8 channels by antidepressant drugs. *Eur. J. Pharmacol.* 764, 395–403. doi: 10.1016/j.ejphar.2015.06.053

Tomita, T., Yasui-Furukori, N., Nakagami, T., Tsuchimine, S., Ishioka, M., Kaneda, A., et al. (2014). Therapeutic reference range for plasma concentrations of paroxetine in patients with major depressive disorders. *Ther. Drug Monit.* 36, 480–485. doi: 10.1097/ftd.0000000000000036

Traiffort, E., Zakaria, M., Laouarem, Y., and Ferent, J. (2016). Hedgehog: a key signaling in the development of the oligodendrocyte lineage. *J. Dev. Biol.* 4:E28. doi: 10.3390/jdb4030028

Uguz, F. (2018). Better tolerance of citalopram in a breastfed infant who could not tolerate sertraline and paroxetine. *Breastfeed. Med.* 13, 89–90. doi: 10.1089/bfm.2017.0168

Uguz, F., and Arpaci, N. (2016). Short-term safety of paroxetine and sertraline in breastfed infants: a retrospective cohort study from a university hospital. *Breastfeed. Med.* 11, 487–489. doi: 10.1089/bfm.2016.0095

Valenti, O., Di Prima, F. A., Renda, E., Faraci, M., Hyseni, E., De Domenico, R., et al. (2011). Fetal cardiac function during the first trimester of pregnancy. *J. Prenat. Med.* 5, 59–62.

van Kesteren, R. E., and Spencer, G. E. (2003). The role of neurotransmitters in neurite outgrowth and synapse formation. *Rev. Neurosci.* 14, 217–231. doi: 10.1515/revneuro.2003.14.3.217

Wang, S., Bates, J., Li, X., Schanz, S., Chandler-Militello, D., Levine, C., et al. (2013). Human iPSC-derived oligodendrocyte progenitor cells can myelinate and rescue a mouse model of congenital hypomyelination. *Cell Stem Cell* 12, 252–264. doi: 10.1016/j.stem.2012.12.002

Welker, E., Armstrong-James, M., Bronchti, G., Ourednik, W., Gheorghita-Baechler, F., Dubois, R., et al. (1996). Altered sensory processing in the somatosensory cortex of the mouse mutant barrelless. *Science* 271, 1864–1867. doi: 10.1126/science.271.5257.1864

Wen, Z., Nguyen, H. N., Guo, Z., Lalli, M. A., Wang, X., Su, Y., et al. (2014). Synaptic dysregulation in a human iPS cell model of mental disorders. *Nature* 515, 414–418. doi: 10.1038/nature13716

Yang, Z., Seif, I., and Armstrong-James, M. (2001). Differences in somatosensory processing in S1 barrel cortex between normal and monoamine oxidase A knockout (Tg8) adult mice. *Cereb. Cortex* 11, 26–36. doi: 10.1093/cercor/11.1.26

Yang, N., Zuchero, J. B., Ahlenius, H., Marro, S., Ng, Y. H., Vierbuchen, T., et al. (2013). Generation of oligodendroglial cells by direct lineage conversion. *Nat. Biotechnol.* 31, 434–439. doi: 10.1038/nbt.2564

Zeskind, P. S., and Stephens, L. E. (2004). Maternal selective serotonin reuptake inhibitor use during pregnancy and newborn neurobehavior. *Pediatrics* 113, 368–375. doi: 10.1542/peds.113.2.368

Zohar, I., Shoham, S., and Weinstock, M. (2016). Perinatal citalopram does not prevent the effect of prenatal stress on anxiety, depressive-like behaviour and serotonergic transmission in adult rat offspring. *Eur. J. Neurosci.* 43, 590–600. doi: 10.1111/ejn.13150

frontiers
in Cellular Neuroscience

Check for
updates

Human Brain Organoids to Decode Mechanisms of Microcephaly

Elke Gabriel†, Anand Ramani†, Nazlican Altinisik and Jay Gopalakrishnan*

Laboratory for Centrosome and Cytoskeleton Biology, Institute für Humangenetik, Universitätsklinikum Düsseldorf, Heinrich-Heine-Universität, Düsseldorf, Germany

Brain organoids are stem cell-based self-assembling 3D structures that recapitulate early events of human brain development. Recent improvements with patient-specific 3D brain organoids have begun to elucidate unprecedented details of the defective mechanisms that cause neurodevelopmental disorders of congenital and acquired microcephaly. In particular, brain organoids derived from primary microcephaly patients have uncovered mechanisms that deregulate neural stem cell proliferation, maintenance, and differentiation. Not only did brain organoids reveal unknown aspects of neurogenesis but also have illuminated surprising roles of cellular structures of centrosomes and primary cilia in regulating neurogenesis during brain development. Here, we discuss how brain organoids have started contributing to decoding the complexities of microcephaly, which are unlikely to be identified in the existing non-human models. Finally, we discuss the yet unresolved questions and challenges that can be addressed with the use of brain organoids as *in vitro* models of neurodevelopmental disorders.

Keywords: centrosomes, primary cilia, neural progenitor cells (NPCs), induced pluripotent stem cells (iPSCs), human brain organoids, microcephaly, neurodevelopmental disorders, neurogenesis

INTRODUCTION

Our knowledge of the mechanisms of human brain development is limited mainly because the human brain is enormously complex in its cell diversity, composition, and architecture (Northcutt and Kaas, 1995; Borrell and Gotz, 2014). Cortical expansion of the human brain is one of the most remarkable evolutionary processes of brain development that is correlated to sophisticated tasks of decision making, emotional, cognitive, and social interactions (Rilling, 2014; Reardon et al., 2018). A highly orchestrated process of neural stem cell maintenance, proliferation, migration, and interactions ensure the accurate and structurally normal cortical expansion. Perturbations in any of these individual steps can lead to neurodevelopmental disorders. Primary microcephaly is one such neurodevelopmental disorder in which brain size is markedly reduced (Jayaraman et al., 2018; Pirozzi et al., 2018).

In mammalians, brain development begins with the massive expansion of the neuroepithelium that generates radial glial stem cells (Borrell and Gotz, 2014; Florio and Huttner, 2014; Florio et al., 2017). Notably, in the human brain, the progenitor zones around the ventricular zone (VZ) are organized extensively. The sub-ventricular region consists of the inner sub-ventricular zone and the outer sub-ventricular zone, separated by an inner fiber layer. The outer sub-ventricular zone constitutes intermediate progenitors and outer radial glia. This compartmentalization, along

with increased heterogeneity of neural precursor populations and their dynamic proliferative characteristics (cell cycle length, mode of division, etc.) collectively underlay the massive expansion of neural stem cells. This could lead to the highest neuron number inducing gyrification and an increase in brain size in humans. Strikingly, rodent brains, which are lissencephalic and lack the inner fiber layer, the outer sub-ventricular zone, and exhibit different dynamics of proliferation and neurogenic period (Zecevic et al., 2005; Cox et al., 2006; Molnar and Clowry, 2012). Thus, when the pathogenesis of microcephaly has been studied in mouse models, they failed to recapitulate the severely reduced brain size seen in human patients. As a result, it has been challenging to study microcephaly in model systems that do not possess the complexity of the human brain. This has been a significant limiting factor for decades and has been a challenge for developmental biologists to model microcephaly since animal models do not mirror the complex embryonic neurodevelopmental disorders occurring in humans.

With recent technological advances identifying the molecular causes of microcephaly, the interplay between genes, cellular structures, and most importantly the recent emergence of powerful 3D *in vitro* brain organoid systems have fortuitously helped to understand the mechanisms of microcephaly and underpinned the fundamental mechanisms of healthy brain development (Mariani et al., 2012; Lancaster et al., 2013; Gabriel et al., 2016; Gopalakrishnan, 2019; Setia and Muotri, 2019). In this review, we will summarize complex cellular processes in the pathogenesis of microcephaly and how the recent 3D brain organoids, also known as "brain mimetics" of the human brain have contributed to unraveling the complexities seen in microcephaly patients. Finally, we outline the critical questions that require immediate attention in the field of microcephaly research and state the current challenges that could be overcome with the use of 3D brain organoids as *in vitro* models of neurodevelopmental disorders.

MICROCEPHALY; DEFINITION AND PATHOGENESIS

The human brain constitutes approximately 2% of the total body mass, also consuming up to 20% of the total energy indicating its vitality for the organism's survival. Deregulation of genes and pathways that have co-evolved with the human brain evolution could result in a small brain, in particular, a smaller frontal cortex, and is clinically termed as primary microcephaly. Microcephaly is classified as primary and secondary. Primary microcephaly is a condition where abnormalities occur at the early onset of brain development resulting in an un-proportional cortical thickness. Secondary microcephaly, on the other hand, develops postnatal during infancy (Basel-Vanagaite and Dobyns, 2010; Alcantara and O'Driscoll, 2014). The term MCPH (autosomal recessive primary microcephaly) has been frequently used in clinical diagnostics of microcephaly. These two categories have been further categorized based on their symptoms. For instance, a microcephaly disorder exhibiting only reduced head circumference with mental retardation belongs

to the non-syndromic type; whereas, microcephaly disorder associated with various neurological and cognitive defects falls under the syndromic type of the disease. Furthermore, the source of primary and secondary microcephaly could also be due to environmental cues as well as viral influence in addition to the well-known genetic causes. Hence they are also called acquired microcephaly. Emerging genetic mutations have further defined another class of syndromic microcephaly, which included malformations of cortices along with whole-body growth shunt, which usually is a clinical feature observed in Seckel syndrome and Microcephalic Osteodysplastic Primordial Dwarfism (MOPD) (Rauch et al., 2008; Pirozzi et al., 2018; Jayaraman et al., 2018). In contrast to Seckel syndrome, MCPH only exhibits retarded brain size (Jayaraman et al., 2018; Pirozzi et al., 2018).

Although several confusing terms and increasing branches of growth-retarded syndromes are emerging, what is undoubtedly intersecting in these disorders is microcephaly. The most frequent abnormality in microcephaly identified by the MRI imaging is diffused cortical gyral pattern where cortical layers are thin and not well layered as seen in the healthy brain (Basel-Vanagaite and Dobyns, 2010). This unambiguously points out the fact that there must be a unifying mechanism that operates in these disorders. Perhaps a tightly coordinated mechanism exists that is critical to maintaining the expanding pool of neural stem cells at the early events of brain development. Alternatively, mutations of genes with different functions, or viral infection leading to intracellular events could be distinct from those activated in genetic forms of microcephaly. However, the disease-relevant cell types of region-specific NPCs could be more prone to undergo depletion or damage under different types of stress. Overall, the depletion of this actively proliferating neural stem cell pool at the early stage of brain development could broadly affect the final mass and function of the human brain.

Congenital microcephaly is mostly caused by autosomal recessive mutations in several genes that regulate centrosome and cilia assembly, which are cellular structures that govern fundamental pathways of microtubule organization, cell proliferation, polarity, migration and cell signaling (**Table 1**). Indeed, the earliest identified microcephaly associated genes were implicated in centrosome biogenesis, and spindle assembly, which include molecules such as CDK5RAP2, CPAP, Cep135, Cep152, PCNT, and MCPH1 where the mutations in these genes were identified in consanguineous populations inherited via an autosomal recessive fashion (Bond et al., 2002; Bond et al., 2005; Rauch et al., 2008; Guernsey et al., 2010; Hussain et al., 2012). As mentioned before, the human neocortex differs from rodents and non-human primates in terms of neuronal numbers, which is an indicator of a positive selection in humans (Bond et al., 2005). This morphological feature suggests a sophisticated regulation of precursor cell numbers and their proliferative/differentiative ratio during neurogenesis. As an example, centrosomal proteins mutations resulting in microcephaly in humans harbor other regions besides conserved domains. Such alterations in amino acid sequences and protein expression levels appear to occur in humans specifically. This allows us to speculate their specific roles in controlling cortical expansion and neuronal number in

TABLE 1 | Genes frequently mutated in primary microcephaly that plays roles in cell cycle regulation, centrosome/cilium formation, spindle orientation, microtubule organization and impaired DNA damage.

Genes	Syndrome	Subcellular localization	Modeled in patient specific brain organoids	Mechanisms revealed	References
MCPH1	Congenital microcephaly	Nucleus	No	Premature NPCs differentiation, premature chromosome condensation	Jackson et al., 2002; Passemard et al., 2011; Zhou et al., 2013; Farooq et al., 2016
ASPM	Congenital microcephaly	Centrosomes	Yes	Decreased NPCs proliferation, Less neuronal activity, cell death	Pulvers et al., 2010; Fujimori et al., 2014
WDR62	Congenital microcephaly, cortical abnormalities	Centrosomes	No	Decreased NPCs proliferation, premature NPCs differentiation	Nicholas et al., 2010; Shohayeb et al., 2019; Zhang et al., 2019
CDK5RAP2	Congenital microcephaly	Centrosomes	Yes	Decreased NPCs proliferation, premature NPCs differentiation	Bond et al., 2005; Barrera et al., 2010; Buchman et al., 2010; Babrowski et al., 2013
CENPJ / CPAP	Congenital microcephaly, Seckel syndrome	Centrosomes	Yes	Decreased NPCs proliferation premature NPCs differentiation	Al-Dosari et al., 2010; McIntyre et al., 2012; Alcantara and O'Driscoll, 2014; Aldape et al., 2019
SAS6	Congenital microcephaly	Centrosomes	No	Decreased NPCs proliferation	Khan et al., 2014; Tang et al., 2016
STIL	Congenital microcephaly	Centrosomes	No	Neural tube defects	Consortium et al., 2009; Amartely et al., 2014
CEP152	Congenital microcephaly, Seckel syndrome	Centrosomes	No	Decreased NPCs proliferation	Guernsey et al., 2010; Kalay et al., 2011
CEP63	Seckel syndrome	Centrosomes	No	Increased neuronal death, increased mitotic error	Alcantara and O'Driscoll, 2014; Marjanovic et al., 2015
NDE1	Congenital microcephaly,	Centrosomes and spindle microtubules	No	Decreased NPCs proliferation	Alcantara and O'Driscoll, 2014; Baffet et al., 2016
PCNT	Congenital microcephaly, Seckel syndrome, MOPD type II	Centrosomes	No	Decreased NPCs proliferation, aberrant mitosis, missegregation of chromosomes	Griffith et al., 2008; Miyoshi et al., 2009; Benmerah et al., 2015
RTTN	Congenital microcephaly, dwarfism, cerebellar abnormalities	Centrosomes	No	Abnormal spindles, centriole structures	Shamseldin et al., 2015; Chen et al., 2017
KIF5C	Cortical dysplasia	Spindles	No	Abnormal microtubule function	Poirier et al., 2013
KIF2A	Cortical dysplasia	Spindles	No	Abnormal axon branching, abnormal microtubule function	Poirier et al., 2013
KIF11	Congenital microcephaly	Centrosomes, spindle, and cilia	No	Abnormal spindles and reduced NPCs proliferation	Ostergaard et al., 2012
KIF14	Congenital microcephaly, Meckel syndrome	Centrosomes, spindle	No	Increased neuronal cell death, abnormal cell migration	Moawia et al., 2017

(Continued)

TABLE 1 | Continued

Genes	Syndrome	Subcellular localization	Modeled in patient specific brain organoids	Mechanisms revealed	References
TUBA1A	Cortical abnormalities, tubulinopathy	Variable, microtubule	No	Abnormal neuronal migration	Wei et al., 2019
TUBG1	Cortical abnormalities, tubulinopathy	Variable, microtubule	No	Abnormal neuronal migration	Poirier et al., 2013
TUBB2B	Cortical abnormalities, tubulinopathy	Variable, microtubule	No	Abnormal neuronal migration	Romaniello et al., 2012
CEP135	Congenital microcephaly	Centrosomes	No	Abnormal centriole structures, disorganized spindles, reduced NPCs proliferation	Hussain et al., 2012; Lin et al., 2013
CDK6	Congenital microcephaly	Centrosomes	No	Abnormal spindle, unknown mechanisms	Hussain et al., 2013
CIT	Congenital microcephaly, dwarfism	Mid body	No	Mitotic delay, impaired cytokinesis, multipolar spindles, genomic instability, cell death	Li et al., 2016; Shaheen et al., 2016
Ninein	Seckel syndrome	Centrosomes	No	Defective migration, neuroectoderm defects	Dauber et al., 2012
NBS1	Congenital microcephaly, Nijmegen breakage syndrome	Nucleus	No	Double strand break repair deficiency	Varon et al., 1998
ATR	Seckel syndrome	Nucleus	No	Mitotic delay, impaired cytokinesis, double strand break repair deficiency	O'Driscoll et al., 2003
XLF/Cernunos	Congenital microcephaly	Nucleus	No	Double strand break repair deficiency	Buck et al., 2006
XRCC2	Congenital microcephaly	Nucleus	No	Double strand break repair deficiency neuronal death	Deans et al., 2000
XRCC4	Congenital microcephaly	Nucleus	No	Double strand break repair deficiency neuronal death	Gao et al., 1998
Ligase IV deficiency	Congenital microcephaly	Nucleus variable	No	Double strand break repair deficiency	Barnes et al., 1998
XPA-XPG	Xeroderma Pigmentosum, Microcephaly, Variable	Nucleus variable	No	Double strand break repair deficiency	Anttinen et al., 2008
ERCC6, ERCC8	Cockayne Syndrome microcephaly	Nucleus variable	No	Nucleotide excision repair and base excision repair deficiency	Jackson et al., 2002; Lin et al., 2005
TTDA	Congenital microcephaly	Nucleus variable	No	Double strand break repair deficiency	Chu and Mayne, 1996; Faghri et al., 2008
DNAPK	Congenital microcephaly, Seizures, Neuronal death	Nucleus variable	No	Double strand break repair deficiency	Vemuri et al., 2001

the humans. Consequently, it is plausible that the interaction partners and biochemical pathways of these microcephaly proteins in humans could have simultaneously co-evolved (Evans et al., 2004; Hill and Walsh, 2005; Ali and Meier, 2008).

Apart from being a centrosome-linked syndrome, microcephaly is also caused by mutations occurring in DNA repair proteins (Jayaraman et al., 2018). In many human DNA repair defects, the repair engine counteracting DNA damage caused exogenously (i.e., radiation and toxic substances) or endogenously (i.e., base mismatch, strand breaks, stalled replication, high amount of reactive oxygen species, etc.) becomes dysfunctional **(Table 1)**. Considering the rapid proliferative capacity of NPCs in the VZ and high level of inherent oxidative DNA damage during embryogenesis, a strictly orchestrated DNA repair pathway must be rendered for the maintenance of these stem cells for healthy brain development.

When this sophisticated system fails, genomic instability occurs, which in turn could trigger NPCs differentiation or cell death (Yoshihara et al., 2017; Henry et al., 2018; Su et al., 2019). Though fate is determined according to the type of repair pathway activated, these aberrations, in each case, could potentially cause microcephaly (Ruzankina et al., 2007; Orii et al., 2006). In this context, patient-specific human brain organoids possess a great potential to decode a broad range of cellular defects occurring during human brain development. Although several DNA repair mutations are attributed to congenital microcephaly, to date, none of the DNA damage-related diseases have been modeled using brain organoids.

Besides the rare incidences of inherited microcephaly, the recent Zika virus (ZIKV) pandemic in the Americas has received significant attention due to its notorious nature of causing microcephaly (Cugola et al., 2016; Qian et al., 2016; Ventura et al., 2016; Gabriel et al., 2017; Wolf et al., 2017). This has further highlighted the vulnerability of the human brain for any developmental defects mediated by viral infections. Nonetheless, the mechanisms underlying the adverse neurodevelopmental abnormalities witnessed in both inherited microcephaly and acquired microcephaly are still mostly unknown. In addition, clinical studies or experiments with model systems that are distantly related to disease relevancy provide insufficient insights for understanding how and why neural stem cells are depleted in the developing human brain.

WHAT ARE 3D BRAIN ORGANOIDS, AND WHY TO USE THEM NOW?

3D brain organoids are self-organized structures derived from human pluripotent stem cells, which have helped to understand several aspects of brain development (Giandomenico and Lancaster, 2017; Gopalakrishnan, 2019; Setia and Muotri, 2019). Importantly, these 3D structures display tissue-like morphologies containing polarized radial glia, intermediate progenitors, and layer-specific cortical neurons recapitulating several aspects of the developing human brain (Mariani et al., 2012, 2015; Kadoshima et al., 2013; Lancaster et al., 2013; Pasca et al., 2015). Organoid culturing methods, which excluded inductive signals, have led to the generation of whole-brain organoids with a primitive cortical plate, including regions mirroring forebrain, hindbrain and midbrain (Lancaster et al., 2013; Gabriel et al., 2016). Strikingly, these 3D structures constituted specific cell types that were spatially restricted apicobasally similar to VZ of the mammalian brain (**Figure 1**). Thus, 3D brain organoids uniquely serve as alternative model systems to address challenging questions in understanding the pathomechanisms of microcephaly using 2D cell culture and rodent models. The uniqueness of brain organoids is substantiated by the growing number of evidence that further urge the use of 3D brain organoids to model human microcephaly. We summarize some of them here as below.

Modeling microcephaly in mice often required the complete ablation of a gene implicated in the assembly of centrosomes, cilia, spindle apparatus, or DNA repair mechanisms (Wang

et al., 2009; Barrera et al., 2010; Buchman et al., 2010; Lizarraga et al., 2010; Alkuraya et al., 2011; McIntyre et al., 2012; Insolera et al., 2014). Such a strong perturbation has been unusually observed in inherited microcephaly in human patients. To date, most of the inherited gene mutations causing microcephaly in human patients included point mutations, single amino acid substitutions, or truncations. In most cases, these mild perturbations led to the generation of at least partially functioning proteins, which still were not sufficient to rescue microcephaly phenotypes. Patient mutations in mouse models, in contrast to knockout models, showed only mild microcephaly phenotypes and didn't give insights into the mechanism at the cellular level. This contrasting difference between the brain phenotypes implies that the human brain is susceptible even when the gene is mildly perturbed.

Moreover, there is yet no evidence that a disease-causing mutation in the human brain could result in the analogous microcephalic brain in mouse models. As examples, CDK5RAP2 or ASPM mutant mice did not exhibit a severely reduced brain size, as was observed in human patients (Barrera et al., 2010; Buchman et al., 2010; Lizarraga et al., 2010; Pulvers et al., 2010). Likewise, Nde1-deficient mice did not display microcephaly phenotypes as, seen in human patients (Alkuraya et al., 2011). In this line, complete ablation of CPAP/Sas-4 was required to view evident microcephaly phenotypes in the mouse brain, suggesting that mouse neural progenitor cells (NPCs) are not as susceptible as human cells (Insolera et al., 2014).

The evidence collected from *in vivo* studies allows us to speculate the presence of a crucial functional difference in brain evolution, explaining why the human brain is much more sensitive and vulnerable than that of rodents. It is possible that mouse NPCs do not extensively proliferate before the onset of neural differentiation. In other words, in the mouse brain, NPCs proliferation and differentiation are not two distinct processes, meaning that there could be an existing steady state of NPCs differentiation, which goes hand in hand with its proliferation. On the other hand, it is likely that in human brain development, NPCs first extensively proliferate to accomplish a sufficient pool of symmetrically expanding NPCs before the onset of neural differentiation, suggesting that in humans, NPCs proliferation and differentiation are seemingly two distinct processes. Verifying this hypothesis in the developing human brain is an arduous task (Rakic, 1995; Huttner and Kosodo, 2005; Geschwind and Rakic, 2013; Florio and Huttner, 2014).

Indeed, 3D brain organoids mirroring early events of human brain development have convincingly helped to verify this aspect. Analyzing the division planes of radial glial cells (RGs) at the early developmental stages of brain organoids revealed that the majority of RGs division planes are horizontally oriented, a signature of symmetric expansion (Lancaster et al., 2013; Gabriel et al., 2016; Gabriel et al., 2017). This is key evidence that human RGs at the early stages of brain development are determined to symmetrically expand to accomplish a sufficiently large pool of NPCs to generate a structurally normal-sized brain. Strikingly, division planes of RGs in rodents do not seem to follow the human rule. In contrast to human RGs, rodent RGs exhibit mixed dynamics displaying both horizontal and vertical division planes
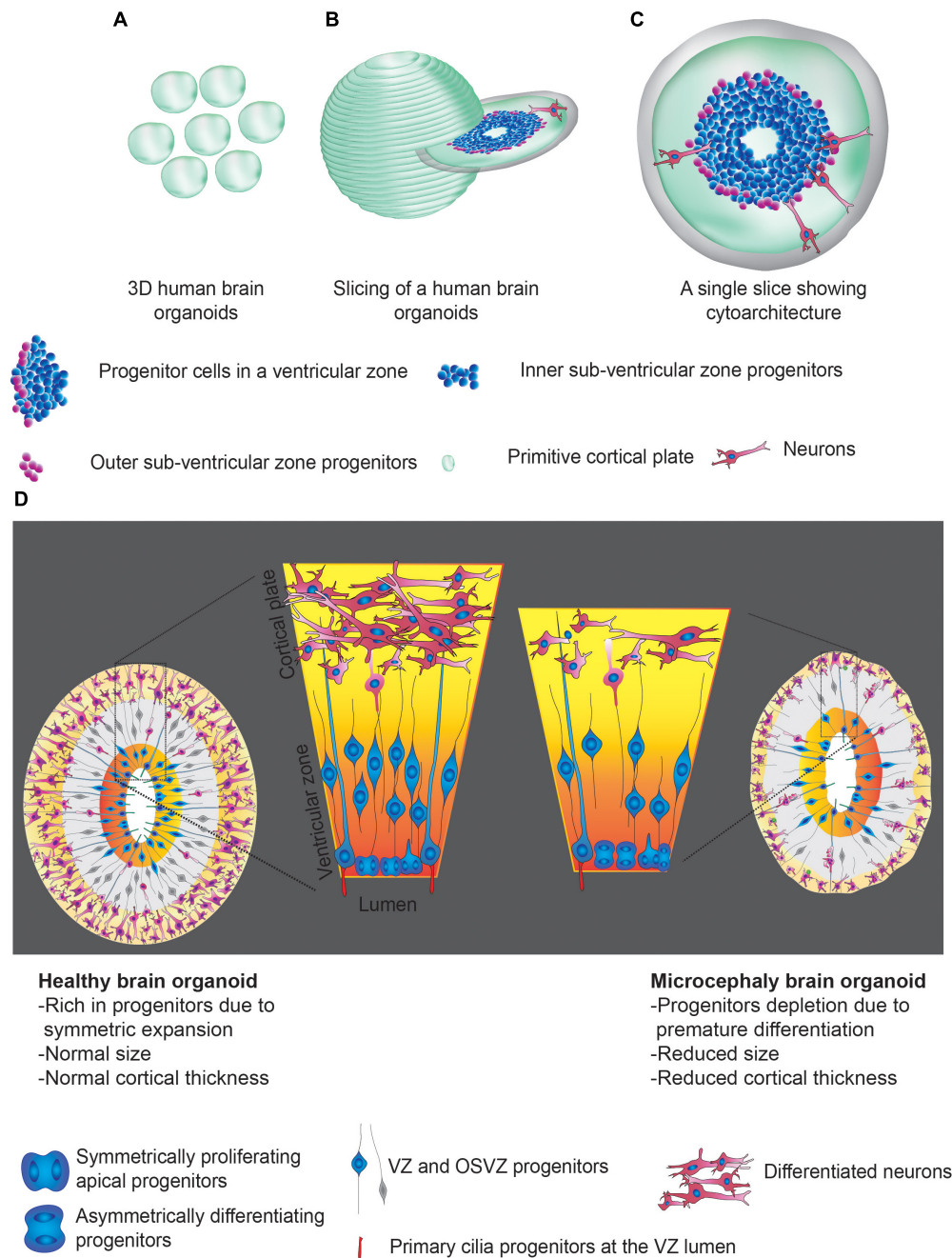
FIGURE 1 | Human brain organoids and their use in modeling the mechanisms of microcephaly. **(A)** Cartoonist representation of 3D human brain organoids. **(A)** Group of brain organoids. **(B)** Slicing off a 3D organoid. **(C)** An exemplary slice showing apicobasal progenitors in a ventricular zone Legends for the specific region or cell types are given. **(D)** Schematics explain possible structural abnormalities that could occur between healthy (left) and microcephaly (right) brain organoids. Microcephaly can be caused by genetic mutations (inherited microcephaly) or ZIKV infections (acquired microcephaly). In both cases, what appears to be shared is premature differentiation of NPCs leading to cortical thinning and overall size reduction. Note that control organoid displays NPCs whose division plane is mostly horizontally oriented to the lumen of the ventricular zone, a signature of symmetric expansion. In microcephaly organoids, the division planes of NPCs are mostly vertical. Legends for the specific region or cell types are given. These figure adapted from Gabriel et al. (2017).

suggesting symmetric expansion is simultaneously coupled to differentiation. Studying the kinetics of RGs division planes with respect to the ventricular lumen of the developing brain is a crucial aspect in understanding the process of early neurogenesis.

3D human brain organoids offer this unique opportunity of analyzing the kinetics of RGs division planes.

In summary, one should appreciate that these mouse-based studies provide valuable insights into the early events of brain

developmental mechanisms; yet, they do not sufficiently shed light on the complexes processes of human microcephaly. This, in turn, necessitates the need of 3D human brain organoids as a complementary model system that reflects the microenvironment of the human brain. The surprising trend, however, is that only a limited number of microcephaly patient-specific brain organoids have been generated to study the pathomechanisms observed in human patients (discussed as below). Nevertheless, these studies have unequivocally identified a surprising mechanism that underlay the formation of small-sized brain organoids as a consequence of impaired proliferation and premature neuronal differentiation of neural progenitors (Lancaster and Knoblich, 2014; Gabriel et al., 2016).

MECHANISMS OF MICROCEPHALY REVEALED BY PATIENT-DERIVED BRAIN ORGANOIDS

So far, only three independent centrosome-related patient-specific brain organoids have been characterized, which were generated from patient-derived iPSCs carrying mutations in CDK5RAP2, CPAP and ASPM (Lancaster et al., 2013; Gabriel et al., 2016; Li et al., 2017; Zhang et al., 2019). Thus, given the vast number of genetic mutations that cause microcephaly in humans, patient-specific microcephaly organoids are remarkably understudied. One of the limiting factors is reduced viability or instability of iPSCs due to mutations affecting centrosome structures, which are critical for fundamental cellular functions. Even then, a few numbers of patient-specific organoids thus far studied have significantly enhanced our understanding of the mechanisms that are derailed in microcephaly. In the first example, Lancaster et al. have successfully generated stable iPSCs from a patient that carried a compound heterozygous nonsense mutation in CDK5RAP2 (Lancaster et al., 2013). Using patient-derived iPSCs, the authors generate brain organoids, which were significantly smaller than the control groups. Thus, the first organoid generation protocol received the most sense of it because they could generate microcephaly brain organoids and elegantly demonstrate that patient-specific organoids exhibit the phenotypes of microcephaly patient brains. CDK5RAP2 is a pericentriolar material (PCM) protein in a centrosome (Zheng et al., 2014; Ramani et al., 2018). PCM is critical for centrosomal functions as it harbors microtubule-organizing centers. Thus, it is the PCM from where spindle microtubules emanate. Mutations in CDK5RAP2 and its homologs in various model systems have resulted in aberrantly functioning centrosomes (Zheng et al., 1995; Avidor-Reiss and Gopalakrishnan, 2012). However, the consequences of aberrantly operating centrosomes in rapidly proliferating human NPCs have never been studied until Lancaster et al. have demonstrated the critical role of centrosomes in symmetrically expanding human NPCs. It is noteworthy that CDK5RAP2 mutant mice did not exhibit a severely reduced brain size, as was observed in human patients (Barrera et al., 2010; Lizarraga et al., 2010).

As a PCM component, CDK5RAP2 is recruited to a centrosome via interacting with another conserved centrosomal

protein CPAP. CPAP is a centriole wall protein required to assemble and recruit PCM proteins to a developing centrosome (Gopalakrishnan et al., 2011; Jingyan and Glover, 2012; Lawo et al., 2012). Loss of function CPAP mutants was embryonic lethal in a variety of model organisms except in flies where the mutant flies could ultimately develop (Basto et al., 2006). Despite successfully developing, these mutant flies were uncoordinated due to the defects in ciliary functions. To date, several independent CPAP mutations have been sequenced in microcephaly patients whose mechanisms underlying microcephaly remained unknown. Besides, whether primary cilium plays a role in microcephaly pathogenesis has never been tested. In the second example, Gabriel et al. generated stable iPSCs from Seckel syndrome patient-derived fibroblasts, which harbored a splice-site mutation in CPAP, resulting in homozygous G-C transition in the last nucleotide of intron 11. This perturbation resulted in the deletion of exons 11, 12, and 13 (Al-Dosari et al., 2010). Brain organoids generated using equivalent starting numbers of iPSCs revealed that patient-specific brain organoids were significantly smaller than that of the control groups again, demonstrating that brain organoid is versatile models to exhibit progenitor biology-related defects due to mutations in centrosomal genes (Gabriel et al., 2016).

By studying the self-renewable and multipotent NPCs from patient-specific organoids, Gabriel et al. have revealed a surprising role of cilia in determining neural stem cell fates (Alcantara and O'Driscoll, 2014; Gabriel et al., 2016). The primary cilium is a cellular antenna that is present in almost all vertebrate cells functioning as a signaling hub. Gabriel and colleagues discovered that besides functioning as a cellular antenna, primary cilia also regulate cell cycle progression of human NPCs. In dividing cells, cilium assembly occurs during cell cycle exit (G1-G0), and disassembly coincides with cell cycle re-entry (G1-S to M). Cilium disassembly at the onset of mitosis is essential for assembling the mitotic spindle apparatus and for cell cycle re-entry. A delay or failure in cilium disassembly acts as a brake, retaining cells in G0/G1 and preventing cell cycle progression (Kim et al., 2011; Alcantara and O'Driscoll, 2014). Thus, the precise timing of cilia assembly and disassembly ensures the length of G1-S transition. These observations have defined the so-called "cilium checkpoint," where the cilium functions as a molecular switch that regulates cell cycle progression.

Using patient-derived brain organoids, Gabriel et al. showed that NPCs harboring a mutation in CPAP has retarded cilia disassembly exhibiting an extended G1-S transition. Importantly, patient-derived brain organoids helped them to uncover that an extended G1-S transition due to a defect in cilia disassembly is sufficient to cause premature differentiation of NPCs into early neurons. Analyzing the kinetics of RGs division planes with respect to the ventricular lumen of developing brain organoids revealed that the majority of RGs of microcephaly brain organoids were vertically oriented, indicating that they tend to differentiate prematurely. This led to an overall reduction in the neural stem cell pool at the ventricular zone and, as a result thinning of the primitive cortical plate (Alcantara and O'Driscoll, 2014; Gabriel et al., 2016). Strikingly, brain

organoids generated from WDR62 ablated pluripotent stem cells also led to a retarded cilium disassembly leading to decreased proliferation and premature differentiation of NPCs (Zhang et al., 2019). In summary, these works using a microcephaly brain organoid has established primary cilia as a molecular switch, regulating the homeostasis of neural epithelial tissues during brain development.

In another example of microcephaly modeling, Li et al. first cultured 3D brain organoids, which strikingly displayed in-vivo neocortex-like processes of ventricular, outer subventricular zones including laminating organization of cortical layers. Using these organoids Li and colleagues have successfully modeled the cellular defects caused by a mutation in abnormal spindle-like microcephaly-associated (ASPM) gene. It is noteworthy that the most common cause of primary human microcephaly is frequently associated with several mutations in the Aspm gene located at the MCPH5 locus. Coherent with the clinical data, patient-derived organoids displayed severe defects in structural organization displaying only a few populations of progenitor cells, which were markedly disorganized as compared to control groups. Although the cellular mechanisms for the loss of progenitor cells remain untested in this model, the smaller sized neural tissues observed in patient-derived organoids were indicative of the severely reduced brain size observed in patients.

As mentioned before, so far, the number of patient-derived organoids studied is meager. However, the mechanistic insights they offered is much more precise than derived from rodent or 2D culture models. It is also noteworthy that the underlying mechanism of NPCs depletion in patient-derived organoids is rather premature differentiation of NPCs than apparent cell death. Strikingly, most mouse models of microcephaly where the candidate genes (CDK5RAP2, CPAP, ASPM, Wdr62, and Plk4) were either completely ablated or highly overexpressed have invariably displayed apoptosis as a prominent mechanism for causing NPCs depletion and microcephaly. Unless and until cell death phenomena are prominently observed in a patient-derived organoid model, premature differentiation of NPCs leading to NPCs depletion makes most physiological sense as a mechanism causing microcephaly.

MECHANISMS REVEALED BY ZIKV INDUCED MICROCEPHALY MODELED BY BRAIN ORGANOIDS

It was scientific serendipity that the emergence of 3D organoid cultures has converged with the global health emergency posed by the ZIKV outbreak. Eventually, human brain organoids have pushed the frontiers of ZIKV research, as numerous studies have revealed the suitability of brain organoids in modeling microcephaly using disease-relevant ZIKV strains (Cugola et al., 2016; Qian et al., 2016; Ventura et al., 2016; Gabriel et al., 2017; Wolf et al., 2017). It is worth mentioning that several initial studies modeling ZIKV infection have used 2D cultures of NPCs and revealed that ZIKV strains are neurotropic and causing apoptosis (Tang et al., 2016). The

apparent cell death phenotypes in 2D experiments did not further allow dissecting the actual cellular mechanism that caused microcephaly (Tang et al., 2016).

Subsequent studies that employed an in-depth analysis of brain organoids exposed to ZIKV at different developmental stages showed that ZIKV could directly target NPCs at the ventricular zones (Cugola et al., 2016; Dang et al., 2016; Gabriel et al., 2017; Qian et al., 2017). Detailed quantitative analysis in brain organoids revealed that ZIKV infection could cause depletion of NPCs leading to the overall size reduction of organoids as seen with genetically inherited primary microcephaly (Cugola et al., 2016; Dang et al., 2016; Gabriel et al., 2017; Qian et al., 2017). Overall, at least two different ways have been profoundly proposed to cause microcephaly phenotypes, namely, either suppression of NPC proliferation or via increased cell death. While the cell death phenotypes are apparent in infected organoids, careful interpretation is required to conclude whether the observed cell death was due to over-loading of the viral particle, increased duration of infection, cytotoxic nature of the strain, disease irrelevant strain or the combination of all.

Few works have attempted to match acquired and genetically caused microcephaly mechanisms and have proposed several causative reasons for suppressing NPC proliferation or depletion. Some of them include upregulation of toll-like receptor 3, upregulation of pro-apoptotic pathways (Dang et al., 2016), p53 activation (El Ghouzzi et al., 2018), cell cycle dysregulation (Gabriel et al., 2017), disrupting RNA-binding protein regulating NPCs growth and differentiation (Chavali et al., 2017), destabilization of adherens junction complex, and premature differentiation of NPCs. The Gargely laboratory has identified a sequence at the 3′ untranslated region of a disease-relevant ZIKV strain, which controls Musashi-1 expression post-transcriptionally. Musashi-1 is a neural RNA-binding protein that regulates the growth and differentiation of NPCs. Intriguingly, a mutation in Musashi-1 is found in primary microcephaly patients (Chavali et al., 2017). The Gargely laboratory further demonstrated that ZIKV disrupts NPCs by interfering or hijacking Musashi-1 binding to its endogenous targets (Chavali et al., 2017). By far, this is the best example showing that there is a shared mechanism between acquired and genetically caused microcephaly. An obvious question that remains unanswered is whether brain organoids derived from Musashi-1 patients exhibit microcephaly due to disrupted proliferation or differentiation equilibrium of NPCs.

While all of these studies have claimed that ZIKV could trigger premature differentiation of NPCs, Gabriel et al. have directly tested the effect of ZIKV infection in altering RGs proliferation at the ventricular zones of developing brain organoids (Gabriel et al., 2017). They showed significantly elevated numbers of RGs exhibiting vertical division planes, an indication of premature differentiation within 5 days of ZIKV infection. By performing ultrastructural analysis, the authors have also identified that there are mild structural defects in centrioles of infected RGs, a critical mechanism that could underlay the premature differentiation of RGs (Gabriel et al., 2017). In summary, these works have identified that there are indeed common mechanisms

between acquired (ZIKV-induced) and genetically inherited microcephaly, which is brought to limelight by the use of human brain organoids as a test system.

CHALLENGES AND OUTLOOK

Even though genetic microcephaly syndromes are relatively rare, examining these disorders provide a unique advantage as they could reveal molecular mechanisms that determine NPCs maintenance, brain development, and human brain evolution in unprecedented detail. Thus, an intense effort needs to be made studying these disorders in a system that closely matches the human brain. In this scenario, the recent progress made with brain organoids strategically positions the field of microcephaly research. From experimental evidence, it has become increasingly clear that human NPCs are much more sensitive than rodents, and as a result, human NPCs are functionally impacted by mutations in the particular genes that cause microcephaly than rodent NPCs. This aspect provides an additional spotlight on the necessity for employing human brain organoids as an alternative model system to decode the most relevant mechanisms of microcephaly.

Recent work from the Kriegstein laboratory utilized large sets of comparative transcriptomes between primary human cortical cells of unknown genetic background, disease status, and brain organ (Bhaduri et al., 2020). The authors concluded that brain organoids do not recapitulate distinct cellular identities, progenitor maturation, and spatial segregation. Interestingly, their reasoning for the infidelity of organoids in this context is the activation of cellular stress pathways. While their work attempts to give a wake-up call for improving the reliability of organoids, their work did not emphasize enough of their organoid quality, since the organoids were grown for extended periods in 96 well plates in the presence of Rho-kinase (ROCK) inhibitor. Prolonged exposure to ROCK inhibitor could change the cell's metabolism and induce the mesendodermal differentiation pathway (Maldonado et al., 2016; Le and Hasegawa, 2019). Thus, from their method, it is impossible to draw a clear boundary until which point of developmental stage organoids are accurate. It is evident that 3D brain organoids would not be able to mimic the physiological functionality of the human brain entirely but owes incredible power in revealing critical aspects of early brain development. Perhaps, their conclusion should be taken into consideration for higher-order developmental issues such as the development of complex circuitry connections in the cerebral cortex.

Comprehensive decoding of the mechanisms of microcephaly requires a repertoire of mutant models, which is the significant bottleneck at the current state of the art. Thus generating a repertoire of iPSCs from microcephaly patients will enable us to generate patient-specific 3D tissues. In our opinion, the organoid generation is less critical than acquiring stable iPSCs that harbor microcephaly mutations. This is particularly true when looking at the extraordinary progress made within the last few years in culturing 3D organoids (Gopalakrishnan, 2019). Addressing questions related to microcephaly mechanisms do not require

brain organoids that are beyond the current state of the art. In other words, these questions do not necessarily depend on the need for further technological developments in the field of 3D organoid cultures. The questions of our interest mostly lie at the level of progenitor biology, and as described, several protocols have elegantly characterized the diversity of progenitors present at the ventricular zone. Introducing mutations in these cell types will allow us to dissect the molecular players and their role at the specific cell types.

An attractive alternative to patient-specific iPSCs is the genome tailoring to acquire disease-relevant patient mutations in pluripotent cells. Of note, CRISPR–Cas9-based genome editing has not been sufficiently utilized in microcephaly research using brain organoids except for a recent report, where authors have successfully eliminated the tight junction protein occludin in human embryonic stem cells. In this regard, CRISPR/Cas9-edited organoids displayed early neuronal differentiation and reduced progenitors (Bendriem et al., 2019). Remarkably, their comparative studies employing both mouse and human NPCs uncovered that human NPCs were more severely affected. Thus, applying genome tailoring in aspics to obtain organoids with patient-specific mutations will serve as a powerful tool and will allow us to generate microcephaly brain organoids to conduct a functional analysis of candidate genes in healthy human brain development.

Besides serving as a powerful *in vitro* system, organoids play a decisive role in dissecting the most likely mechanisms of microcephaly, which is NPCs depletion due to premature differentiation. Experimental evidence for this is derived from studying a few of the causative genes of primary microcephaly or ZIKV infection (Lancaster et al., 2013; Cugola et al., 2016; Gabriel et al., 2016, 2017; Dang et al., 2016; Li et al., 2017; Qian et al., 2017; Zhang et al., 2019). NPC depletion thus leads to overall brain size reduction, thinning of cortices, and impaired cortical expansion (**Figure 1D**). In this scenario, there are a couple of essential questions that stand out which require immediate attention. Firstly, besides standard primary microcephaly genes, several other genes also cause microcephaly, which falls under various mechanistic categories such as DNA damage, accelerated aging, mitotic delay, cytokinesis failure, transmembrane defects, cilia dysfunctions, signaling errors and autophagy (**Table 1**). These discoveries have pointed out that there are a wide variety of molecular and cellular mechanisms in the regulation of brain development and size determination. Do these cellular defects underlay premature NPCs differentiation? If so, during which phase of NPC proliferation, they are most prone to an attack? Studies have elucidated that retarded cilia disassembly leading to an extended G1-S transition is sufficient to trigger NPCs differentiation leading to the depletion of the symmetrically expanding NPCs pool. Thus, it remains to be tested if NPCs are vulnerable to differentiation if they are perturbed at various stages of cell cycle such as G2, and G2-M due to gene mutations that specifically target particular cell cycle stage.

As mentioned before, we are now left with the vast majority of fundamentally essential questions, which require early brain organoids displaying distinct progenitor cell layers with diverse

neural precursor populations. Thus, the brain organoid systems serve as a unique platform to investigate human-specific neurodevelopmental features and hold a great promise for *in vitro* neurobiologists. In conclusion, with the emergence of 3D human brain organoids and various genomic tool kits, we are in an exciting era to dissect mechanisms of microcephaly, which will eventually help us reconstructing the complex process of the human brain development.

AUTHOR CONTRIBUTIONS

JG conceived the concept. EG and AR performed literature survey and helped the concept further. NA involved in conceptualizing the idea of DNA damage in microcephaly.

REFERENCES

Alcantara, D., and O'Driscoll, M. (2014). Congenital microcephaly. *Am. J. Med. Genet. Part C Semin. Med. Genet.* 166, 124–139.

Aldape, K., Brindle, K. M., Chesler, L., Chopra, R., Gajjar, A., Gilbert, M. R., et al. (2019). Challenges to curing primary brain tumours. *Nat. Rev. Clin. Oncol.* 16, 509–520. doi: 10.1038/s41571-019-0177-5

Al-Dosari, M. S., Shaheen, R., Colak, D., and Alkuraya, F. S. (2010). Novel CENPJ mutation causes Seckel syndrome. *J. Med. Genet.* 47, 411–414. doi: 10.1136/jmg.2009.076646

Ali, F., and Meier, R. (2008). Positive selection in ASPM is correlated with cerebral cortex evolution across primates but not with whole-brain size. *Mol. Biol. Evol.* 25, 2247–2250. doi: 10.1093/molbev/msn184

Alkuraya, F. S., Cai, X., Emery, C., Mochida, G. H., Al-Dosari, M. S., Felie, J. M., et al. (2011). Human mutations in NDE1 cause extreme microcephaly with lissencephaly [corrected]. *Am. J. Hum. Genet.* 88, 536–547.

Amartely, H., David, A., Lebendiker, M., Benyamini, H., Izraeli, S., and Friedler, A. (2014). The STIL protein contains intrinsically disordered regions that mediate its protein-protein interactions. *Chem. Commun.* 50, 5245–5247. doi: 10.1039/c3cc45096a

Anttinen, A., Koulu, L., Nikoskelainen, E., Portin, R., Kurki, T., Erkinjuntti, M., et al. (2008). Neurological symptoms and natural course of xeroderma pigmentosum. *Brain J. Neurol.* 131, 1979–1989. doi: 10.1093/brain/awn126

Avidor-Reiss, T., and Gopalakrishnan, J. (2012). Building a centriole. *Curr. Opin. Cell Biol.* 25, 72–77. doi: 10.1016/j.ceb.2012.10.016

Babrowski, T., Romanowski, K., Fink, D., Kim, M., Gopalakrishnan, V., Zaborina, O., et al. (2013). The intestinal environment of surgical injury transforms *Pseudomonas aeruginosa* into a discrete hypervirulent morphotype capable of causing lethal peritonitis. *Surgery* 153, 36–43. doi: 10.1016/j.surg.2012.06.022

Baffet, A. D., Carabalona, A., Dantas, T. J., Doobin, D. D., Hu, D. J., and Vallee, R. B. (2016). Cellular and subcellular imaging of motor protein-based behavior in embryonic rat brain. *Methods Cell Biol.* 131, 349–363. doi: 10.1016/bs.mcb.2015.06.013

Barnes, D. E., Stamp, G., Rosewell, I., Denzel, A., and Lindahl, T. (1998). Targeted disruption of the gene encoding DNA ligase IV leads to lethality in embryonic mice. *Curr. Biol.* 8, 1395–1398.

Barrera, J. A., Kao, L. R., Hammer, R. E., Seemann, J., Fuchs, J. L., and Megraw, T. L. (2010). CDK5RAP2 regulates centriole engagement and cohesion in mice. *Dev. Cell* 18, 913–926. doi: 10.1016/j.devcel.2010.05.017

Basel-Vanagaite, L., and Dobyns, W. B. (2010). Clinical and brain imaging heterogeneity of severe microcephaly. *Pediatr. Neurol.* 43, 7–16. doi: 10.1016/j.pediatrneurol.2010.02.015

Basto, R., Lau, J., Vinogradova, T., Gardiol, A., Woods, C. G., Khodjakov, A., et al. (2006). Flies without centrioles. *Cell* 125, 1375–1386.

Bendriem, R. M., Singh, S., Aleem, A. A., Antonetti, D. A., and Ross, M. E. (2019). Tight junction protein occludin regulates progenitor self-renewal and survival in developing cortex. *eLife* 8:e49376. doi: 10.7554/eLife.49376

FUNDING

ACKNOWLEDGMENTS

Benmerah, A., Durand, B., Giles, R. H., Harris, T., Kohl, L., Laclef, C., et al. (2015). The more we know, the more we have to discover: an exciting future for understanding cilia and ciliopathies. *Cilia* 4:5. doi: 10.1186/s13630-015-0014-0

Bhaduri, A., Andrews, M. G., Mancia, Leon W, Jung, D., Shin, D., Allen, D., et al. (2020). Cell stress in cortical organoids impairs molecular subtype specification. *Nature* 578, 142–148. doi: 10.1038/s41586-020-1962-0

Bond, J., Roberts, E., Mochida, G. H., Hampshire, D. J., Scott, S., Askham, J. M., et al. (2002). ASPM is a major determinant of cerebral cortical size. *Nat. Genet.* 32, 316–320.

Bond, J., Roberts, E., Springell, K., Lizarraga, S. B., Scott, S., Higgins, J., et al. (2005). A centrosomal mechanism involving CDK5RAP2 and CENPJ controls brain size. *Nat. Genet.* 37, 353–355.

Borrell, V., and Gotz, M. (2014). Role of radial glial cells in cerebral cortex folding. *Curr. Opin. Neurobiol.* 27, 39–46. doi: 10.1016/j.conb.2014.02.007

Buchman, J. J., Tseng, H. C., Zhou, Y., Frank, C. L., Xie, Z., and Tsai, L. H. (2010). Cdk5rap2 interacts with pericentrin to maintain the neural progenitor pool in the developing neocortex. *Neuron* 66, 386–402. doi: 10.1016/j.neuron.2010.03.036

Buck, D., Malivert, L., de Chasseval, R., Barraud, A., Fondaneche, M. C., Sanal, O., et al. (2006). Cernunnos, a novel nonhomologous end-joining factor, is mutated in human immunodeficiency with microcephaly. *Cell* 124, 287–299.

Chavali, P. L., Stojic, L., Meredith, L. W., Joseph, N., Nahorski, M. S., Sanford, T. J., et al. (2017). Neurodevelopmental protein Musashi-1 interacts with the Zika genome and promotes viral replication. *Science* 357, 83–88.

Chen, H. Y., Wu, C. T., Tang, C. C., Lin, Y. N., Wang, W. J., and Tang, T. K. (2017). Human microcephaly protein RTTN interacts with STIL and is required to build full-length centrioles. *Nat. Commun.* 8:247. doi: 10.1038/s41467-017-00305-0

Chu, G., and Mayne, L. (1996). Xeroderma pigmentosum, Cockayne syndrome and trichothiodystrophy: do the genes explain the diseases? *Trends Genet.* 12, 187–192.

Consortium, F., Suzuki, H., Forrest, A. R., van Nimwegen, E., Daub, C. O., Balwierz, P. J., et al. (2009). The transcriptional network that controls growth arrest and differentiation in a human myeloid leukemia cell line. *Nat. Genet.* 41, 553–562. doi: 10.1038/ng.375

Cox, J., Jackson, A. P., Bond, J., and Woods, C. G. (2006). What primary microcephaly can tell us about brain growth. *Trends Mol. Med.* 12, 358–366.

Cugola, F. R., Fernandes, I. R., Russo, F. B., Freitas, B. C., Dias, J. L., Guimaraes, K. P., et al. (2016). The Brazilian Zika virus strain causes birth defects in experimental models. *Nature* 534, 267–271. doi: 10.1038/nature18296

Dang, J., Tiwari, S. K., Lichinchi, G., Qin, Y., Patil, V. S., Eroshkin, A. M., et al. (2016). Zika Virus depletes neural progenitors in human cerebral organoids through activation of the innate immune receptor TLR3. *Cell Stem Cell* 19, 258–265. doi: 10.1016/j.stem.2016.04.014

Dauber, A., Lafranchi, S. H., Maliga, Z., Lui, J. C., Moon, J. E., McDeed, C., et al. (2012). Novel microcephalic primordial dwarfism disorder associated with variants in the centrosomal protein ninein. *J. Clin. Endocrinol. Metab.* 97, E2140–E2151. doi: 10.1210/jc.2012-2150

Deans, B., Griffin, C. S., Maconochie, M., and Thacker, J. (2000). Xrcc2 is required for genetic stability, embryonic neurogenesis and viability in mice. *EMBO J.* 19, 6675–6685.

El Ghouzzi, V., Bianchi, F. T., Molineris, I., Mounce, B. C., Berto, G. E., Rak, M., et al. (2018). Correction to: ZIKA virus elicits P53 activation and genotoxic stress in human neural progenitors similar to mutations involved in severe forms of genetic microcephaly. *Cell Death Dis.* 9:1155. doi: 10.1038/s41419-018-1159-8

Evans, P. D., Anderson, J. R., Vallender, E. J., Gilbert, S. L., Malcom, C. M., Dorus, S., et al. (2004). Adaptive evolution of ASPM, a major determinant of cerebral cortical size in humans. *Hum. Mol. Genet.* 13, 489–494.

Faghri, S., Tamura, D., Kraemer, K. H., and Digiovanna, J. J. (2008). Trichothiodystrophy: a systematic review of 112 published cases characterises a wide spectrum of clinical manifestations. *J. Med. Genet.* 45, 609–621. doi: 10.1136/jmg.2008.058743

Farooq, M., Fatima, A., Mang, Y., Hansen, L., Kjaer, K. W., Baig, S. M., et al. (2016). A novel splice site mutation in CEP135 is associated with primary microcephaly in a Pakistani family. *J. Hum. Genet.* 61, 271–273.

Florio, M., Borrell, V., and Huttner, W. B. (2017). Human-specific genomic signatures of neocortical expansion. *Curr. Opin. Neurobiol.* 42, 33–44. doi: 10.1016/j.conb.2016.11.004

Florio, M., and Huttner, W. B. (2014). Neural progenitors, neurogenesis and the evolution of the neocortex. *Development* 141, 2182–2194.

Fujimori, A., Itoh, K., Goto, S., Hirakawa, H., Wang, B., Kokubo, T., et al. (2014). Disruption of Aspm causes microcephaly with abnormal neuronal differentiation. *Brain Dev.* 36, 661–669. doi: 10.1016/j.braindev.2013.10.006

Gabriel, E., Ramani, A., Karow, U., Gottardo, M., Natarajan, K., Gooi, L. M., et al. (2017). Recent Zika Virus isolates induce premature differentiation of neural progenitors in human brain organoids. *Cell Stem Cell* 20, 397–406. doi: 10.1016/j.stem.2016.12.005

Gabriel, E., Wason, A., Ramani, A., Gooi, L. M., Keller, P., Pozniakovsky, A., et al. (2016). CPAP promotes timely cilium disassembly to maintain neural progenitor pool. *EMBO J.* 35, 803–819. doi: 10.15252/embj.201593679

Gao, Y., Sun, Y., Frank, K. M., Dikkes, P., Fujiwara, Y., Seidl, K. J., et al. (1998). A critical role for DNA end-joining proteins in both lymphogenesis and neurogenesis. *Cell* 95, 891–902.

Geschwind, D. H., and Rakic, P. (2013). Cortical evolution: judge the brain by its cover. *Neuron* 80, 633–647. doi: 10.1016/j.neuron.2013.10.045

Giandomenico, S. L., and Lancaster, M. A. (2017). Probing human brain evolution and development in organoids. *Curr. Opin. Cell Biol.* 44, 36–43. doi: 10.1016/j.ceb.2017.01.001

Gopalakrishnan, J. (2019). The emergence of stem cell-based brain organoids: trends and challenges. *BioEssays* 41:e1900011. doi: 10.1002/bies.201900011

Gopalakrishnan, J., Mennella, V., Blachon, S., Zhai, B., Smith, A. H., Megraw, T. L., et al. (2011). Sas-4 provides a scaffold for cytoplasmic complexes and tethers them in a centrosome. *Nat. Commun.* 2, 359.

Griffith, E., Walker, S., Martin, C. A., Vagnarelli, P., Stiff, T., Vernay, B., et al. (2008). Mutations in pericentrin cause Seckel syndrome with defective ATR-dependent DNA damage signaling. *Nat. Genet.* 40, 232–236.

Guernsey, D. L., Jiang, H., Hussin, J., Arnold, M., Bouyakdan, K., Perry, S., et al. (2010). Mutations in centrosomal protein CEP152 in primary microcephaly families linked to MCPH4. *Am. J. Hum. Genet.* 87, 40–51. doi: 10.1016/j.ajhg.2010.06.003

Henry, M. P., Hawkins, J. R., Boyle, J., and Bridger, J. M. (2018). The genomic health of human pluripotent stem cells: genomic instability and the consequences on nuclear organization. *Front. Genet.* 9:623. doi: 10.3389/fgene.2018.00623

Hill, R. S., and Walsh, C. A. (2005). Molecular insights into human brain evolution. *Nature* 437, 64–67.

Hussain, M. S., Baig, S. M., Neumann, S., Nurnberg, G., Farooq, M., Ahmad, I., et al. (2012). A truncating mutation of CEP135 causes primary microcephaly and disturbed centrosomal function. *Am. J. Hum. Genet.* 90, 871–878. doi: 10.1016/j.ajhg.2012.03.016

Hussain, M. S., Baig, S. M., Neumann, S., Peche, V. S., Szczepanski, S., Nurnberg, G., et al. (2013). CDK6 associates with the centrosome during mitosis and is mutated in a large Pakistani family with primary microcephaly. *Hum. Mol. Genet.* 22, 5199–5214. doi: 10.1093/hmg/ddt374

Huttner, W. B., and Kosodo, Y. (2005). Symmetric versus asymmetric cell division during neurogenesis in the developing vertebrate central nervous system. *Curr. Opin. Cell Biol.* 17, 648–657.

Insolera, R., Bazzi, H., Shao, W., Anderson, K. V., and Shi, S. H. (2014). Cortical neurogenesis in the absence of centrioles. *Nat. Neurosci.* 17, 1528–1535. doi: 10.1038/nn.3831

Jackson, A. P., Eastwood, H., Bell, S. M., Adu, J., Toomes, C., Carr, I. M., et al. (2002). Identification of microcephalin, a protein implicated in determining the size of the human brain. *Am. J. Hum. Genet.* 71, 136–142.

Jayaraman, D., Bae, B. I., and Walsh, C. A. (2018). The genetics of primary microcephaly. *Annu. Rev. Genomics Hum. Genet.* 19, 177–200. doi: 10.1146/annurev-genom-083117-021441

Jingyan, F., and Glover, D. M. (2012). Structured illumination of the interface between centriole and peri-centriolar material. *Open Biol.* 2, 120104. doi: 10.1098/rsob.120104

Kadoshima, T., Sakaguchi, H., Nakano, T., Soen, M., Ando, S., Eiraku, M., et al. (2013). Self-organization of axial polarity, inside-out layer pattern, and species-specific progenitor dynamics in human ES cell-derived neocortex. *Proc. Natl. Acad. Sci. U.S.A.* 110, 20284–20289. doi: 10.1073/pnas.1315710110

Kalay, E., Yigit, G., Aslan, Y., Brown, K. E., Pohl, E., Bicknell, L. S., et al. (2011). CEP152 is a genome maintenance protein disrupted in Seckel syndrome. *Nat. Genet.* 43, 23–26. doi: 10.1038/ng.725

Khan, M. A., Rupp, V. M., Orpinell, M., Hussain, M. S., Altmuller, J., Steinmetz, M. O., et al. (2014). A missense mutation in the PISA domain of HsSAS-6 causes autosomal recessive primary microcephaly in a large consanguineous Pakistani family. *Hum. Mol. Genet.* 23, 5940–5949. doi: 10.1093/hmg/ddu318

Kim, S., Zaghloul, N. A., Bubenshchikova, E., Oh, E. C., Rankin, S., Katsanis, N., et al. (2011). Nde1-mediated inhibition of ciliogenesis affects cell cycle re-entry. *Nat. Cell Biol.* 13, 351–360. doi: 10.1038/ncb2183

Lancaster, M. A., and Knoblich, J. A. (2014). Organogenesis in a dish: modeling development and disease using organoid technologies. *Science* 345:1247125. doi: 10.1126/science.1247125

Lancaster, M. A., Renner, M., Martin, C. A., Wenzel, D., Bicknell, L. S., Hurles, M. E., et al. (2013). Cerebral organoids model human brain development and microcephaly. *Nature* 501, 373–379. doi: 10.1038/nature12517

Lawo, S., Hasegan, M., Gupta, G. D., and Pelletier, L. (2012). Subdiffraction imaging of centrosomes reveals higher-order organizational features of pericentriolar material. *Nat. Cell Biol.* 14, 1148–1158. doi: 10.1038/ncb2591

Le, M. N. T., and Hasegawa, K. (2019). Expansion culture of human pluripotent stem cells and production of cardiomyocytes. *Bioengineering* 6:48.

Li, H., Bielas, S. L., Zaki, M. S., Ismail, S., Farfara, D., Um, K., et al. (2016). Biallelic mutations in citron kinase link mitotic cytokinesis to human primary microcephaly. *Am. J. Hum. Genet.* 99, 501–510. doi: 10.1016/j.ajhg.2016.07.004

Li, R., Sun, L., Fang, A., Li, P., Wu, Q., and Wang, X. (2017). Recapitulating cortical development with organoid culture in vitro and modeling abnormal spindle-like (ASPM related primary) microcephaly disease. *Protein Cell* 8, 823–833. doi: 10.1007/s13238-017-0479-2

Lin, S. Y., Rai, R., Li, K., Xu, Z. X., and Elledge, S. J. (2005). BRIT1/MCPH1 is a DNA damage responsive protein that regulates the Brca1-Chk1 pathway, implicating checkpoint dysfunction in microcephaly. *Proc. Natl. Acad. Sci. U.S.A.* 102, 15105–15109.

Lin, Y. C., Chang, C. W., Hsu, W. B., Tang, C. J., Lin, Y. N., Chou, E. J., et al. (2013). Human microcephaly protein CEP135 binds to hSAS-6 and CPAP, and is required for centriole assembly. *EMBO J.* 32, 1141–1154. doi: 10.1038/emboj.2013.56

Lizarraga, S. B., Margossian, S. P., Harris, M. H., Campagna, D. R., Han, A. P., Blevins, S., et al. (2010). Cdk5rap2 regulates centrosome function and chromosome segregation in neuronal progenitors. *Development* 137, 1907–1917. doi: 10.1242/dev.040410

Maldonado, M., Luu, R. J., Ramos, M. E., and Nam, J. (2016). ROCK inhibitor primes human induced pluripotent stem cells to selectively differentiate towards mesendodermal lineage via epithelial-mesenchymal transition-like modulation. *Stem Cell Res.* 17, 222–227. doi: 10.1016/j.scr.2016.07.009

Mariani, J., Coppola, G., Zhang, P., Abyzov, A., Provini, L., Tomasini, L., et al. (2015). FOXG1-dependent dysregulation of GABA/glutamate neuron differentiation in autism spectrum disorders. *Cell* 162, 375–390. doi: 10.1016/j.cell.2015.06.034

Mariani, J., Simonini, M. V., Palejev, D., Tomasini, L., Coppola, G., Szekely, A. M., et al. (2012). Modeling human cortical development in vitro using induced pluripotent stem cells. *Proc. Natl. Acad. Sci. U.S.A.* 109, 12770–12775.

Marjanovic, M., Sanchez-Huertas, C., Terre, B., Gomez, R., Scheel, J. F., Pacheco, S., et al. (2015). CEP63 deficiency promotes p53-dependent microcephaly and reveals a role for the centrosome in meiotic recombination. *Nat. Commun.* 6:7676. doi: 10.1038/ncomms8676

McIntyre, R. E., Lakshminarasimhan Chavali, P., Ismail, O., Carragher, D. M., Sanchez-Andrade, G., Forment, J. V., et al. (2012). Disruption of mouse Cenpj, a regulator of centriole biogenesis, phenocopies Seckel syndrome. *PLoS Genet.* 8:e1003022. doi: 10.1371/journal.pgen.1003022

Miyoshi, K., Kasahara, K., Miyazaki, I., Shimizu, S., Taniguchi, M., Matsuzaki, S., et al. (2009). Pericentrin, a centrosomal protein related to microcephalic primordial dwarfism, is required for olfactory cilia assembly in mice. *FASEB J.* 23, 3289–3297. doi: 10.1096/fj.08-124420

Moawia, A., Shaheen, R., Rasool, S., Waseem, S. S., Ewida, N., Budde, B., et al. (2017). Mutations of KIF14 cause primary microcephaly by impairing cytokinesis. *Ann. Neurol.* 82, 562–577. doi: 10.1002/ana.25044

Molnar, Z., and Clowry, G. (2012). Cerebral cortical development in rodents and primates. *Prog. Brain Res.* 195, 45–70. doi: 10.1016/B978-0-444-53860-4.00003-9

Nicholas, A. K., Khurshid, M., Desir, J., Carvalho, O. P., Cox, J. J., Thornton, G., et al. (2010). WDR62 is associated with the spindle pole and is mutated in human microcephaly. *Nat. Genet.* 42, 1010–1014. doi: 10.1038/ng.682

Northcutt, R. G., and Kaas, J. H. (1995). The emergence and evolution of mammalian neocortex. *Trends Neurosci.* 18, 373–379.

O'Driscoll, M., Ruiz-Perez, V. L., Woods, C. G., Jeggo, P. A., and Goodship, J. A. (2003). A splicing mutation affecting expression of ataxia-telangiectasia and Rad3-related protein (ATR) results in Seckel syndrome. *Nat. Genet.* 33, 497–501.

Orii, K. E., Lee, Y., Kondo, N., and McKinnon, P. J. (2006). Selective utilization of nonhomologous end-joining and homologous recombination DNA repair pathways during nervous system development. *Proc. Natl. Acad. Sci. U.S.A.* 103, 10017–10022.

Ostergaard, P., Simpson, M. A., Mendola, A., Vasudevan, P., Connell, F. C., van Impel, A., et al. (2012). Mutations in KIF11 cause autosomal-dominant microcephaly variably associated with congenital lymphedema and chorioretinopathy. *Am. J. Hum. Genet.* 90, 356–362. doi: 10.1016/j.ajhg.2011.12.018

Pasca, A. M., Sloan, S. A., Clarke, L. E., Tian, Y., Makinson, C. D., Huber, N., et al. (2015). Functional cortical neurons and astrocytes from human pluripotent stem cells in 3D culture. *Nat. Methods* 12, 671–678. doi: 10.1038/nmeth.3415

Passemard, S., El Ghouzzi, V., Nasser, H., Verney, C., Vodjdani, G., Lacaud, A., et al. (2011). VIP blockade leads to microcephaly in mice via disruption of Mcph1-Chk1 signaling. *J. Clin. Invest.* 121, 3071–3087. doi: 10.1172/JCI43824

Pirozzi, F., Nelson, B., and Mirzaa, G. (2018). From microcephaly to megalencephaly: determinants of brain size. *Dialogues Clin. Neurosci.* 20, 267–282.

Poirier, K., Lebrun, N., Broix, L., Tian, G., Saillour, Y., Boscheron, C., et al. (2013). Mutations in TUBG1, DYNC1H1, KIF5C and KIF2A cause malformations of cortical development and microcephaly. *Nat. Genet.* 45, 639–647. doi: 10.1038/ng.2613

Pulvers, J. N., Bryk, J., Fish, J. L., Wilsch-Brauninger, M., Arai, Y., Schreier, D., et al. (2010). Mutations in mouse Aspm (abnormal spindle-like microcephaly associated) cause not only microcephaly but also major defects in the germline. *Proc. Natl. Acad. Sci. U.S.A.* 107, 16595–16600. doi: 10.1073/pnas.1010494107

Qian, X., Nguyen, H. N., Jacob, F., Song, H., and Ming, G. L. (2017). Using brain organoids to understand Zika virus-induced microcephaly. *Development* 144, 952–957. doi: 10.1242/dev.140707

Qian, X., Nguyen, H. N., Song, M. M., Hadiono, C., Ogden, S. C., Hammack, C., et al. (2016). Brain-region-specific organoids using mini-bioreactors for Modeling ZIKV Exposure. *Cell* 165, 1238–1254. doi: 10.1016/j.cell.2016.04.032

Rakic, P. (1995). A small step for the cell, a giant leap for mankind: a hypothesis of neocortical expansion during evolution. *Trends Neurosci.* 18, 383–388.

Ramani, A., Mariappan, A., Gottardo, M., Mandad, S., Urlaub, H., Avidor-Reiss, T., et al. (2018). Plk1/Polo Phosphorylates Sas-4 at the onset of mitosis for an efficient recruitment of pericentriolar material to centrosomes. *Cell Rep.* 25, 3618.e6–3630.e6. doi: 10.1016/j.celrep.2018.11.102

Rauch, A., Thiel, C. T., Schindler, D., Wick, U., Crow, Y. J., Ekici, A. B., et al. (2008). Mutations in the pericentrin (PCNT) gene cause primordial dwarfism. *Science* 319, 816–819. doi: 10.1126/science.1151174

Reardon, P. K., Seidlitz, J., Vandekar, S., Liu, S., Patel, R., Park, M. T. M., et al. (2018). Normative brain size variation and brain shape diversity in humans. *Science* 360, 1222–1227. doi: 10.1126/science.aar2578

Rilling, J. K. (2014). Comparative primate neuroimaging: insights into human brain evolution. *Trends Cogn. Sci.* 18, 46–55.

Romaniello, R., Tonelli, A., Arrigoni, F., Baschirotto, C., Triulzi, F., Bresolin, N., et al. (2012). A novel mutation in the beta-tubulin gene TUBB2B associated with complex malformation of cortical development and deficits in axonal guidance. *Dev. Med. Child Neurol.* 54, 765–769. doi: 10.1111/j.1469-8749.2012.04316.x

Ruzankina, Y., Pinzon-Guzman, C., Asare, A., Ong, T., Pontano, L., Cotsarelis, G., et al. (2007). Deletion of the developmentally essential gene ATR in adult mice leads to age-related phenotypes and stem cell loss. *Cell Stem Cell* 1, 113–126. doi: 10.1016/j.stem.2007.03.002

Setia, H., and Muotri, A. R. (2019). Brain organoids as a model system for human neurodevelopment and disease. *Semin. Cell Dev. Biol.* 95, 93–97.

Shaheen, R., Hashem, A., Abdel-Salam, G. M., Al-Fadhli, F., Ewida, N., and Alkuraya, F. S. (2016). Mutations in CIT, encoding citron rho-interacting serine/threonine kinase, cause severe primary microcephaly in humans. *Hum. Genet.* 135, 1191–1197. doi: 10.1007/s00439-016-1722-2

Shamseldin, H., Alazami, A. M., Manning, M., Hashem, A., Caluseiu, O., Tabarki, B., et al. (2015). RTTN mutations cause primary microcephaly and primordial dwarfism in humans. *Am. J. Hum. Genet.* 97, 862–868. doi: 10.1016/j.ajhg.2015.10.012

Shohayeb, B., Ho, U., Yeap, Y. Y., Parton, R. G., Millard, S. S., Xu, Z., et al. (2019). The association of microcephaly protein WDR62 with CPAP/IFT88 is required for cilia formation and neocortical development. *Hum. Mol. Gene.* 29, 248–263. doi: 10.1093/hmg/ddz281

Su, J., Zhu, D., Huo, Z., Gingold, J. A., Ang, Y. S., Tu, J., et al. (2019). Genomic integrity safeguards self-renewal in embryonic stem cells. *Cell Rep.* 28:e1404. doi: 10.1016/j.celrep.2019.07.011

Tang, H., Hammack, C., Ogden, S. C., Wen, Z., Qian, X., Li, Y., et al. (2016). Zika Virus infects human cortical neural progenitors and attenuates their growth. *Cell Stem Cell* 18, 587–590. doi: 10.1016/j.stem.2016.02.016

Varon, R., Vissinga, C., Platzer, M., Cerosaletti, K. M., Chrzanowska, K. H., Saar, K., et al. (1998). Nibrin, a novel DNA double-strand break repair protein, is mutated in Nijmegen breakage syndrome. *Cell* 93, 467–476.

Vemuri, M. C., Schiller, E., and Naegele, J. R. (2001). Elevated DNA double strand breaks and apoptosis in the CNS of scid mutant mice. *Cell Death. Differ.* 8, 245–255.

Ventura, C. V., Maia, M., Bravo-Filho, V., Gois, A. L., and Belfort, R. Jr. (2016). Zika virus in Brazil and macular atrophy in a child with microcephaly. *Lancet* 387:228.

Wang, X., Tsai, J. W., Imai, J. H., Lian, W. N., Vallee, R. B., and Shi, S. H. (2009). Asymmetric centrosome inheritance maintains neural progenitors in the neocortex. *Nature* 461, 947–955. doi: 10.1038/nature08435

Wei, H., Krishnappa, J., Lin, G., Kavalloor, N., Lim, J. Y., Goh, C. J., et al. (2019). Microcephaly with a simplified gyral pattern in a child with a de novo TUBA1A variant. *Am. J. Med. Genet. Part A* 182, 576–578.

Wolf, B., Diop, F., Ferraris, P., Wichit, S., Busso, C., Misse, D., et al. (2017). Zika virus causes supernumerary foci with centriolar proteins and impaired spindle positioning. *Open Biol.* 7:160231. doi: 10.1098/rsob.160231

Yoshihara, M., Hayashizaki, Y., and Murakawa, Y. (2017). Genomic instability of iPSCs: challenges towards their clinical applications. *Stem. Cell Rev. Rep.* 13, 7–16. doi: 10.1007/s12015-016-9680-6

Zecevic, N., Chen, Y., and Filipovic, R. (2005). Contributions of cortical subventricular zone to the development of the human cerebral cortex. *J.. Comp. Neurol.* 491, 109–122.

Zhang, W., Yang, S. L., Yang, M., Herrlinger, S., Shao, Q., Collar, J. L., et al. (2019). Modeling microcephaly with cerebral organoids reveals a WDR62-CEP170-KIF2A pathway promoting cilium disassembly in neural progenitors. *Nat. Commun.* 10:2612. doi: 10.1038/s41467-019-10497-2

Zheng, X., Gooi, L. M., Wason, A., Gabriel, E., Mehrjardi, N. Z., Yang, Q., et al. (2014). Conserved TCP domain of Sas-4/CPAP is essential for pericentriolar material tethering during centrosome biogenesis. *Proc. Natl. Acad. Sci. U.S.A.* 111, E354–E363. doi: 10.1073/pnas.1317535111

Zheng, Y., Wong, M. L., Alberts, B., and Mitchison, T. (1995). Nucleation of microtubule assembly by a gamma-tubulin-containing ring complex. *Nature* 378, 578–583.

Zhou, Z. W., Tapias, A., Bruhn, C., Gruber, R., Sukchev, M., and Wang, Z. Q. (2013). DNA damage response in microcephaly development of MCPH1 mouse model. *DNA Repair.* 12, 645–655. doi: 10.1016/j.dnarep.2013.04.017

Application of Fused Organoid Models to Study Human Brain Development and Neural Disorders

Augustin Chen [1,2,3†], Zhenming Guo [1,2,4†], Lipao Fang [1,2,3†] and Shan Bian [1,2]*

[1]Institute for Regenerative Medicine, Shanghai East Hospital, School of Life Sciences and Technology, Tongji University, Shanghai, China, [2]Frontier Science Center for Stem Cell Research, Tongji University, Shanghai, China, [3]Molecular Physiology, Center for Integrative Physiology and Molecular Medicine (CIPMM), University of Saarland, Homburg, Germany, [4]Bio-X Institute, Shanghai Jiao Tong University, Shanghai, China

Human brain organoids cultured from human pluripotent stem cells provide a promising platform to recapitulate histological features of the human brain and model neural disorders. However, unlike animal models, brain organoids lack a reproducible topographic organization, which limits their application in modeling intricate biology, such as the interaction between different brain regions. To overcome these drawbacks, brain organoids have been pre-patterned into specific brain regions and fused to form an assembloid that represents reproducible models recapitulating more complex biological processes of human brain development and neurological diseases. This approach has been applied to model interneuron migration, neuronal projections, tumor invasion, oligodendrogenesis, forebrain axis establishment, and brain vascularization. In this review article, we will summarize the usage of this technology to understand the fundamental biology underpinning human brain development and disorders.

Keywords: brain organoid, fusion models, stem cells, brain developement, neural disorder

INTRODUCTION

The human central nervous system (CNS) develops from several distinct vesicles into multiple intertwined regions. During this process, a range of migratory streams arise where progenitors generated in one place migrate and integrate into other areas (Marín et al., 2001; Kwan et al., 2012; Clowry et al., 2018; Molnár et al., 2019), and complex networks emerge, neurons branching and projecting across multiple regions (López-Bendito and Molnár, 2003). Besides, the colonization of the embryonic brain by mesodermal derivatives, namely microglia progenitors from the yolk-sac (Rezaie et al., 2005; Monier et al., 2007), and capillaries from the meningeal inner pial lamella (Marín-Padilla, 2012) adds complexity to the development of the human brain. Yet convoluted, the mechanism underpinning the formation of the human CNS is a highly ordered process that needs to be understood.

Human brain organoids are self-organizing three-dimensional stem cell cultures that recapitulate many aspects of the early developing human brain. These organoids include the formation of cortical progenitors with *in vivo*-like morphology and spatiotemporal organization (Eiraku et al., 2008; Kadoshima et al., 2013; Lancaster et al., 2013, 2017; Pasca et al., 2015; Renner et al., 2017) as well as faithful gene expression and epigenome compared to human fetal brains (Camp et al., 2015; Luo et al., 2016; Quadrato et al., 2017; Amiri et al., 2018; Velasco et al., 2019; Trevino et al., 2020). To recapitulate the first developmental stages of the human CNS, human brain

organoids overcome many limitations imposed by animal models, providing a unique tool to study early stages of the human brain development under both physiological and pathological conditions (Lancaster and Knoblich, 2014b; Fatehullah et al., 2016). Although there are still many limitations, brain organoids have been applied to model human brain development and disorders since the milestone publication by Eiraku et al. (2008) introducing the model for the very first time.

By comparing the cerebral organoids derived from humans and non-human primates, this technology led to the discovery of human-specific developmental features (Mora-Bermúdez et al., 2016; Otani et al., 2016; Kanton et al., 2019; Pollen et al., 2019). Results from clonal analysis and live-imaging experiments converged on the finding that human cortical progenitors spend more time in a proliferative state (Mora-Bermúdez et al., 2016; Otani et al., 2016). This has been supported by the description of a higher activity of the PI3K-AKT-mTOR pathway—involved in the maintenance of pluripotency—specific to human radial glia from outer subventricular zones (Pollen et al., 2019). These studies provide possible developmental mechanisms to the higher number of neurons observed in the human cortex. When grown from patient-derived induced pluripotent stem cell (iPSC), brain organoids can model some aspects of developmental diseases (Amin and Pasca, 2018), such as microcephaly (Lancaster et al., 2013; Omer Javed et al., 2018; Zhang et al., 2019), macrocephaly (Li et al., 2017), lissencephaly (Bershteyn et al., 2017; Iefremova et al., 2017), autism (Mariani et al., 2015), schizophrenia (Ye et al., 2017), Down syndrome (Xu et al., 2019), and neuronal heterotopia (Klaus et al., 2019). When exposed to viral loads, brain organoids provide new insights into prenatal infections like ZIKV (Cugola et al., 2016; Garcez et al., 2016; Qian et al., 2016). Moreover, brain organoids could be used as *in vitro* screening platform for potential therapeutics and gene editing technologies for the introduction or the suppression of oncogene mutations (Bian et al., 2018). In a nutshell, by reproducing many aspects of the intricate development of the CNS, human brain organoids are used to study the impact of genomic and transcriptomic modifications as well as the exposition to various stress factors on the early development of the human CNS (Schwartz et al., 2015; Lee et al., 2017; Zhu Y. et al., 2017; Belair et al., 2018; Wang et al., 2018).

Throughout the embryonic brain, neural progenitors progressively acquire their spatial identities, a process regulated by the successive actions of patterning centers and transcriptional frameworks (Molnár et al., 2019). When grown without additional patterning molecules, one single organoid can differentiate into various brain regions, including dorsal and ventral forebrain, choroid plexus, hippocampus, and retina (Lancaster et al., 2013). Although some organizing centers were observed in brain organoids (Renner et al., 2017), which are critical for regional brain patterning, most of the spatial identities in organoids appeared in an uncontrolled manner, thereby limiting the study of complex interregional interactions. Application of patterning factors and/or chemicals allows us to pattern brain organoids into different brain regions (Eiraku et al., 2008, 2011; Muguruma et al., 2010, 2015; Nakano et al., 2012;
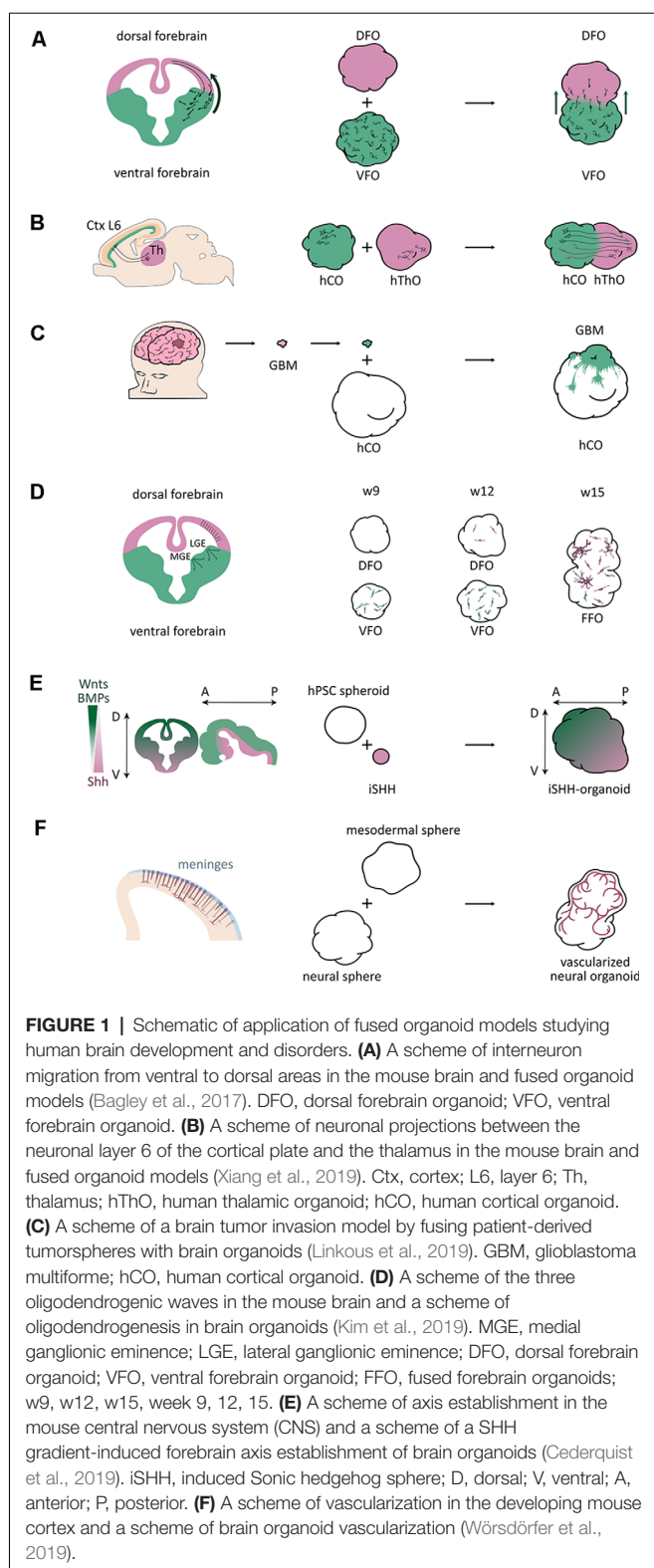
Kadoshima et al., 2013; Sakaguchi et al., 2015; Jo et al., 2016; Qian et al., 2016; Xiang et al., 2019), which provides researchers "LEGO blocks" to establish fused organoid approaches. The development of fused organoids, also called assembloids (Marton and Pasca, 2019), opens a new avenue to investigate interregional dynamics in the embryonic brain. Fusing two brain organoids pre-patterned into different regional identities enables the study of interregional interactions. This organoid fusion technology has already been applied for the study of interneuron migration (Bagley et al., 2017; Birey et al., 2017; Xiang et al., 2017), brain circuits (Giandomenico et al., 2019; Xiang et al., 2019), oligodendrogenesis (Xiang et al., 2017; Kim et al., 2019), and to establish the dorsoventral and anteroposterior axes within forebrain organoids (Cederquist et al., 2019). Organoids made by the fusion approach can help to deconstruct organogenesis by reconstructing the brain piece by piece.

The fusion paradigm should not be limited to the interaction of different brain regions. Any 3D co-culture system involving the assembly of brain organoids with a different tissue can be encompassed in the fusion approaches. This extended definition includes the co-culture of organoids with other cell types, such as endothelial cells (Song et al., 2019; Wörsdörfer et al., 2019) and tumor cells (Ogawa et al., 2018; Linkous et al., 2019; Bhaduri et al., 2020; Zhu et al., 2020). In this review article, we summarize the potential and great diversity of brain organoid fusion and co-culture models in studying human brain development and neural disorders.

INTERNEURON MIGRATION

Inhibitory interneurons, mostly GABAergic cells, are mainly derived from two areas of the human embryonic subpallium (ventral forebrain): the medial ganglionic eminence (MGE) and the caudal ganglionic eminence (CGE; Yuste, 2005; Wonders and Anderson, 2006; Bartolini et al., 2013). After production, post-mitotic interneurons migrate tangentially towards the dorsal forebrain, where, they wire and form functional circuits with locally born excitatory neurons. Defects in interneuron proliferation or impeded migration would disrupt the balance between these two types of neurons and are thought to contribute to many neurological and psychiatric disorders, such as schizophrenia, Down syndrome and autism (Wonders and Anderson, 2006; Bartolini et al., 2013; Bagley et al., 2017; Xu et al., 2019).

Studying interneurons, especially their interaction with excitatory neurons in organoids, would expand our view of these diseases, which are mainly studied using animal models. Although different brain regions, including dorsal and ventral forebrain, can be found in cerebral organoids, they appear in random locations without a stereotyped arrangement (Lancaster et al., 2013, 2017; Lancaster and Knoblich, 2014a), which make it challenging to model interneuron migration in organoids. However, the organoid fusion technique overcame this issue thereby allowing the modeling of human interneuron migration. In 2017, three independent groups generated interneuron migration models using fused organoid approaches (**Figure 1A**; Bagley et al., 2017; Birey et al., 2017; Xiang et al., 2017).

FIGURE 1 | Schematic of application of fused organoid models studying human brain development and disorders. **(A)** A scheme of interneuron migration from ventral to dorsal areas in the mouse brain and fused organoid models (Bagley et al., 2017). DFO, dorsal forebrain organoid; VFO, ventral forebrain organoid. **(B)** A scheme of neuronal projections between the neuronal layer 6 of the cortical plate and the thalamus in the mouse brain and fused organoid models (Xiang et al., 2019). Ctx, cortex; L6, layer 6; Th, thalamus; hThO, human thalamic organoid; hCO, human cortical organoid. **(C)** A scheme of a brain tumor invasion model by fusing patient-derived tumorspheres with brain organoids (Linkous et al., 2019). GBM, glioblastoma multiforme; hCO, human cortical organoid. **(D)** A scheme of the three oligodendrogenic waves in the mouse brain and a scheme of oligodendrogenesis in brain organoids (Kim et al., 2019). MGE, medial ganglionic eminence; LGE, lateral ganglionic eminence; DFO, dorsal forebrain organoid; VFO, ventral forebrain organoid; FFO, fused forebrain organoids; w9, w12, w15, week 9, 12, 15. **(E)** A scheme of axis establishment in the mouse central nervous system (CNS) and a scheme of a SHH gradient-induced forebrain axis establishment of brain organoids (Cederquist et al., 2019). iSHH, induced Sonic hedgehog sphere; D, dorsal; V, ventral; A, anterior; P, posterior. **(F)** A scheme of vascularization in the developing mouse cortex and a scheme of brain organoid vascularization (Wörsdörfer et al., 2019).

Interneurons were produced in the ventral organoids, and migrated into the dorsal regions after fusion.

The first study using brain organoids to model interneuron migration has been is reported by Birey et al. (2017). Based on a cortical spheroid (hCS) protocol (Pasca et al., 2015), Birey et al. (2017) patterned their organoids into ventral forebrain or subpallium identities by adding WNT inhibitor and Sonic Hedgehog (SHH) agonist during early stages of the differentiation protocol. The results of immunostaining and single-cell RNA sequencing (scRNA-seq) revealed that human subpallium spheroids (hSSs) were composed of various ventral progenitors and GABAergic interneurons, which were also found to be functionally active by patch clamping. After fusing hCSs with hSSs, Dlxi1/2b::eGFP labeled hSS cells were found crossing the fusion boundary, moving further into hCSs, generating elaborated branched morphologies, and forming functional synapses with hCS glutamic neurons. FACS followed by scRNA-seq analysis revealed interneuron transcriptional signatures in eGFP$^+$ cells isolated from the hCSs, following previous findings (Zechel et al., 2014). This migration in hSS-hCS fused organoids is consistent with human cortical development. Also, they combined patient-derived iPSCs and the organoid fusion approach to study Timothy syndrome, an L-type calcium channel (LTCCs)-related disorder affecting many organs of the human body including the nervous system. A previous study in mice indicated that LTCCs are associated with interneuron migration (Bortone and Polleux, 2009). Impaired interneuron migration was observed in patient-iPSC derived hSS-hCS, and was rescued by administration of an LTCC blocker.

Bagley et al. (2017) also established a fusion method, but modified from Lancaster's protocol (Lancaster and Knoblich, 2014a). The WNT inhibitor IWP2 and SHH agonist SAG were applied for organoid ventralization, while CycA, an SHH receptor antagonist, was used to dorsalize organoids (Vazin et al., 2014). In GFP$^+$ ventral and dTomato$^+$ dorsal fused organoids, a uni-directional cell migration from ventral into dorsal regions was observed. Rarely, migration was observed within the dorso-dorsal fused organoids. The largest proportion of migrated cells was SOX6$^+$ MGE cells. Also, COUP-TFII$^+$/NR2F2$^+$ and SP8$^+$ lateral ganglionic eminence (LGE)/CGE cells were observed to migrate into dorsal regions. Slice culture of dorso-ventral fusion organoids and time-lapse imaging analysis revealed characteristic interneuron migratory dynamics. Administration of the CXCR4 antagonist AMD3100 onto organoid slice cultures perturbed the migration, supporting a potential application of the fusion platform for drug screening.

Further, Xiang et al. (2017) generated human MGE organoids (hMGEOs) using an *NKX2-1*::GFP reporter human embryonic stem cell (hESC) line. RNA-seq, scRNA-seq, and chromatin accessibility analysis revealed that hMGEOs exhibited a strong correlation with the transcriptional signature of the MGE tissues from of human fetal brain. By fusing human cortical organoids (hCOs) and hMGEOs, they established hMGEOs-hCOs fusion organoids, named hfMCOs. GFP$^+$ but RFP$^-$ interneuron progenitors migrated into the neuronal layer of hCOs. Their migration can be inhibited by the application of blebbistatin, a myosin II inhibitor. Besides, functional synapses in hfMCOs were also observed by calcium imaging analysis.

Furthermore, using a dorsoventral organoid fusion model, Yuan et al. (2020) showed that LHX6 is essential for

GABAergic interneuron migration. Another study implanted patient iPSC-derived ventralized organoids into the mouse brain to investigate the role of OLIG2 in Down syndrome etiology (Xu et al., 2019). All these studies highlight the great potential of using the organoid fusion approaches to investigate the role of interneuron migration during human brain development and neural disorders.

NEURONAL PROJECTIONS

Long distance-projections play essential roles in brain functions. According to recent reports, corticothalamic interactions are relevant for sensorimotor interplay, selective attention, and arousal behaviors (López-Bendito and Molnár, 2003). Recently, Xiang et al. (2019) developed a method to form human thalamic organoids (hThOs) and created a model for corticothalamic projection by merging cortical and thalamic organoids (**Figure 1B**). The expression of the caudal forebrain marker OTX2, ventral thalamic marker DBX1, thalamic marginal zone marker of GBX2, and thalamic marker TCF7L2 significantly increased in the hThOs. Furthermore, scRNA-seq analysis identified specific cell types also found in the human fetal thalamus. After fusing hThOs and hCOs, they found that the axons from both cortex and thalamus reach the other side within 6 days. They also performed whole-cell patch-clamp recordings to examine the functional properties of thalamic neurons. The results revealed that cortico-thalamic neuronal projections might affect the maturation of thalamic neurons. The finding of this study provides a prospect to explore thalamic development and disorders associated with thalamic anomalies, for example, schizophrenia, epilepsy, and autism spectrum disorder.

Another study described the successful formation of neuronal projections between cerebral organoids and the mouse spinal cord (Giandomenico et al., 2019). Giandomenico et al. (2019) applied the air-liquid interface cerebral organoid (ALI-CO) method, which can improve oxygen supply compared to the standard approach, to promote the survival and maturation of brain cells, such as more complex dendrites and dendritic spines. ScRNA-seq indicated that ALI-COs exhibit various neuronal identities correlated with diverse axon morphologies. Interestingly, three-dimensional multi-electrode arrays revealed the highest correlated activity occurred over long distances, suggesting neurons were not limited to nearest-neighbor connections. Using this slice culture approach, they assessed the functionality of subcortically projecting tracts by co-culturing ALI-COs with the spinal cord sections from embryonic mice. Bundles of axon tracts connected to the spinal cord after around 2–3 weeks. Synapses could also be detected between ALI-CO projecting axons and spinal cord neurons. Strikingly, axon tracts could guide mouse muscle contraction when innervated, showing that organoid-derived projections can stimulate spinal cord/muscle explants. This study provides a way to explore neuronal connectivity with both input and output and can be used to study some aspects of neuronal circuit imbalances, degenerative conditions, or spinal cord injury.

Also, Mansour et al. (2018) transplanted human brain organoids into the adult mouse brain. In the chimeric brains, the grafted organoids displayed continuous differentiation and maturation. Moreover, they discovered an extension of axons into various regions of the host brain. Most axon tracts projected out of human organoids into the cortical layers and the corpus callosum. Axons with lower fiber density were observed in the deeper tissues of the host brain, such as the hippocampus and the thalamus, and even the contralateral areas. Furthermore, *in vivo* extracellular recording revealed synaptic connections and neuronal activity within the graft. This study supports the development of cell replacement therapy using brain organoids.

BRAIN TUMOR

Brain tumors are among the most lethal cancers and are the leading cause of cancer deaths in children under the age of 14 (Ostrom et al., 2016a,b). Their study is limited because of the incompleteness of available laboratory models. Brain organoids provide a novel platform to study brain tumor biology. Brain tumor organoid models were established by genetically introducing clinically relevant mutations into cerebral organoids to mimic brain tumor initiation (Bian et al., 2018; Ogawa et al., 2018). However, some studies implanted or fused patient-derived tumor cells into brain organoids to study brain tumor invasion (**Figure 1C**; Ogawa et al., 2018; Linkous et al., 2019; Bhaduri et al., 2020) or therapy (Zhu et al., 2020).

Because of its aggressiveness and invasiveness, glioblastoma multiforme (GBM) is the deadliest and most widespread primary brain tumor in adults. Their property to spread through infiltration in the host brain tissue is associated with high resistance and recurrence rate. To understand the mechanism underpinning this invasive phenotype, organoid-GBM fusion models are particularly appropriate. Ogawa et al. (2018) fused tumorspheres from one patient-derived GBM cell line SK2176 with cerebral organoids and found that SK2176 cells invaded and proliferated within the organoid parenchyma rapidly (Ogawa et al., 2018). In another study, Linkous et al. (2019) used brain organoids to provide a "normal" human brain microenvironment for tumors. They introduced cerebral organoid glioma (GLICO) as a model for tumor infiltration by co-culturing glioblastoma stem cells (GSCs) with cerebral organoids. The GLICO model showed that tumor cells deeply invaded the organoid parenchyma, and proliferated within the host tissues. They also observed the formation of an interconnected network of tumor microtubes, which is critical for tumor invasion. Moreover, in the most recent research, Bhaduri et al. (2020) identified an invasive tumor population similar to outer radial glial (oRG) cells using scRNA-seq analysis of patient specimens. They found that PTPRZ1^{+} cells expanded and invaded into the cerebral organoids after engraftment, and showed that PTPRZ1 plays a crucial role in tumor invasion.

Tumor-organoid fusion models have been used for preclinical therapeutic studies. Previously, the Zika virus (ZIKV) has been proven to be a potential oncolytic virus for brain tumor therapy

because of its tropism towards tumor cells (Zhu Z. et al., 2017). In further investigation, Zhu et al. (2020) used GBM-brain cerebral organoid (GBM-BCO) models to identify the SOX2-integrin $\alpha_v\beta_5$ axis as a potential mechanism for ZIKV tropism. Thus, organoid-GSC fusion models could be used as *in vitro* platforms to characterize GBM invasiveness and screen for potential therapeutics.

OLIGODENDROGENESIS

Oligodendrocytes (OLs) are the myelinating glial cells of the brain and the last type of neural cells to be generated after neurons and astroglial cells during mammalian brain development (Goldman and Kuypers, 2015). Based on the research using animal models, especially rodents, there are three major waves of oligodendrogenesis during forebrain development that have been described. Around embryonic day 12.5 (E12.5) and E15.5 in mice, oligodendrogenesis occurs in the ventral forebrain (Tekki-Kessaris et al., 2001; Kessaris et al., 2006; Chapman et al., 2013). After birth, oligodendrocyte precursors (OPCs) migrate tangentially to the cortex and spread throughout the forebrain. The third wave arises around birth date from the EMX1-expressing precursors in the dorsal forebrain (Kessaris et al., 2006). The dorsally born OPCs migrate locally and replace the OPCs generated from the first two waves. Although oligodendrogenesis has been well studied in animal brains, it remains unclear whether human oligodendrogenesis has any unique features because of the lack of human brain experimental models. The establishment of brain organoids provides a new platform to study human-specific oligodendrogenesis.

In one of the interneuron migration studies, Xiang et al. (2017) observed oligodendrogenesis in hMGEO cultures. They performed chromatin accessibility analysis of hMGEOs by ATAC-seq and found hMGEOs and human MGE shared similar open chromatin regions. Specifically, in ventral organoids, regions of oligodendrocyte-expressing genes were exclusively open. ScRNA-seq analysis showed OLIG1$^+$ cells could be found in hMGEOs at day 80, suggesting an earlier oligodendrocyte generation in human MGE than in the cortex.

Another study used dorsoventral fused organoids to study human developmental processes, particularly the dorsally derived oligodendrogenesis (Kim et al., 2019). They generated an OLIG2-GFP knockin hPSC reporter line to visualize OPC generation, and cultured organoids as dorsal forebrain organoids (DFOs), ventral forebrain organoids (VFOs), or fused forebrain organoids (FFOs) to study oligodendrogenesis. Similar to the first two oligodendrogenic waves in the mouse brain, OPCs first appeared in VFO culture. From week 5 to 7, intensive GFP$^+$ cells were observed in VFOs. In week 9, a big portion of OLIG2-GFP$^+$ OPCs were observed within VFOs (**Figure 1D**). Only until week 12, the GFP$^+$ OPCs were remarkably generated in DFOs, mimicking the third wave of oligodendrogenesis in the mouse brain (**Figure 1D**). More interestingly, when fusing VFO and DFO into FFO, they found that dorsally born OLs outnumber ventral-derived OLs and become dominant in FFOs after long-term culture,

which is also comparable to the oligodendrogenesis in mouse cortex (**Figure 1D**). Although this study did not find human-specific features, it introduced a novel model to study oligodendrogenesis and myelination-related diseases in a human genetic background.

FOREBRAIN AXIS ESTABLISHMENT

During brain development, topographic structures are generated by gradients of various signaling activities, such as WNT, SHH, and BMP (Petros et al., 2011), that regulate cell fate determination and regional identities. Brain organoids can recapitulate histological features of the human brain, but lack reproducible topographic organization. To overcome this drawback, a recent study established a self-organized dorsoventral and anteroposterior axes in forebrain organoids through an SHH protein gradient (Cederquist et al., 2019). By fusing the forebrain organoid with an inducible SHH-expressing hPSC-derived spheroid, Cederquist et al. (2019) introduced a SHH protein gradient into forebrain organoids (**Figure 1E**). SHH-patterned brain organoids exhibited *in vivo*-like topography of major forebrain subdivisions. This study opens the possibility to investigate more subtle neurodevelopmental mechanisms and region-specific neural disorders in a single organoid system.

BRAIN ORGANOID VASCULARIZATION

During brain development, the vasculature is one of the important niche components for neural stem cells and plays critical roles in neurogenesis (Bjornsson et al., 2015). However, due to a lack of cells from the mesodermal lineage during the brain organoid culture procedure, the absence of vascularization represents one of the major limitations of brain organoid models. There were several attempts to vascularize brain organoids using different approaches. Wörsdörfer et al. (2019) fused mesodermal precursor cell (MPC) aggregates with brain organoids for vascularization (**Figure 1F**). They found blood vessel-like structures in the brain organoids. Interestingly, these blood vessel-like tissues exhibited typical blood vessel ultrastructures, such as basement membranes, endothelial cell-cell junctions, and microvesicles. Also, they found IBA1$^+$ microglia-like cells, which are delivered from MPCs, infiltrating the brain organoids. Another study established hybrid neurovascular spheroids by fusing cortical neural precursor cell (iNSC) spheroids, endothelial cell (iEC) spheroids, and mesenchymal stem cells (MSCs; Song et al., 2019). Furthermore, Cakir et al. (2019) mixed wildtype hESCs with engineered hESCs that ectopically express ETS variant 2 (ETV2) to grow brain organoid. During the culture, vascular-like networks were generated within cortical organoids as ETV2 induces differentiation of hESCs into endothelial cells. All these studies open new doors to improve vascularization of brain organoids. However, it is still far from mimic the *in vivo* vascularization during brain development, and significant improvements still need to be done before obtaining functional vascular networks in organoid cultures.

CONCLUDING REMARKS

Brain organoid fusion technology allows us to study more complicated biology during human brain development and neural disorders using hESCs or patient-derived iPSCs, including interneuron migration, and neuronal projections. Using the same technique, researchers can also study other pathological processes and potential mechanisms, such as corpus callosum deformity. Assembling multiple different brain regions would be the next step towards a more complete human "mini-brain," which could then be used to study biological mechanisms requiring the interaction of several brain regions *in vitro*. The fusion strategy should not be limited to the fusion of brain tissues as it can be applied to assemble brain organoids with other types of organoids to study the interaction between different organs. For instance, hepato-biliary-pancreatic organogenesis has been modeled using a multi-organoid fusion approach (Koike et al., 2019). In future studies, investigating the interaction between brain organoids and retinal organoids, inner ear organoids, or even intestinal organoids would be of particular interest.

AUTHOR CONTRIBUTIONS

AC, ZG, and LF wrote the manuscript. AC and ZG prepared the figures. SB directed the manuscript preparation and wrote the manuscript.

FUNDING

ACKNOWLEDGMENTS

REFERENCES

Amin, N. D., and Pasca, S. P. (2018). Building models of brain disorders with three-dimensional organoids. *Neuron* 100, 389–405. doi: 10.1016/j.neuron.2018.10.007

Amiri, A., Coppola, G., Scuderi, S., Wu, F., Roychowdhury, T., Liu, F., et al. (2018). Transcriptome and epigenome landscape of human cortical development modeled in organoids. *Science* 362:eaat6720. doi: 10.1126/science.aat6720

Bagley, J. A., Reumann, D., Bian, S., Lévi-Strauss, J., and Knoblich, J. A. (2017). Fused cerebral organoids model interactions between brain regions. *Nat. Methods* 14, 743–751. doi: 10.1038/nmeth.4304

Bartolini, G., Ciceri, G., and Marín, O. (2013). Integration of GABAergic interneurons into cortical cell assemblies: lessons from embryos and adults. *Neuron* 79, 849–864. doi: 10.1016/j.neuron.2013.04.014

Belair, D. G., Wolf, C. J., Moorefield, S. D., Wood, C., Becker, C., and Abbott, B. D. (2018). A three-dimensional organoid culture model to assess the influence of chemicals on morphogenetic fusion. *Toxicol. Sci.* 166, 394–408. doi: 10.1093/toxsci/kfy207

Bershteyn, M., Nowakowski, T. J., Pollen, A. A., Di Lullo, E., Nene, A., Wynshaw-Boris, A., et al. (2017). Human iPSC-derived cerebral organoids model cellular features of lissencephaly and reveal prolonged mitosis of outer radial glia. *Cell Stem Cell* 20, 435.e4–449.e4. doi: 10.1016/j.stem.2016.12.007

Bhaduri, A., Di Lullo, E., Jung, D., Müller, S., Crouch, E. E., Espinosa, C. S., et al. (2020). Outer radial glia-like cancer stem cells contribute to heterogeneity of glioblastoma. *Cell Stem Cell* 26, 48.e6–63.e6. doi: 10.1016/j.stem.2019.11.015

Bian, S., Repic, M., Guo, Z., Kavirayani, A., Burkard, T., Bagley, J. A., et al. (2018). Genetically engineered cerebral organoids model brain tumor formation. *Nat. Methods* 15, 631–639. doi: 10.1038/s41592-018-0070-7

Birey, F., Andersen, J., Makinson, C. D., Islam, S., Wei, W., Huber, N., et al. (2017). Assembly of functionally integrated human forebrain spheroids. *Nature* 545, 54–59. doi: 10.1038/nature22330

Bjornsson, C. S., Apostolopoulou, M., Tian, Y., and Temple, S. (2015). It takes a village: constructing the neurogenic niche. *Dev. Cell* 32, 435–446. doi: 10.1016/j.devcel.2015.01.010

Bortone, D., and Polleux, F. (2009). KCC2 expression promotes the termination of cortical interneuron migration in a voltage-sensitive calcium-dependent manner. *Neuron* 62, 53–71. doi: 10.1016/j.neuron.2009.01.034

Cakir, B., Xiang, Y., Tanaka, Y., Kural, M. H., Parent, M., Kang, Y.-J., et al. (2019). Engineering of human brain organoids with a functional vascular-like system. *Nat. Methods* 16, 1169–1175. doi: 10.1038/s41592-019-0586-5

Camp, J. G., Badsha, F., Florio, M., Kanton, S., Gerber, T., Wilsch-Bräuninger, M., et al. (2015). Human cerebral organoids recapitulate gene expression programs of fetal neocortex development. *Proc. Natl. Acad. Sci. U S A* 112, 15672–15677. doi: 10.1073/pnas.1520760112

Cederquist, G. Y., Asciolla, J. J., Tchieu, J., Walsh, R. M., Cornacchia, D., Resh, M. D., et al. (2019). Specification of positional identity in forebrain organoids. *Nat. Biotechnol.* 37, 436–444. doi: 10.1038/s41587-019-0085-3

Chapman, H., Waclaw, R. R., Pei, Z., Nakafuku, M., and Campbell, K. (2013). The homeobox gene Gsx2 controls the timing of oligodendroglial fate specification in mouse lateral ganglionic eminence progenitors. *Development* 140, 2289–2298. doi: 10.1242/dev.091090

Clowry, G. J., Alzu'bi, A., Harkin, L. F., Sarma, S., Kerwin, J., and Lindsay, S. J. (2018). Charting the protomap of the human telencephalon. *Semin. Cell Dev. Biol.* 76, 3–14. doi: 10.1016/j.semcdb.2017.08.033

Cugola, F. R., Fernandes, I. R., Russo, F. B., Freitas, B. C., Dias, J. L. M., Guimarães, K. P., et al. (2016). The Brazilian Zika virus strain causes birth defects in experimental models. *Nature* 534, 267–271. doi: 10.1038/nature18296

Eiraku, M., Takata, N., Ishibashi, H., Kawada, M., Sakakura, E., Okuda, S., et al. (2011). Self-organizing optic-cup morphogenesis in three-dimensional culture. *Nature* 472, 51–56. doi: 10.1038/nature09941

Eiraku, M., Watanabe, K., Matsuo-Takasaki, M., Kawada, M., Yonemura, S., Matsumura, M., et al. (2008). Self-organized formation of polarized cortical tissues from ESCs and its active manipulation by extrinsic signals. *Cell Stem Cell* 3, 519–532. doi: 10.1016/j.stem.2008.09.002

Fatehullah, A., Tan, S. H., and Barker, N. (2016). Organoids as an *in vitro* model of human development and disease. *Nat. Cell Biol.* 18, 246–254. doi: 10.1038/ncb3312

Garcez, P. P., Loiola, E. C., Madeiro da Costa, R., Higa, L. M., Trindade, P., Delvecchio, R., et al. (2016). Zika virus impairs growth in human neurospheres and brain organoids. *Science* 352, 816–818. doi: 10.1126/science.aaf6116

Giandomenico, S. L., Mierau, S. B., Gibbons, G. M., Wenger, L. M. D., Masullo, L., Sit, T., et al. (2019). Cerebral organoids at the air-liquid interface generate diverse nerve tracts with functional output. *Nat. Neurosci.* 22, 669–679. doi: 10.1038/s41593-019-0350-2

Goldman, S. A., and Kuypers, N. J. (2015). How to make an oligodendrocyte. *Development* 142, 3983–3995. doi: 10.1242/dev.126409

Iefremova, V., Manikakis, G., Krefft, O., Jabali, A., Weynans, K., Wilkens, R., et al. (2017). An organoid-based model of cortical development identifies non-cell-autonomous defects in wnt signaling contributing to miller-dieker syndrome. *Cell Rep.* 19, 50–59. doi: 10.1016/j.celrep.2017.03.047

Jo, J., Xiao, Y., Sun, A. X., Cukuroglu, E., Tran, H.-D., Göke, J., et al. (2016). Midbrain-like organoids from human pluripotent stem cells contain functional dopaminergic and neuromelanin-producing neurons. *Cell Stem Cell* 19, 248–257. doi: 10.1016/j.stem.2016.07.005

Kadoshima, T., Sakaguchi, H., Nakano, T., Soen, M., Ando, S., Eiraku, M., et al. (2013). Self-organization of axial polarity, inside-out layer pattern, and species-specific progenitor dynamics in human ES cell-derived neocortex. *Proc. Natl. Acad. Sci. U S A* 110, 20284–20289. doi: 10.1073/pnas.1315710110

Kanton, S., Boyle, M. J., He, Z., Santel, M., Weigert, A., Sanchís-Calleja, F., et al. (2019). Organoid single-cell genomic atlas uncovers human-specific features of brain development. *Nature* 574, 418–422. doi: 10.1038/s41586-019-1654-9

Kessaris, N., Fogarty, M., Iannarelli, P., Grist, M., Wegner, M., and Richardson, W. D. (2006). Competing waves of oligodendrocytes in the forebrain and postnatal elimination of an embryonic lineage. *Nat. Neurosci.* 9, 173–179. doi: 10.1038/nn1620

Kim, H., Xu, R., Padmashri, R., Dunaevsky, A., Liu, Y., Dreyfus, C. F., et al. (2019). Pluripotent stem cell-derived cerebral organoids reveal human oligodendrogenesis with dorsal and ventral origins. *Stem Cell Reports* 12, 890–905. doi: 10.1016/j.stemcr.2019.04.011

Klaus, J., Kanton, S., Kyrousi, C., Ayo-Martin, A. C., Di Giaimo, R., Riesenberg, S., et al. (2019). Altered neuronal migratory trajectories in human cerebral organoids derived from individuals with neuronal heterotopia. *Nat. Med.* 25, 561–568. doi: 10.1038/s41591-019-0371-0

Koike, H., Iwasawa, K., Ouchi, R., Maezawa, M., Giesbrecht, K., Saiki, N., et al. (2019). Modelling human hepato-biliary-pancreatic organogenesis from the foregut-midgut boundary. *Nature* 574, 112–116. doi: 10.1038/s41586-019-1598-0

Kwan, K. Y., Šestan, N., and Anton, E. S. (2012). Transcriptional co-regulation of neuronal migration and laminar identity in the neocortex. *Development* 139, 1535–1546. doi: 10.1242/dev.069963

Lancaster, M. A., Corsini, N. S., Wolfinger, S., Gustafson, E. H., Phillips, A. W., Burkard, T. R., et al. (2017). Guided self-organization and cortical plate formation in human brain organoids. *Nat. Biotechnol.* 35, 659–666. doi: 10.1038/nbt.3906

Lancaster, M. A., and Knoblich, J. A. (2014a). Generation of cerebral organoids from human pluripotent stem cells. *Nat. Protoc.* 9, 2329–2340. doi: 10.1038/nprot.2014.158

Lancaster, M. A., and Knoblich, J. A. (2014b). Organogenesis in a dish: modeling development and disease using organoid technologies. *Science* 345, 1247125–1247125. doi: 10.1126/science.1247125

Lancaster, M. A., Renner, M., Martin, C.-A., Wenzel, D., Bicknell, L. S., Hurles, M. E., et al. (2013). Cerebral organoids model human brain development and microcephaly. *Nature* 501, 373–379. doi: 10.1038/nature12517

Lee, C.-T., Chen, J., Kindberg, A. A., Bendriem, R. M., Spivak, C. E., Williams, M. P., et al. (2017). CYP3A5 mediates effects of cocaine on human neocorticogenesis: studies using an *in vitro* 3D self-organized hPSC model with a single cortex-like unit. *Neuropsychopharmacology* 42, 774–784. doi: 10.1038/npp.2016.156

Li, Y., Muffat, J., Omer, A., Bosch, I., Lancaster, M. A., Sur, M., et al. (2017). Induction of expansion and folding in human cerebral organoids. *Cell Stem Cell* 20, 385.e3–396.e3. doi: 10.1016/j.stem.2016.11.017

Linkous, A., Balamatsias, D., Snuderl, M., Edwards, L., Miyaguchi, K., Milner, T., et al. (2019). Modeling patient-derived glioblastoma with cerebral organoids. *Cell Rep.* 26, 3203.e5–3211.e5. doi: 10.1016/j.celrep.2019.02.063

López-Bendito, G., and Molnár, Z. (2003). Thalamocortical development: how are we going to get there? *Nat. Rev. Neurosci.* 4, 276–289. doi: 10.1038/nrn1075

Luo, C., Lancaster, M. A., Castanon, R., Nery, J. R., Knoblich, J. A., and Ecker, J. R. (2016). Cerebral organoids recapitulate epigenomic signatures of the human fetal brain. *Cell Rep.* 17, 3369–3384. doi: 10.1016/j.celrep.2016.12.001

Mansour, A. A., Gonçalves, J. T., Bloyd, C. W., Li, H., Fernandes, S., Quang, D., et al. (2018). An *in vivo* model of functional and vascularized human brain organoids. *Nat. Biotechnol.* 36, 432–441. doi: 10.1038/nbt.4127

Mariani, J., Coppola, G., Zhang, P., Abyzov, A., Provini, L., Tomasini, L., et al. (2015). FOXG1-dependent dysregulation of GABA/glutamate neuron differentiation in autism spectrum disorders. *Cell* 162, 375–390. doi: 10.1016/j.cell.2015.06.034

Marín-Padilla, M. (2012). The human brain intracerebral microvascular system: development and structure. *Front. Neuroanat.* 6:38. doi: 10.3389/fnana.2012.00038

Marín, O., Yaron, A., Bagri, A., Tessier-Lavigne, M., and Rubenstein, J. L. (2001). Sorting of striatal and cortical interneurons regulated by semaphorin-neuropilin interactions. *Science* 293, 872–875. doi: 10.1126/science.1061891

Marton, R. M., and Pasca, S. P. (2019). Organoid and assembloid technologies for investigating cellular crosstalk in human brain development and disease. *Trends Cell Biol.* 30, 133–143. doi: 10.1016/j.tcb.2019.11.004

Molnár, Z., Clowry, G. J., Šestan, N., Alzu'bi, A., Bakken, T., Hevner, R. F., et al. (2019). New insights into the development of the human cerebral cortex. *J. Anat.* 235, 432–451. doi: 10.1111/joa.13055

Monier, A., Adle-Biassette, H., Delezoide, A.-L., Evrard, P., Gressens, P., and Verney, C. (2007). Entry and distribution of microglial cells in human embryonic and fetal cerebral cortex. *J. Neuropathol. Exp. Neurol.* 66, 372–382. doi: 10.1097/nen.0b013e3180517b46

Mora-Bermúdez, F., Badsha, F., Kanton, S., Camp, J. G., Vernot, B., Köhler, K., et al. (2016). Differences and similarities between human and chimpanzee neural progenitors during cerebral cortex development. *Elife* 5:e18683. doi: 10.7554/eLife.18683

Muguruma, K., Nishiyama, A., Kawakami, H., Hashimoto, K., and Sasai, Y. (2015). Self-organization of polarized cerebellar tissue in 3D culture of human pluripotent stem cells. *Cell Rep* 10, 537–550. doi: 10.1016/j.celrep.2014.12.051

Muguruma, K., Nishiyama, A., Ono, Y., Miyawaki, H., Mizuhara, E., Hori, S., et al. (2010). Ontogeny-recapitulating generation and tissue integration of ES cell-derived Purkinje cells. *Nat. Neurosci.* 13, 1171–1180. doi: 10.1038/nn.2638

Nakano, T., Ando, S., Takata, N., Kawada, M., Muguruma, K., Sekiguchi, K., et al. (2012). Self-formation of optic cups and storable stratified neural retina from human ESCs. *Cell Stem Cell* 10, 771–785. doi: 10.1016/j.stem.2012.05.009

Ogawa, J., Pao, G. M., Shokhirev, M. N., and Verma, I. M. (2018). Glioblastoma model using human cerebral organoids. *Cell Rep.* 23, 1220–1229. doi: 10.1016/j.celrep.2018.03.105

Omer Javed, A., Li, Y., Muffat, J., Su, K.-C., Cohen, M. A., Lungjangwa, T., et al. (2018). Microcephaly modeling of kinetochore mutation reveals a brain-specific phenotype. *Cell Rep.* 25, 368.e5–382.e5. doi: 10.1016/j.celrep.2018.09.032

Ostrom, Q. T., Gittleman, H., de Blank, P. M., Finlay, J. L., Gurney, J. G., McKean-Cowdin, R., et al. (2016a). American brain tumor association adolescent and young adult primary brain and central nervous system tumors diagnosed in the united states in 2008–2012. *Neurooncology* 18, i1–i50. doi: 10.1093/neuonc/nov297

Ostrom, Q. T., Gittleman, H., Xu, J., Kromer, C., Wolinsky, Y., Kruchko, C., et al. (2016b). CBTRUs statistical report: primary brain and other central nervous system tumors diagnosed in the united states in 2009–2013. *Neurooncology* 18, v1–v75. doi: 10.1093/neuonc/now207

Otani, T., Marchetto, M. C., Gage, F. H., Simons, B. D., and Livesey, F. J. (2016). 2D and 3D stem cell models of primate cortical development identify species-specific differences in progenitor behavior contributing to brain size. *Cell Stem Cell* 18, 467–480. doi: 10.1016/j.stem.2016.03.003

Pasca, A. M., Sloan, S. A., Clarke, L. E., Tian, Y., Makinson, C. D., Huber, N., et al. (2015). Functional cortical neurons and astrocytes from human pluripotent stem cells in 3D culture. *Nat. Methods* 12, 671–678. doi: 10.1038/nmeth.3415

Petros, T. J., Tyson, J. A., and Anderson, S. A. (2011). Pluripotent stem cells for the study of CNS development. *Front. Mol. Neurosci.* 4:30. doi: 10.3389/fnmol.2011.00030

Pollen, A. A., Bhaduri, A., Andrews, M. G., Nowakowski, T. J., Meyerson, O. S., Mostajo-Radji, M. A., et al. (2019). Establishing cerebral organoids as models of human-specific brain evolution. *Cell* 176, 743.e17–756.e17. doi: 10.1016/j.cell.2019.01.017

Qian, X., Nguyen, H. N., Song, M. M., Hadiono, C., Ogden, S. C., Hammack, C., et al. (2016). Brain-region-specific organoids using mini-bioreactors for modeling ZIKV exposure. *Cell* 165, 1238–1254. doi: 10.1016/j.cell.2016.04.032

Quadrato, G., Nguyen, T., Macosko, E. Z., Sherwood, J. L., Min Yang, S., Berger, D. R., et al. (2017). Cell diversity and network dynamics in photosensitive human brain organoids. *Nature* 545, 48–53. doi: 10.1038/nature22047

Renner, M., Lancaster, M. A., Bian, S., Choi, H., Ku, T., Peer, A., et al. (2017). Self-organized developmental patterning and differentiation in cerebral organoids. *EMBO J.* 36, 1316–1329. doi: 10.15252/embj.201694700

Rezaie, P., Dean, A., Male, D., and Ulfig, N. (2005). Microglia in the cerebral wall of the human telencephalon at second trimester. *Cereb. Cortex* 15, 938–949. doi: 10.1093/cercor/bhh194

Sakaguchi, H., Kadoshima, T., Soen, M., Narii, N., Ishida, Y., Ohgushi, M., et al. (2015). Generation of functional hippocampal neurons from self-organizing human embryonic stem cell-derived dorsomedial telencephalic tissue. *Nat. Commun.* 6:8896. doi: 10.1038/ncomms9896

Schwartz, M. P., Hou, Z., Propson, N. E., Zhang, J., Engstrom, C. J., Santos Costa, V., et al. (2015). Human pluripotent stem cell-derived neural constructs for predicting neural toxicity. *Proc. Natl. Acad. Sci. U S A* 112, 12516–12521. doi: 10.1073/pnas.1516645112

Song, L., Yuan, X., Jones, Z., Griffin, K., Zhou, Y., Ma, T., et al. (2019). Assembly of human stem cell-derived cortical spheroids and vascular spheroids to model 3-D brain-like tissues. *Sci. Rep.* 9:5977. doi: 10.1038/s41598-019-42439-9

Tekki-Kessaris, N., Woodruff, R., Hall, A. C., Gaffield, W., Kimura, S., Stiles, C. D., et al. (2001). Hedgehog-dependent oligodendrocyte lineage specification in the telencephalon. *Development* 128, 2545–2554.

Trevino, A. E., Sinnott-Armstrong, N., Andersen, J., Yoon, S.-J., Huber, N., Pritchard, J. K., et al. (2020). Chromatin accessibility dynamics in a model of human forebrain development. *Science* 367:eaay1645. doi: 10.1126/science.aay1645

Vazin, T., Ball, K. A., Lu, H., Park, H., Ataeijannati, Y., Head-Gordon, T., et al. (2014). Efficient derivation of cortical glutamatergic neurons from human pluripotent stem cells: a model system to study neurotoxicity in Alzheimer's disease. *Neurobiol. Dis.* 62, 62–72. doi: 10.1016/j.nbd.2013.09.005

Velasco, S., Kedaigle, A. J., Simmons, S. K., Nash, A., Rocha, M., Quadrato, G., et al. (2019). Individual brain organoids reproducibly form cell diversity of the human cerebral cortex. *Nature* 570, 523–527. doi: 10.1038/s41586-019-1289-x

Wang, Y., Wang, L., Zhu, Y., and Qin, J. (2018). Human brain organoid-on-a-chip to model prenatal nicotine exposure. *Lab Chip* 18, 851–860. doi: 10.1039/c7lc01084b

Wonders, C. P., and Anderson, S. A. (2006). The origin and specification of cortical interneurons. *Nat. Rev. Neurosci.* 7, 687–696. doi: 10.1038/nrn1954

Wörsdörfer, P., Dalda, N., Kern, A., Krüger, S., Wagner, N., Kwok, C. K., et al. (2019). Generation of complex human organoid models including vascular networks by incorporation of mesodermal progenitor cells. *Sci. Rep.* 9:15663. doi: 10.1038/s41598-019-52204-7

Xiang, Y., Tanaka, Y., Cakir, B., Patterson, B., Kim, K.-Y., Sun, P., et al. (2019). hESC-derived thalamic organoids form reciprocal projections when fused with cortical organoids. *Cell Stem Cell* 24, 487.e7–497.e7. doi: 10.1016/j.stem.2018.12.015

Xiang, Y., Tanaka, Y., Patterson, B., Kang, Y.-J., Govindaiah, G., Roselaar, N., et al. (2017). Fusion of regionally specified hPSC-derived organoids models

human brain development and interneuron migration. *Cell Stem Cell* 21, 383.e7–398.e7. doi: 10.1016/j.stem.2017.07.007

Xu, R., Brawner, A. T., Li, S., Liu, J.-J., Kim, H., Xue, H., et al. (2019). OLIG2 drives abnormal neurodevelopmental phenotypes in human iPSC-Based organoid and chimeric mouse models of down syndrome. *Cell Stem Cell* 24, 908.e8–926.e8. doi: 10.1016/j.stem.2019.04.014

Ye, F., Kang, E., Yu, C., Qian, X., Jacob, F., Yu, C., et al. (2017). DISC1 regulates neurogenesis *via* modulating kinetochore attachment of Ndel1/Nde1 during mitosis. *Neuron* 96, 1041.e5–1054.e5. doi: 10.1016/j.neuron.2017.10.010

Yuan, F., Fang, K.-H., Hong, Y., Xu, S.-B., Xu, M., Pan, Y., et al. (2020). LHX6 is essential for the migration of human pluripotent stem cell-derived GABAergic interneurons. *Protein Cell* 11, 286–291. doi: 10.1007/s13238-019-00686-6

Yuste, R. (2005). Origin and classification of neocortical interneurons. *Neuron* 48, 524–527. doi: 10.1016/j.neuron.2005.11.012

Zechel, S., Zajac, P., Lönnerberg, P., Ibáñez, C. F., and Linnarsson, S. (2014). Topographical transcriptome mapping of the mouse medial ganglionic eminence by spatially resolved RNA-seq. *Genome Biol.* 15:486. doi: 10.1186/s13059-014-0486-z

Zhang, W., Yang, S.-L., Yang, M., Herrlinger, S., Shao, Q., Collar, J. L., et al. (2019). Modeling microcephaly with cerebral organoids reveals a WDR62-CEP170-KIF2A pathway promoting cilium disassembly in neural progenitors. *Nat. Commun.* 10, 2612–2614. doi: 10.1038/s41467-019-10497-2

Zhu, Z., Gorman, M. J., McKenzie, L. D., Chai, J. N., Hubert, C. G., Prager, B. C., et al. (2017). Correction: zika virus has oncolytic activity against glioblastoma stem cells. *J. Exp. Med.* 214:3145. doi: 10.1084/jem.2017109309122017c

Zhu, Y., Wang, L., Yin, F., Yu, Y., Wang, Y., Shepard, M. J., et al. (2017). Probing impaired neurogenesis in human brain organoids exposed to alcohol. *Integr. Biol.* 9, 968–978. doi: 10.1039/c7ib00105c

Zhu, Z., Mesci, P., Bernatchez, J. A., Gimple, R. C., Wang, X., Schafer, S. T., et al. (2020). Zika virus targets glioblastoma stem cells through a SOX2-integrin αvβ5 axis. *Cell Stem Cell* 26, 187.e10–204.e10. doi: 10.1016/j.stem.2019.11.016

Immune Factor, TNFα, Disrupts Human Brain Organoid Development Similar to Schizophrenia—Schizophrenia Increases Developmental Vulnerability to TNFα

Courtney A. Benson[1], Hana R. Powell[1], Michal Liput[1,2], Siddhartha Dinham[3], David A. Freedman[1], Tracey A. Ignatowski[1]*, Ewa K. Stachowiak[1]* and Michal K. Stachowiak[1,3]*

[1]Department of Pathology and Anatomical Sciences, Jacobs School of Medicine and Biomedical Sciences, State University of New York at Buffalo, Buffalo, NY, United States, [2]Department of Stem Cells Bioengineering, Mossakowski Medical Research Centre, Polish Academy of Sciences, Warsaw, Poland, [3]Department of Biomedical Engineering, State University of New York at Buffalo, Buffalo, NY, United States

Schizophrenia (SZ) is a neurodevelopmental genetic disorder in which maternal immune activation (MIA) and increased tumor necrosis factor-α (TNF-α) may contribute. Previous studies using iPSC-derived cerebral organoids and neuronal cells demonstrated developmental malformation and transcriptional dysregulations, including TNF receptors and their signaling genes, common to SZ patients with diverse genetic backgrounds. In the present study, we examined the significance of the common TNF receptor dysregulations by transiently exposing cerebral organoids from embryonic stem cells (ESC) and from representative control and SZ patient iPSCs to TNF. In control iPSC organoids, TNF produced malformations qualitatively similar in, but generally less pronounced than, the malformations of the SZ iPSC-derived organoids. TNF and SZ alone disrupted subcortical rosettes and dispersed proliferating Ki67+ neural progenitor cells (NPC) from the organoid ventricular zone (VZ) into the cortical zone (CZ). In the CZ, the absence of large ramified pan-Neu+ neurons coincided with loss of myelinated neurites despite increased cortical accumulation of O4+ oligodendrocytes. The number of calretinin+ interneurons increased; however, they lacked the preferential parallel orientation to the organoid surface. SZ and SZ+TNF affected fine cortical and subcortical organoid structure by replacing cells with extracellular matrix (ECM)-like fibers The SZ condition increased developmental vulnerability to TNF,

Abbreviations: C, control; SZ, Schizophrenia; MIA, maternal immune activation; TNF-α, Tumor Necrosis Factor-α; ESC, embryonic stem cells; iPSC, induced pluripotent stem cell; NPC, neural progenitor cells; VZ, ventricular zone; CZ, cortical zone; IZ, intermediate zone; FGFR, fibroblast growth factor receptor; INFS, integrative nuclear (n) FGFR1 signaling; CBP, CREB binding protein; ROI, regions of interest; SEM, scanning electron microscopy; TBR1, transcription factor T-Box Brain 1; MBP, myelin basic protein; ECM, extracellular matrix.

leading to more pronounced changes in NPC, pan-Neu^{+} neurons, and interneurons. Both SZ- and TNF-induced malformations were associated with the loss of nuclear (n)FGFR1 form in the CZ and its upregulation in deep IZ regions, while in earlier studies blocking nFGFR1 reproduced cortical malformations observed in SZ. Computational analysis of ChIPseq and RNAseq datasets shows that nFGFR1 directly targets neurogenic, oligodendrogenic, cell migration, and ECM genes, and that the FGFR1-targeted TNF receptor and signaling genes are overexpressed in SZ NPC. Through these changes, the developing brain with the inherited SZ genome dysregulation may suffer increased vulnerability to TNF and thus, MIA.

Keywords: organoids, tumor necrosis factor, schizophrenia, nuclear fibroblast growth factor receptor-1, neural progenitor cell, oligodendrocyte

INTRODUCTION

Schizophrenia (SZ) is a neurodevelopmental psychotic disorder associated with fine changes in the brain cortical structure (Harrison, 1999). Both genetic factors, as well as physical and psychosocial environmental factors play a role in the development of SZ. The combined effect of genetics and environmental factors leads to abnormal circuit formation and consequently, aberrant neurotransmitter and synaptic function and ultimately abnormal behavior in SZ (Na et al., 2014; Estes and McAllister, 2016; Chuye et al., 2018). Evidence points to the primary hypothesis of convergence, in which genes and environmental factors converge and disrupt common developmental mechanism(s) leading to the emergence of SZ (Clarke et al., 2006; Schmitt et al., 2011).

A disrupted "feed forward and gate" signaling by integrative nuclear (n) FGFR1 signaling (INFS) during development acts as a common mechanism in genomic neurodevelopmental deprogramming in SZ patients with different genetic backgrounds (Narla et al., 2017). In cellular development, controlling signals propagate through diverse pathways to their end-point transcription factors. In parallel, these signals are fed forward by nFGFR1 directly to CREB binding protein (CBP), allowing genes to respond in a coordinated manner (Stachowiak and Stachowiak, 2016). Evidence indicates that in SZ, mutations of genes in diverse signaling pathways integrated by nFGFR1 disrupt the INFS function and thus neural development (Narla et al., 2018). Whether pathological environmental factors that contribute to SZ also affect nFGFR1, developmental function is unknown.

One environmental factor linked to the pathogenesis of SZ is infection during pregnancy and early childhood. Viral infection, particularly influenza, has been studied as a factor of SZ prevalence (Buka et al., 2001; Clarke et al., 2006; Patterson, 2009; Dean et al., 2013; Na et al., 2014). Maternal infection could alter immune status of the fetal brain and, along with genetic changes, significantly increase the risk of SZ. Elevated levels of the pro-inflammatory cytokine, tumor necrosis factor-α (TNF-α) have been reported in the placenta, amniotic fluid, and the brain of the fetus from mothers with influenza infection. Activated maternal TNF, and other cytokines, can invade the fetal CNS through various pathways, including disrupting the blood brain barrier (Buka et al., 2001; Clarke et al., 2006; Patterson, 2009; Dean et al., 2013; Na et al., 2014). TNF is one of the cytokines found to be significantly elevated in pregnant mothers that have been infected (Buka et al., 2001; Dean et al., 2013). TNF has been reported to affect neuronal growth, differentiation, synaptic scaling, and apoptosis in cultured cells and *in vivo* (Na et al., 2014).

Pregnant mice at mid-gestation infected with human influenza virus showed brain cortical layer and region-specific changes in the expression of the presynaptic marker, SNAP-25, iNOS, and Reelin (Patterson, 2009). Pyramidal cells were more densely packed, similar to what is observed in SZ (Patterson, 2009). Adult mice that were born to the infected mothers displayed an abnormality in neuronal migration to layer 2/3 in the cortex, which is similar to findings of downregulated DISC1 in SZ (Patterson, 2009) and in a recent SZ iPSC cerebral organoid study (Stachowiak et al., 2017). In mice, behavioral deficits were also observed in the offspring, including social interaction and open field and novel object exploration (Patterson, 2009), similar as in the FGFR1(TK-) transgenic mouse SZ model (Klejbor et al., 2006, 2009; Stachowiak et al., 2013). Increased levels of proinflammatory cytokines, including TNF, have consistently been reported in the blood and CSF of SZ patients during first and acute episodes (Buka et al., 2001; Clarke et al., 2006; Patterson, 2009; Dean et al., 2013; Na et al., 2014). Upregulated cytokine levels have been found in the adult brain of SZ patients, which could represent a permanent state of brain immune dysregulation (Buka et al., 2001; Clarke et al., 2006; Patterson, 2009). Increased TNF, inflammation and neuro-immune dysregulations have also been linked to autism spectrum disorders (Siniscalco et al., 2018).

In order to better understand the neurodevelopment of SZ, organoids, or "mini brains," generated from patient iPSC, provided for the first time, an insight into early disease etiology, parallel to the *in utero* development of the fetal brain during disease development (Stachowiak et al., 2017). These cerebral organoids mimic and closely model human brain development by generating the cerebral cortex, ventral telencephalon, choroid plexus, and retinal identities, among other brain regions (Chuye et al., 2018). The production of organoids *in vitro* can be used for studies of migration, differentiation, basic early neurodevelopment, as well as disease development and

progression. The cerebral organoids allowed for the first time to relate the broad INFS-linked transcriptional dysregulations found in SZ iPSC neural progenitor cells (NPCs; Narla et al., 2017) to development of the human brain malformations in SZ phenotype (Stachowiak et al., 2017). These genomic and tissue structural dysregulations were found in patients with different genomic backgrounds and may constitute a common developmental signature of the SZ phenotype (Chuye et al., 2018; Narla et al., 2018).

According to the "two-hit" theory of SZ, during gestation, genomic dysregulations (first hit) increase the fetus vulnerability to pathogenic factors, such as maternal immune activation (MIA) or hypoxia (second hit). This interaction between genetics and epigenetics could potentially affect histone acetylation and the methylation of DNA, and other gene regulatory mechanisms with lasting effects on neural development (Schmitt et al., 2011; Estes and McAllister, 2016). Despite having one of the two "hits," there is a possibility of a child being born without the disease. However, having both "hits" seems to skew the statistics unfavorably against healthy neurodevelopment.

This study aimed to explore a potential interaction between genetic disease modeled in SZ iPSC cerebral organoids and in MIA modeled by organoid exposure to the cytokine TNF.

MATERIALS AND METHODS

Cerebral Organoid Growth and TNF Exposure

Cerebral organoids derived from human (h) embryonic stem cells (ESC) and induced pluripotent stem cells (iPSCs) were grown according to our established protocol (Stachowiak et al., 2017) modified from the original studies of (Lancaster et al., 2013; Lancaster and Knoblich, 2014). The organoids had developed for 2 weeks (days 1–14) and at days 15–23 were transiently exposed to TNF (human recombinant TNFα, R&D Systems, Minneapolis, MN, USA). After an additional 2 weeks of recovery without TNF, the organoids were harvested on day 37. Fresh TNF was resupplied every 3 days along with medium change. Control organoids received fresh medium without TNF.

ESC organoids were developed from the hESC line, HUES8-iCas9n as previously described (Stachowiak et al., 2017). The initial experiment was designed to determine the effective TNF concentration; 1 or 10 ng/ml of TNF was added to organoid cultures. These concentrations were based on earlier cell culture studies, which showed moderate effects of 20 ng/ml TNF on human neuronal viability (Talley et al., 1995), stimulation of gliogenesis and inhibition of neurogenesis by human brain NPC (Lan et al., 2012). Both 1 and 10 ng/ml concentrations affected the overall organoid development (**Figure 1**, **Supplementary Figures S1, S2**) and subsequently lower TNF concentrations (50 and 250 pg/ml) were used.

IPSC organoids were developed from one representative control (healthy individual) iPSC line BJ#1, and one SZ patient line, 1835 (Narla et al., 2017; Stachowiak et al., 2017). These representative lines were selected from four control and four SZ lines, which showed consistent differences in neuronal

development (Brennand et al., 2015), gene expression including TNF receptor and signaling genes (Narla et al., 2017; Stachowiak et al., 2017), and in organoid corticogenesis between the apparently healthy and diverse SZ patients (Stachowiak et al., 2017). In the initial experiments leading to the current study TNF affected development of organoids of all these lines (CB, Ph.D. Thesis, 2017, University at Buffalo). The iPSC lines were originally obtained from Coriell Cell Repository, Camden New Jersey, NJ, USA. The iPSC organoids were exposed to 50 or 250 pg/ml TNF producing similar results. The four groups of iPSC organoids generated were control (C), control with TNF (C+TNF), schizophrenia (SZ), and schizophrenia with TNF (SZ+TNF) organoids. The organoids were grown and treated in separate batches including all treatment conditions. After freezing, the organoids were combined into common same treatment pools of which four organoids of the same treatment were randomly selected for analysis.

The organoid ventricular zone (VZ) is defined as cells surrounding rosette's ventricle-like lumen, cortical zone (CZ) as the organoid cortex, and intermediate zone (IZ) as the intervening region. These zones were additionally characterized in Stachowiak et al. (2017) and in the present study as regions containing proliferating Ki67+ cells and non-differentiated stem-like radial glia adjacent to the rosettes' lumen (VZ), migrating differentiating DCX+ neuroblasts (IZ), and βIII tubulin+ and differentiated pan-Neu+ neurons and calretinin+ interneuronsneurons (CZ). The intervening subplate region (between IZ and CZ) was earlier identified by anti-Reelin staining (Stachowiak et al., 2017).

Immunohistochemistry

For each treatment group (C, C+TNF, SZ, SZ+TNF) four individual organoids were harvested, and sectioned at 30 μm. The immunohistochemistry was performed simultaneously on series of sections (as previously in Stachowiak et al., 2017), including of the four iPSC organoid groups with four organoids per group analyzed. The sections were incubated with the primary antibodies overnight at 4°C, rinsed 3× in 1× PBS and subsequently incubated with fluorescent secondary antibody in the dark for 2 h as described in (Stachowiak et al., 2017). Microscopic slides containing organoid sections were cover slipped with mounting medium (Fluoro Gel II with DAPI). The primary and secondary antibodies used are listed in **Supplementary Table S1**.

All the stains, except for FGFR1, were observed and imaged using a Zeiss Axio Imager Upright Fluorescence microscope equipped with Zen Blue 2.3 software. Images were taken at 10× and 20× magnification. For FGFR1 a Leica Upright Fluorescence microscope with LAS X software was used. The Ki67 images were analyzed using a MatLab script (Stachowiak et al., 2017). This script recognized individual cells with a red stain by selectively extracting information related to the red light channel. The individual red + cells in regions of interest (ROIs) were counted as a single event using catchment basin identification that used the regional maxima values to create distinct regions around individual events. Calretinin-expressing neurons were counted in ROIs and their longest axis marked by hand. A further

MatLab-based calculation measured the angle of deviation of the axis of calretinin[+] interneurons relative to overlaying organoid's cortex using comprehensive program described in Stachowiak et al. (2017).

Pan-Neu and Olig4 Fluorescence Intensity Measurements were performed using Zen 2.0 Blue Imaging software in randomly selected ROIs within organoid regions (CZ and IZ) listed in the figure legends. As previously (Stachowiak et al., 2017), all images acquired were in the linear range of the camera. Images of sections from C, C+TNF, SZ, and SZ+TNF organoids were acquired under identical illumination conditions and identical camera gain, offset, and exposure times. Background images (outside the tissue sections) were taken and subtracted from the images of stained sections. The total area of each ROI image was recorded, as well as the number of threshold pixels and their integrated intensity. Each channel was converted into the 8-bit grayscale and the mean intensity was calculated.

Cells with nuclear FGFR1 (nFGFR1) immunostaining colocalized with the DAPI stain were counted in six CZ and six IZ ROIs using Visiopharm stereological software, as previously described (Stachowiak et al., 2017).

A recent study revealed the presence of neural crest cells in brain stem organoids (Eura et al., 2019). The presence of neural crest cells in the cerebral organoids was not investigated in the present study.

Scanning Electron Microscopy (SEM)

SEM was performed along with fluorescent microscopy to verify the morphological differences in cortical surface in control and SZ organoids and following TNF exposure.

The 30 μm sections representing individual experimental conditions were fixed in 2% glutaraldehyde for 1.5 h at 4°C. The sections were dehydrated by successive immersion in gradients of ETOH (30, 50, 70, 90, and 100%) 15 min each, followed by dip in 100% hexamethyldisilanzane and air-drying. The dehydrated sections were mounted onto a SEM stage and processed for 10 min through a vacuum chamber, where a very thin carbon layer closely coated the entire surface of the sample to secure conductivity. Representative organoid sections from each of the four conditions were examined under a bright field microscope. The ROIs were identified and imaged on Hitachi S4000 (Field Emission SEM) with IXRF Energy-Dispersive X-Ray Spectrometer; University of Buffalo's Instrument Center.

Images were taken at three different regions of each section with a special focus on the cortical and subcortical areas. At each region, images were taken at five increasing magnifications (500×, 1,500×, 2,500×, 5,000×, and 10,000×) without moving the stage. Circular ROIs were outlined, and numbers of cells/ROI were counted.

RNAseq and ChIPseq Data Analysis

The RNAseq analysis was performed in our earlier study (Narla et al., 2017, 2018) using homogenous cultures of NPC differentiated from four control and four SZ patients' iPSC lines. To induce neuronal committed cells, NPC were treated with 20 ng ml^{-1} BDNF (Peprotech), 20 ng ml^{-1} GDNF (Peprotech), 1 mM dibutyryl-cyclic AMP (Sigma), and 200 nM ascorbic acid

(Sigma; Narla et al., 2017) for 2 days. The current analyses were performed on the RNAseq datasets (Narla et al., 2017) with the accession code: GSE92874. The ChIPseq data were generated from the NPC of two SZ and two control iPSC lines (Narla et al., 2017). The ChIPseq datasets analyzed in the present study can be accessed at GSE92873.

Statistical Analyses

IBM SPSS was used to conduct one-way, two-way or three-way ANOVA followed by Fisher's Least Significant Difference (LSD) *post hoc* analyses (Stachowiak et al., 2017). The details of sample sizes are listed in figure legends and fulfill the requirement of statistical significance.

RESULTS

Human ESC Cerebral Organoids Recapitulate Cortical Development—Disruption by TNF

The initial experiments were performed on organoids generated from the human ESC line, HUES8, to test effects of different concentrations of TNF. Initially, the concentrations tested, 1 and 10 ng/ml, were based on cell culture studies, which showed their moderate effect on human neuronal viability (Talley et al., 1995), stimulation of gliogenesis, and inhibition of neurogenesis by human brain NPC (20 ng/ml; Lan et al., 2012).

HUES8 organoids were developed for 2 weeks in kinetic cultures and then incubated with 1 or 10 ng/ml of TNF for 9 days with fresh cytokine replenished every 3 days. After an additional 2 weeks of recovery in medium lacking TNF, organoids were harvested at day 37, the 5th week of the organoid development. In the control organoids, the culture medium lacking TNF was also exchanged every 3 days. At least six organoids were used per condition. At 5 weeks, the organoids reached 4–5 mm size and in the control TNF- lacking organoids, formation of multiple neurogenic rosettes (**Figure 1A1**) was observed. Similarly, as previously observed in ESC (H9) and iPSC organoids, there were three distinct regions, the VZ in the center of the rosettes, the surrounding IZ, and the peripheral CZ.

Incubation with TNF 1 ng/ml (**Figure 1A2**) or 10 ng/ml (not shown) disrupted the general organoid and rosette structures. The TNF exposed organoids stained with cresyl violet (Nissl staining) frequently displayed a scar-like tissue and their rosettes were irregular (**Figure 1A**). The scar-like regions contained displaced highly concentrated pan-Neu stained neurons (**Figure 1C2**) as well as GFAP stained glia (**Supplementary Figure S1B**). The latter may reflect a gliosis-like response to TNF observed *in vivo* (Livne-Bar et al., 2016; Galinsky et al., 2020).

At 5 weeks, the cortical rosettes of control HUES8 organoids contained Ki67^{+} proliferating NPC surrounding the central VZ lumen (**Figure 1B1**). Few Ki67^{+} cells were present in the IZ, and only single Ki67^{+} cells were occasionally found in the CZ. In 1 ng/ml (**Figure 1B2**) or 10 ng/ml (**Figure 1B3**), TNF-exposed organoids, Ki67^{+} proliferative cells were dispersed throughout the organoids, further illustrating the disruption
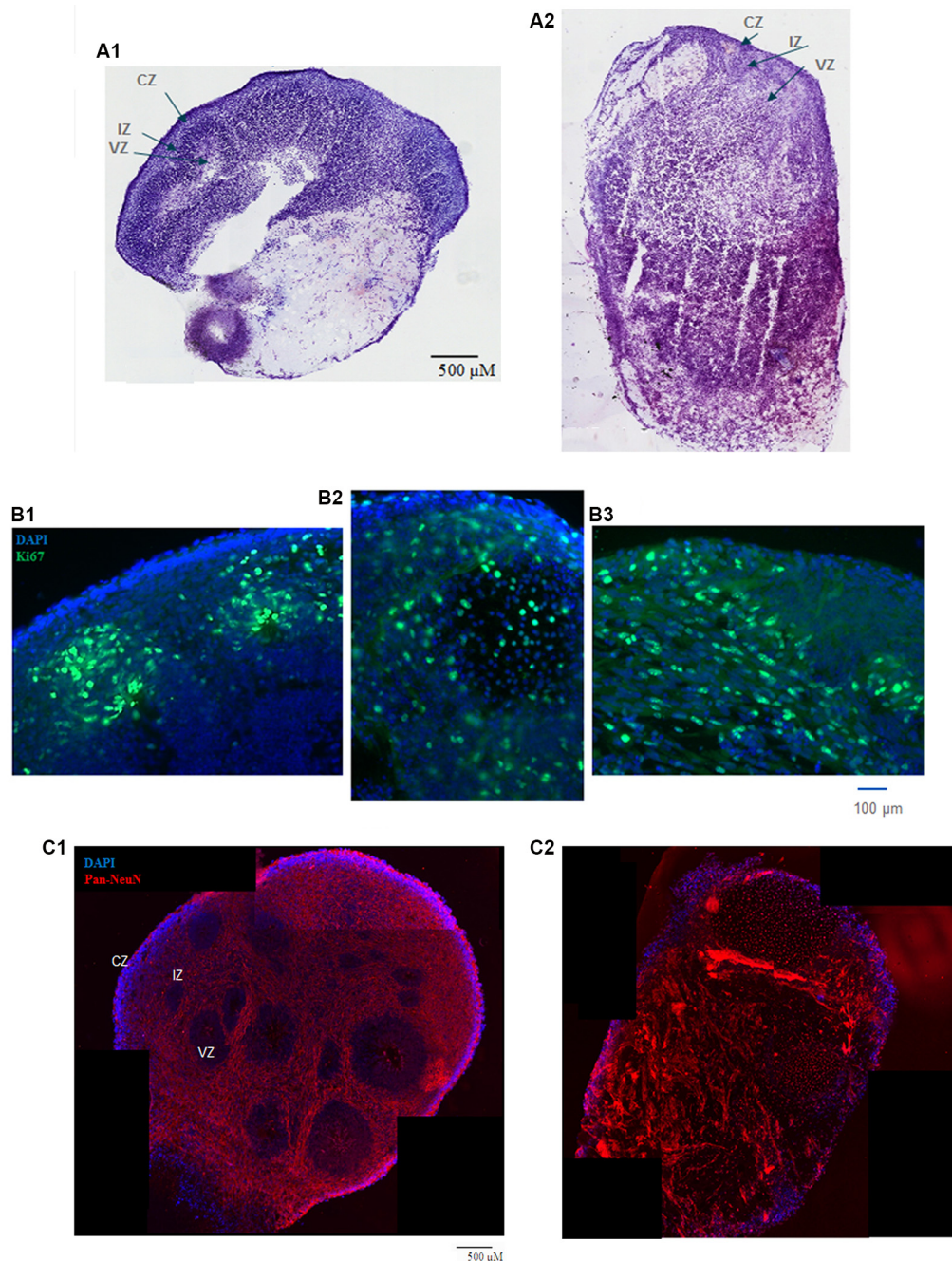
FIGURE 1 | (A) HUES8s organoid at 5 weeks—tile scanning of NISSL staining. Representative images are shown of **(A1)** control, non-treated organoid, and **(A2)** Tumor Necrosis Factor-α (TNF-α) (1 ng/ml) treated organoid. **(B)** Rosette formation in HUES8 organoids at 5 weeks—immunostaining of Ki67+ proliferating cells (green immunostaining) and DAPI stained nuclei (blue). **(B1)** Control HUES8 organoids not exposed to TNF formed cortical rosettes with Ki67+ proliferative cells. **(B2)** In HUES8, organoids exposed to 1 ng/ml TNF and **(B3)** in HUES8 organoids exposed to 10 ng/ml TNF Ki67 positive cells were dispersed throughout the organoids. **(C)** Neuronal development in HUES8 organoids at 5 weeks, pan-Neu immunostaining—red, DAPI—blue, tile scanning. **(C1)** In control organoids, pan-Neu+ neurons were located throughout the organoids outside of the ventricular zones (VZ), in the intermediate zone (IZ) and were concentrated in the cortical zone (CZ). **(C2)** HUES8 organoids exposed to 1 ng/ml TNF exhibited disorganized pan-Neu neuronal development, with clusters of pan-Neu+ cells dispersed throughout the tissue, and concentrated in the scar-like region. Note fewer pan-Neu+ neurons in the CZ of TNF-exposed organoids.

of the rosette organization. Ki67+ cells spread throughout all zones including the CZ (**Figures 1B2,B3**) and were present in the scar-like damaged tissue (not shown). GFAP positive radial glia, the brain stem cells, which in control HUES8 organoids outlined the VZ (**Supplementary Figure S1**). The GFAP+ glia, were dispersed throughout the TNF-exposed organoids

(**Supplementary Figure S1B**). Similar to the proliferating Ki67^{+} NPC, the GFAP-stained glia were found in the CZ and formed clusters in the scar-like regions of the TNF-exposed organoids.

Pan-Neu antibody cocktail, which stains mature neuron proteins of axons, dendrites, soma, and nuclei, showed neuronal development outside of the VZ. The pan-Neu^{+} neurons were concentrated in the CZ (**Figure 1C1**) and present in the subcortical area of the IZ around the VZ. TNF exposure markedly disorganized this neuronal pattern (**Figure 1C2**). Neurons appeared in dense clusters throughout the organoids, including in the scar-like tracts and were no longer outlining the rosettes and defining the CZ.

During brain development, a low level of apoptosis underlies cellular pruning. This process involves DNA binding by the effector caspase-3 (Prokhorova et al., 2018) and appears ongoing in the control cerebral organoids in which we found few apoptotic nuclei marked with anti-caspase 3 antibody (**Supplementary Figure S2**). Their occurrence increased in 1 and 10 ng/ml TNF-exposed HUES8 organoids, along with tissue damage and scar-like formation.

In summary, 1–10 ng/ml TNF exposure induced gross tissue damage throughout the organoids, formation of scar-like structures, increased apoptosis, disrupted neurogenic rosettes, and displaced neuronal formation.

Dispersion of Ki67^{+} NPC in Schizophrenia iPSC Organoids and by TNF

The HUES8 organoids exposed to 1 or 10 ng/ml TNF accrued gross structural damage, along with fine cellular disruptions. Hence, in the subsequent iPSC experiments, we employed lower concentrations, 50 and 250 pg/ml of TNF to assess potential differences in the susceptibility of the control (C) and schizophrenia (SZ) iPSC organoids to TNF. The iPSC organoids were developed for 2 weeks and exposed for 9 days to TNF, and then maintained in TNF-free medium until day 37, as described for the HUES8 organoids.

At 37 days, we observed no gross differences of size, shape, or macroscopic deformities in the TNF exposed control (C+TNF) or schizophrenia (SZ+TNF) organoids compared to the C or SZ organoids that did not receive the cytokine (**Supplementary Figure S3**). Organoids receiving TNF at 250 pg/ml (**Supplementary Figure S3**) or 50 pg/ml (not shown) lacked the scar-like tissue that developed in organoids receiving 1 ng/ml and in 10 ng/ml TNF. Consistent with the previous study (Stachowiak et al., 2017), no gross structural differences were observed between the C and SZ organoids (**Supplementary Figure S3**).

Images of the C+TNF, SZ, and SZ+TNF organoid sections stained for Ki67^{+} and counterstained for DAPI nuclei revealed noticeable differences in the distribution of proliferating Ki67^{+} NPC (**Figure 2A**). In the C iPSC organoids, similar to C HUES8 organoids, the rosettes showed strong presence of Ki67^{+} proliferating NPC surrounded by blue (DAPI) rings of densely packed nuclei (**Figure 2A1**). The Ki67^{+} NPC were typically confined to the periventricular zone of the rosettes, fewer in the IZ, and only single in the superficial cortex. In the SZ and SZ+TNF organoids, the rosettes were less discernable as

their Ki67+ cells appeared dispersed and spread into the CZ (**Figures 2A3,A4**). C+TNF organoids showed similar changes in the distribution of Ki67^{+} NPC as the SZ organoids, but these changes appeared less pronounced than in the SZ organoids (**Figure 2A2**).

To quantify changes in the distribution of the Ki67^{+} NPC, we counted cell densities within the CZ (5–6 cells deep in rectangular ROIs) and in the subcortical circular ROIs centered on the rosettes, including surrounding the IZ but excluding the cortical surface (examples on **Figure 2A1**).

In the IZ region, there was an overall significant effect of SZ, on the Ki67^{+} NPC density and nearly significant ($p = 0.08$) effect of TNF. The LSD *post hoc* analysis showed a significant reduction of Ki67^{+} cells in SZ and in SZ+TNF organoids compared to C. There was no significant additional loss of the NPC caused by TNF in the SZ organoids (**Figure 2B1**).

In the CZ, there was an overall significant effect of SZ ($p < 0.0001$), but no effect of TNF on the NPC density (**Figure 2B2**). The density of Ki67^{+} NPC increased over 2-fold in SZ and in SZ+TNF organoids. A similar trend observed in C+TNF organoids was not statistically significant.

Schizophrenia and TNF Induce Changes in Cortical and Subcortical pan-Neu[+] Neuronal Population

The images of pan-Neu-stained organoid sections indicated a reduction in the neurons in cortical region CZ in all experimental conditions and less pronounced changes in the immediate underlying subcortical region of the IZ (**Figures 3A1–A4**). High density of pan-Neu+ cells and fibers precluded counting of the individual cells. To quantify changes in the pan-Neu^{+} neurons, we analyzed the intensity of Pan-Neu immunofluorescence in the cortical and subcortical IZ areas (**Figures 3B1,B2**). In the C organoids, the resulting intensity values indicated higher densities of the differentiated pan-Neu^{+} neurons in cortical region compared to the underlying subcortical IZ area (**Figure 3B**). These mature neurons formed a dense network of processes along with the networks in experimental conditions (**Supplementary Figure S4**).

Analysis of pan-Neu[+] immunofluorescence intensity was performed by three-way ANOVA, which compared the effects of disease (C vs. SZ), TNF exposure (no TNF vs. TNF), and the organoid region: (CZ vs. subcortical IZ region; **Figure 3B**). ANOVA revealed a main effect of disease $p < 0.001$, whereby SZ conditions were associated with an overall decrease in neuronal staining intensity compared to non-disease organoids. There was a significant overall effect of TNF, $p < 0.001$, leading to decreased intensity of the pan-Neu staining. There were overall significant differences between the organoid regions, with the CZ being more intensely stained than the subcortical IZ region. There was a significant interaction between SZ and the organoid area, and between TNF and the organoid area, showing that the effects of the disease and of TNF were different in the CZ and IZ tissues.

Post hoc analysis using LSD verified that the intensity of the cortical region pan-Neu[+] networks in C organoids was significantly greater than in C+TNF ($p < 0.001$), SZ
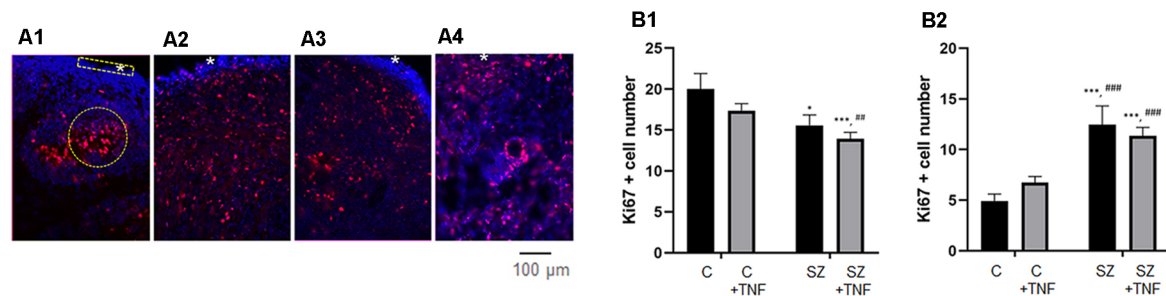
FIGURE 2 | **(A)** Disorganized migration of proliferating cells in SZ and TNF exposed 5-week control (C) organoids; **(A1)**—C, **(A2)**—C+TNF, **(A3)**—SZ, **(A4)**—SZ+TNF. The images show organoids were immunostained for Ki67 (red) used to quantify cell densities in cortical regions of interest (ROIs; rectangle), *marks superficial cortical region. In organoids shown in **(A2–A4)**, note the dispersion of proliferating (Ki67+) cells outside the VZ into IZ and CZ. Examples of ROIs—circular—IZ, rectangular—CZ. **(B)** Changes in ki67+ cell densities. **(B1)** IZ—Density of Ki67+ cells in IZ was analyzed in circular ROIs [four sections per organoid of each of the four iPSC organoid groups (C, C+TNF, SZ, SZ+TNF), 1–3 ROIs per section]. Bars represent average ROI cell numbers per section. Two-way ANOVA compared—main effect of SZ, $F = 10.44$, $p < 0.005$; TNF, $F = 3.07$, $p = 0.08$. LSD *post hoc* analysis: *,***Different from C, $p < 0.05$, $p < 0.0001$; ##,###different from C+TNF. **(B2)** CZ—Density of Ki67+ cells in CZ was analyzed in rectangular ROIs (two to four sections per organoid of each group, three to seven ROI per section). Bars represent average ROI cell numbers per section. Two-way ANOVA—main effects of SZ, $F = 40.2$, $p < 0.0001$; no effect of TNF $F = 0.139$, $p = 0.7$; no significant interaction $F = 2.34$. *,***Different from C, $p < 0.05$, $p < 0.0001$; ##,###different from C+TNF.

($p < 0.001$), or SZ+TNF ($p < 0.001$), indicating that both SZ and the addition of TNF disrupted the neuronal networks (**Figure 3B**). In contrast, in the subcortical region of IZ only SZ ($p < 0.001$) and SZ+TNF ($p < 0.001$) had depleted the pan-Neu+ neurons. TNF had an additional significant reducing effect on the IZ as well on the CZ neuronal networks in SZ + TNF compared to SZ. In control organoids TNF (C+TNF) had no significant effect on the pan-Neu+ network in the IZ, indicating that in SZ the pan-Neu+ neurons became vulnerable to TNF.

The severe cortical neuronal losses in SZ and SZ+TNF were reflected in the changes of the cortical structure as revealed by SEM. The SEM, magnification 1,500×, showed a number of changes in the cortical structure of the organoids exposed to TNF and in SZ organoids (**Figures 3C1–C4**). In SZ and in SZ+TNF organoids there were fewer cell bodies, more fibrous extracellular matrix-like (ECM) material and fewer unoccupied areas (lacking cell or fibers) than in C organoids (**Figure 3C**). Quantification of cell densities in identical size ROIs at 500× (**Figures 3D1–D5**) revealed a statistically significant reduction in the number of cells in the SZ and SZ+TNF organoids. A small reduction in C+TNF organoids did not attain statistical significance. Thus, the severe cortical neuronal loss in SZ and SZ+TNF is accompanied by a reduced density of the cortical cells, replaced by the ECM fibers, as detected by SEM.

Distinct Effects of TNFα on Calretinin Expressing Interneurons in Control and SZ Organoids

Calretinin is a protein expressed by a subpopulation of cortical GABAergic interneurons, which form intracortical connections of the cortical columns (Rogers, 1987), largely in the basal CZ and upper IZ (**Figures 4A1–A4**). We counted the numbers of calretinin+ interneurons within circular ROIs outlined in the cortical area (**Figure 4A**) and found a complex pattern of SZ and TNF-induced changes in calretinin+ cell density (**Figures 4B, C1–C4**). Two-way ANOVA analysis showed an overall (main)

significant effect of SZ and a significant interaction between the disease and TNF exposure. Thus, SZ influenced the action of the cytokine. This was specified by *post hoc* LSD comparisons of the individual conditions, which revealed that TNF significantly increased the numbers of calretinin+ cells in C+TNF organoids compared to C ($p < 0.001$). A small increase observed in the SZ organoids was not significant; however, addition of TNF to the SZ organoids markedly depleted the calretinin+ interneurons compared to SZ ($p < 0.001$) and to C ($p < 0.001$) organoids (**Figure 4B**). Thus, while in the C organoids, TNF alone increased the number of calretinin+ cells, the combined actions of disease and TNF largely eliminated these interneurons.

Cortical interneurons connect cortical microcolumns by extending parallel largely to the cortical surface (Barinka et al., 2010). We measured the orientation angle of the individual cells' long axes relative to the cortical surface using image J-based methodology. In C organoids, the greatest numbers of cells formed low angles (10–30°) with the cortical surface. This prevailing "near parallel" directionality of calretinin interneurons was maintained in C+TNF but was lost in SZ and in SZ+TNF organoids. ANOVA verified the significant effect of the angle factor on the cell frequency within different angle bins in C organoids and in C+TNF organoids and lack of such effects in SZ and in SZ+TNF organoids (**Figure 4C**).

Changes in Neuronal Precursor Cells in Schizophrenia iPSC Organoids

The antibody against autism-linked transcription factor T-Box Brain 1 (TBR1), identifies developing neuroblasts of the subplate and cortical plate, which provide the first pioneer neurons of the developing cortical networks (Kolk et al., 2006). TBR1 is necessary for neuronal differentiation of NPC and is a potential master regulator in autism spectrum disorders (Chuang et al., 2015) and SZ (Stachowiak et al., 2017). At 5 weeks of the control iPSC organoid development, cells expressing moderate levels of TBR1 were distributed throughout the entire CZ
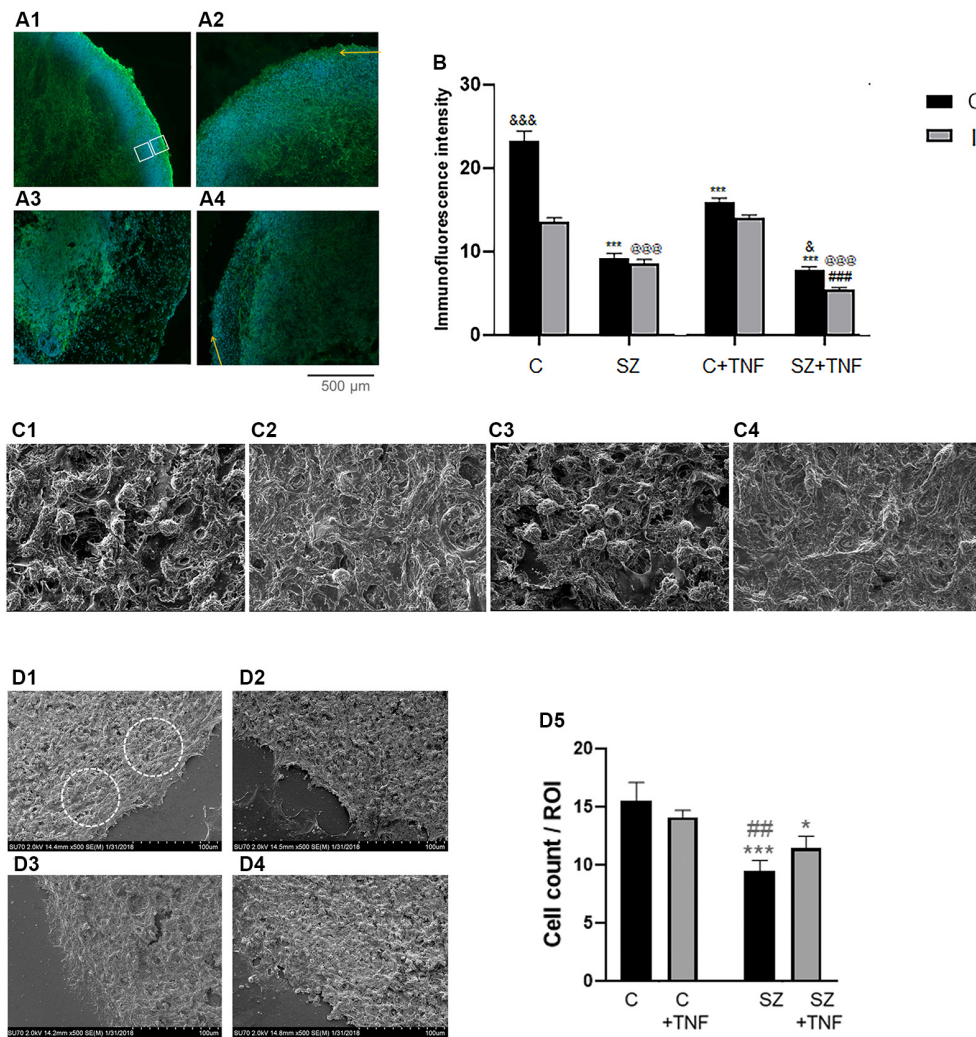
FIGURE 3 | (A) Analysis of pan-Neu+ neuronal networks in 5-week iPSC organoids. Examples of the pan-Neu antibody stained images depicting the pan-Neu neuronal networks. In each image, pan-Neu immunofluorescence intensity was measured in five ROIs each in the cortical area (CZ), five in subcortical region of the IZ (examples on **A1**). Five additional ROIs placed outside the tissue were used for background subtraction (not shown), **(A1)**—C; **(A2)**—C + TNF, **(A3)**—SZ; **(A4)**—SZ + TNF. Yellow arrows point to cortical surface. **(B)** Quantitative analysis of pan-Neu intensity numbers in analyzed ROIs. Sixteen organoids, four from each condition and 10 sections from each organoid were analyzed for the pan-Neu immunofluorescence intensity as indicated on panel **(A)**; black bars—CZ, gray bars—subcortical IZ. Bars represent average ROI fluorescence intensity per section. Three-way ANOVA: significant main effects of SZ, $F = 531.8$ ($p < 0.0001$), TNF $F = 55.33$ ($p < 0.0001$), and organoid region $F = 86.57$ ($p < 0.0001$), as well as significant interactions ($p < 0.0001$), disease × organoid region, $F = 29.22$, and TNF × organoid region $F = 15.91$. In C organoids, the pan-Neu+ neuronal density was significantly higher in CZ than subcortical zone region of the IZ ($p < 0.0001$). *Post hoc* LSD: CZ, ***different from C ($p < 0.0001$), and different from SZ ($p < 0.05$); IZ, [@@@]different from C ($p < 0.0001$), [###]different from SZ ($p < 0.0001$). **(C)** Scanning electron microscopy (SEM) images of different organoid conditions: **(C1)**—C, **(C2)**—SZ, **(C3)**—C + TNF, **(C4)**—SZ + TNF; magnification 2,500×. Note reduced cell density and increased ECM fiber density in SZ and in SZ + TNF. **(D)** Cell densities were counted within circular ROIs (examples shown) in organoid images: **(D1)**—C, **(D2)**—SZ, **(D3)**—C + TNF and **(D4)**—SZ + TNF; magnification 500×. Panel **(D5)** shows results of cell counting. Two-way ANOVA: significant main effect of SZ, $F = 15.73$, $p < 0.005$. LSD: different from C (***$p < 0.001$; *$p < 0.05$); different from C + TNF ([##]$p < 0.01$).

(**Supplementary Figure S5**). As previously found, in the SZ iPSC organoids, the neuroblasts expressing high levels of TBR1 concentrated predominantly in the VZ proximal to the rosettes but were absent from the CZ region and were depleted in the cortical subplate IZ region. TNF exposure vastly depleted TBR1 cells in the CZ and IZ, as shown in the C+TNF organoids and TNF+SZ organoids, which displayed loss of TBR1 similar to SZ organoids that were not exposed to TNF (**Supplementary** Figure S5). Thus, impaired development of cortical neurons is associated with the absence of the cortical pioneer TBR1^{+} neuroblasts.

SZ and TNF Influence Distribution of Oligodendrocytes in Developing Organoids

The O4 antibody stains late oligodendrocyte progenitors, by reacting with a sulfated glycolipid antigen (Proligodendrocyte
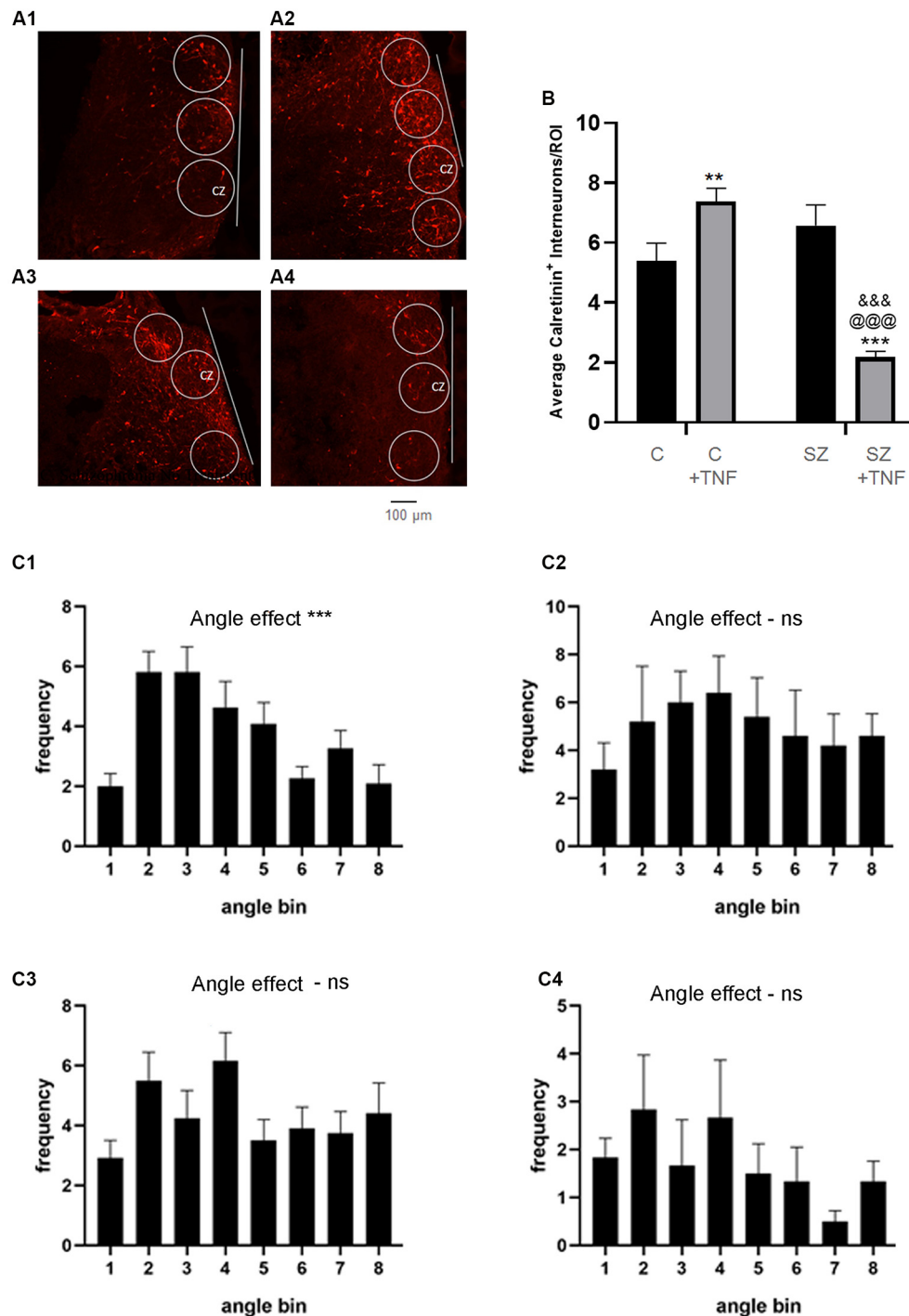
FIGURE 4 | (A) Density and orientation of cortical calretinin interneurons. **(A)** Images of organoids immunostained for calretinin (red): **(A1)**—C, **(A2)**—C+TNF, **(A3)**—SZ and **(A4)**—SZ+TNF. ROIs were outlined in which densities and orientation (angles) of the Calretinin+ interneurons long axis relative to the organoid surface (indicated by line) were measured. Sixteen organoids were analyzed, four from each condition. A total 117 ROIs were placed across the CZ of the four conditions (27–30/condition). **(B)** The average cell density of the calretinin+ interneurons/ROI is shown. Two-way ANOVA analysis, showed a main significant effect of SZ $F_{(1,115)} = 18.09$, $p < 0.001$, main significant effect of TNF ($p < 0.05$) and a significant interaction between the disease and TNF exposure, $F_{(1,115)} = 45.05$, $p < 0.0001$. *Post hoc* LSD: **,***different from C ($p < 0.0001$, $p < 0.005$), @@@different from C+TNF ($p < 0.0001$), &&&different from SZ ($p < 0.0001$). **(C)** Angles between the long axis of each calretinin+ cell and the cortical surface organoids were computed as described in the "Materials and Methods" section. Graph shows average frequency distribution of cells in ROIs in bins corresponding to the deviation angles from the cortical surface. Bin 1: 0–10°; 2: 10–20°; 3: 20–30°, etc. **(C1)**—C, c2—SZ, **(C3)**—C+TNF, **(C4)**—SZ+TNF. One-way ANOVA: main angle effect: **(C1)** $F_{(8,90)} = 6.635$, ***$p < 0.0001$, **(C2)** $F_{(8,36)} = 0.97$, $p = 0.47$, **(C3)** $F_{(7,88)} = 1.65$, **(C4)** $F_{(8,45)} = 0.92$, $p = 0.5$. ns = non-significant.

Antigen, POA). It also reacts with oligodendrocytes that have entered terminal differentiation, in which case it reacts with sulfated galactosylcerebroside, sulfatide (Ohnishi et al., 2013).

In C organoids, the O4^{+} oligodendrocytic cells followed radial patterns extending from the VZ of subcortical rosettes, through the IZ and to the CZ (**Figures 5A1–A4**). However, in all experimental conditions, C+TNF, SZ, and in SZ+TNF this radial pattern were lost. The VZ regions were devoid of O4 cells, while the majority appeared restricted into the cortical region. To quantify these changes, the intensity of the O4 immunofluorescence was measured in two areas: CZ and subcortical IZ, and the results are shown on **Figures 5B1,B2**, respectively. In the CZ, two-way ANOVA showed significant main effects of SZ, TNF, and their interaction. *Post hoc* LSD test verified significant increases in O4 densities in C+TNF, SZ, and SZ+TNF compared to C. In the IZ, we found a significant main effect only of TNF. The O4 cell density was reduced by TNF only in SZ (SZ+TNF < SZ).

In addition, three-way ANOVA of the combined CZ and IZ results showed significant main effects of SZ, TNF, organoid region (IZ vs. CZ) as well as significant interactions of SZ × organoid region and TNF × organoid region (in contrast, the pan-Neu+ neuronal density was significantly higher in CZ than in the subcortical zone region of the IZ (**Figure 3B**). Thus, the effects of TNF differed between the C and SZ organoids and between the IZ and CZ. Interestingly, the effects of SZ and TNF on the CZ O4 oligodendrocytic cells (**Figure 5B1**) and pan-Neu neurons (**Figure 3B**), were opposite, resulting in accumulation of oligodendrocytes and loss of neurons from the organoid cortical area.

To assess if the changes in the distribution of O4 oligodendrocytes were reflected in neuronal myelination, we stained the organoid sections for myelin basic protein (MBP) along with pan-Neu. In the C organoids, we observed closely co-localized pan-Neu[+] and MBP[+] staining indicating the presence of myelinated neurons in the CZ and IZ (**Supplementary Figure S6A**). In SZ organoids, we observed fewer myelinated neurons in the CZ and IZ (**Supplementary Figure S6A**) indicating lack of myelination. In C+TNF organoids, pan-Neu and MBP co-staining persisted in the CZ similar to C organoids, thus, the generation of myelinated fibers in the CZ was unchanged. However, consistent with loss of subcortical and deep IZ O4 oligodendrocytes, the myelin staining in deep areas of the C+TNF organoids was markedly reduced (**Supplementary Figure S6A**). In the SZ, as well as the SZ+TNF organoids, the CZ had reduced neuronal staining and lacked myelinated fibers while the IZ contained unmyelinated neurons (**Supplementary Figure S6A**).

Expression of nFGFR1 Protein Is Reduced in the Cortex of the SZ and TNF Exposed Organoids

The nuclear form of FGFR1 (nFGFR1) is a central signaling protein of the Integrative Nuclear FGFR1 Signaling (INFS). nFGFR1 activates coordinated gene programs, which promote neuronal development and inhibits the genes involved in

oligodendrogenesis (Stachowiak and Stachowiak, 2016; Narla et al., 2017). In contrast, cytoplasmic/plasma membrane associated FGFR1 is expressed in proliferating non-differentiated cells, including NPC, and stimulates cell proliferation (Stachowiak and Stachowiak, 2016).

Five-week-old organoids were imaged for anti-FGFR1 immunofluorescence along with DAPI (**Figures 6A1–A6**) to identify its subcellular distribution. In C organoids, strong nFGFR1 staining was observed in the CZ where it colocalized with the DAPI DNA stain, thus representing nFGFR1. nFGFR1 staining in the IZ was weaker, with fewer cells showing FGFR1/DAPI colocalized stains, while some cells displayed cytoplasmic FGFR1. In SZ organoids, as shown previously (Stachowiak et al., 2017) the nuclear presence of FGFR1 in the CZ was reduced, while it appeared increased in the IZ. This altered pattern of nFGFR1 expression was observed also in C+TNF and in SZ+TNF organoids (**Figure 6A**).

To quantify these changes, we counted nFGFR1+ cells, where nFGFR1 immunostaining co-localized with the nuclear DAPI stain. Counting was performed in rectangular ROIs within the CZ and IZ regions as illustrated in **Figures 6A1–A4**. The effects of disease (C vs. SZ) and TNF (no TNF vs. TNF) on the number of nFGFR1 positive cells were compared using a two-way ANOVA (**Figures 6B1,B2**). In the CZ, significant main effects of both SZ ($p < 0.000$) and TNF ($p < 0.01$) were found. There was also a significant interaction between the disease and TNF ($p < 0.0001$), thus, SZ affected the organoid response to TNF. *Post hoc* analysis verified that both TNF and SZ depleted cortical nFGFR1^{+} cells and that their effects were not additive. In the IZ, both SZ and TNF had main significant effects ($p < 0.005$ and $p < 0.05$, respectively), but no interactions were found. *Post hoc* comparisons showed a significant increase in the numbers of FGFR1^{+} cells in SZ and an additional increase in SZ+TNF organoids. The increase observed in C+TNF did not reach statistical significance. These results indicated an overactivity of INFS in the IZ cells of SZ and SZ+TNF organoids and a loss of INFS activity in the CZ cells of all disrupted conditions.

nFGFR1 Regulates Genes of Neuronal and Oligodendrocytic Differentiation, Cell Migration, ECM, and TNF Signaling

The study by Narla et al. (2017, 2018) identified genes dysregulated in SZ NPC as belonging to the general Gene Ontology categories of neuronal development (overexpressed genes) and oligodendrogenesis (underexpressed genes). The exemplary genes of these two categories were found to be affected by nFGFR1: stimulated (neuronal genes: TH, DISC1, Wnt7B, NeuroD) and inhibited (oligodendrocytic genes: Olig 2, Olig 1; Narla et al., 2017). We recently reported that dysregulation of nFGFR1 in the developing NPC progeny directly affected genes representing additional ontogenic processes, including cell migration and ECM, all of which were disrupted in SZ and in organoids exposed to TNF (Stachowiak et al., 2017). Many of the SZ dysregulated genes had promoters targeted by nFGFR1 (Narla et al., 2017; ChIpseq datasets GSE92873)
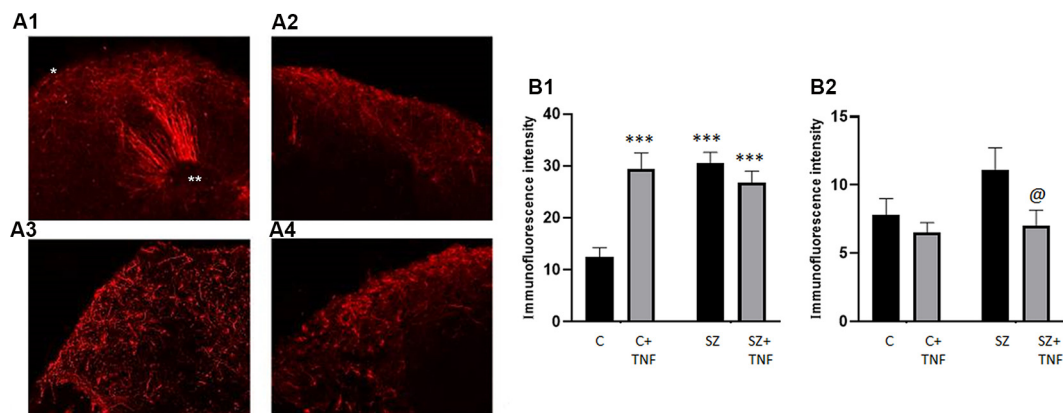
FIGURE 5 | Distribution of O4 Oligodendrocytes is affected in SZ and by TNFα. Panel **(A)** shows the florescent microscopy images of O4 antibody stained organoids (red). **(A1)**—C, **(A2)**—C+TNF, **(A3)**—SZ, **(A4)**—SZ+TNF. The radial scaffolding of migrating O4 cells emanating from ventricular rosettes towards the cortex in the C organoids **(A1)** was largely lost in C+TNF, SZ, and SZ+TNF organoids **(A2–A4)**. In TNF-treated and in SZ organoids, conditions O4 oligodendrocytes were largely restricted to the cortical region. *CZ, **VZ. **(B)** Changes in O4+ immunofluorescence intensity induced by TNF and in SZ. A total of 16 organoids were analyzed, four from each condition; CZ—cortical region, IZ—subcortical region. A total of 128 ROIs were analyzed, with eight ROIs/image, four in CZ—cortical region, four in IZ—subcortical region. In each image, four additional ROIs were placed outside and use for background subtraction, but were not part of the total count. **(B1)**—CZ, two-way ANOVA: significant main effect of SZ $F = 11.04$, $p < 0.05$, TNF $F = 8.088$, $p < 0.05$, SZ × TNF interaction $F = 19.81$, $p < 0.0001$. **(B2)**—IZ, two-way ANOVA: significant effect of TNF $F = 5.054$, $p < 0.05$. LSD: ***different from C ($p < 0.0001$); @different from SZ ($p < 0.05$). In addition a three-way ANOVA of combined CZ and IZ showed significant main effects of SZ $F = 13.67$ ($p = 0.0003$), and organoid region $F = 163.4$ ($p < 0.0001$) as well as significant interactions, disease × TNF $F = 20.1$ ($p < 0.0001$), disease × organoid region $F = 4.915$ ($p = 0.0285$), TNF × organoid region $F = 12.65$ ($p = 0.0005$) and disease × TNF × organoid region $F = 11.74$ ($p = 0.0008$).

and were directly affected by the changes of nFGFR1 signaling (Narla et al., 2017). Here, we analyzed nFGFR1 binding to the promoters of the exemplary genes involved in generation and function of neurons, oligodendrocytes, cell migration, and ECM using the NCBI Genome Browser and ChIP-seq datasets GSE92873. Genome browser illustrations of nFGFR1 binding to its promoters are shown in **Supplementary Figures S7–S10**. The analysis of our FGFR1 ChiPseq data revealed that nFGFR1 binds directly to the promoters of genes that underwrite neuronal development: WNT7B, Disc1, Neurofilament NEFL, NEFM and NEFL (**Supplementary Figure S7**); to the promoters of oligodendrogenic genes: Olig 2 and Sox9 (**Supplementary Figure S8**), ECM genes: ITGB3, NCOA3, POMT1, ANXA2, ADAMTS14 (**Supplementary Figure S9**) and cell migration genes: Ema4G, MSN, Syne2 (**Supplementary Figure S10**). Thus, changes in nFGFR1 expression in the IZ and CZ may provide a direct mechanism through which the ontogenic processes became dysregulated in the SZ and TNF exposed organoids.

Mechanisms by which SZ could affect the responses of NPC in organoids to TNF were explored by comparing the expression of TNF receptors and signaling genes in the RNAseq datasets (GSE92874) from control and SZ NPC deposited along with (Narla et al., 2017). The genes upregulated in SZ NPC included TNFRSF1B encoding TNFR2, TNFRSF10B (so called "Death Receptor" 5.5 log2), and genes for proteins that transduce TNF receptor signals, PAK1 (3.3 log 2), and PAK7 (2.2 log2; P21 protein activated kinases). These genes were affected by transfected constitutively active and/or dominant negative nuclear FGFR1 FGFR1(SP-/NLS) (Stachowiak et al., 2017;

RNAseq datasets GSE103307) that have promoters targeted by nFGFR1 (**Supplementary Figure S11**). These findings indicate that overactive TNF signaling in developing SZ NPC may be instated by overactive INFS and affect the responses of the SZ organoids to TNF.

DISCUSSION

SZ is a polygenetic disorder in which environmental influences, such as MIA, are thought to play an enabling or exacerbating role. With over 300 genes linked to SZ, it has been proposed that these genes converge on a common developmental mechanism, the disruption of which increases the risk of the disease (Cannon and Keller, 2006; Chuye et al., 2018). In support of this model, recent studies demonstrated a common dysregulated transcriptome of over 1,300 genes in developing neurons shared by SZ patients with different SZ-linked mutations (Narla et al., 2017). The pan-ontogenic INFS mechanism, in which SZ-linked genes converge, is dysregulated in all such patients. Over 80% of dysregulated genes are targeted by nFGFR1, and the changes in nFGFR1 signaling disrupt the ontogenic gene programs that lead to developmental malformations as found in SZ NPC and in cerebral organoids (Narla et al., 2017).

Our present study shows that TNF, similar to SZ, alters nFGFR1 signaling, NPC, and neurons in developing cerebral organoids that together negatively affects brain development modeled in organoids. The dysregulation of INFS instigated by SZ genetic changes is reproduced by TNF, and thus, may serve as the converging point in the genetic-environmental etiology of SZ
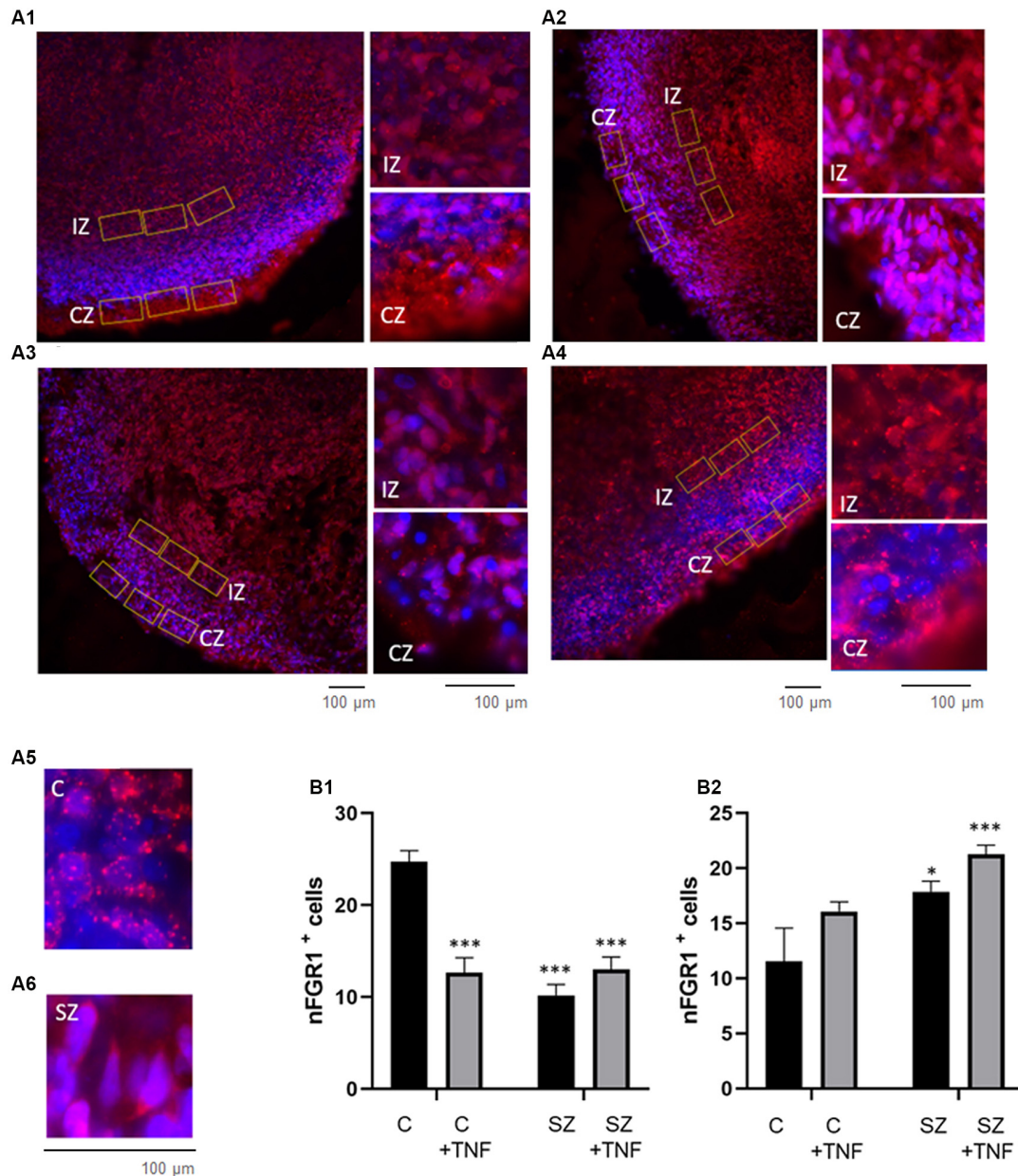
FIGURE 6 | Increases in nFGFR1 expression in subcortical cells and loss of nFGFR1 expression in cortical cells in SZ organoids and induced by TNF. **(A)** Immunostaining of FGFR1 (red) and co-staining with DAPI (blue). Organoids: **(A1)**—C, **(A2)**—C+TNF, **(A3)**—SZ, **(A4)**—SZ+TNF. In C organoids the nFGFR1 was highly expressed in the CZ cells and less expressed in the IZ cells. This pattern was reversed in SZ and TNF conditions, where nFGFR1 was depleted in the CZ and more highly concentrated in the IZ. Examples of different subcellular localization of FGFR1 staining: nuclear in C **(A5)** and cytoplasmic in C **(A6)**, CZ organoid area. Red/pink speckles on a blue DAPI background represent nFGFR1, while cytoplasmic FGFR1 forms red cytoplasmic staining surrounding the blue DAPI stained nuclei. For each image, three of the same ROIs were placed in the CZ and three in the IZ. **(B)** Sixteen organoids, four from each condition and four images from each organoid were analyzed for the number of cells with nFGFR1 (colocalized FGFR1 and DAPI stains). For each image, the total number of cells with nFGFR1were counted in three ROIs in CZ **(B1)** and in three ROIs in the IZ **(B2)**. Bars represent average total number of nFGFR1+ cells per image. **(B1)**—CZ—two-way ANOVA main effects of SZ $F = 27.81$ ($p < 0.0001$) and TNF $F = 11.84$ ($p < 0.005$); significant interaction between the SZ and TNF $F = 30.48$ ($p < 0.0001$). **(B2)**—IZ, main effect of SZ $F = 10.71$ ($p < 0.005$), TNF $F = 0.641$ ($p < 0.05$). LSD: *,***different from C $p < 0.05$, $p < 0.0001$.

and related disorders. In addition, exposure of the SZ patient's cerebral organoids to TNF exacerbates a number of cellular malformations and thus, may contribute to the development of brain pathology in SZ.

TNF in Schizophrenia

One environmental factor, which significantly increases the odds of SZ in at-risk individuals, is MIA. When an expectant mother undergoes an infection-induced immune activation, the

increased levels of the maternal cytokines can be transmitted across the placenta and potentially affect neurodevelopment of the human fetus (Toder et al., 2003; Estes and McAllister, 2016). TNF is a cytokine, whose effects can be either protective or harmful, dependent on its source, concentration and the existing brain environment (Perry et al., 2002). In the absence of MIA, endogenous brain TNF acts as a neuromodulator that supports normal brain development. However, when the brain becomes inflamed, the additional TNF produced by microglia and macrophages becomes neurotoxic (Perry et al., 2002). In the rodent brain, ischemia-induced inflammation switches the TNF function from neuroprotective to neurotoxic (Perry et al., 2002). While there is no evidence that fetal brain inflammation occurs in SZ, studies have shown elevated serum TNF levels that correlate with the incidence of SZ (Lee et al., 2017). Patient studies revealed elevated TNF blood levels, indicating an overall increase in TNF production (Ajami et al., 2014; Zhu et al., 2018). The risk of SZ increases as the immune cytokine levels are increased during pregnancy (Canetta and Brown, 2012). Specifically, the mothers of offspring who later went on to develop SZ had significantly elevated levels of TNF and interleukin-8 in the second and early third trimester, relative to the mothers of offspring who did not develop SZ (Canetta and Brown, 2012).

Furthermore, changes in brain chemistry and structure caused by broad dysregulation of genes, including TNF signaling proteins shown in our investigation, could alter the response of the developing brain stem cells, neurons, and oligodendrocytes to TNF (Narla et al., 2017; Stachowiak et al., 2017). During MIA, the increased levels of the maternal produced TNF may become transmitted across the placenta and act on the developing brain as a harmful neurotoxin (Toder et al., 2003; Estes and McAllister, 2016).

TNF pg/ml serum concentrations have been reported in human studies (Díez et al., 2002). The ED_{50} of TNF is ≤ 1 ng/ml and similar concentrations are frequently used in cell culture studies (Talley et al., 1995; Lan et al., 2012). The 1 ng/ml and 10 ng/ml TNF doses used initially in our study resulted in gross morphological malformations, as well as cellular disruptions in HUES8 cerebral organoids. The fine cellular malformations were observed with 200-fold lower concentrations of TNF, indicating that relatively small concentrations of TNF carry a significant risk of affecting brain development and have increased pathogenicity in the SZ organoids. Hence, cerebral organoids emerge as an effective model to study the neurotoxic effects of cytokines and other brain-affecting factors.

TNF and SZ Induced Malformations in Developing Brain and Interplay of TNF and SZ

We previously described a time-dependent generation and development of organoids, recapitulating the inside-out pattern of human cortical development (Stachowiak et al., 2017), similar to other laboratories that pioneered this new technology (Lancaster et al., 2013; Lancaster and Knoblich, 2014). The VZ in the center of the organoid rosettes contained GFAP⁺

radial glia and proliferating NPC, the IZ contained migrating doublecortin⁺ neuroblasts and immature βIII-tubulin⁺ neurons, and the CZ incorporated pioneer neurons (TBR1⁺) and built cortical-like layers of the βIII-tubulin⁺, pan-Neu⁺ neurons, and calretinin⁺ interneurons (Stachowiak et al., 2017). These cellular structures, zones, and their development were consistently reproduced among organoids generated from multiple hESC lines and control iPSC lines but were noticeably disrupted in SZ iPSC organoids. The same structural and cellular disruptions were established in the organoids of patients carrying different SZ-linked mutations (Stachowiak et al., 2017), similar to the present results, indicating that they are general features of the developing SZ brain. We show that with addition of TNF to either ESC or iPSC organoids, the C+TNF and SZ organoids were similar on many accounts, but different from the C organoids. One of the most striking features of the SZ organoids and of the TNF exposed ESC and iPSC organoids was the disruption of their developmental strata. Specifically, we observed a movement of proliferating Ki67⁺ NPC from the rosettes in the VZ into the CZ. In the organoids developed from either hESC or control iPSC, the proliferating cells were restricted to two to three layers surrounding the lumen of the VZ rosettes. Relatively few cells that migrated to the IZ remained in a proliferative state, and essentially, no such cells were found in the CZ. In contrast, in C+TNF and SZ+TNF, similar as in the SZ organoids, much of the Ki67⁺ cells were dispersed out from the VZ and accumulated in the CZ. Thus, the endogenous disease and the introduction of TNF reduced the number of active proliferating NPC in the neurogenic rosettes, verified by cell counting, and caused their dispersion into other organoid zones. The disorganization of the neurogenic rosettes by TNF was also revealed by dispersion of GFAP⁺ radial glia, neural stem cells, which similar to Ki67⁺ NPC, appeared outside the rosettes across the organoid interior. Hence, we conclude that both the immune cytokine, TNF, and the diseased brain state, caused rampant migration of the proliferating cells outside the normal confines of the VZ. Such dispersion of the NPC was accompanied by an abnormal formation of neuronal foci in deep subcortical regions of the organoids and excessive numbers of cortical oligodendrocytes.

Despite expanded subcortical neurogenesis and cortical oligodendrogenesis, there were fewer mature neurons expressing high levels of pan-Neu neuronal markers in the cortex of SZ organoids (see also Stachowiak et al., 2017) and in TNF-exposed organoids, both C and SZ. This was shown by a significant reduction in cortical pan-Neu intensity (**Figure 3B**) and was corroborated by visibly diminished pan-Neu fibers in the SZ and in the organoids exposed to TNF (**Supplementary Figure S2**). The loss of cortical neurons was indicated as well as by fewer cortical cells as shown by SEM in **Figure 3D**.

In C+TNF, SZ, and SZ+TNF organoids, the specific depletion of the neurons in the cortex, but not in the IZ, where formation of abnormal neuronal foci was observed, was accompanied by the reduced cortical migration of TBR1⁺ neuroblasts and their accumulation in the IZ (**Supplementary Figure S3**). The present study verified our earlier observations and indicate an abnormal subcortical arrest of pioneer TBR1 neurons

(Stachowiak et al., 2017) and lack of their cortical migration in the SZ organoids (Stachowiak et al., 2017). In SZ organoids, the reduced cortico-petal migration of TBR1+ neuroblasts and immature neurons correlated with the diminished deposition of reelin in the organoid cortex (Stachowiak et al., 2017). Further studies will be carried out to determine if an impaired reelin guidance may underlie the reduced formation of the cortical neuronal layers in TNF organoids, similar to SZ. Together, these findings illuminated an abnormal subcortical neuronogenesis in SZ and by TNF and were consistent with the premature neuronal generation predicted from the transcriptome studies of the NPC derived from SZ iPSC (Narla et al., 2017, 2018).

In SZ organoids, as shown in **Figure 3B**, and in the previous study (10), there was a reduced formation of the pan-Neu mature neurons in the top and basal regions of the cortex. In contrast, in control organoids, TNF depleted only superficial cortical neurons (**Figure 3B**), similarly as observed in mouse studies of immune activation during fetal neurodevelopment (Soumiya et al., 2011). However, in SZ organoids, TNF augmented the overall cortical neuronal loss, especially in the basal cortex, pointing to an increased vulnerability of the disease-affected cortex to this cytokine. These findings reinforce the notion that SZ and exogenous TNF have a cumulative negative effect on human cortical development, as modeled by cerebral organoids. The interaction of the SZ disease and TNF was also evident in the changes in calretinin+ interneurons, the density of which was not affected in SZ organoids, increased in C+TNF organoids, but was markedly depleted in SZ+TNF organoids. Although pyramidal neurons comprise more than 90% of cortical neurons and they project to target regions, local inhibitory interneurons shape pyramidal cell firing and their timing. The altered relationship between excitatory neurons of the vertical microcortical columns and the connecting horizontal GABAergic interneurons (of which calretinin positive neurons are a subtype) has been suggested in relation to the development of SZ in humans (Reynolds et al., 2002; Murray et al., 2014). Specifically the reduced function of inhibitory interneurons has been linked to deprograming of SZ patients cortical circuits (Sullivan and O'Donnell, 2012). Our study suggests that TNF induced a decrease in interneuron numbers in SZ organoid cortex, and their altered directionality in SZ and following TNF exposure may affect cortical connections and communication in SZ following MIA. Whether the disorientation of calretinin interneurons (**Figure 4**) could be a consequence of the disorganized proliferating progenitor cells (**Figure 2**) is currently unknown.

SZ and TNF Have Opposite Effects on Oligodendrocytic Development in the Cortex (Increases) and Subcortical Zone (Decreases) and Affect Neuronal Myelination

A striking feature of both the SZ and TNF exposed organoids were marked increases in the O4+ cells within the cortical layers. The increased O4 intensity may reflect increased expression of O4 by individual cortical cells, potentially a result of an accelerated differentiation of cortical oligodendrocyte progenitors (OPC) to O4 oligodendrocytes. Alternatively or in addition to the proposed above, the higher O4 intensity could reflect increased numbers of the developed oligodendrocytes. The latter is consistent with increased presence of proliferating Ki67+ cells, some of which may represent OPCs. The presence of oligodendrocytic cells in human cerebral organoids was shown in this study and consistent with this finding, we observed the pan-Neu+ and MBP co-stained axons of the myelinated neurons. In 5-week organoids, as the dense neuronal network formed, the occurrence of the myelinated fibers was noticed within the CZ and IZ. The development of myelinated neurons was conspicuously diminished in the SZ organoids, in C+TNF organoids and no additional effect of TNF could be noted in SZ+TNF. Despite the increased presence of O4+ oligodendrocytic cells in cerebral organoids, the diminished developing population of pan-Neu+ neurons remained largely unmyelinated. Further transmission electron microscopy (TEM)-based analysis will be required to ascertain whether the MBP+ associated neuronal fibers have mature dense, myelin wrappings.

Given the changes found in myelination in adult SZ brains (Kubicki et al., 2007; Samartzis et al., 2014; Wheeler and Voineskos, 2014), these early changes in neuronal and oligodendrocytic development and myelination revealed in the organoid model support a delayed and abnormal development of mature myelinated neuronal systems and the SZ disconnection syndrome associated with white matter loss in the frontal and temporal lobes, as well as in the corpus callosum and internal capsule (Vanes et al., 2018).

SZ and TNF Change Microstructure of the Organoid Cortex

The changes in neuronal cortical networks revealed by pan-Neu immunocytochemistry in SZ in an earlier study (Stachowiak et al., 2017) and the current study, and the changes in SZ+TNF, and relatively smaller changes in C+TNF organoids in the present study, were further illuminated by SEM. In all conditions that led to cortical underdevelopment (SZ, C+TNF, SZ+TNF), the paucity of the cell bodies was accompanied by increased spaces between cells that were "vacant" in C+TNF but became filled with the ECM fibrous material in SZ and in SZ+TNF organoids. This suggests that SZ promotes ECM development, consistent with the presence of ECM regulating genes within the SZ dysregulated transcriptome (Narla et al., 2018). Such changes may alter the mechanical properties (surface tension) of the developing cortex, which could further influence the development of the brain cortex (Kroenke and Bayly, 2018) and, potentially, lead to mild cerebral atrophy observed in SZ patients (Weinberger et al., 1979).

The cerebral organoid findings are consistent with MRI data of brains from patients with SZ that showed a specific decrease in both cortical thickness and complexity (sulci and gyri), along with enlarged ventricles. The areas that were the most heavily impacted were the temporal and frontal lobes. The authors also note that these changes may be rooted in the abnormal neural development that occurs *in utero* (Haukvik et al., 2013).
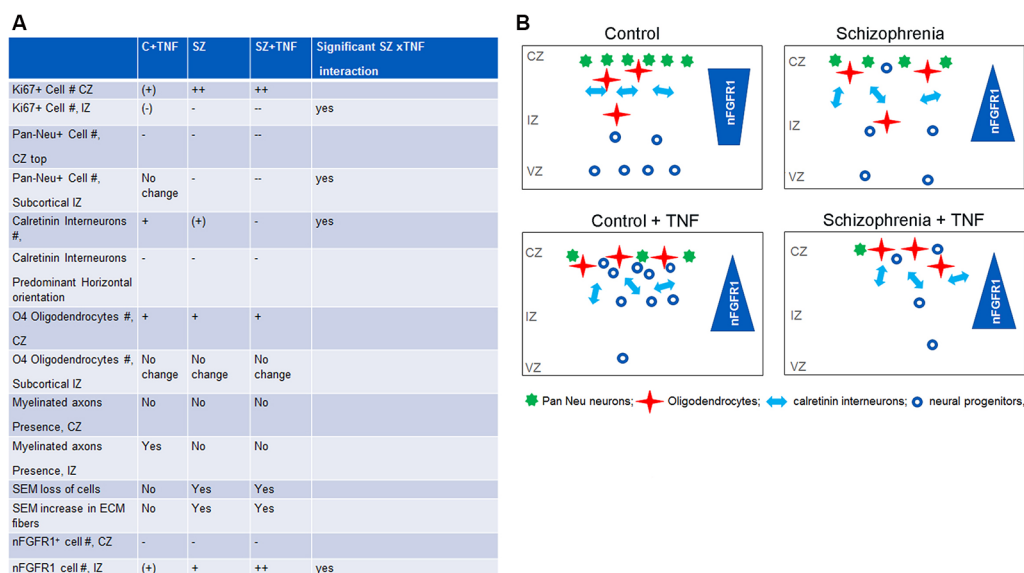
A

	C+TNF	SZ	SZ+TNF	Significant SZ xTNF interaction
Ki67+ Cell # CZ	(+)	++	++	
Ki67+ Cell #, IZ	(-)	-	--	yes
Pan-Neu+ Cell #, CZ top	-	-	--	
Pan-Neu+ Cell #, Subcortical IZ	No change	-	--	yes
Calretinin Interneurons #,	+	(+)	-	yes
Calretinin Interneurons - Predominant Horizontal orientation	-	-	-	
O4 Oligodendrocytes #, CZ	+	+	+	
O4 Oligodendrocytes #, Subcortical IZ	No change	No change	No change	
Myelinated axons Presence, CZ	No	No	No	
Myelinated axons Presence, IZ	Yes	No	No	
SEM loss of cells	No	Yes	Yes	
SEM increase in ECM fibers	No	Yes	Yes	
nFGFR1+ cell #, CZ	-	-	-	
nFGFR1 cell #, IZ	(+)	+	++	yes

FIGURE 7 | Comparisons of the effects of TNF, SZ, and their combined effect on the organoid development. **(A)** Significant increase: +; significant decrease: −; significant differences: +/++,−/−−; non-significant trend (+), (−). The effects of TNF were either similar or less pronounced than of SZ. In some cellular changes, the effects of SZ+TNF were bigger than the individual factors. In one case, density of calretinin interneurons, the interaction between TNF and SZ reversed their individual effects (increases) to a marked loss of interneurons by SZ+TNF. **(B)** The relationship of INFS and altered neuronogenesis and oligodendrogenesis by TNF and in SZ. During brain development, the nuclear location of nFGFR1, which programs neuronal development, gradually increases as the proliferating neural progenitor cells (NPC) progress through neuroblasts to differentiating neurons that form cortical layers. The diverse SZ-linked mutations that disturb developmental signals and an increased TNF promote premature nuclear FGFR1 location leading to increased formation of neurons already within the VZ and IZ and reduced subcortical oligodendrocytic development. However, when cells reach the organoid surface, nFGFR1 is turned off, possibly by increased ECM signals (Stachowiak et al., 2017). The loss of nFGFR1 reduces formation of dense cortical neuronal networks, while increasing numbers of short calretinin interneurons, diminishing their preferred horizontal orientation, and promoting oligodendrocytes. The TNF-induced changes in C organoids are similar, although generally less pronounced than those occurring in SZ. On the other hand, the combined effect of SZ and TNF are often more pronounced or even opposite (loss of calretinin interneurons) from their individual effects, likely reflecting INFS dysregulation of TNF receptor signaling. Our findings suggest that the combined effects of the SZ genomic dysregulations and maternal immune activation (MIA) may increase the risk and/or severity of SZ.

Mechanisms of Cellular Changes—Role of INFS

In the VZ and IZ of the control organoids, FGFR1 was predominantly cytoplasmic and became increasingly nuclear as the cells reached the CZ (also Stachowiak et al., 2017). This is consistent with the changing function of FGFR1, initially as the mitogenic plasma membrane receptor in the VZ and IZ, gradually to the differentiation programing nuclear protein in the IZ and CZ. The increased numbers of IZ cells with nFGFR1 in SZ+TNF, similar to the albeit pronounced trend in C+TNF and SZ, and the significantly enhanced by TNF in SZ organoids, indicated that both factors, disease and TNF, stimulate INFS in the IZ in a synergistic manner (**Figure 7A**).

The current investigation confirmed the loss of nFGFR1 in cortical cells of the SZ organoids (Stachowiak et al., 2017), and showed that, like in SZ, TNF disruption of cortical development (**Figure 3**) coincides with the loss of nFGFR1 expressing cells in the developing cortex. Thus, excess TNF appears to impair pan-developmental INFS, essential for cortical neuronal development.

The overactivation of INFS in the subcortical region and its inactivation in the cortex is thought to underlie the premature NPC development in subcortical loci and an impaired development in the organoid cortex, as shown in cultured NPC and organoids (Stachowiak et al., 2017; Chuye et al., 2018). The relationship of INFS and altered neuronogenesis and oligodendrogenesis by TNF and in SZ are summarized in **Figure 7B**.

In studies of SZ iPSC NPC, it was shown that dysregulation of INFS had opposite effects on the expression of genes involved in the generation of oligodendrocytes and neurons (Narla et al., 2017). nFGFR1 was shown to inhibit oligodendrogenic genes and activate neuronogenic genes. These findings can now be translated into the cellular data of the present organoid study. Increased subcortical nFGFR1 in disrupted conditions was accompanied by pan-Neu[+] neuronal foci, but with fewer IZ cells expressing O7294. The opposite changes were found in the cortex, where upon with the loss of nFGFR1, pan-Neu^{+} cells were restricted from the cortex and Olig4^{+} cells were more abundant than in control (non-TNF exposed) organoids. These opposite changes in the distribution of oligodendrocytic and neuronal cells may reflect the effects of nFGFR1 on neuronal (stimulation) and glial/oligodendrocytic (inhibition) genes in developing NPC (Narla et al., 2017). The current in-silico analyses revealed direct nFGFR1 targeting of the promoters of these critical genes in human developing NPC, and its

increase in SZ, as the genes became dysregulated. Hence, the changes in nFGFR1, as they occur in SZ and induced by TNF, may directly affect these critical genes and cell lineage developmental decisions.

The significant interaction of SZ and TNF in eliciting changes in neuronal and oligodendrocytic populations (**Figure 7A**) and in nFGFR1 indicated an increased sensitivity of the developing SZ brain to TNF, and thus, MIA. The analyses of the dysregulated genes in SZ NPC enlightens changes in the expression of TNF receptors and signaling pathway genes as a potential mechanism for the increased TNF sensitivity in SZ NPC. In all four SZ patients, a multifold upregulation of the TNF receptor-II genes TNFRSF1B and TNFRSF10B, dubbed the "death receptor," as well as TNF receptor 1 signaling genes PAK1 and PAK7, was found. The serine/threonine-protein kinases, PAK1 and PAK7, which influence a wide variety of cellular processes, including directional motility and growth and are overexpressed in many diseases, showed multi-fold upregulation in SZ cells (GSE92874; Narla et al., 2017).

TNF is a strong candidate gene for SZ. Serum levels of TNF were significantly increased in SZ, associated with more severe symptoms of SZ and with a higher risk of developing SZ (Suchanek-Raif et al., 2018). The mining of the existing FGFR1 ChIpseq data from our laboratory revealed that nFGFR1 direct binding to TNF receptor genes, as well as to the component genes of their receptor pathways, was increased in SZ (**Supplementary Figure S11**). Through these changes, the developing SZ brain with inherited genome dysregulations may suffer increased vulnerability to TNF, which is neurotoxic when in excess. This further lends support to the proposal that MIA could be a significant contribution for genetically at-risk fetuses for the expression of SZ.

Since a single representative SZ iPSC line was used for the extensive quantitative-computational anatomical analyses in the present studies, whether the supersensitivity to TNF similarly extends to the other SZ lines, as well as the extent to which individual genotypes may affect the response to TNF and the potential treatments are the subject of ongoing studies. The genomic changes in TNF receptors and their signaling pathway genes found in multiple SZ patients' iPSCs (Narla et al., 2017) are consistent with the SZ patient-derived organoid supersensitivity to TNF.

In conclusion, cerebral organoid and genomic-based models offer plausible cellular and molecular mechanisms for TNF-dependent neurodevelopmental pathology of SZ and its induction by MIA.

REFERENCES

Ajami, A., Abedian, F., Hamzeh Hosseini, S., Akbarian, E., Alizadeh-Navaei, R., and Taghipour, M. (2014). Serum TNF-α, IL-10 and IL-2 in schizophrenic patients before and after treatment with risperidone and clozapine. *Iran. J. Immunol.* 11, 200–209.

Barinka, F., Druga, R., Marusic, P., Krsek, P., and Zamecnik, J. (2010). Calretinin immunoreactivity in focal cortical dysplasias and in non-malformed epileptic cortex. *Epilepsy Res.* 88, 76–86. doi: 10.1016/j.eplepsyres.2009.09.021

DATA AVAILABILITY STATEMENT

AUTHOR CONTRIBUTIONS

CB: doctoral student, dissertation project, performed the major portion of experiments, analyzed the data, and assisted with writing the manuscript. HP: Master's student thesis project, performed some of the experiments and assisted with manuscript writing and editing. ML: assisted with experiments and contributed to manuscript preparation and editing. SD and DF: performed some of the experiments and contributed to manuscript preparation and editing. TI: contributed to experimental design, data interpretation, and contributed to manuscript writing and editing. ES: contributed to experimental design, data analysis, and writing of the manuscript. MS: overall project design, oversee all aspects of project, data analysis and interpretation, and wrote the manuscript.

FUNDING

ACKNOWLEDGMENTS

SUPPLEMENTARY MATERIAL

The Supplementary Material for this article can be found online at: https://www.frontiersin.org/articles/10.3389/fncel.2020.00233/full#supplementary-material

Brennand, K., Savas, J. N., Kim, Y., Tran, N., Simone, A., Hashimoto-Torii, K., et al. (2015). Phenotypic differences in hiPSC NPCs derived from patients with schizophrenia. *Mol. Psychiatry* 20, 361–368. doi: 10.1038/mp.2014.22

Buka, S. L., Tsuang, M. T., Torrey, E. F., Klebanoff, M. A., Wagner, R. L., and Yolken, R. H. (2001). Maternal cytokine levels during pregnancy and adult psychosis. *Brain Behav. Immun.* 15, 411–420. doi: 10.1006/brbi.2001.0644

Canetta, S. E., and Brown, A. S. (2012). Prenatal infection, maternal immune activation, and risk for schizophrenia. *Transl. Neurosci.* 3, 320–327. doi: 10.2478/s13380-012-0045-6

Cannon, T. D., and Keller, M. C. (2006). Endophenotypes in the genetic analyses of mental disorders. *Annu. Rev. Clin. Psychol.* 2, 267–290. doi: 10.1146/annurev.clinpsy.2.022305.095232

Chuang, H. C., Huang, T. N., and Hsueh, Y. P. (2015). T-brain-1—a potential master regulator in autism spectrum disorders. *Autism Res.* 8, 412–426. doi: 10.1002/aur.1456

Chuye, L. B., Dimitri, A., Desai, A., Handelmann, C., Bae, Y., Johari, P., et al. (2018). Brain organoids: expanding our understanding of human development and disease. *Results Probl. Cell Differ.* 66, 183–206. doi: 10.1007/978-3-319-93485-3_8

Clarke, M. C., Harley, M., and Cannon, M. (2006). The role of obstetric events in schizophrenia. *Schizophr Bull.* 32, 3–8. doi: 10.1093/schbul/sbj028

Dean, B., Gibbons, A. S., Tawadros, N., Brooks, L., Everall, I. P., and Scarr, E. (2013). Different changes in cortical tumor necrosis factor-α-related pathways in schizophrenia and mood disorders. *Mol. Psychiatry* 18, 767–773. doi: 10.1038/mp.2012.95

Díez, J. J., Hernanz, A., Medina, S., Bayón, O., Iglesias, P. (2002). Serum concentrations of tumour necrosis factor-alpha (TNF-α) and soluble TNF-alpha receptor p55 in patients with hypothyroidism and hyperthyroidism before and after normalization of thyroid function. *Clin. Endocrinol.* 57, 515–521. doi: 10.1046/j.1365-2265.2002.01629.x

Estes, M. L., and McAllister, A. K. (2016). Maternal immune activation: implications for neuropsychiatric disorders. *Science* 353, 772–777. doi: 10.1126/science.aag3194

Eura, N., Matsui, T. K., Luginbühl, J., Matsubayashi, M., Nanaura, H., Shiota, T., Kinugawa, K., et al. (2019). Brainstem organoids from human pluripotent stem cells contain neural crest population. *Front. Neurosci.* 14:538.

Galinsky, R., Dhillon, S. K., Dean, J. M., Davidson, J. O., Lear, C. A., Wassink, G., et al. (2020). Tumor necrosis factor inhibition attenuates white matter gliosis after systemic inflammation in preterm fetal sheep. *J. Neuroinflammation* 17:92. doi: 10.1186/s12974-020-01769-6

Harrison, P. J. (1999). The neuropathology of schizophrenia. A critical review of the data and their interpretation. *Brain* 122, 593–624. doi: 10.1093/brain/122.4.593

Haukvik, U. K., Hartberg, C. B., and Agartz, I. (2013). Schizophrenia–what does structural MRI show? *Tidsskr. Nor. Laegeforen.* 133, 850–853. doi: 10.4045/tidsskr.12.1084

Klejbor, I., Kucinski, A., Wersinger, S. R., Corso, T., Spodnik, J. H., Dziewiatkowski, J., et al. (2009). Serotonergic hyperinnervation and effective serotonin blockade in an FGF receptor developmental model of psychosis. *Schizophr. Res.* 113, 308–321. doi: 10.1016/j.schres.2009.06.006

Klejbor, I., Myers, J. M., Hausknecht, K., Corso, T. D., Gambino, A. S., Morys, J., et al. (2006). Fibroblast growth factor receptor signaling affects development and function of dopamine neurons—inhibition results in a schizophrenia-like syndrome in transgenic mice. *J. Neurochem.* 97, 1243–1258. doi: 10.1111/j.1471-4159.2006.03754.x

Kolk, S. M., Whitman, M. C., Yun, M. E., and Shete, P., Donoghue, M. J. (2006). A unique subpopulation of Tbr1-expressing deep layer neurons in the developing cerebral cortex. *Mol Cell Neurosci* 32, 200–214. doi: 10.1016/j.mcn.2005.08.022

Kroenke, C. D., and Bayly, P. V. (2018). How forces fold the cerebral cortex. *J. Neurosci.* 38, 767–775. doi: 10.1523/jneurosci.1105-17.2017

Kubicki, M., McCarley, R., Westin, C. F., Park, H. J., Maier, S., Kikinis, R., et al. (2007). A review of diffusion tensor imaging studies in schizophrenia. *J. Psychiatr. Res.* 41, 15–30. doi: 10.1016/j.jpsychires.2005.05.005

Lan, X., Chen, Q., Wang, Y., Jia, B., Sun, L., and J. Zheng and Peng, H. (2012). TNF-α affects human cortical neural progenitor cell differentiation through the autocrine secretion of leukemia inhibitory factor. *PLoS One* 7:e50783. doi: 10.1371/journal.pone.0050783

Lancaster, M. A., and Knoblich, J. A. (2014). Generation of cerebral organoids from human pluripotent stem cells. *Nat. Protoc.* 9, 2329–2340. doi: 10.1038/nprot.2014.158D

Lancaster, M. A., Renner, M., Martin, C. A., Wenzel, D., Bicknell, L. S., Hurles, M. E., et al. (2013). Cerebral organoids model human brain development and microcephaly. *Nature* 501, 373–379. doi: 10.1038/nature12517

Lee, E. E., Hong, S., Martin, A. S., Eyler, L. T., and Jeste, D. V. (2017). Inflammation in schizophrenia: cytokine levels and their relationships to demographic and clinical variables. *Am. J. Geriatr. Psychiatry* 25, 50–61. doi: 10.1016/j.jagp.2016.09.009

Livne-Bar, I., Lam, S., Chan, D., Guo, X., Askar, I., Nahirnyj, A., et al. (2016). Pharmacologic inhibition of reactive gliosis blocks TNF-α-mediated neuronal apoptosis. *Cell Death Dis.* 7:e2386. doi: 10.1038/cddis.2016.277

Murray, J. D., Anticevic, A., Gancsos, M., Ichinose, M., Corlett, P. R., Krystal, J. H., et al. (2014). Linking microcircuit dysfunction to cognitive impairment: effects of disinhibition associated with schizophrenia in a cortical working memory model. *Cereb. Cortex* 24, 859–872. doi: 10.1093/cercor/bhs370

Na, K. S., Jung, H. Y., and Kim, Y. K. (2014). The role of pro-inflammatory cytokines in the neuroinflammation and neurogenesis of schizophrenia. *Prog. Neuropsychopharmacol. Biol. Psychiatry* 48, 277–286. doi: 10.1016/j.pnpbp.2012.10.022

Narla, S. T., Decker, B., Sarder, P., Stachowiak, E. K., and Stachowiak, M. K. (2018). Induced pluripotent stem cells reveal common neurodevelopmental genome deprograming in schizophrenia. *Results Probl. Cell Differ.* 66, 137–162. doi: 10.1007/978-3-319-93485-3_6

Narla, S. T., Lee, Y. W., Benson, C. A., Sarder, P., Brennand, K. J., Stachowiak, E. K., et al. (2017). Common developmental genome deprogramming in schizophrenia—role of integrative nuclear FGFR1 signaling (INFS). *Schizophr. Res.* 185, 17–32. doi: 10.1016/j.schres.2016.12.012

Ohnishi, Y., Iwatsuki, K., Shinzawa, K., Ishihara, M., Moriwaki, T., Umegaki, M., et al. (2013). Adult olfactory sphere cells are a source of oligodendrocyte and Schwann cell progenitors. *Stem Cell Res.* 11, 1178–1190. doi: 10.1016/j.scr.2013.08.005

Patterson, P. H. (2009). Immune involvement in schizophrenia and autism: etiology, pathology and animal models. *Behav. Brain Res.* 204, 313–321. doi: 10.1016/j.bbr.2008.12.016

Perry, S. W., Dewhurst, S., Bellizzi, M. J., and Gelbard, H. A. (2002). Tumor necrosis factor-alpha in normal and diseased brain: Conflicting effects via intraneuronal receptor crosstalk? *J. Neurovirol.* 8, 611–624. doi: 10.1080/13550280290101021

Prokhorova, E. A., Kopeina, G. S., Lavrik, I. N., and Zhivotovsky, B. (2018). Apoptosis regulation by subcellular relocation of caspases. *Sci. Rep.* 8:12199. doi: 10.1038/s41598-018-30652-x

Reynolds, G. P., Beasley, C. L., and Zhang, Z. J. (2002). Understanding the neurotransmitter pathology of schizophrenia: selective deficits of subtypes of cortical GABAergic neurons. *J. Neural Transm.* 109, 881–889. doi: 10.1007/s007020200072

Rogers, J. H. (1987). Calretinin: a gene for a novel calcium-binding protein expressed principally in neurons. *J. Cell Biol.* 105, 1343–1353. doi: 10.1083/jcb.105.3.1343

Samartzis, L., Dima, D., Fusar-Poli, P., Kyriakopoulos, M. (2014). White matter alterations in early stages of schizophrenia: a systematic review of diffusion tensor imaging studies. *J. Neuroimaging* 24, 101–110. doi: 10.1111/j.1552-6569.2012.00779.x

Schmitt, A., Hasan, A., Gruber, O., Falkai, P. (2011). Schizophrenia as a disorder of disconnectivity. *Eur. Arch. Psychiatry Clin. Neurosci.* 261, S150–S154. doi: 10.1007/s00406-011-0242-2

Siniscalco, D., Schultz, S., Brigida, A. L., and Antonucci, N. (2018). Inflammation and neuro-immune dysregulations in autism spectrum disorders. *Pharmaceuticals* 11:56. doi: 10.3390/ph11020056

Soumiya, H., Fukumitsu, H., Furukawa, S. (2011). Prenatal immune challenge compromises the normal course of neurogenesis during development of the mouse cerebral cortex. *J. Neurosci. Res.* 89, 1575–1585. doi: 10.1002/jnr.22704

Stachowiak, E. K., Benson, C. A., Narla, S. T., Dimitri, A., Chuye, L. E. B., Dhiman, S., et al. (2017). Cerebral organoids reveal early cortical maldevelopment in schizophrenia—computational anatomy and genomics, role of FGFR1. *Translational Psychiatry* 7:6. doi: 10.1038/s41398-017-0054-x

Stachowiak, M. K., and Stachowiak, E. K. (2016). Evidence-based theory for integrated genome regulation of ontogeny–an unprecedented role of nuclear FGFR1 signaling. *J. Cell Physiol.* 231, 1199–1218. doi: 10.1002/jcp.25298

Stachowiak, M. K., Kucinski, A., Curl, R., Syposs, C., Yang, Y., Narla, S., et al. (2013). Schizophrenia: a neurodevelopmental disorder–integrative genomic hypothesis and therapeutic implications from a transgenic mouse model. *Schizophr Res.* 143, 367–376. doi: 10.1016/j.schres.2012.11.004

Suchanek-Raif, R., Raif, P., Kowalczyk, M., Paul-Samojedny, M., Kucia, K., Merk, W., et al (2018). Promoter polymorphisms of TNF-α gene as a risk factor

for schizophrenia. *Arch. Med. Res.* 49, 248–254. doi: 10.1016/j.arcmed.2018.
09.007

Sullivan, E. M., and O'Donnell, P. (2012). Inhibitory interneurons, oxidative
stress, and schizophrenia. *Schizophr. Bull.* 38, 373–376. doi: 10.1093/schbul/
sbs052

Talley, A. K., Dewhurst, S., Perry, S. W., Dollard, S. C., Gummuluru, S.,
Fine, S. M., et al. (1995). Tumor necrosis factor α-induced apoptosis in
human neuronal cells: protection by the antioxidant N-acetylcysteine and the
genes bcl-2 and crmA. *Mol. Cell Biol.* 15, 2359–2366. doi: 10.1128/mcb.15.
5.2359

Toder, V., Fein, A., Carp, H., and Torchinsky, A. (2003). TNF-α in pregnancy
loss and embryo maldevelopment: a mediator of detrimental stimuli or
a protector of the fetoplacental unit? *J. Assist. Reprod. Genet.* 20, 73–81.
doi: 10.1023/a:1021740108284

Vanes, L. D., Mouchlianitis, E., Wood, T. C., and Shergill, S. S. (2018). White
matter changes in treatment refractory schizophrenia: does cognitive control
and myelination matter? *NeuroImage Clin.* 18, 186–191. doi: 10.1016/j.nicl.
2018.01.010

Weinberger, D. R., Torrey, E. F., Neophytides, A. N., and Wyatt, R. J. (1979).
Structural abnormalities in the cerebral cortex of chronic schizophrenic

patients. *Arch. Gen. Psychiatry* 36, 935–939. doi: 10.1001/archpsyc.1979.
01780090021002

Wheeler, A. L., and Voineskos, A. N. (2014). A review of structural neuroimaging
in schizophrenia: from connectivity to connectomics. *Front. Hum. Neurosci.*
8:653. doi: 10.3389/fnhum.2014.00653

Zhu, F., Zhang, L., Liu, F., Wu, R., Guo, W., Ou, J., et al. (2018). Altered
serum tumor necrosis factor and interleukin-1β in first-episode drug-naive and
chronic schizophrenia. *Front. Neurosci.* 12:296. doi: 10.3389/fnins.2018.00296

Advantages of publishing in Frontiers

OPEN ACCESS
Articles are free to read
for greatest visibility
and readership

FAST PUBLICATION
Around 90 days
from submission
to decision

HIGH QUALITY PEER-REVIEW
Rigorous, collaborative,
and constructive
peer-review

TRANSPARENT PEER-REVIEW
Editors and reviewers
acknowledged by name
on published articles

Frontiers
Avenue du Tribunal-Fédéral 34
1005 Lausanne | Switzerland

Visit us: www.frontiersin.org
Contact us: info@frontiersin.org | +41 21 510 17 00

REPRODUCIBILITY OF RESEARCH
Support open data
and methods to enhance
research reproducibility

DIGITAL PUBLISHING
Articles designed
for optimal readership
across devices

FOLLOW US
@frontiersin

IMPACT METRICS
Advanced article metrics
track visibility across
digital media

EXTENSIVE PROMOTION
Marketing
and promotion
of impactful research

LOOP RESEARCH NETWORK
Our network
increases your
article's readership